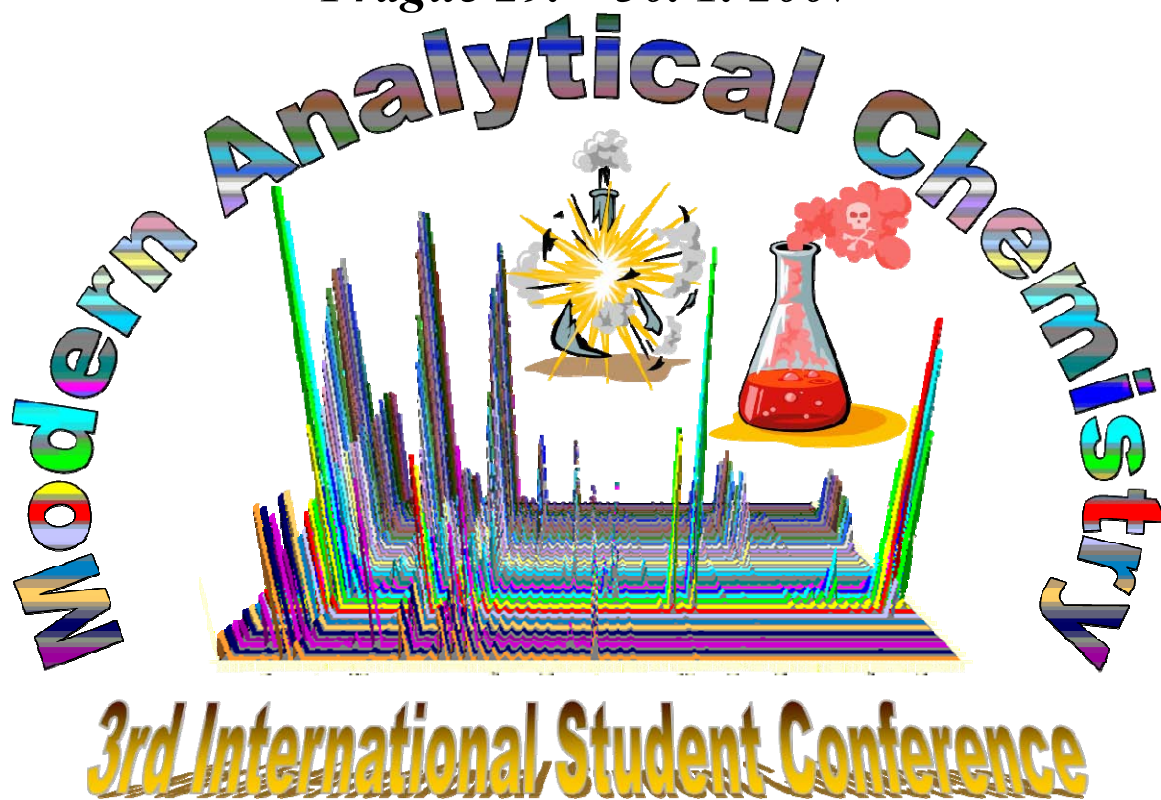


Charles University in Prague, Faculty of Science, Department of
Analytical Chemistry, *Hlavova 2030, 12843, Prague2, Czech Republic*

Prague 29. – 30. 1. 2007



3rd International Student Conference

Book of Proceedings



Prague 2007

Published by the Czech Chemical Society

ISBN 80 - 86238 - 96 - 2

We are very grateful to our sponsors for their kind support:

ZENTIVA

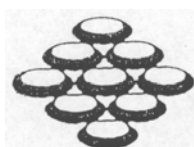
<http://www.zentiva.cz/>

Waters

<http://www.waters.com/>



<http://www.quinta.cz>



PharmaTech s.r.o.

<http://www.medicainfo.cz/jmr/jmr1604.htm>

Charles University in Prague, Faculty of Science, Department of Analytical Chemistry, Hlavova 2030, 12843, Prague2, Czech Republic

3rd International Student Conference

“Modern Analytical Chemistry”

Prague 29. – 30. 1. 2007

Book of Proceedings



Prague 2007

Published by

**Česká společnost chemická
Czech Chemical Society**

ISBN 80 - 86238 - 96 – 2

Vydala Česká společnost chemická. Za obsah veškerých textů nesou plnou zodpovědnost autoři. Publikace neprošla odbornou ani jazykovou úpravou a je určena pro účastníky semináře a členy pořádajících organizací. Není určena k volnému prodeji. Zveřejněné informace mohou být dále použity za předpokladu úplného citování původního zdroje. Přetiskování, kopírování či převádění této publikace do jakékoliv tištěné či elektronické formy a její prodej je možný pouze na základě písemného souhlasu vydavatele. (Bona fide vědečtí pracovníci si mohou pořídit jednotlivé xerox kopie).

Published by the Czech Chemical Society in collaboration with organizers of the conference. This publication is made available for the conference participants, members of the organizing institutions and for documentary purposes.

Some products named or cited in this publication and other materials of the congress are registered as trademarks or proprietary names even in the case this fact is being explicitly shown or acknowledged. It is not to be considered as fail to notice the ownership or authorship by the publisher. All the texts are published with the full responsibility of authors for their content. The publication was not content or language-polished. Its content could be used on the condition of full acknowledgement and citation of the source. Direct reprinting, transformation to any means of electronic form is restricted (bona fide scientist may xerox single copies in accordance of their local copyright laws and regulations) and is possible upon written agreement with the publisher only.

Vydala / Published By



Česká společnost chemická
Czech Chemical Society

Novotného lávka 5, CZ 116 68, Praha 1

v roce 2007

1. vydání, brož., náklad 50 výtisků

© Charles University in Prague

ISBN 80 - 86238 - 96 – 2

An Invitation to the 3rd International Student Conference

“Modern Analytical Chemistry”

to be held

on January 29 – 30, 2007

*at the lecture hall CH5, Faculty of Science,
Chemical Departments Building, Hlavova 2030, Prague 2*

organized by

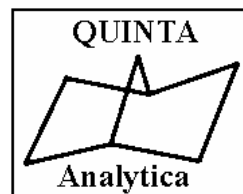
Charles University in Prague, Faculty of Science
Department of Analytical Chemistry

and

sponsored by

ZENTIVA

Waters



PharmaTech s.r.o.

Monday January 29th

Morning

9.00

M. Braun^a, M. Adam^a, K. Štulík^b

^aInstitute of Rheumatology, Experimental Connective Tissue Research Laboratory Prague and ^bCharles University in Prague, Faculty of Science, Department of Analytical Chemistry

High Performance Separation of Collagen and Elastin Cross-Links 9

9.30

M. Vadinská^a, Z. Bosáková^a, E. Tesařová^b

Charles University in Prague, Faculty of Science, Departments of Analytical^a and Physical and Macromolecular^b Chemistry

Study of Enantioseparation Behaviour of Profen Nsaids on the Teicoplanin Aglycone-Based Chiral Stationary Phase by HPLC. 17

10.00

L. Loukotková^a, Z. Bosáková^a, E. Tesařová^b

Charles University in Prague, Faculty of Science, Departments of Analytical^a and Physical and Macromolecular^b Chemistry

Study of the Influence of Experimental Conditions on the Retention and Enantioseparation of Series of Newly Synthesized Disubstituted Binaphthyls 28

10.30

H. Dejmková, J. Zima, J. Barek

Charles University in Prague, Faculty of Science, Department of Analytical Chemistry

HPLC-ED Determination of Aminonitrophenols 40

11.00

V. Šolínová, D. Koval, V. Kašička, M. Česnek, A. Holý

Institute of Organic Chemistry and Biochemistry, Academy of Sciences of the Czech Republic, Prague

Determination of Acid-Base Dissociation Constants of Acyclic Nucleoside Phosphonates and Related Compounds by Capillary Zone Electrophoresis 49

11.30

J. Kratzer^{a,b}, J. Dědina^a, P. Rychlovský^b

^aAcademy of Sciences of the Czech Republic, Institute of Analytical Chemistry, Prague, Czech Republic and ^bCharles University in Prague, Faculty of Science, Department of Analytical Chemistry

As and Se Hydride Trapping at the Quartz Surface - a Step Forward to In-situ Trapping in Quartz Tube Atomizers for AAS 59

Sponsored lunch

Monday January 29th

Afternoon

13.30

**Ž. Krkošová^a, R. Kubinec^a, H. Jurdáková^a, J. Blaško^a, B. Meľuchová^a, I. Ostrovský^a,
L. Soják^a, J. Ševčík^b, J. Višňovský^c**

^a*Chemical Institute, Faculty of Natural Sciences, Comenius University, Bratislava*

^b*Charles University in Prague, Faculty of Science, Department of Analytical Chemistry,*

^c*CMS Chemicals, s. r. o., Nobelova 34, P. O. Box 44, SK-836 03 Bratislava*

**Very Fast Gas Chromatography with a Ballistic Heating and Ultra Fast Cooling of the
Column** 68

14.00

**B. Meľuchová^a, V. Valkovská^a, H. Jurdáková^a, Ž. Krkošová^a, J. Blaško^a, P. Příkryl^b,
R. Kubinec^a, J. Ševčík^b, I. Ostrovský^a, L. Soják^a, V. Berezkin^c**

^a*Chemical Institute, Faculty of Natural Sciences, Comenius University, Bratislava*

^b*Charles University in Prague, Faculty of Science, Department of Analytical Chemistry,*

^c*A. V. Topchiev Institute of Petrochemical Synthesis, Russian Academy of Sciences, Moscow*

**Needle Concentrator and Solid Phase Micro-Extraction for Gas Chromatographic
Determination of BTEX from Aqueous Samples** 81

14.30

**H. Jurdáková, L. Soják, R. Kubinec, Ž. Krkošová, J. Blaško, B. Meľuchová,
E. Pavlíková**

Chemical Institute, Faculty of Natural Sciences, Comenius University, Bratislava

**GC Structure-Retention Relation and Mass Spectrometry for Identification of
Polyalkenes Decomposing Products** 94

15.00

**J. Blaško, L. Soják, R. Kubinec, Ž. Krkošová, H. Jurdáková, B. Meľuchová,
E. Pavlíková**

Chemical Institute, Faculty of Natural Sciences, Comenius University, Bratislava

Analysis of Conjugated Linoleic Acid Isomers in Ewe Milk Products by GC-MS 107

15.30

O. Grossová^{a,b}, J. Dědina^a

^a*Academy of Sciences of the Czech Republic, Institute of Analytical Chemistry, Prague*

^b*Charles University, Faculty of Science, Prague, Czech Republic*

Development of L-Shaped Hydride Multiatomizer for Atomic Absorption Spectrometry 119

16.00

J. Musilová^a, J. Barek^a, K. Pecková^a

^a*Charles University in Prague, Faculty of Science, Department of Analytical Chemistry*

**Use of Boron-Doped Diamond Electrode in Voltammetry of Biologically Active Organic
Compounds** 126

**Social Meeting at the Department of Analytical Chemistry
(from 17 o'clock)** (Chemical Departments building)

Tuesday January 30th

Morning

9.00

V. Vyskočil^a, J. Barek^a, K. Čížek^a, Z. Zawada^b

^a Charles University in Prague, Faculty of Science, Department of Analytical Chemistry, UNESCO Laboratory of Environmental Electrochemistry, Prague

^b Charles University in Prague, Faculty of Pharmacy in Hradec Králové, Department of Inorganic and Organic Chemistry, Hradec Králové

Study of Electrochemical Behavior of 2,7-dinitro-9-fluorenone 132

9.30

A. Daňhel, J. Barek, B. Yosypchuk, K. Pecková

Charles University in Prague, Faculty of Science, Department of Analytical Chemistry, Prague

Voltammetric Determination of Genotoxic Nitrocompounds Using Silver Amalgam Electrodes 142

10.00

E. Svobodová, M. Vadinská, Z. Bosáková

Charles University in Prague, Faculty of Science, Department of Analytical Chemistry, Prague

Capillary Electrophoresis of Anthraquinone Dyes Employed in Works of Art 151

10.30

Z. Jemelková, J. Zima, J. Barek

Charles University in Prague, Faculty of Science, Department of Analytical Chemistry, Prague

HPLC - ED Determination of Epinephrine at Carbon Paste Electrode 160

11.00

R. Pospíchal, K. Nesměrák, P. Rychlovský

Charles University in Prague, Faculty of Science, Department of Analytical Chemistry, Prague

FIA Determination of Chondroitin Sulfate by Azure B with Spectrophotometric Detection 167

11.30

I. Jiránek^a, J. Barek^a, B. Yosypchuk^b, K. Pecková^a, K. Čížek^a

^a Charles University in Prague, Faculty of Science, Department of Analytical Chemistry, UNESCO Laboratory of Environmental Electrochemistry, Prague

^b J. Heyerovský Institute of Physical Chemistry, Academy of Science of the Czech Republic, Prague

Voltammetric Determination of Trace Amounts of Nitro and Amino Derivatives of Quinoline 177

Sponsored lunch

13.30

V. Červený, J. Hraníček, P. Rychlovský

Charles University in Prague, Faculty of Science, Department of Analytical Chemistry, Prague

Postcolumn Electrochemical Hydride Generation Used For Speciation Analysis of Arsenic Compounds 188

14.00

M. Hlína, M. Hrabovský, V. Kopecký, M. Konrad, T. Kavka, S. Skoblja

Institute of Plasma Physics, ASCR, Prague and ^bDepartment of Gas, Coke and Air Protection, Institute of Chemical Technology, Prague

Production of Gas with Low Content of Tar in Plasma Gasification Reactor 197

HIGH PERFORMANCE SEPARATION OF COLLAGEN AND ELASTIN CROSS-LINKS

Martin Braun ^{a,b}, Milan Adam ^a and Karel Štulík ^b

^a *Institute of Rheumatology, Experimental Connective Tissue Research Laboratory
Na Šlupí 4, 128 50 Prague 2, Czech Republic; e-mail: braun@revma.cz*

^b *Charles University, Faculty of Science, Department of Analytical Chemistry
Albertov 8, 128 40 Prague 2, Czech Republic*

Abstract

This work concerns the development and application of high performance separation methods suitable for determination of clinically considerable fragments of collagen and elastin as the most important proteins of connective tissues. For their analyses we utilized various chromatographic and electrophoretic methods, including high performance liquid chromatography (HPLC), capillary zone electrophoresis (CZE) and micellar electrokinetic liquid chromatography (MEKC).

Our aim was optimizing of analytical separation procedures and their utilization for determination of clinically important markers of connective tissue degradation.

In the presented work we described high performance methods which were suggested and optimized for separation and quantitative determination of pentosidine, pyridinolines and desmosines as the most important collagen and elastin cross-links. The methods were already successfully applied in analysis of real patient's samples and obtained results utilized in clinical practice.

Keywords

HPLC; Capillary Electrophoresis; Collagen; Elastin; Pentosidine; Pyridinoline; Desmosine; Connective Tissue; Cross-link

1. Introduction

Pathological changes of connective tissues are reflected at first by specific biochemical findings in the organism. Collagen and elastin cross-links are clinically important molecules and their elevated concentrations in the body could indicate serious metabolic disorders. Their quantification by means of sensitive analytical methods helps to monitor the pathological modifications of these proteins with long biological half-life as well as kinetics of their degradation.

From the analytical point of view there are some specific aspects in this work, given by the nature of used samples of biological materials (body fluids and joint compartment tissues) as well as low concentration of the studied analytes, complexity of the raw material, tendency to disintegrability and low amount of available sample.

These obstacles demanding sophisticated sample treatment were solved using a sequence of separation and preconcentration steps, high-performance separation methods and sensitive detection with respect to sample consideration during treatment.

Characteristics of the studied analytes:

All the monitored analytes (pentosidine, pyridinolines and desmosines) are cross-links which represent covalent linkage among the individual fibrils of collagen or elastin (Fig. 1). These cross-links are formed by post-translational modifications of connective tissue proteins which occurs usually within pathobiochemical processes *in vivo*, in chronic joint diseases or another pathological states affecting connective tissues. The cross-links are during breakdown of collagen or elastin secreted into blood and urine, where are monitored as indicators of kinetics of osteoclastic activity and markers of bone, cartilage or elastic tissues resorption.

Incorrect crosslinkage of collagen and elastin leads to higher rigidity of their structures and in rheumatic or other patients can be manifested as connective tissue diseases associated with decreased elasticity of tissue proteins, increased fragility and even reduced resistance to proteases. As a consequence, release of the mentioned cross-links from these most important molecules of the supportive tissues has negative influence on their physico-chemical and functional properties and leads to their disintegration.

Pentosidine (PEN) belongs to one of the best chemically defined representative of the group of Advanced Glycation End-products (AGEs) formed by non-enzymatic glycation. This naturally fluorescent cross-link of proteins (especially those with long biological half-life) come up, as well as other AGEs, by so called Maillard reaction which is a sequence of condensation reactions where amino-groups of lysine and arginine residues from the polypeptide chains of proteins are combined with aldehyde group of reducing carbohydrates, mainly pentose (such a ribose which is the most reactive). In this way Schiff base is formed as an early glycation product. Increased concentration of carbohydrates in blood, extracellular matrix and tissues is thus one of the crucial reasons which induce pathological level of glycation. Later occurs rearrangement of Schiff base to Amadori products (which are stable to hydrolysis). These intermediate products of glycation are harmless itself, but during months or years are irreversibly transforming with involvement of free oxygen radicals to more reactive carbonyl compounds, AGEs. PEN is the best example of such compounds formed spontaneously by Maillard reaction which enable pathological cross-linking of modified protein chains and is considered to be an indicator of general collagen breakdown and glycooxidation. Markedly increased PEN levels are associated mainly with inflammation processes, oxidative & carbonyl stress (e.g. in chronic joint disease such as in arthritis), in diabetes mellitus, renal insufficiency, neurological diseases, and other symptoms related to ageing of connective tissues. Accumulation of PEN (which is not further metabolized) *in vivo* can have toxic effects to the whole organism.

The other markers reflecting bone catabolism are pyridinoline (PD) and deoxypyridinoline (DPD). They both are stable, fluorescent, non-reducible trifunctional cross-links, specifically binded to collagen. PD and DPD are formed from the lysine and hydroxylysine residues in the presence of lysyl oxidase and their urinary concentrations are utilized as markers of bone collagen, mainly in chronic and degenerative rheumatic diseases and those associated with bone mass loss (e.g. osteoporosis and osteoarthritis).

Analogical cross-links as pyridinolines in collagen are formed also in elastin – in this case they are called desmosine (DES) and isodesmosine (IDES). Both the isomers are formed in the presence of

lysylloxidase by condensation of four lysine residues contained in tropoelastin resulting to pyridine cycle structures and absorb in UV spectrum range. They are specifically binded to elastin and were not observed in other proteins, but their occurrence is very rare – approximately 2 DES or IDES residues among 1000 of other amino acid residues within elastin molecule. Determination of desmosines can indicate elastin degradation in pathological metabolic actions where soft and elastic connective tissues are afflicted (such as blood vessels, elastic cartilage, lungs, skin etc.).

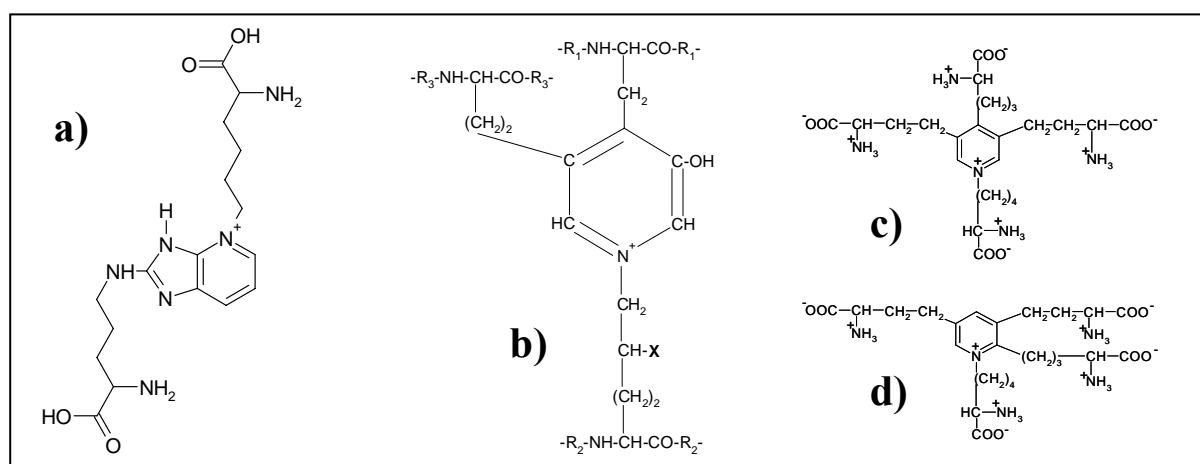


Fig. 1 Chemical structure of the studied analytes:

a) pentosidine; b) pyridinoline ($X = OH$), resp. deoxypyridinoline ($X = H$); c) desmosine; d) isodesmosine.

2. Experimental

2.1. Sample pretreatment

Acid hydrolysis (in aliquot of 12M HCl), purification and preconcentration by solid phase extraction (SPE using Supelco vacuum manifold extractor), vacuum evaporation of excessive solvents using SpeedVac rotary concentrator (Savant, USA) for about 6 hours and reconstitution in mobile phase, injection into HPLC.

2.2 HPLC - apparatus and experimental conditions:

Pentosidine analysis:

The method developed in our lab for PEN determination is based on reversed phase HPLC separation using programmable gradient flow of mobile phase and sensitive fluorescent detection. For analysis we used on-line PC controlled HPLC system SHIMADZU (Kyoto, Japan) operated by CLASS VP software (version 5.03) consisting of liquid chromatograph (model: LC 10ADvp) equipped with autosampler, quaternary pump, column oven and fluorescence detector (set at $\lambda_{exc/em} = 335/385$ nm). The separation was performed using compact glass column CGC Separon SGX C18 packed with spherical silica gel particles (diameter 7 μ m) embedded with octadecyl group, sized 150x3 mm (Tessek, Prague, Czech Republic); mobile phase (degassed with He): 0.02 M heptafluorobutyric acid, 0.01M $(NH_4)_2SO_4$ and linear gradient was given by variable concentration of acetonitrile (12.5–25 % ACN within 20 minutes), column temperature was 40°C, flow rate 0.5 ml/min and time of HPLC run 30 min. (including returning of the mobile phase composition to the initial conditions); 10-25 μ l of sample reconstituted in mobile phase was applied into the HPLC column.

Analysis of pyridinolines:

The method used for simultaneous determination of PD and DPD was isocratic ion-exchange HPLC with fluorescent detection (wavelength set at $\lambda_{exc/em} = 297/400$ nm); CGC Separon HEMA-BIO 1000 column (150x3 mm) filled with sulphobutyl was used as stationary phase, mobile phase consisted of 0.3M CH_3COOH (pH=3.0) and 0.45 mol/l Na_2SO_4 , column temperature was 48°C, flow rate 0.3 ml/min. and time of the HPLC run was 12 minutes.

Analysis of desmosines:

Possibility of HPLC separation of DES and IDES was tested as well. From several alternatives the best results were obtained with slightly modified method used for pentosidine analysis. In this case gradient of ACN was 5-17,5 %, and fluorescent detection was replaced with UV. Under these conditions with UV wavelength set at

$\lambda = 273$ nm, optimal separation of DES and IDES peaks was obtained within 30 minutes, which enable calibration of the method using commercial DES and IDES standards (ICN ,Costa Mesa, CA, USA).

2.3. Capillary Electrophoresis

For separation of desmosine isomers (DES & IDES) were made attempts using also capillary zone electrophoresis (CZE) and micellar electrokinetic chromatography (MEKC) with UV detection. For both modes was used CRYSTAL CE System (Unicam, Cambridge, UK) combined with UV spectrophotometric detector Spectra 100 (TSP, USA). Separation was performed in open tube silica capillary TWC-S50 (i.d.=50 μ m; $l_t/l_d = 65/50$ cm; CACO, Slovakia) and voltage from 10 to 30 kV was applied during experiments, hydrodynamic injection of sample was usually 30 mbar/0.1 min. Within the work experimental conditions were optimized by means of different composition and concentration of the background electrolyte, pH, separation voltage and λ). In CZE experiments the following electrolytes were tested: H_3PO_4 , NaH_2PO_4 and $Na_2B_4O_7$; in MEKC we used 30 mM $Na_2B_4O_7$ buffer (pH=9.2) with addition of 50 mM sodium dodecyl sulphate.

3. Results and discussion

The individual separation conditions were optimized for the best analysis performance to enable utilization of the described methods for quantitative determination of collagen cross-links in various types of samples. According to our present measurements, the applied HPLC methods appear to be very reliable and provide relevant quantitative results in quite short time. Reproducibility of PEN determination was 98.8%, of the whole method (including sample hydrolysis & purification) was 4.44%; recovery of the whole method $77 \pm 3.5\%$ and limit of detection 17.6 femtomols, in pyridinolines the limit of detection for both PD and DPD was about 200 femtomols. Examples of separation of studied cross-links are shown in Fig. 2a, 2b.

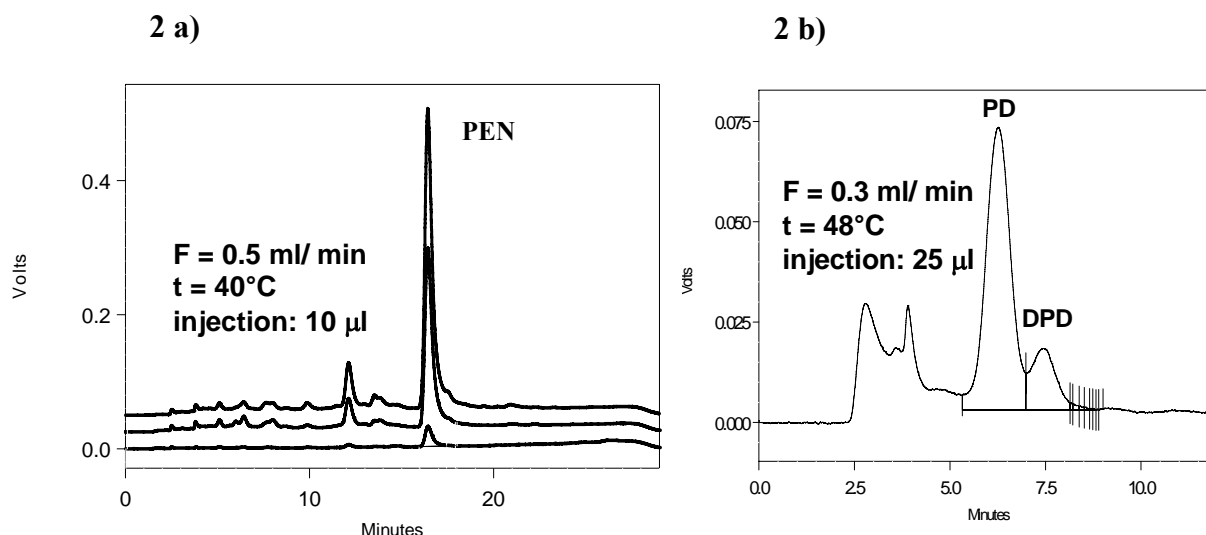


Fig. 2 Examples of HPLC separation of collagen cross-links

- a) gradient separation of PEN in joint tissues from patient with advanced osteoarthritis (OA): synovial membrane (top line), cartilage (middle line), subchondral bone (bottom line)
b) isocratic separation of PD and DPD in urine of patient with advanced OA

For determination of elastin cross-links (DES and IDES) were tested both capillary electrophoretic methods and HPLC. The best results were obtained in MEKC mode with UV detection ($\lambda=273$ nm) where 30 mM $\text{Na}_2\text{B}_4\text{O}_7$ (pH=9,2) with 50 mM SDS was used as separation electrolyte (Fig. 3a). The separation of both isomers was successful in model mixture of standards but not suitable and sensitive enough for practical analysis of urinary desmosines in real patient's samples.

Another approach was separation of DES and IDES isomers by HPLC (Fig. 3b). In this case was observed good separation of both elastin cross-links using analogical method as for PEN determination but with UV detection (set at $\lambda=273$ nm). Nevertheless for quantitative measurements of both DES and IDES in real urine samples, preconcentration is crucial and there is a need of pooling samples from large volume due to very low concentration.

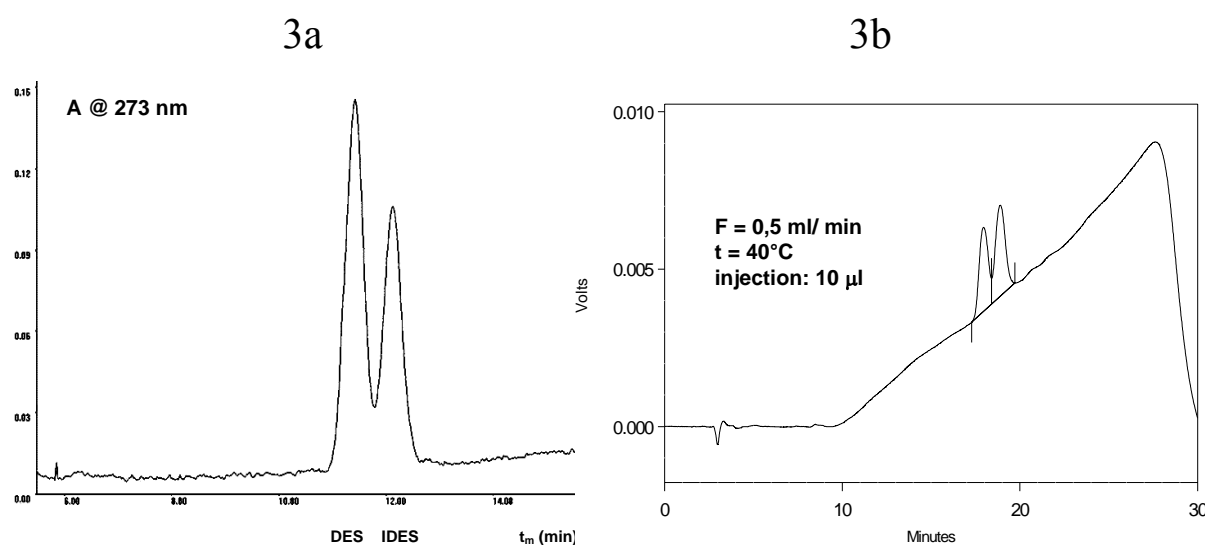


Fig. 3 Examples of elastin cross-links separation (DES / IDES standard mixture)

a) MEKC – experimental conditions: capillary TWC-S50 (i.d.=50 µm; $l_t / l_d = 65/50$ cm), 30mM $Na_2B_4O_7$ (pH=9.2) + 50mM SDS; $U=30$ kV, $\lambda = 273$ nm; 30 mbar/ 0.1 min.

b) Gradient RP-HPLC separation of DES and IDES using CGC Separon SGX C18 column (150x3 mm); mobile phase: 0.02M heptafluorobutyric acid + 0.01M $(NH_4)_2SO_4$ with linear gradient of acetonitrile (5-17,5 %), UV detection at $\lambda=273$ nm.

4. Conclusions

The elaborated analytical procedure and methods were successfully applied in real samples of body fluid or tissues of patients suffering from connective tissue diseases. Reliable quantitative determination of the selected biomarkers of connective tissue degradation seems to be a useful tool within the scope of special laboratory diagnostics and the achieved results were already applied in clinical practice.

Acknowledgment:

This work supported Czech Ministry of Health / IGA (research projects Nos. 00023728, NR/ 7895-3, NR/ 8447-4, NR/ 7886-3).

STUDY OF ENANTIOSEPARATION BEHAVIOUR OF PROFEN NSAIDs ON TEICOPLANIN AGLYCONE-BASED CHIRAL STATIONARY PHASE BY HPLC

Marie Vadinská¹, Zuzana Bosáková¹, Eva Tesařová²

¹ Department of Analytical Chemistry, Faculty of Science, Charles University, Albertov 2030, 128 40 Prague 2, Czech Republic

² Department of Physical and Macromolecular Chemistry, Faculty of Science, Charles University, Albertov 2030, 128 40 Prague 2, Czech Republic

Abstract

The teicoplanin aglycone-based chiral stationary phase (CSP) was used for study of retention and enantioselective behaviour of profen non-steroidal anti-inflammatory drugs (NSAIDs), ibuprofen, fenoprofen, flurbiprofen, indoprofen, carprofen, suprofen, flobufen and ketoprofen. Reversed-phase separation mode with mobile phases composed of methanol and 0.1 or 1.0% triethylamine acetate (TEAA) buffer (pH 3.0 - 6.0) in various volume ratios was applied. In general, lower methanol contents (40 vol. %), higher concentration of TEAA buffer (1.0%) and buffer pH of 4.0 or 4.5 are suitable for enantioresolution of all studied profen NSAIDs with the exception of fenoprofen.

1. Introduction

Teicoplanin aglycone (TAG) (Fig.1) belongs to macrocyclic antibiotics' (MAs) chiral selectors. This new group of chiral selectors is very successful for enantioseparation of a wide variety of analytes. MAs dispose of many stereogenic centers and functional groups such as hydroxyl, amine and carboxylic groups, aromatic moieties and hydrophobic pockets that offer multiple interaction possibilities for many chiral molecules.¹ Among MAs, glycopeptides, namely vancomycin, ristocetin A, avoparcin, teicoplanin and teicoplanin aglycone, are mostly applied chiral selectors in high performance liquid chromatography. MAs-based chiral stationary phases (MA CSPs) constitute of covalently bonded glycopeptides on a 5 µm silica

gel. The ligands are attached by multiple linkages to establish high stability CSPs.

The teicoplanin aglycone is prepared by removing three carbohydrate moieties from the teicoplanin molecule. This modification leaves intact the remaining eight chiral centers surrounding the four pockets (cavities). The peptide chain contains hydrogen donor and hydrogen acceptor chiral sites that are in close proximity to the aromatic rings, which make up the inclusion pockets, and act as anchor sites.² The structure of teicoplanin aglycone is depicted in Figure 1.

Profen NSAIDs (2-arylpropionic acids) represent an important group of non-steroidal anti-inflammatory drugs, exhibiting analgesic, antipyretic and antirheumatic effects. The mechanism of their therapeutic effect consists of non-selective inhibition of cyclooxygenase. Due to the inhibition of this enzyme, production of prostaglandines, which play important role in genesis of inflammations and pains, is blocked.³

Polar profens are characterized by a stereogenic center adjacent to the carboxylic acid moiety. Several direct or indirect liquid chromatographic methods involving a variety of CSPs were reported for enantiomeric analysis of profens. The most frequently used CSPs are based on cyclodextrins⁴, polysaccharides⁵, ergot alkaloids⁶ and macrocyclic antibiotics^{7,8}. From the group of MAs' chiral selectors, only vancomycin⁷ and teicoplanin⁸ were applied.

The aim of this work is a study of retention and enantioseparation of the selected chiral profens (see Fig. 2) on teicoplanin aglycone-based chiral stationary phase (TAG CSP) in reversed-phase separation mode by HPLC.

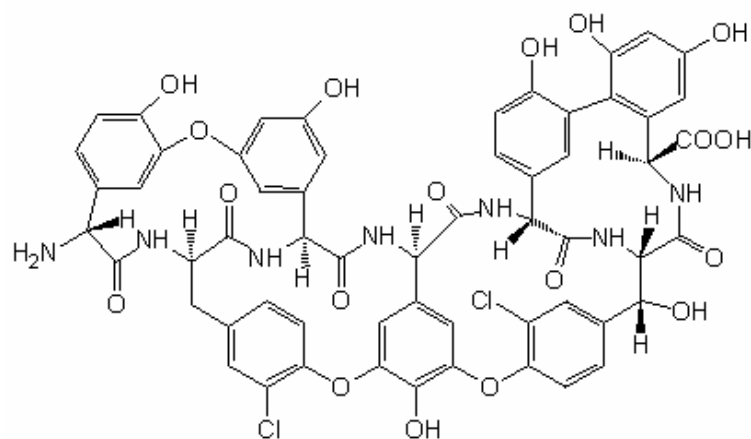
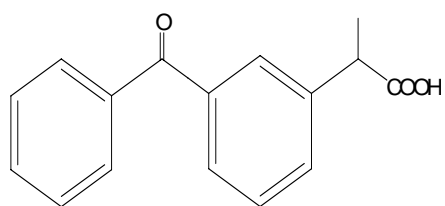
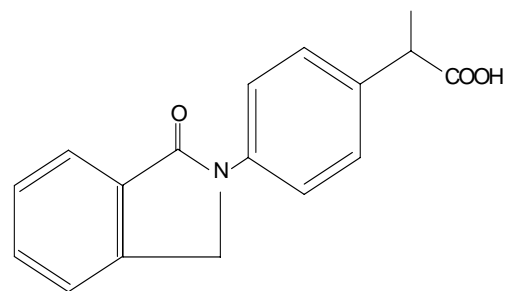


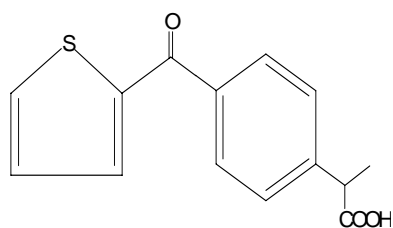
Figure 1. Structure of teicoplanin aglycone



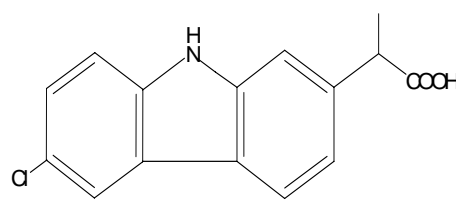
Ketoprofen (Ket)



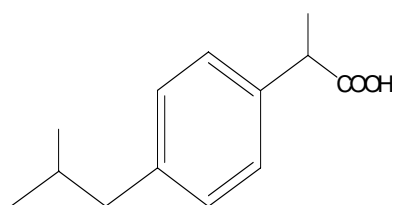
Indoprofen (Ind)



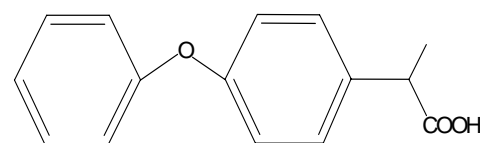
Suprofen (Sup)



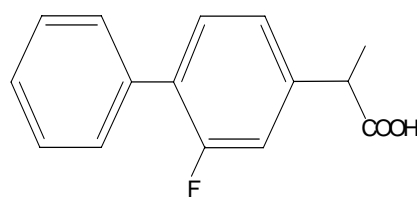
Carprofen (Car)



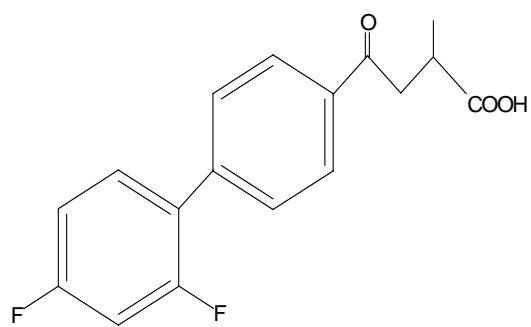
Ibuprofen (Ibu)



Fenoprofen (Fen)



Flurbiprofen (Flu)



Flobufen (Flo)

Figure 2. Structures of the studied profen NSAIDs

2. Experimental

2.1. Chemicals

The mobile phases were prepared from the following compounds and solvents: methanol, (Chromasolv®Riedel-de Haën, Seelte, Germany); triethylamine, purity > 99 %, (Sigma Aldrich, St. Louis, MO, USA); acetic acid, p.a. 99 %, (Lachema, Brno, Czech Republic). Deionized water was used throughout the experiments (Milli-Q water purification system Millipore, Milford, MA, USA).

All the tested standards of profens (i.e. ibuprofen, indoprofen, carprofen, ketoprofen, suprofen, flurbiprofen and fenoprofen) were purchased from Sigma Aldrich (St. Louis, MO, USA).

2.2. Equipment and chromatographic conditions

The commercially available steel column (250 mm x 4.6 mm i.d.), with teicoplanin aglycone bonded to silica gel support, particle size 5 µm – CHIROBIOTIC TAG (ASTEC, Whippany, NY, USA) was used. Measurements were performed on a DeltaChrom SDS 030 liquid chromatograph (Watrex, Prague, Czech Republic) consisting of SDS 030 pump, Rheodyne 7125 injector with 20 µl loop and UV-VIS detector. Clarity 2.1 software was used for process control and data handling. Triethylamine acetate (TEAA) buffers, 0.1 or 1.0%, pH 3.0 – 6.0, containing various percentages of methanol (80 – 40 vol. %) were used as mobile phases. The flow rate was 0.7 ml·min⁻¹. The measurements were carried out at laboratory temperature (22 ± 2 °C). The detection wavelength was 230 for ibuprofen, indoprofen, carprofen, flurbiprofen and fenoprofen and 270 nm for suprofen, flobufen and ketoprofen. The methanolic stock solutions of individual analytes were prepared in the concentration of 1.0 mg·ml⁻¹.

3. Results and discussion

With respect to our results obtained for profens on teicoplanin bonded chiral stationary phase we decided to work also with the teicoplanin aglycone bonded CSP in the reversed-phase separation system. We studied the influence of mobile phase composition on

retention and enantiodiscrimination of selected profen NSAIDs in the present work. The effect of methanol (MeOH) contents and pH values of 1.0% TEAA buffer in the mobile phase on retention factors (k), selectivity (α) and enantioresolution (R) values can be seen in Table 1. It is obvious that the retention of all the studied profens increases with decreasing content of methanol in all the tested mobile phases. Increasing of pH values of 1.0% TEAA buffer leads to decreased retention of the majority of profens. From the three different measured values of buffer pH the worst results were obtained for pH 6. The best chiral separation for ibuprofen, indoprofen, carprofen, suprofen and flobufen was achieved at pH 4 while for flurbiprofen and ketoprofen at pH 5 in the mobile phases with 40 % content of methanol.

Analogous measurements were carried out in the mobile phases with 0.1% concentration of TEAA buffer. Comparison of the chromatographic data obtained with 1.0% and 0.1% buffers in the mobile phase composed of 40 % MeOH and 60 % of the individual TEAA buffers is given in Table 2. These results can be summarized as follows: Lower concentration of TEAA resulted in increased retention of the profen NSAIDs (except of flobufen, which has a different structure) at pH 4 while the opposite results were obtained if buffers of higher pH were used. The corresponding enantioresolution values were lower with 0.1% TEAA buffers in the whole pH range.

Table 1 Effect of methanol and 1.0% TEAA buffer of various pH values on chromatographic data of the studied profens.

Experimental conditions: TAG CSP, mobile phase - methanol/1.0% TEAA, (pH 4.0 – 6.0) in various ratios (v/v); k_1 - retention factor of the first eluted enantiomer, α - selectivity, R - enantioresolution.

TEAA pH 4.0	80 % MeOH			60 % MeOH			40 % MeOH		
	k_1	α	R	k_1	α	R	k_1	α	R
Ibuprofen	0.00	1.00	0.00	0.83	1.00	0.00	4.52	1.11	0.51
Indoprofen	0.99	1.18	0.62	2.82	1.14	0.64	12.44	1.14	0.80
Fenoprofen	0.24	1.00	0.00	1.08	1.00	0.00	5.27	1.00	0.00
Carprofen	0.63	1.00	0.00	2.62	1.09	0.32	18.79	1.08	0.50
Flurbiprofen	0.31	1.32	0.50	1.37	1.19	0.69	7.37	1.16	0.78
Ketoprofen	0.40	1.00	0.00	1.38	1.00	0.00	6.54	1.00	0.00
Suprofen	0.61	1.32	0.90	1.88	1.21	0.97	8.23	1.17	1.05
Flobufen	0.27	1.00	0.00	1.47	1.00	0.00	10.64	1.07	0.29
pH 5.0	k_1	α	R	k_1	α	R	k_1	α	R
Ibuprofen	0.00	1.00	0.00	0.87	1.00	0.00	3.80	1.04	0.14
Indoprofen	1.11	1.23	0.59	2.90	1.18	0.55	10.42	1.15	0.43
Fenoprofen	0.00	1.00	0.00	1.05	1.00	0.00	4.47	1.00	0.00
Carprofen	0.70	1.00	0.00	2.81	1.00	0.00	15.58	1.00	0.00
Flurbiprofen	0.00	1.00	0.00	1.50	1.35	0.70	6.62	1.28	1.03
Ketoprofen	0.36	1.12	0.17	1.28	1.13	0.28	4.94	1.15	0.53
Suprofen	0.63	1.37	0.76	1.98	1.32	0.94	6.90	1.26	1.03
Flobufen	0.00	1.00	0.00	1.14	1.00	0.00	7.03	1.03	0.12
pH 6.0	k_1	α	R	k_1	α	R	k_1	α	R
Ibuprofen	0.00	1.00	0.00	0.73	1.00	0.00	3.70	1.00	0.00
Indoprofen	0.84	1.28	0.56	2.46	1.21	0.52	8.50	1.15	0.38
Fenoprofen	0.00	1.00	0.00	0.85	1.00	0.00	3.81	1.00	0.00
Carprofen	0.51	1.00	0.00	2.28	1.00	0.00	11.93	1.00	0.00
Flurbiprofen	0.00	1.00	0.00	1.17	1.42	0.96	5.62	1.34	1.06
Ketoprofen	0.00	1.00	0.00	1.01	1.18	0.37	4.13	1.19	0.57
Suprofen	0.50	1.44	0.71	1.60	1.35	0.84	6.06	1.28	0.90
Flobufen	0.00	1.00	0.00	0.80	1.00	0.00	4.71	1.00	0.00

Table 2 Effect of the buffer concentration on chromatographic data of the studied profens.

Experimental conditions: TAG CSP, mobile phase - 40/60 (v/v) methanol/0.1 and 1.0% TEAA, the abbreviations as in Tab. 1.

pH 4.0	0.1% TEAA			1.0% TEAA		
	k_1	α	R	k_1	α	R
Ibuprofen	5.59	1.24	0.54	4.52	1.11	0.51
Indoprofen	14.54	1.13	0.66	12.44	1.14	0.80
Fenoprofen	6.86	1.00	0.00	5.27	1.00	0.00
Carprofen	26.57	1.08	0.29	18.79	1.08	0.50
Flurbiprofen	9.67	1.07	0.26	7.37	1.16	0.78
Ketoprofen	7.33	1.00	0.00	6.54	1.00	0.00
Suprofen	8.12	1.08	0.30	8.23	1.17	1.05
Flobufen	12.48	1.07	0.31	10.64	1.07	0.29
pH 5.0	k_1	α	R	k_1	α	R
Ibuprofen	2.67	1.06	0.39	3.80	1.04	0.14
Indoprofen	6.16	1.14	0.53	10.42	1.15	0.43
Fenoprofen	3.71	1.00	0.00	4.47	1.00	0.00
Carprofen	16.20	1.00	0.00	15.58	1.00	0.00
Flurbiprofen	3.83	1.13	0.29	6.62	1.28	1.03
Ketoprofen	2.66	1.00	0.00	4.94	1.15	0.53
Suprofen	3.58	1.12	0.36	6.90	1.26	1.03
Flobufen	6.28	1.04	0.13	7.03	1.03	0.12
pH 6.0	k_1	α	R	k_1	α	R
Ibuprofen	0.76	1.00	0.00	3.70	1.00	0.00
Indoprofen	2.13	1.07	0.19	8.50	1.15	0.38
Fenoprofen	0.84	1.00	0.00	3.81	1.00	0.00
Carprofen	3.61	1.00	0.00	11.93	1.00	0.00
Flurbiprofen	1.22	1.24	0.36	5.62	1.34	1.06
Ketoprofen	0.98	1.00	0.00	4.13	1.19	0.57
Suprofen	1.32	1.26	0.30	6.06	1.28	0.90
Flobufen	1.92	1.00	0.00	4.71	1.00	0.00

Based on the fact that mobile phases with 40 % content of methanol yielded the best results, the effect of the buffer pH was studied in these mobile phases in more detail. The results are shown in Table 3.

Table 3 Effect of the buffer pH on chromatographic data of the studied profens.

Experimental conditions: TAG CSP, mobile phase - 40/60 (v/v) methanol/1.0% TEAA, the abbreviations as in Tab. 1.

		pH 3.0	pH 3.5	pH 4.0	pH 4.5	pH 5.0	pH 6.0
Ibuprofen	k_I	2.79	3.81	4.52	4.35	3.80	3.70
	α	1.08	1.11	1.11	1.12	1.04	1.00
	R	0.44	0.62	0.51	0.70	0.14	0.00
Indoprofen	k_I	8.25	11.06	12.44	13.46	10.42	8.50
	α	1.09	1.11	1.14	1.13	1.15	1.15
	R	0.48	0.65	0.80	0.64	0.30	0.38
Fenoprofen	k_I	3.81	4.79	5.27	5.50	4.47	3.81
	α	1.00	1.00	1.00	1.00	1.00	1.00
	R	0.00	0.00	0.00	0.00	0.00	0.00
Carprofen	k_I	10.80	15.27	18.79	20.15	15.58	11.93
	α	1.08	1.09	1.08	1.09	1.00	1.00
	R	0.44	0.47	0.50	0.40	0.00	0.00
Flurbiprofen	k_I	4.84	6.42	7.37	7.54	6.62	5.62
	α	1.05	1.08	1.16	1.16	1.28	1.34
	R	0.27	0.55	0.78	1.17	1.03	1.06
Ketoprofen	k_I	4.25	5.14	6.54	6.70	4.94	4.13
	α	1.00	1.00	1.00	1.00	1.15	1.19
	R	0.00	0.00	0.00	0.00	0.53	0.57
Suprofen	k_I	4.99	6.53	8.23	8.01	6.90	6.06
	α	1.07	1.10	1.17	1.18	1.26	1.28
	R	0.36	0.54	1.05	1.11	0.95	0.90
Flobufen	k_I	6.30	7.82	10.64	9.47	7.03	4.71
	α	1.05	1.07	1.07	1.09	1.03	1.00
	R	0.28	0.33	0.29	0.48	0.12	0.00

The selectivities slightly increased in the whole range of tested pH of the buffer and enantioresolution was improved with increasing buffer pH up to pH 4.0 or 4.5 (except of fenoprofen) and then it decreased again towards pH 6.0. The influence of pH of the TEAA buffer on retention and chiral resolution is demonstrated for ibuprofen in Fig. 3. The highest enantiomeric resolution of the individual profens was achieved in the mobile phase 40/60 (v/v) methanol/1.0% TEAA buffer, pH 4.0, for indoprofen and carprofen or pH 4.5 for indoprofen, flurbiprofen, suprofen and flobufen. No partial enantioresolution of fenoprofen was observed in any tested mobile phases. For illustration, the best enantioseparation achieved for flurbiprofen and suprofen is shown in Fig. 4.

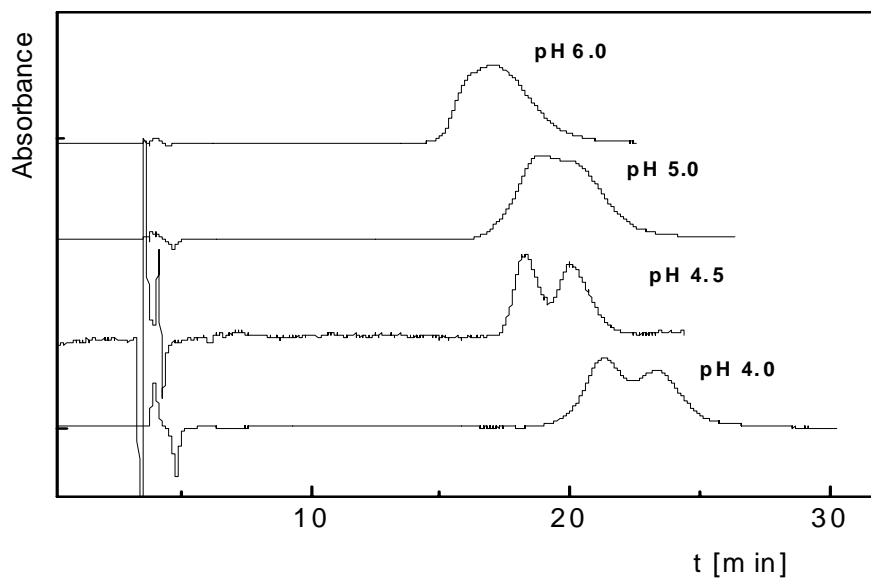


Fig. 3. Effect of the buffer pH on separation of ibuprofen.

Experimental conditions: TAG CSP; mobile phase - methanol/1.0% TEAA 40/60 (v/v).

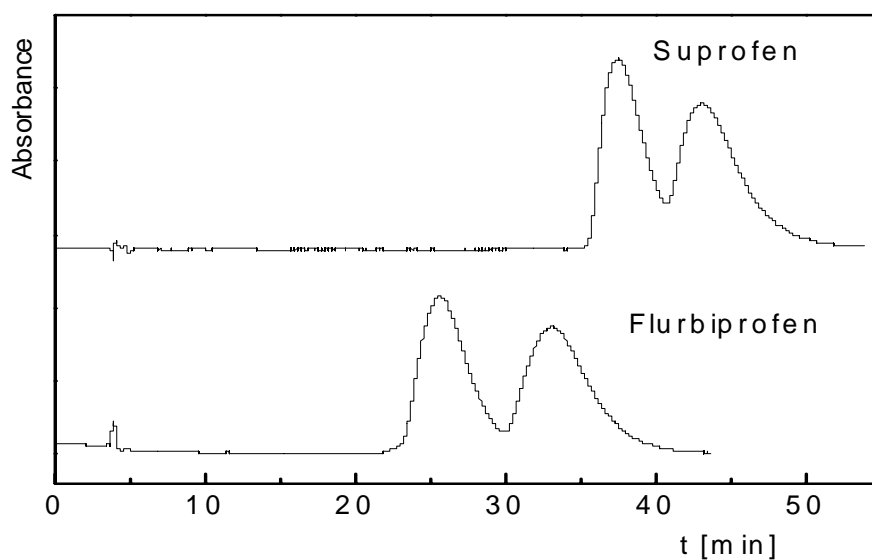


Fig. 4. Chromatograms of suprofen and flurbiprofen under the optimized separation conditions:

TAG CSP; mobile phase - methanol/1.0% TEAA 40/60 (v/v), pH 4.5.

4. Conclusion

Teicoplanin aglycone-based chiral stationary phase proved to be suitable for enantioseparation of selected profen non-steroidal anti-inflammatory drugs. Lower methanol content (40 % vol.) and higher concentration of TEAA buffer (1.0%) in the mobile phase were essential for enantioselective interactions of the studied profen NSAIDs. Significant influence of pH on retention and chiral resolution was observed. The highest values of enantioresolution were achieved at buffer pH 4.0 or 4.5.

Acknowledgement

The authors acknowledge financial support of the Ministry of Education, Youth and Physical Training of the Czech Republic and GAUK No. 63307.

References

1. Chirobiotic Handbook, Advanced Separation Technology, Whippany, NY, USA, 2006.
2. Alcaro S.; D'Acquarica I.; Gasparini F.; Misiti D.; Pierini M.; Villani C.: *Asymmetry* **13** (2002) 69-75.
3. Dannhardt G.; Kiefer W.: *Eur. J. Med. Chem.* **36** (2001) 109-126.
4. Riering H.; Sieber M.: *J. Chromatogr. A* **728** (1996) 171-177.
5. Gyllenhaal O.; Stefansson M.: *Chirality* **17** (2005) 257-265.
6. Olšovská J.; Flieger M.; Bachechi F.; Messina A.; Sinibaldi M.: *Chirality* **11** (1999) 291-300.
7. Bosáková Z.; Cuřínová E.; Tesařová E.: *J. Chromatogr. A* **1088** (2005) 94-103.
8. Kafková B.; Bosáková Z.; Tesařová E.: *J. Chromatogr. A* **1088** (2005) 82-93.

**STUDY OF THE INFLUENCE OF EXPERIMENTAL CONDITIONS
ON THE RETENTION AND ENANTIOSEPARATION OF SERIES OF
NEWLY SYNTHESIZED DISUBSTITUTED BINAPHTHYLS**

Lucie Loukotková^a, Zuzana Bosáková^a and Eva Tesařová^b

^a Department of Analytical Chemistry, Faculty of Science, Charles University, Albertov 8, 128 40 Prague 2, Czech Republic

^b Department of Physical and Macromolecular Chemistry, Faculty of Science, Charles University Albertov 8, 128 40 Prague 2, Czech Republic

Abstract:

Two chiral stationary phases (CSPs) based on β -cyclodextrin (β -CD) and hydroxypropyl- β -cyclodextrin (HP- β -CD) were used for study of the retention and separation of newly synthesized chiral 2,2'-disubstituted 1,1'-binaphthyls and 8,3'-disubstituted 1,2'-binaphthyls. Normal and reverse-phase separation modes were tested with both CSPs. HP- β -CD CSP in normal phase mode was proved to be suitable for separation of various mixtures of binaphthyl derivatives but no enantioresolution was achieved. Reversed phase separation mode utilizing the same CSP provided partial or even baseline enantioseparation of 8,3'-disubstituted 1,2'-binaphthyls. The retention mechanism was proved to be independent on temperature.

Keywords:

HPLC, chiral separation, beta-cyclodextrin based chiral stationary phases, disubstituted binaphthyls

Introduction:

In the last decades, a lot of stereoselective reactions, which allow preparing chiral compounds with high enantiomeric purity, have been discovered. Pure enantiomers of various chemical compounds are widely used in different branches of pharmacy, medicine, organic chemistry and other scientific disciplines.

Generally, two methods can be used for preparation of optically pure or enriched compounds. The first approach is based on a synthesis of racemic mixture that is subsequently transformed to diastereoisomers, which can be resolved into enantiomers via distillation, crystallisation, enzymatically or by other methods. The second approach is a direct synthesis of enantiomers, using suitable enantiomers of catalysts (ligands). This type of synthesis is called asymmetric synthesis. Compounds potentially usable as chiral ligands in asymmetric reactions must have sufficiently stable configuration, it means that they must be resistant towards racemization.

2,2'-substituted 1,1'-binaphthyls belong to the group of important chiral catalysts which have played a major role in the development of asymmetric synthesis [1, 2]. This type of chiral compounds does not possess an asymmetric carbon atom but an axis of chirality. The common feature of 1, 1'-binaphthyl is the chiral axis connecting individual naphthyl rings which creates a chiral cavity. This type of chirality is called atropisomerism and is caused by restricted rotation of atoms or groups of atoms around single bond at the binaphthyl skeleton [3].

Whilst the classical first generation of disubstituted binaphthyls possessed identical substituents (e.g. 2,2'-dihydroxy 1,1'-binaphthyl (BINOL), 2,2'-diamino-1,1'-binaphthyl (BINAM) and 2,2'-bis(diphenylphosphino)-1,1'-binaphthyl (BINAP)), development of new catalysts is characterized by non-identical groups in different positions [4, 6] and also a shift of the classical 1,1'-chiral axis into other positions is tested. The effort in molecular architecture of these ligands is oriented to create a stable chiral environment providing the high degree of enantioselectivity.

High-performance liquid chromatography with chiral stationary phase has been proved to be a suitable technique for determination of optical purity of synthesized asymmetric ligands. Some disubstituted binaphthyl derivatives were resolved into enantiomers on chiral stationary phases based on cellulose and its derivatives [4]. A previous adjustment of the binaphthyl structure is needed sometimes [5]. Chiral stationary phases based on binaphthyls were also prepared and employed for enantioseparations of other binaphthyl derivatives [1].

The type of CSP and mobile phase composition strongly affect the retention and enantioseparation behaviour of optically active

compounds. Another important factor influencing retention and chiral separation is temperature. Moreover, enantiomers can undergo interconversion that is strongly affected by temperature. There are several theories describing determination of the enantiomerization barrier such as Eyring's model [7, 8, 9]. Construction of van't Hoff plots [10] ($\ln k$ vs $1/T$) leads to a simple prediction whether the retention and enantioseparation mechanism is temperature dependent or not. The retention mechanism is independent on temperature when the van't Hoff plots are linear. Comparable slopes of the van't Hoff plots indicate that the enantioseparation selectivity is not temperature dependent.

The aim of this work is to find a suitable system for separation of series of newly synthesized 2, 2'-substituted 1,1'-binaphthyls and 8,3'-substituted 1,2'-binaphthyls. Various experimental conditions (e.g. type of β -cyclodextrin based CSPs, mobile phase composition and temperature) are tested. Dependency of the retention mechanism and system selectivity on temperature is also examined.

Experimental:

Reagents:

Methanol, propan-2-ol, *n*-hexane, triethylamine and acetonitril were purchased from Sigma-Aldrich (St. Louis, MO, USA), each HPLC grade. Glacial acetic acid was purchased from Lachema (Brno, Czech republic). Deionised water was used throughout the experiments (Milli-Q water purification system Millipore, Milford, MA, USA).

All the studied analytes (Fig. 1) have been synthesized as racemates at the Department of Organic Chemistry, Faculty of Sciences, Charles University in Prague. The structure of the derivatives has been confirmed by ^1H NMR, ^{13}C NMR, MS, HRMS and by UV spectrophotometry [11, 12].

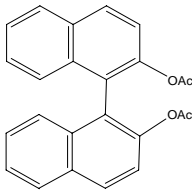
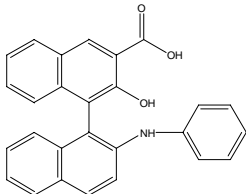
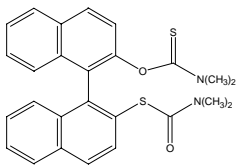
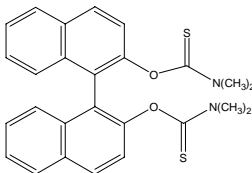
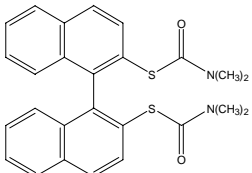
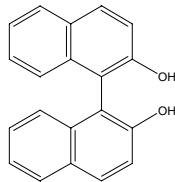
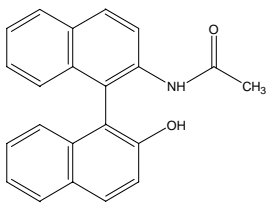
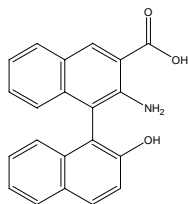
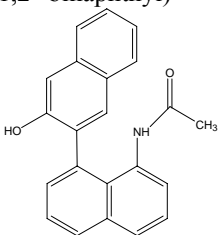
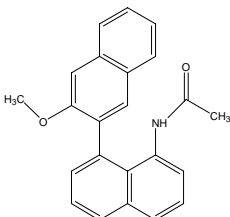
<p>Sample 1 2,2'-diacetoxy-1,1'-binaphthyl (OBIN diAc)</p> 	<p>Sample 2 3-carboxy-2-hydroxy-2'-naphthylamide-1,1'-binaphthyl (3-COOH-2-OH-2'-NH(C₆H₅)-1,1'-binaphthyl)</p> 
<p>Sample 3 2-(N,N-dimethylthiocarbamoyloxy)-2'-(N,N-dimethylcarbamoylthio)-1,1'-binaphthyl (2-OCSN(Me)₂-2'-SCON(Me)₂-1,1'-binaphthyl)</p> 	<p>Sample 4 2,2'-bis(N,N-dimethylthiocarbamoyloxy)-1,1'-binaphthyl (2-OCSN(Me)₂-2'-OCSN(Me)₂-1,1'-binaphthyl)</p> 
<p>Sample 5 2,2'-bis(N,N-dimethylcarbamoylthio)-1,1'-binaphthyl (2-SCON(Me)₂-2'-SCON(Me)₂-1,1'-binaphthyl)</p> 	<p>Sample 6 2,2'-dihydroxy-1,1'-binaphthyl (OBIN, BINOL, BINAFTOL)</p> 
<p>Sample 7 2-acetylamid-2'-hydroxy-1,1'-binaphthyl (2-NHAc-2'-OH-1,1'-binaphthyl)</p> 	<p>Sample 8 3-carboxy-2-amino-2'-hydroxy-1,1'-binaphthyl (3-COOH-2-NH₂-2'-OH-1,1'-binaphthyl)</p> 
<p>Sample 9 8-acetylamino-3'-hydroxy-1,2'-binaphthyl (8-NHAc-3'-OH-1,2'-binaphthyl)</p> 	<p>Sample 10 8-acetylamino-3'-methoxy-1,2'-binaphthyl (8-NHAc-3'-OMe-1,2'-binaphthyl)</p> 

Figure 1: Structure of the studied newly synthesized binaphthyls

Instrumentation:

The HPLC equipment (Pye Unicam, Cambridge, UK) comprised a PU 4015 pump, an UV detector type PU 4020 and a Rheodyne injection valve Model 7725i (Cotati, CA, USA) with a 20 μ L sample loop. The samples were injected with Hamilton syringe (Reno, Nevada, USA). Signal was exquisted and data were handled with the PC CSW 32 Software.

Temperature was controlled using a Mistral column thermostat Model Spark (Mistral, The Netherlands). Ultrasound bath Ultrasonic LC 30H (Germany) served for degassing the mobile phases. The buffer pH was adjusted with pH-meter Model 3510 purchased from Jenway (UK).

Two commercially available steel columns were purchased by ASTEC (Whippany, NY, USA):

Cyclobond I 2000 (250 \times 4.6 mm I.D., β -cyclodextrin bonded to silica gel, particle size 5 μ m)

Cyclobond I 2000 RSP (250 \times 4.6 mm I.D., hydroxypropyl- β -cyclodextrin bonded to silica gel, particle size 5 μ m).

Separation conditions:

Normal separation mode: Mobile phases consisted of *n*-hexane and propan-2-ol in various volume ratios.

Reversed-phase separation mode: The mobile phases contained water or 0.5% triethylamine acetate (TEAA) buffer, pH 3.0 or 6.0, and methanol (MeOH) or acetonitrile (ACN) as the organic modifiers. The buffer pH was adjusted with acetic acid to the required value before the organic modifier was added. The amount of organic modifiers present in the mobile phase was varied. Pure methanol and acetonitrile were also used as the mobile phases.

2,2'-disubstituted 1,1'-binaphthyls were diluted in methanol, 8,3'-disubstituted 1,2'-binaphthyls in acetonitrile and concentrations of the injected solutions were 0.5 mg/mL. The samples were stored at 5 °C.

The mobile phase flow rate was 0.7 mL/min.

Detection was performed at the wavelength of 254 nm.

The measurements were carried out at temperatures ranging from 5°C to 40°C.

Results and discussion:

Separation on β -cyclodextrin – bonded CSP

The enantioseparation was carried out in two separation modes – normal and reverse-phase. The molecules of substituted binaphthyls have a non-polar character so for that reason the normal separation mode was used as the first choice. The mobile phases consisted of *n*-hexane/propan-2-ol in various volume ratios. As the amount of *n*-hexane in mobile phase increased, retention of the analytes increased too, but no enantioseparation was observed (results not shown).

The reverse-phase separation mode was carried out in binary mobile phases consisted of organic modifier (ACN, MeOH) and water. Water was later replaced by triethylamine acetate buffer of two different pH values – 3.0 and 6.0.

When acetonitrile was used as the organic modifier all the analytes eluted in death time, while in the mobile phase containing methanol as organic modifier better results were observed.

High amount of methanol (50 - 100 vol. %) in mobile phases led to short retention times with no enantioseparation. As the amount of methanol decreased, the analytes were more retained and the enantioseparation was observed in some cases. The appropriate mobile phase composition was proved to be MeOH/water 30/70 (v/v) in which all the analytes eluted with retention times ranging from 6 to 12 minutes, except of 3-COOH-2-OH-2'-NH (C₆H₅)-1,1'-binaphthyl (sample 2 in Fig. 1) which had the retention time 119 minutes. This long retention indicates a strong interaction between the naphthyl substitution group and the cavity of chiral selector – β -cyclodextrin. Just one representative of the group of 2,2'-substituted 1,1'-binaphthyls, OBIN diAc, was partly separated into enantiomers with the resolution value $R = 0.5$.

The best resolution of 8,3'-substituted-1,2'-binaphthyls was achieved in mobile phases consisted of MeOH/water 20/80 (v/v) and 30/70 (v/v) for 8-NHAc-3'-OH-1,2'-binaphthyl and 8-NHAc-3'-OMe-1,2'-binaphthyl, respectively. The measured data are shown in Table 1.

Table 1: Retention parameters of binaphthyl derivatives separated on Cyclobond I 2000 column

mobile phase MeOH/water, flow rate 0.7 mL/min and detection wavelength 254 nm.

MeOH/H ₂ O (v/v)	20/80			30/70		
	<i>k</i> ₁	<i>R</i>	α	<i>k</i> ₁	<i>R</i>	α
OBIN diAc	2.9	0.5	1.2	0.8	0.2	1.1
8-NHAc-3'-OH-1,2'-binaphthyl	2.1	2.2	1.3	1.1	0.4	1.2
8-NHAc-3'-OMe-1,2'-binaphthyl	2.5	0.5	1.3	1.1	0.9	1.1

As shown in Table 2, mobile phase pH affected the elution time significantly. Replacement of water for 0.5% triethylamine acetate buffer, pH 3.0, provided considerable retention decrease which indicates more effective reduction of silanophyl interactions between analyte and silica gel. These interactions are characteristic for this type of chiral column. Higher pH led also to shorter retention times in comparison with the mobile phase consisted of MeOH and water. The peak symmetry, resolution and efficiency were not affected by the change of the mobile phase composition.

Table 2: Retention factors of the studied compounds obtained on Cyclobond I 2000 columnmobile phase 20/80 (v/v) MeOH/H₂O and 20/80 (v/v) MeOH/0.5% TEAA, pH 3.0 or 6.0, flow rate 0.7 ml/min and detection wavelength 254 nm.

Sample	MeOH/H ₂ O	MeOH/0.5% TEAA	
	<i>k</i>	pH 3.0 <i>k</i>	pH 6.0 <i>k</i>
OBIN diAc	2.9	0.3	1.9
3-COOH-2-OH-2'-NH(C ₆ H ₅)-1,1'-binaphthyl	-	2.9	14.2
2-OCSN(Me) ₂ -2'-SCON(Me) ₂ -1,1'-binaphthyl	7.8	0.5	3.8
2-OCSN(Me) ₂ -2'-OCSN(Me) ₂ -1,1'-binaphthyl	10.1	0.5	4.7
2-SCON(Me) ₂ -2'-SCON(Me) ₂ -1,1'-binaphthyl	8.5	0.7	4.3
OBIN	2.4	1.2	4.3
2-NHAc-2'-OH-1,1'-binaphthyl	1.5	0.2	0.8
3-COOH-2-NH ₂ -2'-OH-1,1'-binaphthyl	24.4	0.4	2.3
8-NHAc-3'-OH-1,2'-binaphthyl	2.2	2.1	2.7
8-NHAc-3'-OMe-1,2'-binaphthyl	2.9	2.7	2.6

^ Analyte did not eluted in 150 minutes

Separation on hydroxypropyl- β -cyclodextrin – bonded CSP

As the results have shown, the chiral stationary phase based on β -cyclodextrin is not effective for the enantioseparations of the studied compounds. Strong inclusion complexes are probably formed in reverse-phase separation mode in the binary mobile phase consisted of methanol and low water amounts, but this interaction does not have any stereodiscriminative character. In further experiments hydroxypropyl- β -cyclodextrin was used as a chiral selector. The hydroxyl group is bonded to the second carbon atom in the glucose structure and in this way the molecule of the substituted cyclodextrin is enlarged and offers more other interaction possibilities for the analytes (steric repulsions, hydrogen bonds).

Normal separation mode

Firstly the normal separation mode was studied but no enantioseparation occurred. The retention factors acquired with β -CD CSP were lower than these obtained with HP- β -CD CSP, whereas the asymmetry values were proved to be better on the latter column. Non-chiral separations of binaphthyl mixtures can be applied in normal separation mode, because mixtures of binaphthyl derivatives can occur during the process of asymmetric synthesis as the required derivative accompanied by some side products. Results of the analysis of these mixtures could be helpful for planning the following steps of the synthesis.

Reverse-phase separation mode

The mobile phases composed of acetonitrile and water provided very short retention times and no enantioseparation was observed on β -cyclodextrin-based column, so this mobile phase type was not employed on HP- β -CD CSP. Thus the binary mobile phase contained methanol and water, where the percentage of methanol was in the range of 30 - 40% (Table 3). The higher amount of MeOH in mobile phase, the faster was the elution and the enantioseparation was suppressed. The retention gained on the derivatized β -CD column was in most cases higher than the retention on β -CD based CSP. In the case of 3-COOH-2-OH-2'-NH(C₆H₅)-1,1'-binaphthyl the retention time on β -CD CSP was

almost two times shorter. This short retention might be caused by the mutual steric effects of the cyclodextrin cavity and the analyte which do not allow sufficient inclusion interaction. In spite of the higher retention and better values of asymmetry, the experiments carried out on hydroxypropyl- β -cyclodextrin column did not lead to enantioseparation of all the studied analytes. OBIN diAc as the representative of the group of disubstituted 1,1'-binaphthyls was separated in 23 minutes with resolution value $R = 1.0$.

Table 3: Retention parameters of the studied compounds obtained on Cyclobond I 2000 RSP column

mobile phase MeOH/water, flow rate 0.7 ml/min and detection wavelength 254 nm.

MeOH/H ₂ O (v/v)	30/70			35/65			40/60		
	k_1	$R_{1,2}$	$\alpha_{1,2}$	k_1	$R_{1,2}$	$\alpha_{1,2}$	k_1	$R_{1,2}$	$\alpha_{1,2}$
OBIN diAc	2.8	0.7	1.2	1.4	0.5	1.2	1.2	0.4	1.1
3-COOH-2-OH-2'-NH(C ₆ H ₅)-1,1'-binaphthyl	3.0	1.0	1.4	4.0	0.1	1.1	4.0	0.4	1.1
2-OCSN(Me) ₂ -2'-SCON(Me) ₂ -1,1'-binaphthyl	10.8	0.2	1.1	4.8	-	1.0	2.1	-	1.0
2-OCSN(Me) ₂ -2'-OCSN(Me) ₂ -1,1'-binaphthyl	8.6	-	1.0	4.2	-	1.0	2.0	-	1.0
2-SCON(Me) ₂ -2'-SCON(Me) ₂ -1,1'-binaphthyl	7.6	-	1.0	3.6	-	1.0	1.8	-	1.0
OBIN	4.0	0.8	1.4	3.1	-	1.0	1.9	-	1.0
2-NHAc-2'-OH-1,1'-binaphthyl	2.5	-	1.0	1.6	-	1.0	0.99	-	1.0
3-COOH-2-NH ₂ -2'-OH-1,1'-binaphthyl	1.8	-	1.0	0.75	-	1.0	1.2	-	1.0
8-NHAc-3'-OH-1,2'-binaphthyl	3.4	1.9	1.6	1.8	0.9	1.6	1.2	0.8	1.5
8-NHAc-3'-OMe-1,2'-binaphthyl	4.0	1.1	1.4	2.2	0.4	1.3	1.3	0.5	1.3

Both studied 8,3'-substituted 1,2'-binaphthyls were successfully separated into enantiomers in mobile phase consisted of MeOH/water 30/70 (v/v) with the value of resolution $R = 1.9$ for 8-NHAc-3'-OH-1,2'-binaphthyl and $R = 1.1$ for 8-NHAc-3'-OMe-1,2'-binaphthyl. The analytes eluted in 23 minutes.

Triethylamine acetate buffer (pH 3.0 or 6.0) instead of water was studied also as the mobile phase constituent. The mobile phase composition 30/70 (v/v) MeOH/0.5% TEAA, pH 3.0, rendered higher resolution value in comparison with water for OBIN diAc with contemporary decrease of the asymmetry and the detector response. There was no change in enantiomeric behaviour for the other 1,1'-binaphthyls.

Most convenient pH for enantioseparation of 8-NHAc-3'-OH-1,2'-binaphthyl was 6.0 where the value of resolution was $R = 1.9$. The second representative, 8-NHAc-3'-OMe-1,2'-binaphthyl, had the resolution value $R = 1.5$ at pH 3.0. At pH 6.0 the asymmetry and the peak shape of this analyte were worsened as it is shown in Figure 2.

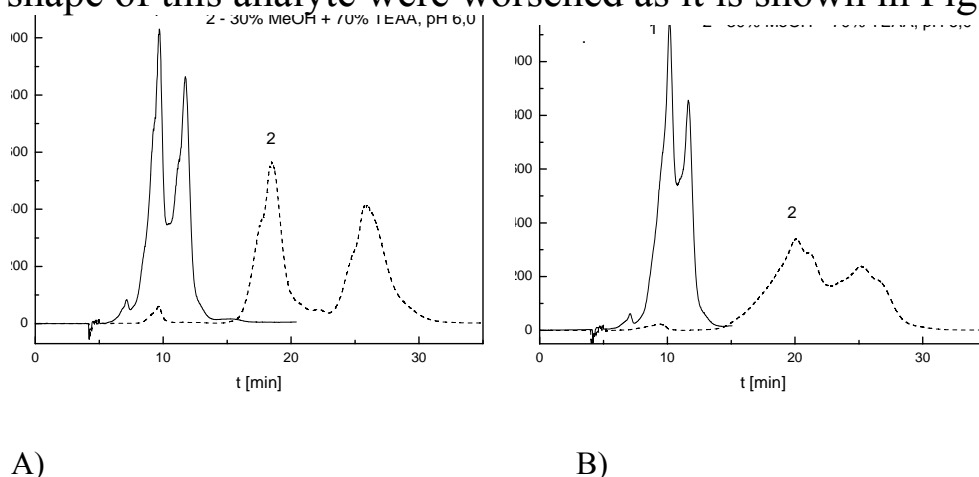


Figure 2: A) 8-NHAc-3'-OH-1,2'-binaphthyl: Cyclobond I 2000 RSP

mobile phase 30/70 (v/v) MeOH/TEAA, pH 3.0 and 6.0, flow rate 0.7 ml/min, UV detection at 254 nm.

B) 8-NHAc-3'-OMe-1,2'-binaphthyl: Cyclobond I 2000 RSP

mobile phase 30/70 (v/v) MeOH/TEAA, pH 3.0 and 6.0, flow rate 0.7 ml/min, UV detection at 254 nm.

Temperature effect

The HP- β -CD column was employed for temperature studies because of better peak symmetry and higher values of resolution which were obtained on this column in comparison with β -CD. The mobile phase consisted of MeOH/water 30/70 (v/v) was used because it was shown to be the most convenient mobile phase in the previous measurements. The temperature ranged from 5 to 40 °C.

Lower temperature yielded increased retention of the analytes but it did not improve the enantioseparation of OBIN diAc, 8-NHAc-3'-OH-1,2'-binaphthyl and 8-NHAc-3'-OMe-1,2'-binaphthyl. Same tendency in retention behaviour was noticed for OBIN diAc and both 8,3'-disubstituted 1,2'-binaphthyls. As the temperature decreased, the capacity factors became higher, the resolution enhanced, but the selectivity was not changed extensively.

Constructed van't Hoff plots were linear so independency of the retention mechanism on temperature was confirmed (Table 4).

Enantioselectivity of the separation system is a little dependent on temperature because the van't Hoff straight – lines plotted for individual enantiomers were not parallel.

Table 4: Parameters of the van't Hoff dependency ($\ln k$ on $1/T$).

Sample	Retention factor	Slope [K]	Regression coefficient
OBIN diAc	k_1	3059.5	0.9831
	k_2	3432.9	0.9898
8-NHAc-3'-OH-1,2'-binaphthyl	k_1	2600.5	0.9744
	k_2	3025.4	0.9839
8-NHAc-3'-OMe-1,2'-binaphthyl	k_1	2479.4	0.9447
	k_2	2845.0	0.9628

Conclusion:

β -cyclodextrin based chiral stationary phases did not provide sufficient enantioseparation ability for the studied analytes but these chiral selectors can be successfully used for separations of mixtures of these compounds produced during the synthesis process. The temperature studies confirmed the retention mechanism independency on temperature.

In future studies we will focus on finding an appropriate enantioseparation system for newly synthesized substituted binaphthyls using other chiral stationary phases.

Acknowledgments:

Financial support from the Ministry of Education, Youth and Physical Training of the Czech Republic and Grant Agency of Charles University (Project No. 59507) is gratefully acknowledged.

References:

1. S. Oi, M. Shijo, H. Tanaka and S. Miyano, *J. Chromatogr.*, **645** (1993) 17-28.
2. C. Rosini, L. Franzini, A. Raffaelli and P. Salvadori, *Synthesis*, (1992) 503.
3. M. L. Magri, N. vanthuynne, Ch. Roussel, M. B. García and L. R. Orelli, *J. Chromatogr. A*, **1069** (2005) 203-208
4. Š. Vyskočil, L. Meca, I. Tišlerová, I. Císařová, M. Polášek, S. R. Harutyunyan, Y. N. Belokon, R. M. J. Stead, L. Farrugia, S. C. Lockhart, W. L. Mitchell and P. Kočovský, *Chem. Eur. J.*, **8** (2002) 4633-4648
5. F. Toda, K. Yoshizawa, S. Hyoda, S. Toyota and S. Chatziefthimiou, *Org. Biomol. Chem.* **2** (2004) 449-451
6. P. Kočovský, Š. Vyskočil and M. Smrčina, *Chem. Rev.*, **103** (2003) 3213-3245
7. O. Trapp, G. Schoetz and V. Schurig, *Chirality* **13** (2001) 403-414
8. M. Jung and V. Schurig, *J. Am. Chem. Soc.* **114** (1992) 529-534
9. R. A. Keller, J.C. Giddings, *J. Chromatogr.*, **3** (1960) 205-220
10. E. Tesařová, Z. Bosáková, *Chem. Anal. (Warsaw)* **48** (2003) 439
11. Meca, L.: Diplomová práce, Univerzita Karlova v Praze, Přírodovědecká fakulta, Praha, 2000
12. Smrčina, M.: Kandidátská práce, Univerzita Karlova v Praze, Přírodovědecká fakulta, Praha, 1991

HPLC-ED DETERMINATION OF AMINONITROPHENOLS

Hana Dejmková, Jiří Zima , Jiří Barek

Charles University in Prague, Faculty of Science, Department of Analytical Chemistry,
UNESCO Laboratory of Environmental Electrochemistry, Hlavova 2030, 12843 Prague 2,
Czech Republic; e-mail: hdejmкова@seznam.cz

Abstract

RP-HPLC method with UV spectrophotometric detection and amperometric detection based on glassy carbon paste electrode detector was developed for the determination of 2-amino-3-nitrophenol, 2-amino-4-nitrophenol, 2-amino-5-nitrophenol, 4-amino-2-nitrophenol and 4-amino-3-nitrophenol. Methanol and phosphate buffer pH 8 were used as a mobile phase with methanol content varying from 45 % to 65 % (v/v) according to the gradient programme. Potential +0.4 V was used for electrochemical detection. The sensitivity of both kinds of detection is comparable with limits of detection around $1 \cdot 10^{-8} \text{ mol} \cdot \text{L}^{-1}$.

Keywords

HPLC-ED, aminonitrophenols, glassy carbon paste electrode

1 Introduction

The main usage of aminonitrophenols used to be their inclusion in hair dyes, particularly for obtaining light and red tones. However, these substances are suspected mutagens and carcinogens^{1,2} and are also proven or suspected sensitizers, causing skin dermatitis³. This led to banning them in European Union⁴ and therefore, it's necessary to develop methods for their determination. Moreover, aminonitrophenols are metabolites of dinitrophenols, chemicals used in dye industry, and they can serve as a marker to their exposition⁵.

HPLC with diode array detection is most often used^{6,7} but the presence of two oxidizable groups offers to employ electrochemical

detection and hence, to take advantage of its selectivity and sensitivity.

The advantages of carbon pastes are associated mainly with their broad potential window, low background current and ease of renewal of the working surface of the carbon paste electrode. Another advantage of this type of electrode is the possibility to employ it both for oxidation and reduction of organic substances. Last, but not least, their price is very reasonable⁸. The use of classical carbon paste electrodes in HPLC is rather limited as the organic modifiers of the mobile phases quickly degrade the paste. However, it was shown that pastes based on glassy carbon spherical microparticles are compatible with high contents of methanol and acetonitril in mobile phase⁹. The main drawback of carbon paste electrodes is lower repeatability of the measurements.

The aim of this work was to develop an HPLC method with electrochemical detection using carbon paste electrodes for the determination of 2-amino-3-nitrophenol, 2-amino-4-nitrophenol, 2-amino-5-nitrophenol, 4-amino-2-nitrophenol and 4-amino-3-nitrophenol.

2 Experimental

2.1 Chemicals

Studied substances were 2-amino-3-nitrophenol (2A3NP, CAS Number 603-85-0), 2-amino-4-nitrophenol (2A4NP, CAS Number 99-57-0), 2-amino-5-nitrophenol (2A5NP, CAS Number 121-88-0), 4-amino-2-nitrophenol (4A2NP, CAS Number 119-34-6), 4-amino-3-nitrophenol (4A3NP, CAS Number 610-81-1), all by Aldrich. The stock solutions ($c = 1 \cdot 10^{-3} \text{ mol} \cdot \text{L}^{-1}$) were prepared by dissolving the exact amount of the substances in methanol and were kept at laboratory temperature. It was observed spectrophotometrically, that the solutions are stable for at least three months.

Carbon paste electrode was prepared from 90 μL of mineral oil (Fluka) and 250 mg of spherical microparticles of glassy carbon with a diameter from 0.4 to 12 μm (Alfa Aesar, Germany).

Solutions of phosphate buffers were prepared from 0.01 $\text{mol} \cdot \text{L}^{-1}$ sodium dihydrogenphosphate. Its pH was adjusted to the desired value

by concentrated phosphoric acid or 0.2 mol·L⁻¹ sodium hydroxide (all Lachema Brno, Czech Republic). Other used chemicals were methanol (for HPLC, Chromservis, Czech Republic) and deionized water (Millipore).

2.2 Apparatus

An HPLC system consisted of degasser, high-pressure pump Beta 10, injector valve with 20 µL loop, Gemini 3µm C18 110A, 150 × 4.6 mm column (Phenomenex, USA) with chemically bonded C18 phase, UV/VIS detector Sapphire 800 (all Ecom, Czech Republic) and amperometric detector ADLC 2 (Laboratorní přístroje, Czech Republic) connected in series. The HPLC system was controlled via Clarity 2.3 software (DataApex, Czech Republic) working under Windows XP (Microsoft). The three-electrode wall-jet system was used for electrochemical detection with an Ag/AgCl (1 M KCl) reference electrode, a platinum wire auxiliary electrode and a glassy carbon paste working electrode adjusted against the outlet capillary at a controlled distance. The working electrode body was made from teflon with a 3 mm inner diameter. The surface of the electrode was renewed once a day by wiping out with wet filtration paper.

The pH measurements were performed with the combined glass electrode using 3510 pH Meter (Jenway, UK). The room temperature was kept throughout.

2.3 Procedures

Samples for injection were prepared by exact dilution of the stock solutions to contain the required concentration of the analyte in 50% methanol (v/v in water). The concentration of 1·10⁻⁴ mol·L⁻¹ was used for the optimization. During the optimization, only UV spectrophotometric detection was used. Detection wavelength 216 nm was selected from UV spectra of the analytes. 0.5 mL·min⁻¹ mobile phase flow rate was used throughout the measurements.

Calibration dependences were evaluated by least squares linear regression method. The detection limits were calculated as the concentration of an analyte which gave a signal three times the background noise ($S/N = 3$).

3 Results and Discussion

3.1 HPLC separation

The presence of both amino and hydroxy groups gives amphoteric character to aminonitrophenols and interesting behaviour can be expected both in acid and alkaline media and therefore, the column Gemini C-18 with stability in a wide range of pH was chosen.

The mobile phase consisted of methanol and 0.01 mol·L⁻¹ phosphate buffer to ensure sufficient conductivity for electrochemical detection. The first step of optimization of the composition of the mobile phase dealt with pH of the buffer; it was performed with 40% (V/V) methanol content, whose choice was based on earlier works⁶. The effect of pH in the value range from 2 to 9 on the retention times of the analytes is shown in Fig. 1. The compounds are not ionized between pH values 4 to 6, their retention times are almost constant and similar for 2A4NP, 2A5NP, 4A2NP and 4A3NP, on the other hand, 2A3NP elutes markedly later. For more acidic and alkaline pH, retention times generally lower because of polar groups ionization. The optimum resolution of the analytes was at pH 8 and therefore, this value was chosen for further study.

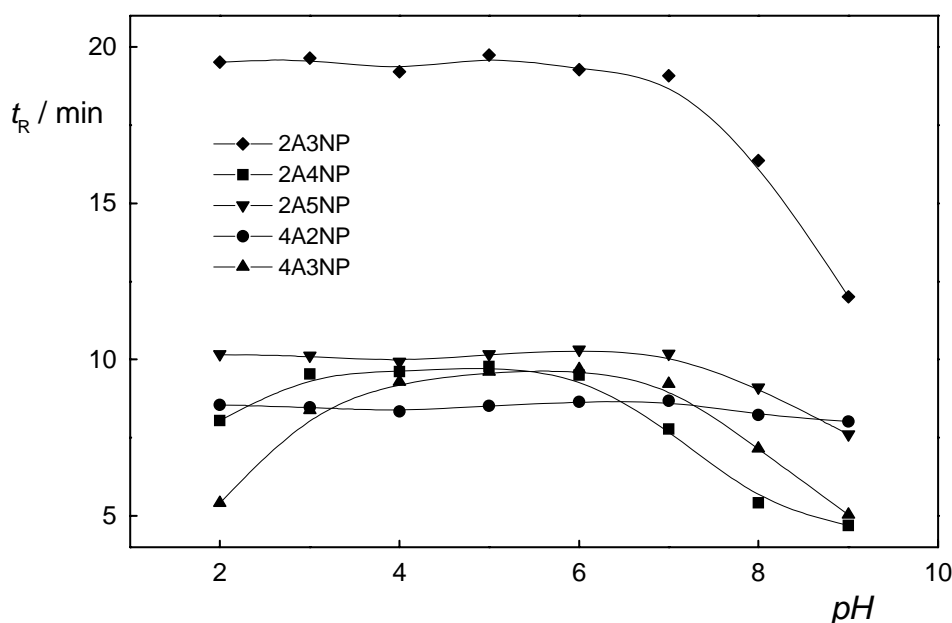


Fig. 1 Dependence of retention times of studied compounds on pH.

(Gemini 3 μ m C18 110A, 150 \times 4.6 mm column, 0.01 mol·L⁻¹ phosphate buffer:methanol = 60:40(v/v) mobile phase, injected 20 μ L of a solution with $c = 1 \cdot 10^{-4}$ mol·L⁻¹ of each analyte, $\lambda_{DET} = 216$ nm)

The next step was optimization of methanol content in the mobile phase. Good resolution of the peaks allowed to increase the content of methanol from 40 % to 45 % (v/v). However, there was still unsatisfactory long time of analysis caused by the high difference of retention time of 2A3NP and the other four compounds. To reduce it, gradient elution was employed. From the beginning of the analysis to 3.5 min, the methanol content was kept on 45 % (v/v), until 4.5 min it was linearly changed to 65 % and maintained on this concentration until the end of analysis in 11 min. Time of analysis decreased from earlier 13 min to 10.5 min.

3.2 Amperometric detection

To determine the optimal detection potential, hydrodynamic voltammograms were measured (Fig. 2). The substances are easily oxidizable and the response of the detector is stable within the range +0.4 to +0.9 V. For that reason, the potential of +0.4 V was chosen as optimal, because it grants not only a sufficient sensitivity, but also a high selectivity and a very low-noise baseline with the absence of drifting.

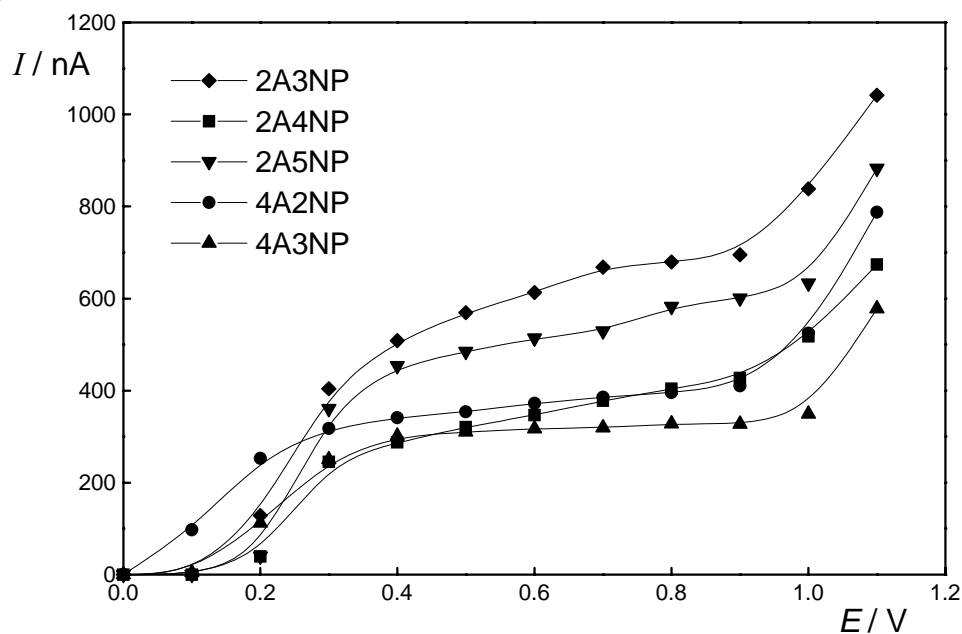


Fig. 2 Hydrodynamic voltammograms of 2A3NP, 2A4NP, 2A5NP, 4A2NP and 4A3NP

(Gemini 3 μ m C18 110A, 150 \times 4.6 mm column, 0.01 mol·L⁻¹ phosphate buffer:methanol = 60:40(v/v) mobile phase, injected 20 μ of a solution with $c = 1 \cdot 10^{-4}$ mol·L⁻¹ of each analyte)

The chromatograms obtained using spectrophotometric and electrochemical detection are shown in Fig 3.

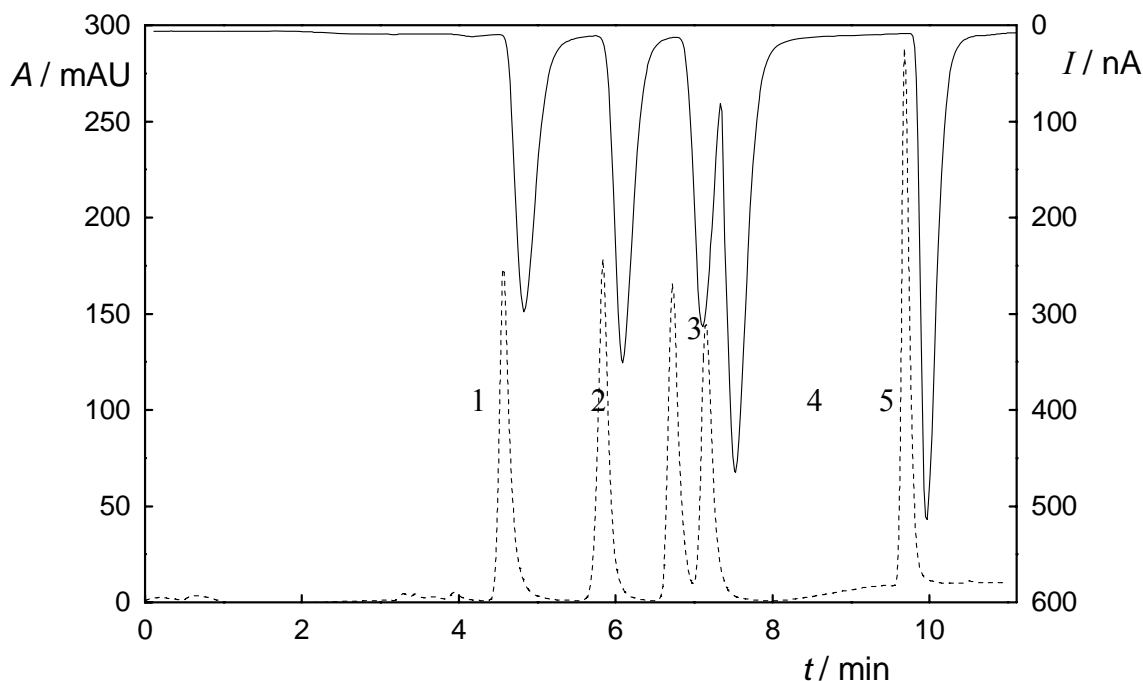


Fig. 3 Chromatograms of 2A3NP (5), 2A4NP (1), 2A5NP (4), 4A2NP (3) and 4A3NP (2) obtained using spectrophotometric (dashed) and electrochemical (solid line) detection

(Gemini 3 μ m C18 110A, 150 \times 4.6 mm column, 0.01 mol·L⁻¹ phosphate buffer:methanol = 60:40(v/v) mobile phase, injected 20 μ L of a solution with $c = 1 \cdot 10^{-4}$ mol·L⁻¹ of each analyte, $\lambda_{DET}=216$ nm, $E_{DET} = +0.4$ V)

3.3. Calibration dependences and detection limits

Under optimized conditions, calibration dependences for both spectrophotometric and electrochemical detection were measured. Limits of detection were determined as the concentration of an analyte which gave a signal three times the background noise. Results calculated from the peak heights are summarized in Table 1.

Table 1. Characteristics of calibration dependences of tested analytes calculated from the peak heights.

Analyte	Concentration range (mol·L ⁻¹)	Correlation coefficient	Limit of detection (mol·L ⁻¹)
Spectrophotometric detection			
2A3NP	4·10 ⁻⁸ - 1·10 ⁻⁵	0.9992	1.7·10 ⁻⁸
2A4NP	4·10 ⁻⁸ - 1·10 ⁻⁵	0.9987	1.6·10 ⁻⁸
2A5NP	4·10 ⁻⁸ - 1·10 ⁻⁵	0.9990	1.5·10 ⁻⁸
4A2NP	4·10 ⁻⁸ - 1·10 ⁻⁵	0,9991	1.6·10 ⁻⁸
4A3NP	4·10 ⁻⁸ - 1·10 ⁻⁵	0,9963	7.0·10 ⁻⁹
Electrochemical detection			
2A3NP	2·10 ⁻⁸ - 1·10 ⁻⁵	0.9977	1.1·10 ⁻⁸
2A4NP	2·10 ⁻⁸ - 1·10 ⁻⁵	0.9922	1.4·10 ⁻⁸
2A5NP	2·10 ⁻⁸ - 1·10 ⁻⁵	0.9990	1.2·10 ⁻⁸
4A2NP	2·10 ⁻⁸ - 1·10 ⁻⁵	0.9971	8.7·10 ⁻⁹
4A3NP	2·10 ⁻⁸ - 1·10 ⁻⁵	0.9944	8.6·10 ⁻⁹

The dependences are linear in the whole concentration range; the correlation coefficients show the electrochemical detection as slightly less precise. Sensitivity of both methods is similar with limits of detection reaching from 7.0·10⁻⁹ to 1.7·10⁻⁸ mol·L⁻¹ for spectrophotometric detection and from 8.6·10⁻⁹ to 1.4·10⁻⁸ mol·L⁻¹ for electrochemical detection. However, low selectivity of spectrophotometric detection causes baseline drifts and interferences, which complicate evaluation particularly at lower analyte concentrations (Fig. 4).

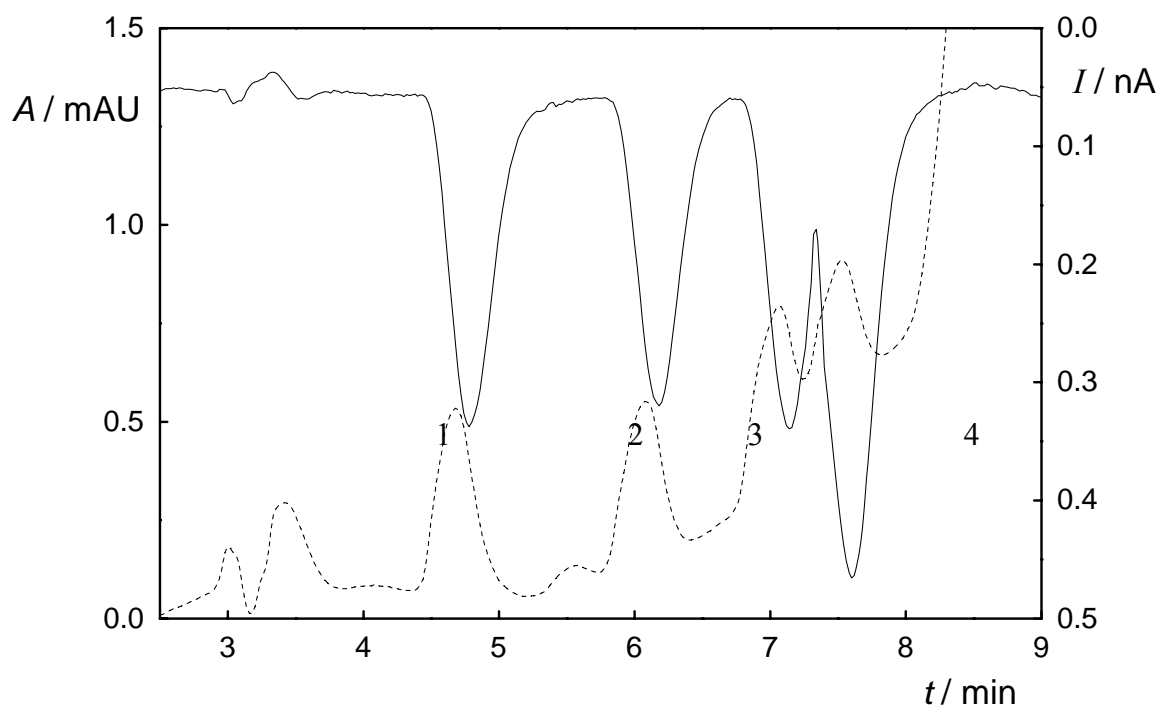


Fig. 4 Chromatograms of equimolar mixture of 2A4NP (1), 2A5NP (4), 4A2NP (3) and 4A3NP (2) of $c = 6 \cdot 10^{-7} \text{ mol} \cdot \text{L}^{-1}$ obtained using spectrophotometric (dashed) and electrochemical (solid line) detection

(Gemini $3 \mu\text{m}$ C18 110A, $150 \times 4.6 \text{ mm}$ column, $0.01 \text{ mol} \cdot \text{L}^{-1}$ phosphate buffer:methanol = 60:40(v/v) mobile phase, injected $20 \mu\text{L}$ of solution, $\lambda_{\text{DET}}=216 \text{ nm}$, $E_{\text{DET}} = +0.4 \text{ V}$)

4 Conclusion

RP-HPLC with electrochemical detection based on glassy carbon paste electrode detector can be used for determination of five isomers of aminonitrophenol. The sensitivity of electrochemical detection is comparable with UV spectrophotometric, reaching limit of detection around $1 \cdot 10^{-8} \text{ mol} \cdot \text{L}^{-1}$, but electrochemical detection offers higher selectivity.

Acknowledgement

This work was financially supported by the Grant Agency of the Czech Republic (project No. 203/04/0136) and the Czech Ministry of Education, Youth and Sports (projects No. LC 06035 and No. MSM0021620857).

References

- [1] Zahm, S.H.; Weisenburger, D.D.; Babbit, P.A.; Saal, R.C.; Vaught, J.B.; Blair, A.: *Am. J. Public Health* **82(7)** (1992) 990-997
- [2] <<http://monographs.iarc.fr/ENG/Classification/crthgr03list.php>> [cit. November, 14th, 2006].
- [3] Sorsted H.; Basketter D.A.; Estrada, E.; Johansen, J.D.; Patlewics, G.Y.: *Contact Dermatitis* **51** (2004), 241-254
- [4] Twenty-sixth Commission Directive 2002/34/EC of 15 April 2002 adapting to technical progress Annexes II, III and VII to Council Directive 76/768/EEC on the approximation of the laws of the Member States relating to cosmetic products.
- [5] Hayes, W.J., Jr.; Laws, E.R., Jr.: *Handbook of Pesticide Toxicology. Volume 3. Classes of Pesticide*. New York, Academic Press 1991, p. 1195
- [6] Wang, S.P.; Chen, H.J.: *J. Chromatogr. A* **979** (2002), 439-446
- [7] Nageswara, R. R.; Bhavani, T.; Husain, S.: *J. High Res. Chromatogr.* **18(7)** (1995), 449-451
- [8] Švancara, I.; Vytrás, K.; Barek, J.; Zima, J.: *Crit. Rev. Anal. Chem.* **31(4)** (2001), 311-345
- [9] Barek, J.; Muck, A.; Wang, J.; Zima, J.: *Sensors* **4** (2004), 47-57

DETERMINATION OF ACID-BASE DISSOCIATION CONSTANTS OF ACYCLIC NUCLEOSIDE PHOSPHONATES AND RELATED COMPOUNDS BY CAPILLARY ZONE ELECTROPHORESIS

Veronika Šolínová, Dušan Koval, Václav Kašička, Michal Česnek and Antonín Holý

Institute of Organic Chemistry and Biochemistry, Academy of Sciences of the Czech Republic, Flemingovo nám. 2, 166 10 Prague 6, Czech Republic, zimova@uochb.cas.cz

Abstract

Capillary zone electrophoresis (CZE) has been applied as an alternative method to traditional potentiometric and spectrophotometric titrations for determination of acid-base dissociation constants (pK_a) of ionogenic groups of amino- and (amino)guanidinopurine nucleotide analogues, such as acyclic nucleoside phosphonates and related compounds. These compounds bear characteristic pharmacophores contained in various important biologically active substances, such as cytostatics and antivirals. The knowledge of pK_a values of potentially new drugs is of great importance since from the pK_a values the occurrence of ionic forms of particular compounds at given pH of their water solution can be determined. The pK_a values of the ionogenic groups of the above compounds were determined by the nonlinear regression analysis of the experimentally measured pH dependence of effective electrophoretic mobility of these compounds. The effective electrophoretic mobility was measured by CZE performed in a series of background electrolytes in a broad pH range (3.50-11.25) and constant ionic strength (25 mM) and temperature (25°C). Dissociation constant of the protonated guanidinyll group was estimated to be in the range 8.29-10.32; pK_a of phosphonic acid to the second dissociation degree was found to be in the range 6.64-6.86, depending on the structure of the analyzed compounds.

Keywords:

Acyclic nucleoside phosphonates; Aminopurine nucleosides; Guanidinopurine nucleosides; Capillary electrophoresis; Dissociation constant (pK_a)

1 Introduction

The knowledge of physicochemical characteristics of new synthetic compounds, such as water solubility, lipophilicity and acid-base properties, is necessary when these compounds start to be tested as new drug candidates. The determination of these characteristics is an important step in the optimization stage of a new drug development project. Particularly, the acid-base dissociation constant (pK_a) is a key parameter for compounds containing at least one ionogenic (acidic or basic) functional group for understanding the passage of drugs into and across cell membranes, for estimation of the concentration of the individual ionic forms of the drug in blood, for assessment of reaction rate and for investigation of the biological uptake and metabolism mechanism. Moreover, the knowledge of pK_a values is important for prediction of the effective charge, effective electrophoretic mobility and migration order of the analytes in capillary zone electrophoresis (CZE), which has become a method of choice for determination of pK_a values [1]. In comparison with the traditional potentiometric and spectrophotometric titration methods, the particular advantage of CZE is that it allows working with a very small amount of sample (nanolitre applied sample volume per analysis) and knowledge of the analyte precise concentration is not necessary. In addition, the analyte need not to be perfectly pure, since its potential admixtures are separated during the analysis.

Newly synthesized amino and (amino)guanidino 9-alkylpurines [2, 3, 4] and their acyclic nucleoside phosphonates bear characteristic pharmacophores contained in various important biologically active substances, such as cytostatics and antivirals. The acid-base dissociation constants of selected acyclic nucleoside phosphonates, acyclic nucleoside phosphonate diesters and related compounds were determined in our recent paper [5]. The derivatives of 9-alkylpurines also show a broad spectrum of biological activity, they influence the metabolic pathway of cytokinins and cyclin-dependent kinases. 6-

Amino group plays an important role in purine derivatives, it is essential for substrate/inhibitor binding to diverse enzymes of purine metabolism as well as in important regulatory pathways. The inhibitors of the influenza virus neuramidinase, inhibitors of polyamine synthesis and the minor groove binding agent netropsin belong to the biologically active compounds bearing the guanidinyl group.

The aim of this work was to develop CZE method for determination of the thermodynamic dissociation constants (pK_a) of ionogenic groups of amino- and guanidinopurines and their analogues, particularly pK_a of the protonated guanidinyl group and pK_a of phosphonic acid to the second dissociation degree in acyclic nucleoside phosphonates of (amino)guanidino 9-alkylpurines (**1**, **2**, **3** and **4**), see Figure 1.

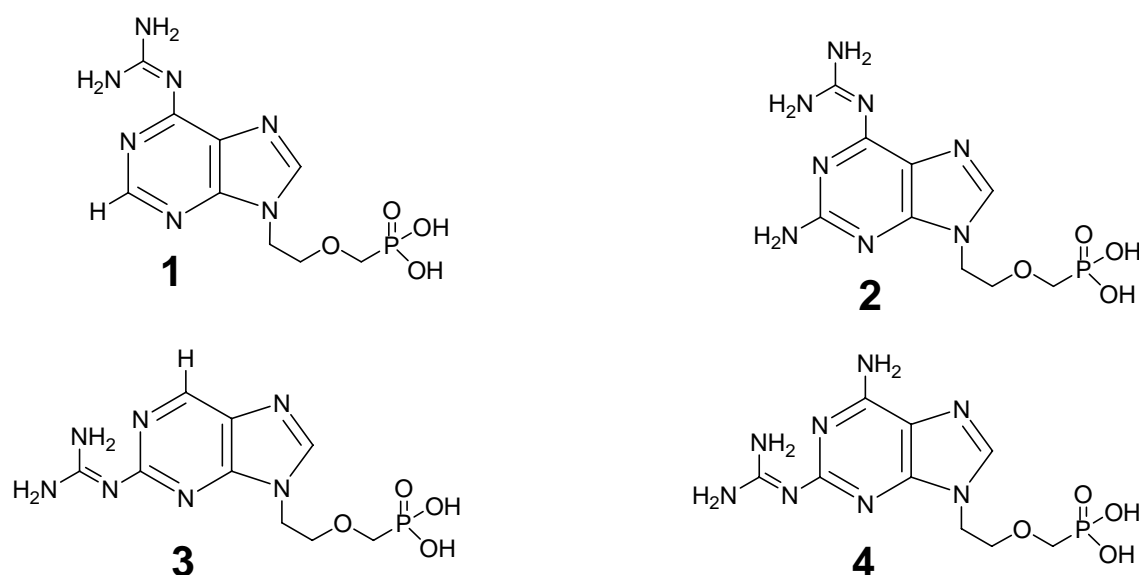


Figure 1 Molecular structures of acyclic nucleoside phosphonates of guanidino- and amino-guanidino 9-alkylpurines

2 Experimental

CZE analyses were carried out in the capillary electrophoretic analyzer P/ACE MDQ (Beckman Coulter, Fullerton, CA, USA) using the software 32 Karat System, version 7.0 for data acquisition and evaluation. The analyzer was equipped with the internally uncoated fused silica capillary with outer polyimide coating, total/effective length 394/292 mm, ID/OD 75/360 μm (Polymicro Technologies,

Phoenix, AR, USA). The analytes were detected by UV-Vis spectrophotometric photodiode array detector (190-600 nm) set to operate in the range 190-300 nm. Absorbance of analyzed compounds and of electroosmotic flow markers (DMSO or isophorone) was monitored at 225 nm and 250 nm, respectively. The analyses were performed at constant temperature of the BGE inside the capillary, 25°C. BGE solutions with pH values covering a broad pH range (3.50-11.25) with 0.25 pH unit increment were prepared by mixing the appropriate amounts of stock solutions listed in Table 1 and then diluted to the constant ionic strength 25 mmol/L.

Table 1 Composition of the stock solutions and pH range of the BGEs, applied separation voltage, *U*, and electric current, *I*, of the CZE analyses

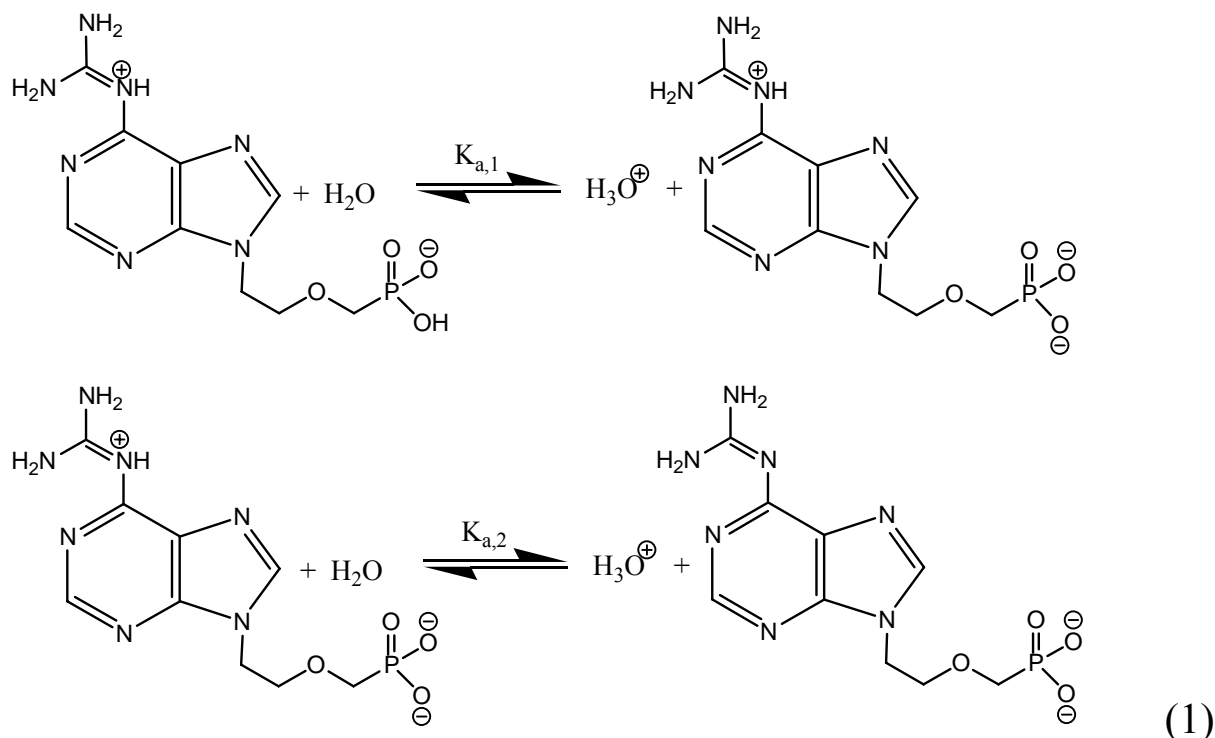
BGE number	Composition of stock solutions	pH range	<i>U</i> range (kV)	<i>I</i> range (μA)
BGE I-IV	0.95 M HCOOH, 0.7 M Tris	3.50-4.25	9.8-10.7	26.4-24.1
BGE V-X	1 M CH ₃ COOH, 1 M NaOH	4.25-5.50	8.6-10.6	30.0-24.4
BGE XI-XV	0.4 M MES, 1 M NaOH	5.50-6.50	11.0-11.5	24.8-23.4
BGE XVI-XX	0.4 M MOPS, 1 M NaOH	6.50-7.50	11.3-11.5	23.4-21.7
BGE XXI-XXVI	0.4 M Tricine, 1 M NaOH	7.50-8.75	11.1-12.3	23.1-19.7
BGE XXVII-XXXI	0.5 M CHES, 1 M NaOH	8.75-9.75	11.0-11.5	23.5-22.5
BGE XXXII-XXXVIII	0.4 M CAPS, 1 M NaOH	9.75-11.25	10.0-13.0	27.1-19.8

3 Theoretical

3.1 Acid-base equilibria of the acyclic nucleoside phosphonates of (amino)guanidino 9-alkylpurines

The acyclic nucleoside phosphonates of (amino)guanidino 9-alkylpurines behave as zwitterions with effective charge close to zero in acidic BGEs, where the positive charge of the protonated guanidinyll group is compensated by the negative charge of hydrogenphosphonate. With the increasing pH of the BGE the effective charge of these compounds is becoming negative due to the dissociation of hydrogenphosphonate (-1) to phosphonate (-2) at around neutral pH and due the deprotonation of the guanidinyll group at alkaline pH. Using 6-guanidino-9-[2-(phosphonomethoxy)ethyl]-

9*H*-purine (**1**) as a representative of these types of compounds, their dissociation equilibrium can be described as follows:



The corresponding thermodynamic dissociation constant ($K_{a,1}$) and mixed dissociation constant ($K_{a,1}^{mix}$) of phosphonic acid group to the second dissociation degree can be expressed as:

$$K_{a,1} = \frac{a_{H_3O^+} a_{A^{2-}BH^+}}{a_{HA^-BH^+}} = \frac{a_{H_3O^+} c_{A^{2-}BH^+} \gamma_{A^{2-}BH^+}}{c_{HA^-BH^+} \gamma_{HA^-BH^+}} = K_{a,1}^{mix} \gamma_{A^{2-}BH^+} \quad (2)$$

where $a_{HA^-BH^+}$, ($c_{HA^-BH^+}$) and $a_{A^{2-}BH^+}$, ($c_{A^{2-}BH^+}$) are activities (concentrations) of zwitterionic and single charged anionic forms of this type of analytes, respectively, and the activity coefficient of the zwitterion, $\gamma_{HA^-BH^+}$, is supposed to be unity.

The relation between thermodynamic and mixed dissociation constants can be expressed in the logarithmic form as:

$$pK_{a,1} = pK_{a,1}^{mix} - \log \gamma_{A^{2-}BH^+} \quad (3)$$

Thermodynamic and mixed dissociation constants of the dissociation of the protonated guanidinylic group, $K_{a,2}$ and $K_{a,2}^{mix}$, respectively, are defined as:

$$K_{a,2} = \frac{a_{H_3O^+} a_{A^{2-B}}}{a_{A^{2-BH^+}}} = \frac{a_{H_3O^+} c_{A^{2-B}} \gamma_{A^{2-B}}}{c_{A^{2-BH^+}} \gamma_{A^{2-BH^+}}} = \frac{K_{a,2}^{mix} \gamma_{A^{2-B}}}{\gamma_{A^{2-BH^+}}} \quad (4)$$

where $a_{A^{2-BH^+}}$, $(c_{A^{2-BH^+}})$ and $a_{A^{2-B}}$, $(c_{A^{2-B}})$ are activities (concentrations) of single charged and double charged anions of these type of analytes.

In the logarithmic form (and regarding the relationship $\log \gamma_{A^{2-B}} = 4 \log \gamma_{A^{2-BH^+}}$) the relation between thermodynamic and mixed dissociation constants can be expressed as:

$$pK_{a,2} = pK_{a,2}^{mix} - 3 \log \gamma_{A^{2-BH^+}} \quad (5)$$

The dependence of the effective mobility of these types of analytes on pH is given by Eq. (6):

$$m_{eff} = \frac{m_{A^{2-B}} 10^{pK_{a,2}^{mix} - pH} - m_{A^{2-BH^+}} 10^{pH - pK_{a,1}^{mix}}}{1 + 10^{pH - pK_{a,1}^{mix}} + 10^{pK_{a,2}^{mix} - pH}} \quad (6)$$

where $m_{A^{2-BH^+}}$ and $m_{A^{2-B}}$ are the actual ionic mobilities of the ionic forms A^{2-BH^+} and A^{2-B} , respectively.

4 Results and discussion

4.1 Selection of experimental conditions

For pK_a determination by CZE it is important to select experimental conditions in such a way that the measured effective mobilities are obtained as precisely and accurately as possible. As stated above, the actual ionic and effective mobilities depend on ionic strength and temperature. Consequently, the mobilities should be measured in the BGEs of constant ionic strength and at constant temperature. Measurements of effective mobilities in the pH range 3.50-11.25 allowed us to use the BGEs of constant ionic strength, 25 mM. The appropriate mixtures of the buffering anionic constituents with pK_a values close to pH of the BGE ($pH_{BGE} = pK_a \pm 0.7$) and strong cationic counterion (Tris for formic acid-based BGEs, pH 3.50-4.25, sodium for the other BGEs) were used for preparation of BGEs with this constant ionic strength and also with sufficient buffering capacity, see Table 1. The mobility measurement at constant temperature of 25°C was ensured by thermostating the outer polyimide capillary surface to constant temperature of 24°C and by

setting the input power to the value of 0.66 W per meter of the capillary length, which causes 1°C temperature increase inside the capillary, resulting in the constant temperature of 25°C inside the capillary.

4.2 Determination of thermodynamic dissociation constants

The calculation of mixed dissociation constants was accomplished by non-linear fitting of the sets of experimentally determined effective electrophoretic mobilities within a broad pH range using the computer program Origin with appropriate regression function, Eq. (6). The courses of this function for the zwitterionic to divalent anionic acyclic nucleoside phosphonates of (amino)guanidino 9-alkylpurines (1, 2, 3, 4) are depicted in Figure 2. The values of correlation coefficient, mixed dissociation constants and actual anionic mobilities of the individual ionic species of the analyzed compounds are presented in the text parts of the figures. Thermodynamic dissociation constants, pK_a , were recalculated from mixed dissociation constants using Eqs. (3) and (5) for dissociation of phosphonic acid group to the second degree and dissociation of protonated guanidinyll group, respectively. Thermodynamic pK_a of a phosphonic acid group to the second dissociation degree (-2) was found to be in the range 6.64-6.86 and pK_a of dissociation of protonated guanidinyll group was in the range 8.29-10.32. The values of thermodynamic pK_a with their standard deviations are presented in Table 2.

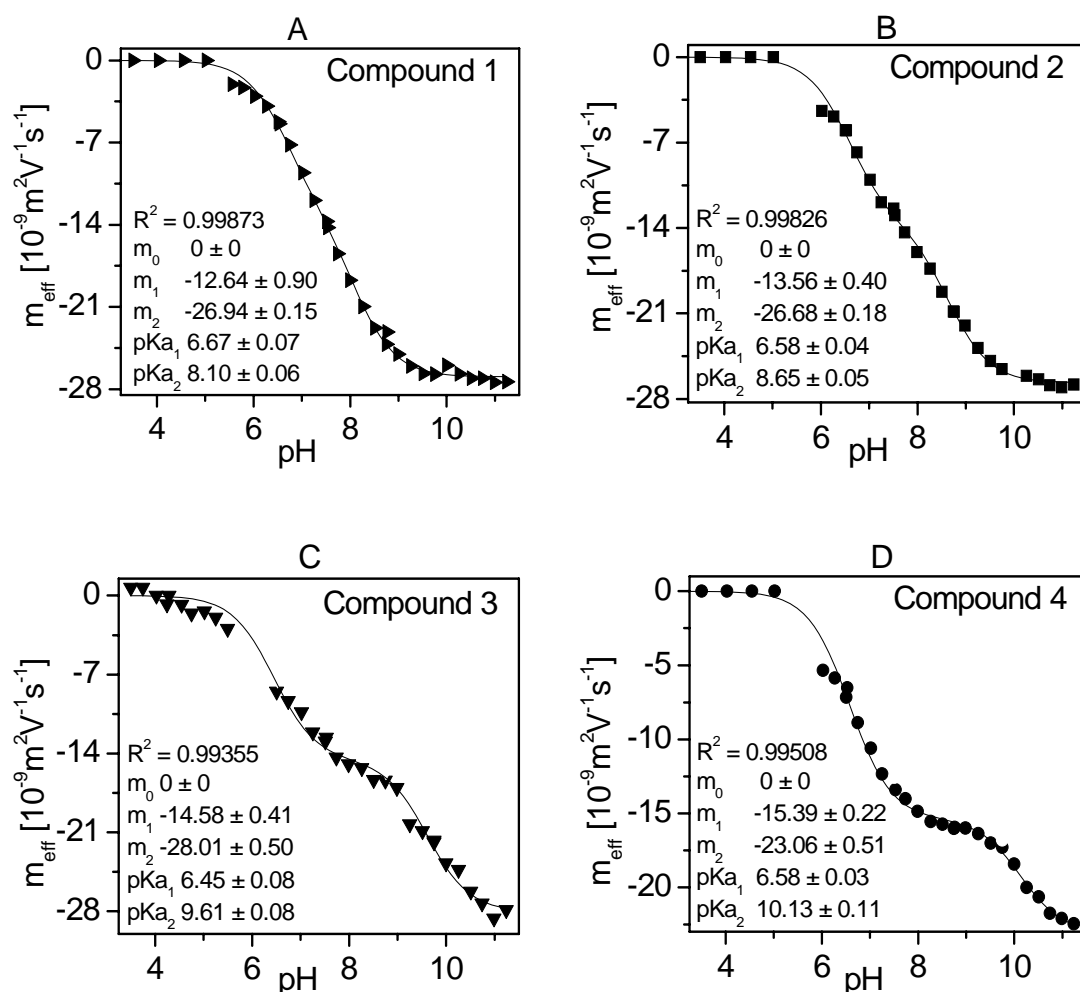


Figure 2 Dependencies of effective electrophoretic mobilities, m_{eff} , of acyclic nucleoside phosphonates of (amino)guanidino 9-alkylpurines on pH.

R , correlation coefficient; m , actual ionic mobility; pK_a , mixed dissociation constant.

From the results it is evident that basicity of the amino-guanidino derivatives is higher than that of the guanidino derivatives (ca by the 0.5 unit difference in pK_a), see the pairs 2 (pK_a 8.84) vs. 1 (pK_a 8.29) and 4 (pK_a 10.32) vs. 3 (pK_a 9.80).

Table 2 Thermodynamic pK_a values of ionogenic groups of analyzed compounds (at 25 °C)

Compound	pK_a	
	$P(OH)O^-/P(O)_2^{2-}$	$(G)H^+/(G)$
1	6.86 ± 0.06	8.29 ± 0.06
2	6.77 ± 0.04	8.84 ± 0.05
3	6.64 ± 0.08	9.80 ± 0.08
4	6.77 ± 0.03	10.32 ± 0.11

$P(OH)O^-/P(O)_2^{2-}$ – dissociation of phosphonic acid group to the second degree (-2);
 $(G)H^+/(G)$ – dissociation of protonated guanidinyll group

5 Conclusions

CZE has proved to be suitable and useful method for determination of dissociation constants (pK_a) of amino and (amino)guanidinopurine nucleotide analogues, such as acyclic nucleoside phosphonates and related compounds, in a microscale, applying only few nanoliter sample volumes of 0.1 mM analyte solution per analysis. The determination of pK_a values of series of the above related compounds allowed to quantify their basicity and to detect certain correlations between the basicity and the structure of these analytes.

Acknowledgements

The work was supported by gacr, grants no. 203/04/0098, 203/05/2539, 203/06/1044, and by research project z40550506 of ascr. It was performed within the frame of projects of the centre for new antivirals and antineoplastics id 1m0508 of the ministry of education, youth and sports of the czech republic.

References

- [1] Poole, S. K., Patel, S., Dehring, K., Workman, H., Poole, C. F., *J. Chromatogr. A* **1037** (2004), 445-454.
- [2] Česnek, M., Holý, A., Masojídková, M., *Tetrahedron* **58** (2002), 2985-2996.
- [3] Česnek, M., Holý, A., Masojídková, M., Zídek, Z., *Bioorg. Med. Chem.* **13** (2005), 2917-2926.
- [4] Česnek M., Masojídková M., Holý A., Šolínová V., Koval D., Kašička V., *Collect. Czech. Chem. Commun.* **71** (2006), 1303-1319.
- [5] Šolínová V., Koval D., Kašička V., Česnek M., Holý A.: *Electrophoresis* **27** (2006), 1006-1019.

As AND Se HYDRIDE TRAPPING AT THE QUARTZ SURFACE - A STEP FORWARD TO IN-SITU TRAPPING IN QUARTZ TUBE ATOMIZERS FOR AAS

Jan Kratzer^{a,b}, Jiří Dědina^a and Petr Rychlovský^b

^a Academy of Sciences of the Czech Republic, Institute of Analytical Chemistry, Public Research Institution, Vídeňská 1083, 142 20 Prague 4, Czech Republic

^b Charles University in Prague, Faculty of Science, Albertov 8, 128 40 Prague 2, Czech Rep.

Abstract

A novel quartz device has been designed to trap arsine and selenium hydride and subsequently to volatilize the collected analyte and atomize it for atomic absorption spectrometric detection. The device is actually the multiple microflame quartz-tube atomizer (multiatomizer) with inlet arm modified to serve as the trap and to accommodate the oxygen-delivery capillary used to combust hydrogen during the trapping step. The effect of relevant experimental conditions (trap temperature during trapping and hydrogen flow rate and trap temperature during volatilization) on collection and volatilization efficiency was investigated. Under the optimum conditions collection and volatilization efficiency for arsenic and selenium were 50 and 70%, respectively.

Keywords

HG-AAS; AsH₃; SeH₂; Preconcentration; Quartz surface; Quartz multiatomizer; Hydride trapping

1. Introduction

Hydride forming elements in general but As and Se especially are important analytes even at ultratrace levels. Moreover, increased interest in element speciation calls for introduction of routine techniques - cheap and reliable on the one hand but also sensitive on the other. Hydride generation atomic absorption spectrometry¹ (HG-AAS) meets the requirements on price and reliability, but not on sensitivity at ultratrace levels. The sensitive ICP-MS is very expensive

regarding operation and investment costs. Thus, a simple preconcentration step of the hydride prior to detection by AAS seems to be a suitable solution.

Besides the established technique of the in-situ trapping in graphite furnaces², other materials suitable for hydride trapping were explored. In last 5 years, graphite, metal and quartz preconcentration devices (traps) were tested.

Quartz traps can be simply interfaced to quartz atomizers predominantly used for hydride atomization. Moreover, conditions for in-situ trapping in the atomizer^{3,4} might be found. Our experiments indicated that the incomplete trapping/volatilization at the quartz surface was due to trapping losses unavoidable in the presence of hydrogen developed in hydride generator. It appeared that the solution was to burn hydrogen out in the collection step adding a stoichiometric excess of oxygen. Also a temperature minimum between the trap and the atomizer should be avoided. Otherwise, uncontrolled trapping takes place there.

The aim of this work was to develop a temperature minimum free apparatus design for the trapping studies and to optimize conditions for collection/volatilization of As and Se at quartz surface with subsequent atomization in the quartz multiatomizer.

2. Experimental

Reagents

All reagents were of analytical reagent grade or higher purity. Deionized water was used to prepare solutions. Working As and Se standards were prepared from 1 mg ml⁻¹ stock solutions (BDH Laboratory Reagents) by dilution in 1.0 mol l⁻¹ HCl. The blank was 1.0 mol l⁻¹ HCl. The reductant was 0.5% (m/v) solution of NaBH₄ (Sigma) in 0.4% (m/v) KOH (Merck) filtered after preparation and stored frozen.

Spectrometer

The Varian SpectrAA300/400 model equipped with hollow cathode lamps (As -10 mA, 193.7 nm, 0.5 nm band pass and Se – 10

mA, 196.0 nm, 1.0 nm band pass) was employed without background correction.

Hydride generator

An in-house made, continuous flow hydride generation system was employed as described elsewhere^{3,4}. Sample and reductant solutions were delivered and the waste from the gas-liquid separator was removed by a peristaltic pump. In all experiments, sample and reductant flow rates were 4.0 ml min⁻¹ and 1.2 ml min⁻¹, respectively.

Atomizer and trap device

A T-shaped multiple microflame atomizer (multiatomizer) was used. Its inlet arm served as a trap (8 cm length, 2 mm i.d., 3 mm o.d.). A 6-cm length of heating coil made from 40 cm canthal wire (4.17 Ω m⁻¹, 0.65 mm diameter) covered the downstream part of the inlet arm. The mains voltage, 220 V, was reduced to 80 V by use of an autotransformer. Another autotransformer controlled the potential applied to the heating coil and the current was monitored by means of an ammeter. A current between 0 to 9 A resulted in a temperature in the range 80–1100 °C. Deactivated fused silica capillary tubing (Supelco, 0.53 mm i.d.) centred in the inlet arm served for the oxygen delivery (see Fig. 1 for the schematic view of the apparatus). Two PTFE channels (1 mm i.d.) were employed to introduce: (1) the gases from the hydride generator in the trapping step (75 ml min⁻¹ Ar, analyte hydride + ca 15 ml min⁻¹ of H₂ evolved from NaBH₄ decomposition) and (2) auxiliary H₂ in the volatilization step.

The horizontal arm (aligned in the optical path of the spectrometer) was heated to 900 °C by the commercial heating unit (RMI, Lázně Bohdaneč). The arm was made of two concentric tubes: the inner (optical) one was evenly perforated with 14 orifices. A flow of gas (outer gas) was introduced from the sides into the cavity between both tubes of the horizontal arm and then passed through the orifices into the inner tube. Hydrogen at the flow rate of 25 ml min⁻¹ was introduced as the outer gas during the trapping step of the procedure. A 3-way valve was used to switch between air and hydrogen (see Fig. 1). 25 ml min⁻¹ air was employed as the outer gas during the volatilization step (see Procedure).

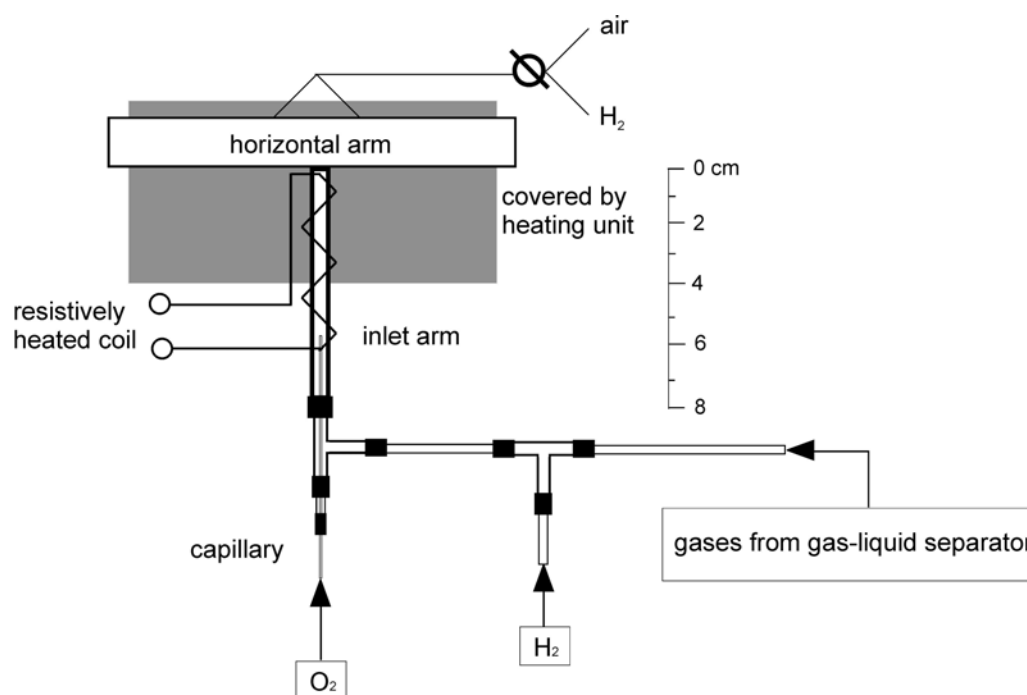


Fig. 1 – Schematic diagram of the apparatus arrangement

Procedure

Measurements were performed either in the preconcentration mode or in the direct transfer mode. Comparing the preconcentration mode with the direct transfer mode the trapping efficiency was estimated.

The collection mode procedure consisted of two steps: trapping - analyte is trapped in the inlet arm of the atomizer; volatilization - trapped analyte is released and transferred into the optical arm of the atomizer and trap device and atomized there.

Trapping step:

The inlet arm heating was set to the actual trapping temperature. The peristaltic pump was switched on; a standard was introduced to the sample channel for 30 s, then it was replaced by the blank for 30 s to flush the system. The oxygen channel was opened simultaneously with switching on the pump to deliver 10 ml min^{-1} O_2 to the capillary. The introduction of O_2 in the stoichiometric excess over 15 ml min^{-1} H_2 , evolved from NaBH_4 decomposition, resulted in an ignition of a flame burning at the tip of the capillary. The pump was stopped at the end of trapping step. Hydrogen at the flow rate of 25 ml min^{-1} was introduced as the outer gas into the cavity between both tubes of the horizontal arm during the trapping step and the signal of analyte

breaking through the trap and atomized in the optical tube was recorded. The "breakthrough" signal integration was thus performed for 90 s beginning at the start of the standard introduction.

Volatilization step:

The inlet arm heating was changed to the actual volatilization temperature. After 60 s the steady state temperature was reached. To volatilize collected analyte species, the oxygen channel was closed and after 5 s delay the hydrogen channel was opened. Simultaneously with opening the hydrogen channel, the signal of volatilized analyte atomized in the optical tube was recorded and integrated for 15 s.

If explicitly stated, an additional volatilization step was introduced: The oxygen channel was opened and the inlet arm temperature was changed to 920 °C and 570 °C, respectively, in the case of As and Se determination. After 60 s when the steady state temperature was reached, the volatilization procedure described above was repeated: the oxygen channel was closed and the hydrogen channel was opened with the 5 s delay time and the signal of additionally volatilized analyte was recorded and integrated for 15 s.

In the direct transfer mode, the inlet arm was unheated, the oxygen channel was closed, the hydrogen channel was open, the peristaltic pump was on and the signal of analyte atomized in the optical tube was continuously monitored. Air was always employed as the outer gas. An actual standard was introduced to the sample channel for 30 s and it was subsequently replaced by the blank for 30 s. The signal was integrated for 90 s.

3. Results and discussion

Atomizer and trap device

The capillary setup of the device (see Fig. 1) makes possible to fix the H₂/O₂ flame at the end of the oxygen delivery capillary during the trapping step. The flame is ignited by starting oxygen introduction regardless the trap is heated or not: in the case of low trap temperature the flame is ignited in the hot optical tube and immediately flashed back to burn stable at the tip of the capillary. Under oxygen excess the analyte hydrides are converted to oxides which are retained at the quartz surface. At the elevated quartz surface temperature and under

the hydrogen excess, the interactions between analyte oxides and quartz surface probably become weaker and/or the analyte oxides are reduced by hydrogen. Analyte species are thus volatilized and transported to the optical arm to be atomized there. Hydrogen is employed as outer gas in the trapping step. It enables to reverse the O₂ to H₂ ratio in the optical arm. Only under H₂ excess non-trapped analyte species breaking through can be atomized and detected.

Arsenic

Optimum trapping temperature was found in a broad range between ambient and (the maximum checked) 950 °C and there was no breakthrough signal observed. The volatilization curve and the influence of volatilization temperature on the signal of additionally volatilized analyte is presented in Fig. 2. The figure shows that volatilization temperature around 650 to 800 °C is optimal. For lower volatilization temperature, a fraction of analyte is retained in the trap to be subsequently released and atomized in the additional volatilization step (see Fig. 2).

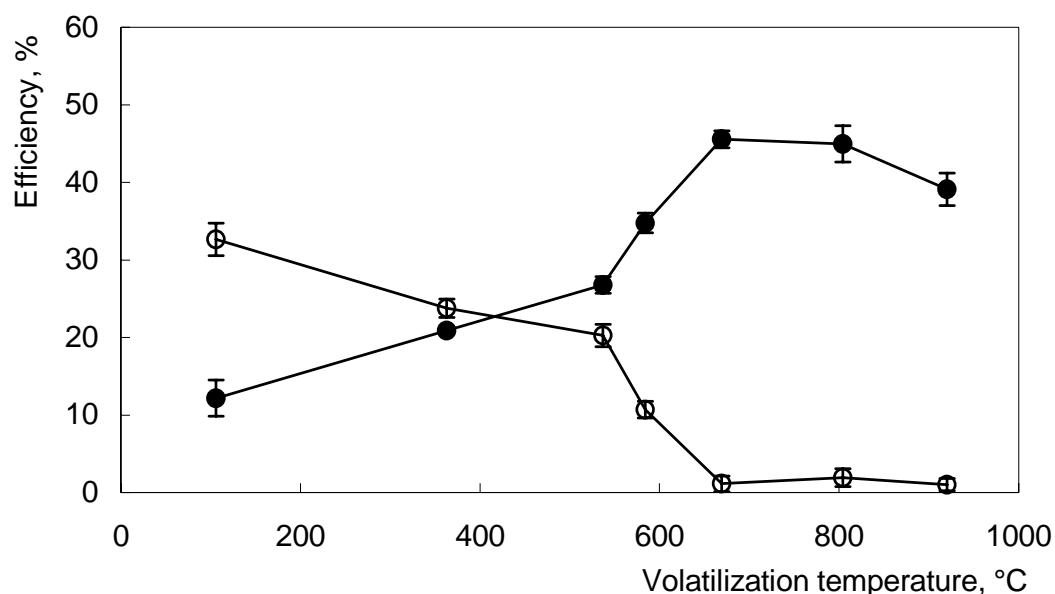


Fig. 2 Volatilization curve (●) and additional volatilization step at 920 °C (○) trapping temperature 150 °C; volatilization hydrogen flow rate 100 ml min⁻¹

Selenium

Fig. 3 illustrates that there are substantial breakthrough signals observed for the trap temperature above 400 °C. The optimum trapping temperature is below 200 °C.

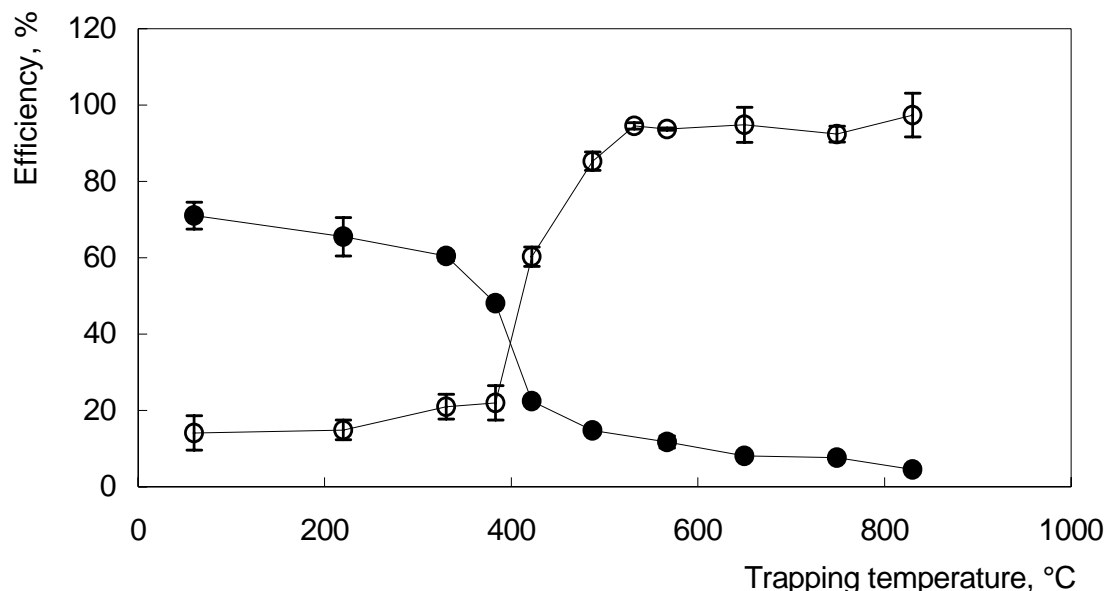


Fig. 3 Trapping curve (●) and breakthrough signal (○)
volatilization temperature 570 °C; volatilization hydrogen flow rate 50 ml min⁻¹

The volatilization curve and the influence of volatilization temperature on the signal of additionally volatilized analyte is presented in Fig. 4. The optimum volatilization temperature ranges around 570 - 650 °C. For lower volatilization temperature, a fraction of analyte is retained in the trap to be subsequently released and atomized in the additional volatilization step. For the volatilization temperature above 650 °C the efficiency dramatically decreases. The decrease is due to analyte losses during the 5 s period, when the trap is heated to the volatilization temperature without oxygen supply.

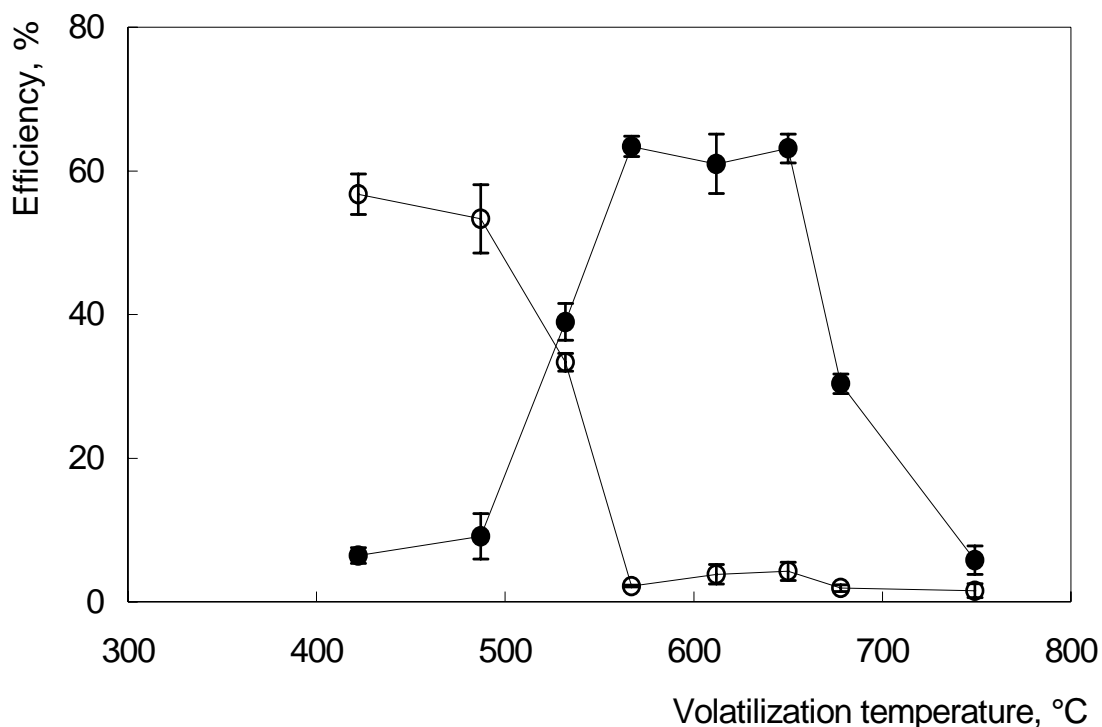


Fig. 4 Volatilization curve (●) and additional volatilization step at 570 °C (○) trapping temperature 80 °C; volatilization hydrogen flow rate 50 ml min⁻¹

4. Conclusions

Our results indicate the potential of this novel approach for preconcentration of As and Se hydride in analytical practice. Under the optimized conditions, rapid analyte volatilization is achieved. In addition, carryover for arsenic and selenium is negligible under the optimized conditions. The capacity of the trap estimated from the calibration plots is sufficient for ultratrace analysis (>4 ng analyte).

Experiments are in progress to find the explanation for and, subsequently, to improve the 50% preconcentration efficiency for As. For Se, the reasons for the 70% preconcentration efficiency were found. The objective of forthcoming experiments is to prevent losses in both the trapping and volatilization steps.

Acknowledgment

Financial support from the Grant Agency of the ASCR (Project No. A400310507), the Grant Agency of Charles University (Project No. GAUK 306/2006/B-CH/PrF), and the Ministry of Education, Youth and Sports FRVS (Project No. 1011/2006/G6) is gratefully acknowledged.

References

- [1] Dědina, J.; Tsalev, D.: *Hydride Generation Atomic Absorption Spectrometry*. Chichester, 1995.
- [2] Matusiewicz, H.; Sturgeon, R.E.: *Spectrochim. Acta B* **51** (1996), 377–397
- [3] Kratzer, J.; Dědina, J.: *Spectrochim. Acta B* **60** (2005), 859–864
- [4] Kratzer, J.; Dědina, J.: *J. Anal. At. Spectrom.* **21** (2006), 208–210

VERY FAST GAS CHROMATOGRAPHY WITH A BALLISTIC HEATING AND ULTRA FAST COOLING OF THE COLUMN

Žofia Krkošová^a, Róbert Kubinec^a, Helena Jurdáková^a,
Jaroslav Blaško^a, Beáta Meľuchová^a, Ivan Ostrovský^a,
Ladislav Soják^a, Jiří Ševčík^b, Jozef Višňovský^c

^a*Chemical Institute, Faculty of Natural Sciences, Comenius University, Mlynská dolina CH-2, SK-845 45 Bratislava, Slovakia*

^b*Department of Analytical Chemistry, Faculty of Natural Sciences, Charles University, Hlavova 2030, CZ-128 40 Prague, Czech Republic*

^c*CMS Chemicals, s. r. o., Nobelova 34, P. O. Box 44, SK-836 03 Bratislava, Slovakia*

Abstract

An overview of the existing methods for minimization of the analysis time in gas chromatography (GC) is given and a new system for fast temperature programming and very fast cooling down is evaluated. In this study, a system of coaxial tubes, a heating/cooling module (HC–M), has been developed and studied, with a capillary column placed inside the HC–M module. The module itself is heated by the GC oven and cooled down by an external cooling medium. The HC–M module is heated up at rates of up to 330 °C min⁻¹ and cooled down at a rate of 6 000 °C min⁻¹. The GC system is prepared for the next run within a few seconds. The HC–M module permits good separation reproducibility, comparable with that of conventional GC, expressed in terms of the reproducibilities of the relative retention times and the peak areas of analytes. The HC-M module can be used within any commercial gas chromatograph.

Keywords:

Fast temperature programming, Very fast chromatography, Ultra fast cooling, Phenols

Introduction

Since the introduction of GC in 1952, there has been continuous interest in increasing its separation speed [1]. Fast gas chromatographic separation is a generally beneficial option, since the decreased total time of analysis results in an increased sample throughput and, consequently, the laboratory operating costs can be reduced significantly [2]. The principles and theory of fast chromatography were established as early as in the 1960s. Since that time, many studies on the theoretical background of fast GC, development of suitable instrumentation and applications of the technique have been published [3].

The primary objective of chromatographic analysis is to achieve the desired resolution of compounds of a mixture, or of a critical pair of compounds, within the shortest possible time. Most analyses that have been performed with conventional capillary GC (columns with the internal diameter, I. D., 0.2–0.32 mm) require analysis times of 10–60 min., depending on the sample character, the number of components to be analyzed and the experimental conditions employed [1]. The analysis time can be reduced either by changing the column parameters (the column internal diameter and length) or changing the operational parameters (heating rate, flow rate, type of stationary phase) [4] or by combining the two approaches.

The temperature has an essential influence on gas chromatographic separations, regarding the operational parameters. Since isothermal GC is still restricted to analyze of samples with a relatively narrow boiling point range, fast temperature programming is considered for a majority of samples. An optimization process has to determine an optimum heating rate in temperature programmed GC that represents the best compromise between the quality of separation and the speed of analysis [5]. In, practice, fast temperature programming can be accomplished: (1) with conventional GC ovens, (2) by resistive heating [6], (3) using a microwave oven [7, 8] or heating by a 150 W halogen lamp [1, 9].

(1) Fast temperature programming with conventional GC ovens usually combines optimized conditions, such as narrow-bore capillary columns and thin films of stationary phases, with a powerful oven heater. The thermal capacity of the GC oven limits the heating and

cooling rates and common GC ovens provide maximum temperature programming rates of 1-2 °C s⁻¹. Not only fast temperature programming rates during the GC separation, but also a minimum cooling-down period between two adjacent runs can significantly contribute to increasing the sample throughput [10].

(2) One means of generating very rapid heating rates is provided by resistive heating of the column [11]. Resistive heating rate techniques (EZ-Flash) eliminate the conventional air bath ovens. Electrical current is employed to heat a conductive material (a metal) located very close to the column. The thermal capacity is minimized and the heating up and cooling down can be very fast. Commercial systems have recently become available in which a fused silica capillary column is inserted into a resistively heated tube or enclosed in thermal wrapping tape. Temperature programming rates of up to 20 °C s⁻¹ have been attained [12].

(3) Microwave heating of GC columns is an attractive alternative to conventional heating because of fast microwave heating rates, a lower power needed and a relatively straightforward procedure for integration into existing GC instruments. Microwave heating also permits faster cooling rates because only the column has been directly heated. Microwave ovens have attained temperature-programming rates of up to 360 °C min⁻¹ [13].

The total time of a GC analysis includes the time for resetting the system, i. e. the cooling/re-equilibration time of the GC oven and, if necessary, of the injector [14]. In addition, for high speed separations, the lengthy cooling down time of convection ovens limits the sample throughput [15]. The total analysis time of fast GC separations strongly depends on the complexity of the mixture analyzed. For very complex samples with many compounds, minimum separation times will typically be in the range of minutes [1].

Van Deursen et al. [6], Blumberg and Klee [16] and Magni et al. [17] suggested a classification of fast GC methods into the groups of the fast, very fast and ultra fast GC, based on the resulting peak widths and the total analysis times.

The present paper deals with the construction of a heating/cooling module for very fast GC, enabling the very fast ballistic heating and ultra fast cooling of capillary column. The system

developed consists of coaxial tubes enabling ultra-fast cooling. It has been tested and briefly applied to analyze of several compound classes. The analysis time, the separation efficiency and the precision of the retention times and the peak areas were the main parameters monitored [14, 18, and 19].

Experimental

Materials

A newly constructed heating/cooling module (HC-M) consists of coaxial stainless steel tubes 2.5 m long with an outer diameter (o.d.)/inner diameter (i.d.) of 5/3.1 mm and 1.59/0.76 mm, purchased from Supelco, USA.

Temperature measurements on the HC-M module were carried out by a thermo element from a tungsten wire with an outer diameter of 0.03 mm, an electrical resistance of $125 \Omega \text{ m}^{-1}$ (purchased from CACO, SAV, Bratislava), which was inserted into a capillary column of $3 \text{ m} \times 0.32 \text{ mm}$ (CACO, SAV, Bratislava).

The cooling medium (1.100 L min^{-1}) was circulated by a pump (Wagner International AG, Switzerland) at a pressure of 0.9 MPa and regulated by means of solenoid valve switching (Type M5 – G 1/8“, KV Limited, United Kingdom). The HC-M module and the pump tubing were connected by a copper tubes ASTM B-280, $6.35 \text{ mm} \times 4.83 \text{ mm} \times 20 \text{ m}$ (Supelco, USA) with tubing fittings 402-1 “1/4“, 202-1 “1/8“ (Supelco, USA). A constant temperature of the cooling medium – paraffin oil (Merck KgaA, Germany) was maintained in a thermostat (LAUDA, Type RE 104, Germany).

All the analyses were carried out using a capillary column Petrocol DH 150 $2.5 \text{ m} \times 0.25 \text{ mm i.d.} \times 1 \mu\text{m}$ from Supelco, USA. This capillary column was inserted into the HC-M module. The data on the temperature rates were processed on a CSW 1.7 computer module.

Samples

The *n*-alkanes (C₇ – C₂₀) were purchased from Sigma – Aldrich Chemie GmbH, Germany and the longer *n*-alkanes (C₂₂ – C₅₀) from Polywax 655, Catalog. No. 4 – 8 477, Supelco, USA. A mixture of the *n*-alkanes was dissolved in chloroform at concentrations of 300 µg mL⁻¹. A standard solution of phenols (phenol; 2-chlorophenol; 2-nitrophenol; 2,4-dimethylphenol; 2,4-dichlorophenol, each at a concentration of 500 µg mL⁻¹; 2,4,6-trichlorophenol; 2,4-dinitrophenol, each at a concentration of 1 500 µg mL⁻¹, and 4-chloro-3-methylphenol; 4-nitrophenol; 2-methyl-4,6-dinitrophenol; pentachlorophenol, each at a concentration of 2 500 µg mL⁻¹) was obtained from Supelco, USA.

GC analysis

The GC analyses were carried out using a GC System 6890N (1530N) instruments, equipped with a split-split less injector, a flame ionization detector (FID) and a 7683 Series auto sampler, all from Agilent Technologies (USA). The carrier gas was hydrogen at a pressure of 30 kPa in the injection port. The split injection with a split ratio of 20:1 for the phenols and splitless injection with 0.3 minutes for the *n*-alkanes was used, with a liner of 5 mm i.d., and at the injection port temperature 300 °C. The injected sample volume was 1 µL. An oven temperature was maintained constant at 350 °C. The HC–M module with the directly heated column was placed in the GC oven. The detector temperature was maintained at 350 °C. The data acquisition was performed using the GC ChemStation Rev. A. 09.01 [1206] Software.

Results and discussion

Design of the heating/cooling module

The HC-M module developed is shown in Fig. 1. The module consists of coaxial stainless tubes that are fixed and sealed and the space between them is filled up with a cooling medium, paraffin oil with a suitable viscosity and temperature stability. The capillary column can be replaced, if needed. The developed system was installed in a conventional GC oven by inserting HC–M to the GC

oven and connecting the capillary column to the injector and detector. The host GC oven was maintained at a constant temperature and because of a low thermal capacity of the HC-M module, the fast heating was attained. The flowing of the cooling medium provided fast cooling of the capillary column. Adjacent analysis (between the temperature of GC oven 350 °C and the final temperature of capillary column 25 °C) could be started in 8 seconds. The HC-M module does not require additional instrumentation, except for an additional remote control of the solenoid valve.

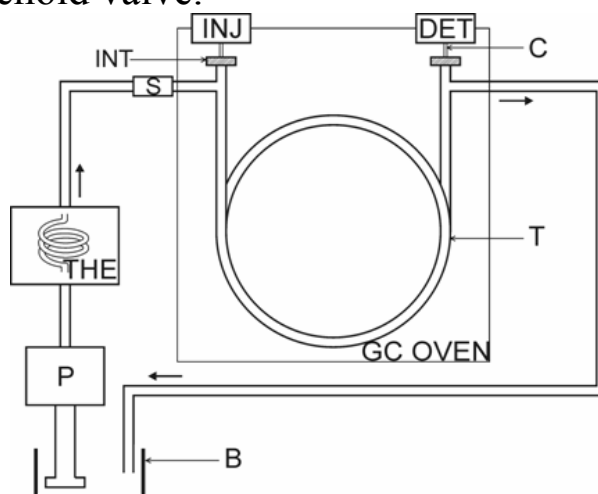


Fig. 1. Schematics of the HC-M module.

S – solenoid valve, *P* – pump, *B* – box with cooling medium, *INT* – connectors, *T* – system of tubes (HC-M), *C* – capillary column inserted into HC-M module, *THE* – thermostat, *INJ* – injector, *DET* – detector.

As shown in Fig. 1, the module can be used with any commercially available GC.

Temperature monitoring

The temperature gradients were monitored by a thermo element made of a tungsten wire, inserted into the capillary column.

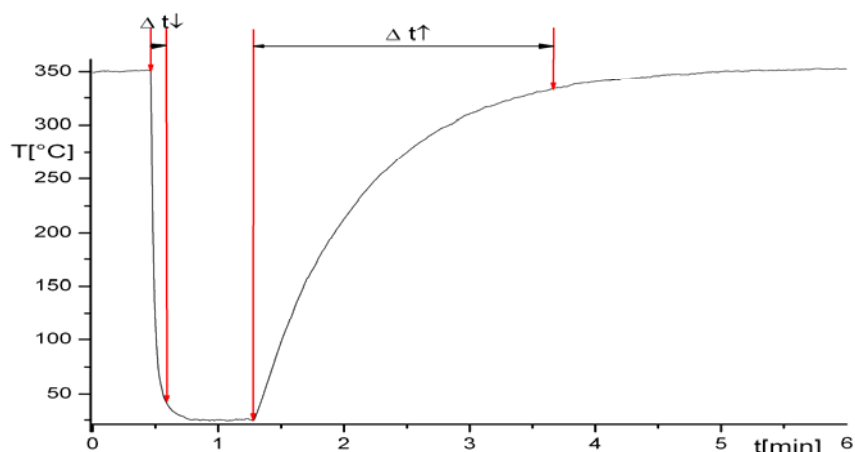


Fig. 2. Temperature program obtained with HC-M module

at the temperature of GC oven of 350 °C, with the cooling medium temperature 25 °C and its flow rate of 1.100 L min⁻¹. Δt↑ - the time of heating up and Δt↓ - the time of cooling down.

Fig. 2 shows the temperature rates provided by HC-M module at the GC oven temperature of 350 °C. The maximum temperature gradients and times for the heating and cooling, for the HC-M and a conventional GC oven, are given in Table 1. The ballistic temperature rise is quantitatively described by Equation 1. It holds that

$$T = 351,2 - 335,2 * \exp\left(-\frac{x}{488,1}\right) \quad (1)$$

where x is the time of heating in seconds.

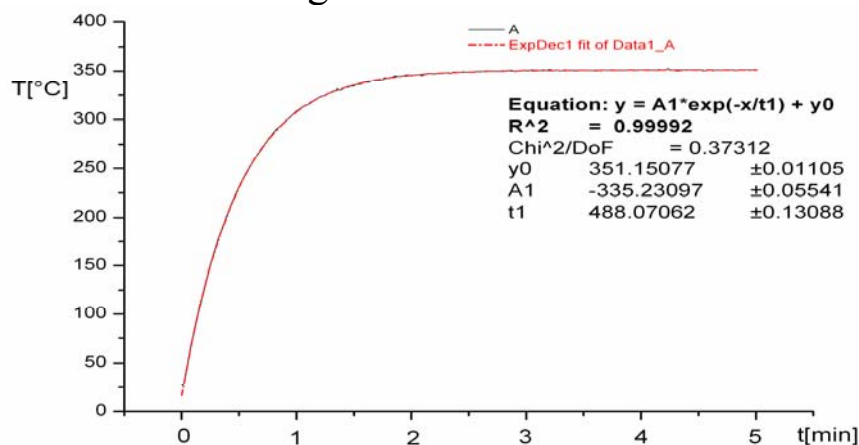


Fig. 3. Temperature program of HC-M module.

The validity of Eq. 1 is proved by the high correlation, $R^2 = 0.99992$, and the coefficient of variation of the equation parameters better than 0.1 %, as demonstrated in Fig. 3.

Table 1: The temperature gradients and the times of heating and cooling for HC-M system developed and laboratory GC oven.

	Conventional GC oven	Prepared system of tubes
Maximal gradient of heat up [$^{\circ}\text{C}.\text{min}^{-1}$]	155	330
Maximal gradient of cool down [$^{\circ}\text{C}.\text{min}^{-1}$]	205	6 000
Time of heat up Δt_{\uparrow} [s]	232	143
Time of cool down Δt_{\downarrow} [s]	355	8

As shown in Table 1, the HC-M module is about two times faster in heating up and 30 times faster by cooling down than a conventional chromatographic oven. Our results were in a good agreement with this; (1.5 times faster heating up and 44 times faster cooling down). We found that the cooling down gradient was independent of the column oven temperature and was only determined by the material of the tubes used, their flow resistance and the volume of the cooling medium.

Chromatographic characterization

The GC separation speed may influence the separation capability of a chromatographic system. The parameters currently used to define the metrics of GC separations are the resolution, R (separation of two peaks) [10, 20], the separation number, SN (the number of well – separated peaks within any homologous pair), the peak capacity, n (the maximum number of peaks that can be separated by a chromatographic system with a given resolution) [10].

Here we can demonstrate that separations of hydrocarbon mixtures with the HC-M module take much less time without loss in the chromatographic performance.

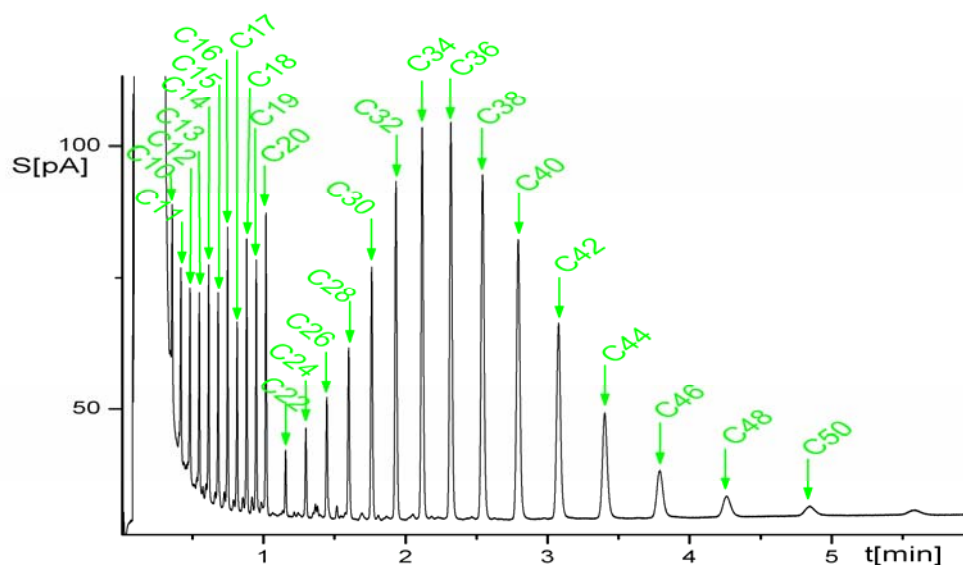


Fig. 4. GC–FID separation of mixture *n*-alkanes in the HC-M system.

The potential of the system designed is demonstrated on a separation of a mixture containing twenty six *n*-alkanes in the range of *n*-C₁₀ to *n*-C₅₀, (Fig. 4). Separations of *n*-alkanes have been used to study the effect of the heating rate on the separation capability (criteria *SN*, *n*) and the analysis time. We have found that the separation number *SN* was in a range from 7.9 (for C₁₀-C₁₂) to 3.4 (for C₄₈-C₅₀), while the peak capacity was *n* = 107 and the speed of analysis was 25 *SN* min⁻¹.

Table 2: Repeatability of the retention time and of the peak area of *n*-alkanes mixture.

<i>n</i> -alkanes	Retention time [min]	RSD [%]	Area [pA.s]	RSD [%]
<i>n</i> -decane	0.36	0.35	18.40	4.29
<i>n</i> -dodecane	0.48	0.29	19.86	0.63
<i>n</i> -tetradecane	0.62	0.21	24.06	1.61
<i>n</i> -hexadecane	0.75	0.20	29.13	1.42
<i>n</i> -octadecane	0.88	0.19	29.05	0.95
<i>n</i> -icozane	1.02	0.19	34.46	1.09
<i>n</i> -docozane	1.16	0.16	7.94	1.34
<i>n</i> -tetracozane	1.30	0.17	11.13	2.11
<i>n</i> -hexacozane	1.45	0.18	16.66	0.97
<i>n</i> -octacozane	1.60	0.20	26.12	1.83
<i>n</i> -triacontane	1.76	0.22	39.47	2.26
<i>n</i> -dotriacontane	1.93	0.28	59.27	2.73
<i>n</i> -tetratriacontane	2.12	0.28	75.76	3.34
<i>n</i> -hexatriacontane	2.32	0.29	88.11	4.03
<i>n</i> -octatriacontan	2.54	0.28	88.82	4.54
<i>n</i> -tetracontane	2.79	0.29	81.74	4.51
<i>n</i> -dotetracontane	3.07	0.34	63.26	5.79
<i>n</i> -tetratetracontane	3.40	0.29	42.00	5.06
<i>n</i> -hexatetracontane	3.79	0.29	22.82	8.24
<i>n</i> -octatetracontane	4.26	0.27	13.14	5.48
<i>n</i> -pentacontane	4.84	0.32	7.07	9.30

RSD – Relative standard deviation

Table 2 contains qualitative and quantitative results obtained with the HC-M system. The reproducibility of the peak retention times, obtained from six repeated measurements, was RSD = 0.25 % on average. The reproducibility of the peak area expressed in terms of RSD was in a range from 0.63 % for *n*-dodecane to 9.3% for *n*-pentacontane.

Applications

The hydrocarbon oil index (HOI) is defined as the total amount of compounds which can be extracted from the sample (potable water, surface water and waste water) with a non – polar solvent having a boiling point between 39°C and 69°C. In addition, the compounds must not absorb on Florisil and must elute between *n* – decane (C₁₀H₂₄) and *n* - tetracontane (C₄₀H₈₂) when analyzed by GC using an apolar analytical column.

The method is suitable for HOI determinations in concentrations above 0.1 mg.l⁻¹ in drinking waters, surface waters, waste waters and waters from sewage treatment plants.

Table 3: Equation calibration curve and correlation coefficient of oil R 932 and diesel fuel.

	Equation calibration curve	Correlation coefficient
Oil R 932	$y = 18,64x + 2772,5$	0,9997
Diesel fuel	$y = 21,609x + 187,13$	0,9997

y – peak area
x – concentration (ppm), range 2,5 – 50 000 ppm for oil R 932 and 3 – 5 000 ppm for diesel fuel

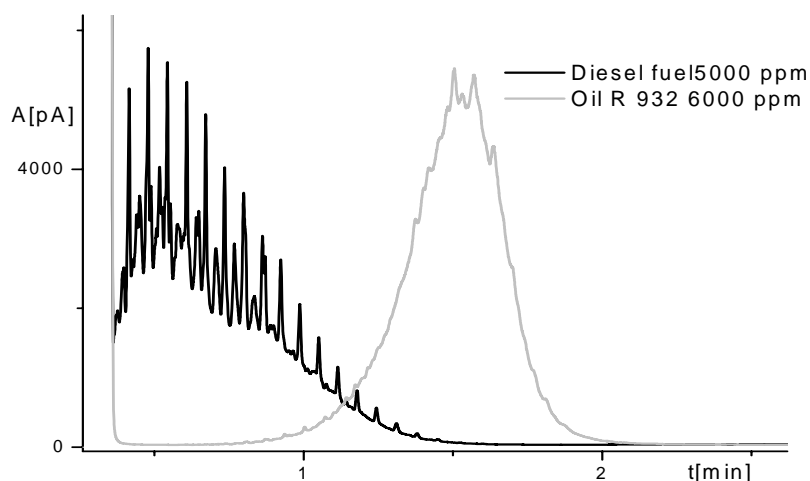


Fig. 5. GC – FID analysis of oil R932 (6000 ppm) and diesel fuel (5000 ppm).

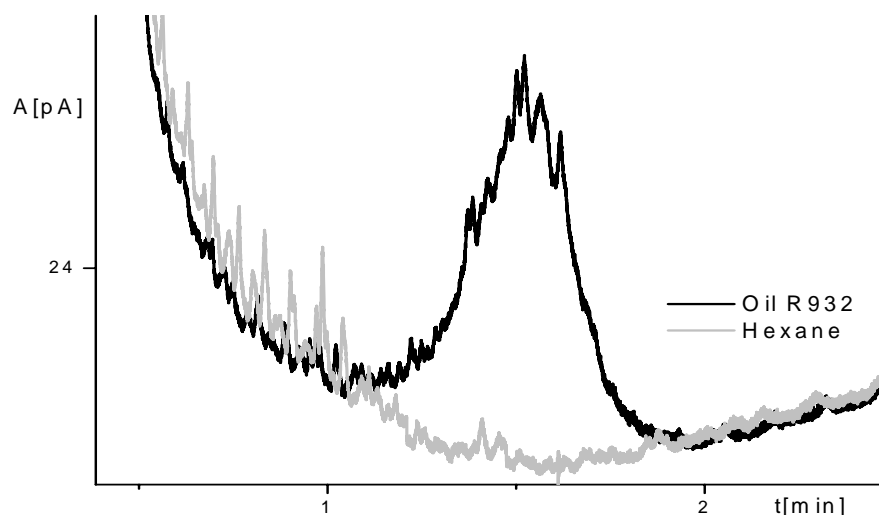


Fig. 6. GC – FID analysis of oil R932 (2,5 ppm) and hexane.

Conclusions

The HC-M system for heating GC columns is an attractive alternative to conventional GC instrumentation. The developed system is suitable for high speed GC separations of wide boiling point range mixtures. In the HC-M system, the temperature can be increased by 300 - 600 °C min⁻¹ and decreased by 5 500 – 6 000 °C min⁻¹. The cooling-down period is thus less than 9 seconds and a next analysis can be started in a rapid succession.

The system developed was chromatographically characterized by separation of a mixture of *n*-C₁₀ - *n*-C₅₀. The mixture of *n* - alkanes was eluted in less than 5 minutes with a total peak capacity of 107 peaks, applying a heating rate of 330 °C.min⁻¹ and a cooling rate of 5 500 °C.min⁻¹. A higher peak-capacity value was obtained with lower programming rates.

At present, when the productivity of a laboratory is the most important criterion, increasing the speed of analytical measurements is imperative and the developed system could contribute significantly to increasing the sample throughput.

The HC-M system developed permits:

- 1 A good repeatability of the retention times and peak areas.
- 2 Fast temperature gradients, plus 300 to 600 °C min⁻¹ and minus 6000 °C min⁻¹.
- 3 Short times of the cooling period, about 3 – 9 seconds.
- 4 Application to any commercial GC oven.

Acknowledgements

The authors thank the Grant Agency VEGA Slovakia (1/2467/05), and ESF (No. 54/04-I/32-DP, ITMS 131201 10048) for the financial support of this research.

References

- [1] Korytár P, Janssen HG, Matisová E, Brinkman UATh (2002) Trends Anal. Chem. 21: 558.
- [2] Maštovská K, Hajšlová J, Godula M, Křivánková J, Kocourek V (2001) J Chromatogr A 907: 235 – 245.
- [3] Van Es A, Janssen J, Cramers CA, Rijks J (1988) J High Resol Chromatogr Chromatogr Commun 11: 852.
- [4] Blumberg LM, Klee MS, www.richrom.com.
- [5] Blumberg LM, Klee MS (2000) Anal Chem 72: 4080 – 4089.
- [6] Van Deursen MM, Beens J, Janssen HG, Leclercq PA, Cramers CA (2000) J Chromatogr A 878: 205.
- [7] www.antekhon.com.
- [8] www.iscpubs.com.
- [9] Matz G, Harder A, Walte A, Münchmeyer W, www.tu-harburg.de.
- [10] Bicchi C, Brunelli C, Cordero Ch, Rubiolo P, Galli M, Sironi A (2004) J of Chromatogr A 1024: 195 – 207.
- [11] McNair HM, Reed GL (2000) J Microcolumn Separations 12(6): 351 – 355.
- [12] Dallüge J, Vreuls RJJ, Van Iperen DJ, Van Rijn M, Brinkman Th (2002) J Sep Sci 25: 608.
- [13] www.antekhon.com/pdf/misc.
- [14] Dallüge J, Ou-Aissa R, Vreuls JJ, Brinkman UATh, Veraart JV (1999) J High Resol Chromatogr 22: 459 – 464.
- [15] Grall A, Leonard C, Sacks R (2000) Anal Chem 72: 591 – 598.
- [16] Blumberg LM, Klee MS, Sandra P (26 – 29 May 1998) Proceedings of 20th International Symposium of Capillary Chromatography, Riva del Garda, Italy, PL9.
- [17] Magni P, Facchetti R, Cavagnino D, Trestianu S, Sandra P (13 – 17 May 2002) Proceedings of 25th International Symposium of Capillary Chromatography, Riva del Garda, Italy, KLN05, and references cited therein.
- [18] Mustacich R, Everson J, Richards J (2003) Fast GC, American Laboratory.
- [19] Giddings JC (1962) Anal Chem 34: 314.
- [20] Cramers CA, Janssen HG, Van Deursen MM, Leclercq PA, J Chromatogr A 856 (1999) 315-329.

NEEDLE CONCENTRATOR AND SOLID PHASE MICRO-EXTRACTION FOR GAS CHROMATOGRAPHIC DETERMINATION OF BTEX FROM AQUEOUS SAMPLES

B. Meľuchová², Viera Valkovská², H. Jurdáková², Ž. Krkošová²,
J. Blaško², P. Prikryl¹, R. Kubinec², J. Ševčík¹, I. Ostrovský²,
L. Soják², V. Berezkin³

¹*Department of Analytical Chemistry, Faculty of Natural Sciences, Charles University, Hlavova 2030, CZ-12843 Prague, Czech Republic*

²*Chemical Institute, Faculty of Natural Sciences, Comenius University, Mlynská dolina CH-2, SK-842 15 Bratislava, Slovakia*

³*A. V. Topchiev Institute of Petrochemical Synthesis, Russian Academy of Sciences, Leninsky Prosp. 29, 119991 Moscow, Russia*

A method of solventless extraction of volatile organic compounds (BTEX) from aqueous samples was developed and validated. A new arrangement of the full volume inside needle capillary adsorption trap device filled with Porapak Q as a sorbent material and wet alumina as a source of desorptive water vapour flow is presented. The developed device has been applied for head-space sampling of BTEX from water sample and compared to solid phase micro-extraction method. The analytical characteristics of developed device are better than that of solid phase micro-extraction method for BTEX compounds under the same sampling conditions. The limits of detection and of the quantification are lower than 0.5 µg L⁻¹.

Keywords:

Gas chromatography, Solid phase micro-extraction, Needle concentrator, Volatile organic compounds in aqueous samples

Introduction

The analytical methods based on solventless sample preparation techniques for environmental samples which allow elimination of liquid solvents in the analytical procedures at low concentration levels as well as the reduction of the sample preparation time are permanently in development [1]. Among this enrichment of the analytes techniques is in progress the technique of the inside needle capillary adsorption trap (INCAT) or in-tube extraction [2-12]. In this device the sampling of a gaseous or aqueous analyzed mixture can be done by drawing a fixed volume of a sample through the sorbent placed as adsorbent layer on the interior surface or in full inside volume of stainless steel needle. The volatile analytes sorbed on the sorbent, which can be adsorbent or liquid coated onto a support, are thermally desorbed in the heated injection port of a gas chromatograph and then directly swept by the carrier gas into the capillary column for analysis. Procedure of solid phase dynamic extraction of organics using a wall coated syringe needle was automated [8].

The main advantages of INCAT device lie in the simple methodology, easiness, and rapidity of the analyses [5]. The drawbacks involve the fact that the samples collected can be not particularly large, the desorption temperature is limited by that of the gas chromatographic injection port, and the elution zones of analytes are slightly dispersed [5]. Other problems consist in competitive effects and variation in sampling efficiencies for the different analyzed compounds as the result of the low capacity of the sorbent [7]. These drawbacks were overcome by a new arrangement of the full inside volume needle capillary adsorption trap device with Porapak Q as a sorbent material and wet alumina as a source of desorptive water vapour flow in a closed analytical system. The INCAT sampling method was verified, optimized and validated compared to purge-and-trap (PTI) technique and was described in our previous paper [13]. In this work are analyzed aromatics from headspace of water sample in difference to previous work where were analyzed direct water sample.

Solid phase micro-extraction (SPME) presents many advantages over traditional analytical methods by combining sampling, preconcentration, and the transfer of the analytes into a standard gas chromatograph [14]. The sensitivity of solid (or mixed-phase) SPME

coatings, such as PDMS and divinylbenzene (PDMS/DVB) and Carboxen/PDMS, was reported to be very high for extracting VOCs. However, competitive adsorption and displacement effects make mass calibration and quantification particularly challenging. The solid coatings can extract (via adsorption) great amounts of VOCs, but short sampling times and nonequilibrium conditions have to be used and operating conditions must be carefully adjusted too. The new INCAT device could overcome these disadvantages as will be shown later.

The volatile aromatic compounds such as benzene, toluene, ethylbenzene, *ortho*-, *meta*-, *para*-xylene (BTEX) are fuel components commonly found in ground water contamination. The normalized quality limit for drinking water is for benzene 1, toluene 50 and for xylenes 100 $\mu\text{g L}^{-1}$, respectively [15]. The analysis of BTEX in aqueous samples is usually achieved by purge-and-trap-gas chromatography [16] and or by nowadays often used SPME method. The aim of this work was to make a comparative study of the new INCAT technique and SPME method for the headspace sampling and preconcentration BTEX from aqueous samples at same operating conditions. The present paper shows several advantages of sampling with new INCAT device compared to sampling volatiles with adsorption coating SPME fibers.

Experimental

Materials

Porapak Q 0.15 – 0.18 mm with a specific surface area of 550 $\text{m}^2 \text{g}^{-1}$ and aluminium oxide with a grain size of 0.2 – 0.4 mm as packed materials for needle concentrator were purchased from Waters Assoc., Inc. (Framingham, Mass., USA) and Merck (Darmstadt, Germany), respectively. Standards BTEX (benzene, toluene, ethylbenzene, *p*-xylene and *o*-xylene) were from Slovak Institute of Metrology (Bratislava, Slovakia), and methanol (gradient grade) from Merck (Darmstadt, Germany).

Stainless steel needles (cannula) 90 mm long with an outer / inner diameter of 1.3 mm / 1.1 mm, and 1.1 mm / 0.9 mm were from Nissho (Osaka, Japan), and from this material were prepared also O-rings (3 mm x 1.1 mm O.D. / 0.9 mm I.D.). Stainless steel frits (20 μm porosity and 0.16 mm depth) were from Carlo Erba (Milano, Italy),

1000 Series GASTIGHT Syringes TEFLON® luer lock (TLL) for gas or liquid sampling (volume 100 ml) from Hamilton Company (Reno, Nevada, USA), MTB Sampling Valve from Hamilton Company (Reno, Nevada, USA).

Restrictor as an uncoated deactivated silica capillary column of 0.7 m x 0.1 mm from Caco (Bratislava, Slovakia) was used for investigation of the sorption-desorption process of analytes in INCAT device, and a DB-1 30 m x 0.53 mm I. D. x 3 µm (J&W Scientific, Blue Ravine Road, Folsom, USA) column was employed for analytical separation of desorbed aromatic hydrocarbon standards.

Sampling

INCAT

Drinking water samples were prepared by direct spiking 8 mL of destilated water with 8 µL of methanolic stock solutions containing 0.2 - 5000 µg L⁻¹ of each BTEX in the 16 mL vials. Concentration of each BTEX in drinking water models were 0.2, 0.5, 1, 2.5, 5, 10, 20, 50, 100, 200, 500, 1000, 2000, 5000 µg L⁻¹. Sample vial was then thermostated at temperature 40 °C and thin stainless steel needle with active carbon plug was inserted to prevent depressurization during dynamic sampling. Headspace extraction was carried out 20 minutes at speed 0.4 mL min⁻¹ by INCAT device and propelled by glass syringe.

SPME

The SPME was used as an comparative method for headspace sampling of volatiles from aqueous matrices. The SPME fiber with 65µm PDMS/DVB coating (Supelco, Bellefonte, PA, USA) was chosen as a similar sorbent to Porapak Q.

The above listed aromatic hydrocarbons solutions were extracted with PDMS/DVB fibers. Extractions were performed with magnetic stirring speed 600 rpm and extraction time 15 min at temperature 40 °C. Position of the fiber in the vial was 0.6 cm from the center always at constant high. The extracted analytes were desorbed and analyzed immediately after the extraction.

GC analysis

The GC measurements were performed on gas chromatograph HP 5890 SERIES II Hewlett-Packard (Avondale, USA) equipped with flame ionization detector (FID) and a split-splitless injector. The carrier gas was helium with a pressure of 30 kPa in the injection port. The detectors temperature was maintained at 250 °C. Injections for separation of desorbed aromatic standards from INCAT and SPME device were made in the splitless mode (closed split valve during analysis) at injection port temperature 270 °C, and oven temperature 40 °C and heated quickly 10 °C min⁻¹ to 170 °C. The inner diameters of used liners were 0.75 mm and 4 mm for SPME and INCAT, respectively.

For investigation of INCAT device was used a model mixture of BTEX without *m*-xylene because of its coelution with *p*-xylene in used GC column. Results of real samples coelutate given as sum of *m*-, *p*-xylene because these isomers show similar recovery and response. In the case of required individual analyse of these isomers is necessary by use other GC column which separates *m*- and *p*-xylenes.

Results and discussion

A new INCAT device with adsorbent inside of the whole volume of stainless steel needle was developed for the preconcentration of trace volatile organic compounds (BTEX) from headspace of aqueous samples. As can be seen from Fig. 1 it comprises a stainless steel needle N, stainless steel O-ring O, stainless steel frits F, sampling on/off valve V, adsorbent Porapak Q 0.15 – 0.18 mm (15 mg, 50 mm length of needle) P, and alumina 0.2 – 0.4 mm (3 mg, 7 mm length of needle) A.

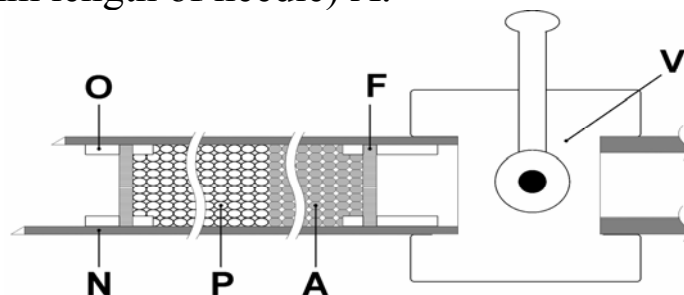


Fig. 1. Scheme of INCAT system.

N – stainless steel needle, *O* – stainless steel O-ring, *F* – stainless steel frits, *P* – adsorbent Porapak Q, *A* – adsorbent alumina, *V* – MTB sampling on/off valve.

Fig. 2 and Table 1 represent single steps of adsorption and desorption of BTEX from INCAT device. Aqueous sample is purged by 80 mL of air through the stainless steel needle by means of a syringe with 100 mL volume at speed about 0.4 mL min⁻¹ and stripped BTEX are retained in INCAT device (Fig. 2A). Subsequently the INCAT device is flushed by cca 0.1 mL of distilled water to wet alumina (Fig. 2B) and then by cca 0.5 mL of air to remove residual water (approx. of 30 µL) (Fig. 2C) at temperature 40 °C. Then the valve is closed and the INCAT device is introduced to GC injection port with 1 mL liner in the splitless mode at 270 °C. Adsorbed analytes are thermally desorbed from hydrophobic Porapak Q and displaced to the injection port with gradually purging water steam formed by evaporation of water from hydrophilic alumina sorbent (approx. of 9 µL water, determined by weighing of alumina sorbent). Various materials were tested for the water reservoir in needle concentrator, e.g. silica and molecular sieve, but the alumina was found to be most suitable. Desorbed analytes are separated by capillary gas chromatography and detected by FID detector (Fig. 2D). Once the analyse is finished the valve on INCAT device is open and residual organic compounds are removed by stream of helium with flow of 70 mL min⁻¹ within 2 minutes (Fig. 2E).

Table 1

The steps from sampling of aqueous samples headspace to cleaning of INCAT device.

Fig.	Step	Vent position	Plunger movement	Needle position
A	Sampling	ON	UP	Headspace over sample
B	Alumina wetting	ON	UP	Water
C	Residual water removing	ON	UP	Air
D	Desorption	OFF	-	GC injector
E	Cleaning	ON	-	GC injector

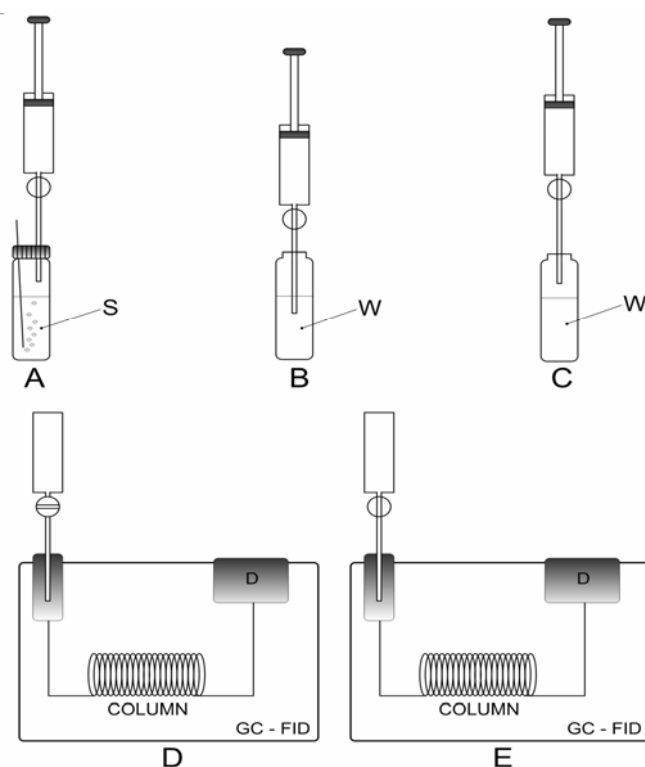


Fig. 2. Scheme of sorption and desorption process of INCAT device.

A – purging and sampling of aqueous samples, B – flushing of INCAT device by water to wet alumina, C – removing of residual water, D – desorption, E – cleaning. S – sample; W – water; D – detector

Sorption processes in INCAT device

Breakthrough volumes of BTEX had to be determined before sampling to prevent loss of the most volatile compounds. Sorption processes were studied at temperature 40 °C and INCAT device was used as a chromatographic column. The deactivated restrictors were used to fast transfer of analytes through INCAT device into the detector. Each pure standard was injected at injection port temperature 270 °C in split mode. Fig. 3 illustrates chromatographic elution of benzene and toluene in INCAT device. It's evident that benzene starts to elute at 80 mL and toluene at 350 mL of passed carrier gas. Ethylbenzene and xylenes do not elute from INCAT device until the gas volume 2000 mL at temperature 40 °C.

Stripping of BTEX from water

To determine an optimal volume of air necessary for quantitative extraction of all BTEX from aqueous sample, the vial of volume 16 mL filled with 8 mL of distilled water was placed in GC, connected with injector and detector by capillary restrictors, thermostated at 40 °C and purged by carrier gas at flow 20 mL min⁻¹.

Positions of capillary restrictors in vial are same as in the case of INCAT and SPME extraction. Each standard of BTEX and methane was injected directly to water and purged profiles were examined. Results are shown in Fig. 4 and it can be seen that all purged profiles have similar shapes and approximately 70 % of BTEX are stripped by gas volume 80 mL. Purged profile of methane characterizes band spreading of compounds in the vial and is represented by gas volume about 20 mL. Obtained results, exponentially decrease of volatile analytes concentration with purging time (as well as in purge-and-trap method), are in coincidence with literature [19].

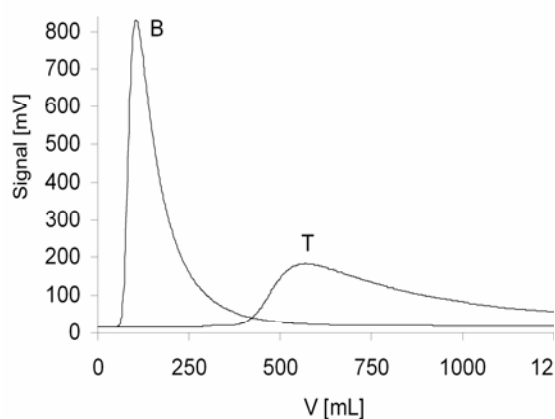


Fig. 3. The dependence of signal magnitude of benzene (B) and toluene (T) on the volume of carrier gas purged by INCAT device at the temperature of 40 °C and the flow rate of 20 mL min⁻¹.

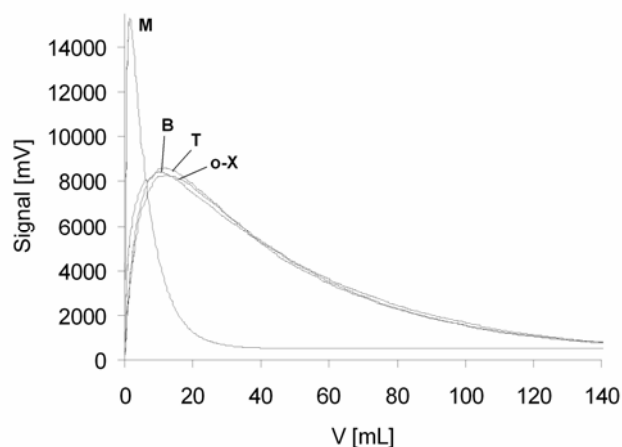


Fig. 4. The dependence of signal magnitude on the volume of stripping gas for individual BTEX and the methane at the temperature of 40 °C and the flow rate of 20 mL min⁻¹.

M – methane; B – benzene;
T – toluene; o-X – o-xylene.

Recoveries and sample capacity of INCAT device and SPME

The recoveries and sample capacity were studied at injection port temperature of 270 °C using of capillary column DB-1 and FID detector that has linear response in studied trace concentration range for BTEX compounds. Fig. 5 shows the dependences of BTEX peak areas on the concentration in water sample for INCAT device. It is evident that the peak area of benzene decreases from concentration approx. 2000 $\mu\text{g L}^{-1}$ which is a caused by oversaturation of INCAT device.

Fig. 6 illustrates the dependences of BTEX peak area on the concentration in water sample for SPME device. In this case, the dependences of BTEX peak areas do not follow linear trend and extracted amounts are much lower than for INCAT device.

There was an appreciable difference in recoveries too. INCAT recoveries of toluene, ethylbenzene and xylenes lie in range 65 - 90 % and slightly increase with increasing concentration. Values of benzene recovery are about 10 % lower in concentration range 0.2 - 2000 $\mu\text{g L}^{-1}$. It can be caused by breakthrough of benzene in INCAT device. Large decrease of recovery at concentration 5000 $\mu\text{g L}^{-1}$ is due to oversaturation of INCAT device. BTEX recoveries for SPME are much lower and very dependent on concentration (up to 20 % in concentration range 50 – 5000 $\mu\text{g L}^{-1}$ and maximum 45 % for lower concentration), which results from low sorption capacity and single extraction step of SPME fiber in comparison with new INCAT device.

In Fig. 7 are shown the chromatograms of BTEX compounds at concentration of 100 $\mu\text{g L}^{-1}$ individual aromatics obtained by INCAT and SPME methods. It is evident that the INCAT device provides much higher peaks than SPME method. In case of INCAT there is a shift of retention time of benzene and is probably caused by co-elution with water as solvent peak.

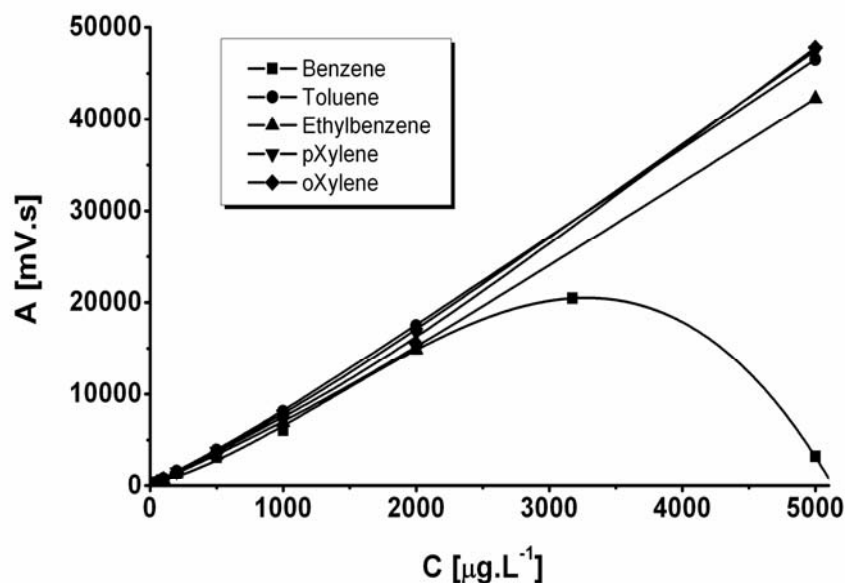


Fig. 5. The dependence of peak areas of individual BTEX on their concentration after the desorption from INCAT device.

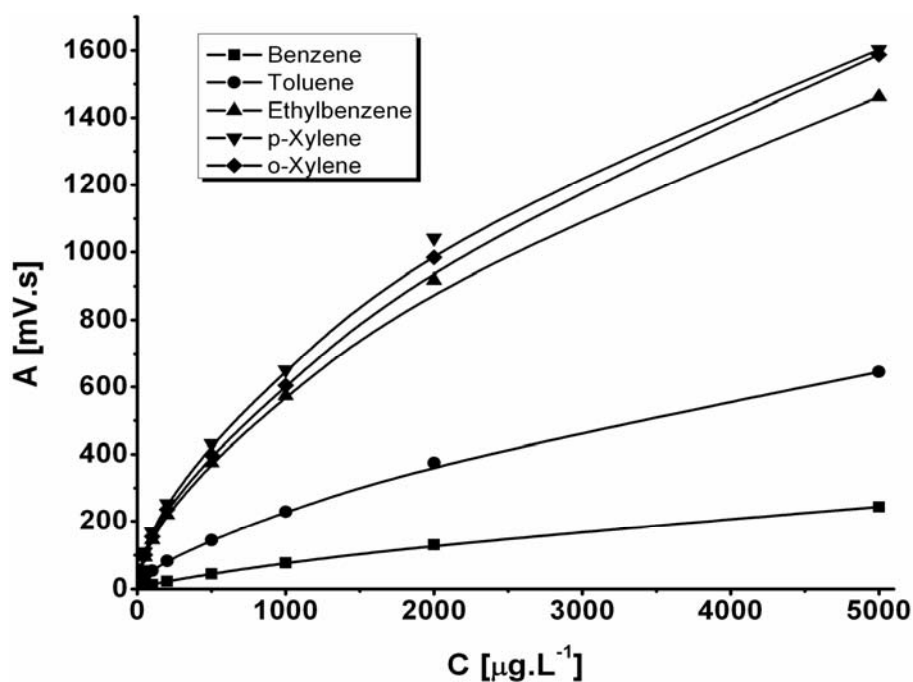


Fig. 6. The dependence of peak areas of individual BTEX on their concentration after the desorption from SPME fiber.

For INCAT method the limits of detection (LOD) values of BTEX are from 0.019 to 0.125 $\mu\text{g L}^{-1}$ and for SPME method are in the range from 0.027 – 0.382 $\mu\text{g L}^{-1}$ (Table 2). The LOD value is 3-times higher for benzene achieved by SPME method in comparison with

those achieved by INCAT method. The LOD values of toluene, ethylbenzene and xylenes are practically same for both methods. The INCAT method provides higher noise in comparison with SPME, which is caused by decomposition products from INCAT device during thermal desorption. Regression coefficients (R^2) for INCAT device are in range 0.998 - 0.999 in concentration range 0.2 - 100 $\mu\text{g L}^{-1}$ (benzene and o-xylene) and 0.2 - 200 $\mu\text{g L}^{-1}$ (toluene, ethylbenzene and p-xylene). Linearity of INCAT device in this range was verified by Mandel's fitting test what indicate values F_{cal} and F_{crit} for all tested components (Table 2).

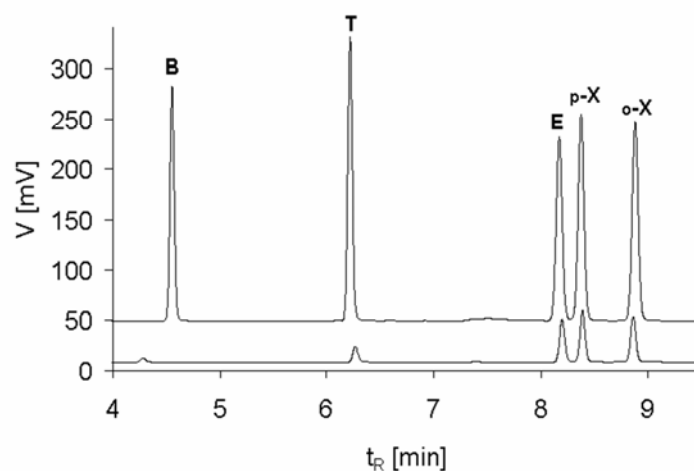


Fig. 7. Chromatograms of BTEX at concentration of 100 $\mu\text{g L}^{-1}$ for SPME (lower chromatogram) and INCAT device (upper chromatogram). *B* – benzene; *T* – toluene; *E* – ethylbenzene; *p-X* – p-xylene; *o-X* – o-xylene.

Table 2

The values of limits of quantification (LOQ), detection (LOD), noise and Mandel's fitting test for SPME and INCAT methods.

Analytes	SPME			INCAT			R^2	F_{crit}	F_{calc}
	LOQ	LOD	Noise	LOQ	LOD	Noise			
	[$\mu\text{g L}^{-1}$]	[$\mu\text{g L}^{-1}$]	[mV]	[$\mu\text{g L}^{-1}$]	[$\mu\text{g L}^{-1}$]	[mV]			
Benzene	1.042	0.382	0.032	0.341	0.125	0.056	0.99846 ^a	13.75	3.63
Toluene	0.393	0.144	0.030	0.284	0.104	0.067	0.99990 ^b	12.25	6.84
Ethylbenzene	0.207	0.075	0.031	0.199	0.073	0.074	0.99998 ^b	12.25	4.07
p-Xylene	0.074	0.027	0.031	0.052	0.019	0.050	0.99999 ^b	12.25	0.76
o-Xylene	0.185	0.068	0.048	0.161	0.059	0.053	0.99998 ^a	13.75	5.08

^a 9 points in graph (0.2 – 100 $\mu\text{g L}^{-1}$)

^b 10 points in graph (0.2 – 200 $\mu\text{g L}^{-1}$)

Conclusions

A new arrangement of the full inside volume needle capillary adsorption trap device with Porapak Q as a sorbent material and wet alumina as a source of desorptive water vapour flow enables high efficiency and repeatability of adsorption and desorption of trace quantities of BTEX from headspace of water matrix. The developed INCAT device is suitable for the analysis of BTEX in drinking and waste water samples. The limit of detection as well as limit of quantification of BTEX compounds analysed in INCAT device is comparable with those for SPME method. The main advantages of INCAT device in comparison with SPME device lie mainly in substantially higher extraction capacity, mechanically robustness and is easy to operate and optimize. Not negligible advantage is robustness to operating conditions changes during the sampling mode. The drawbacks involve the coelution of benzene and toluene with water as a solvent peak causing slightly worse detection and quantification limits in comparison with ethylbenzene and xylenes. Water also limits the use of the narrower column with thin film of stationary phase. Other potential problem is the rise in decomposing products of Porapak Q [20].

Acknowledgements

The authors thank the Slovak Grant Agency VEGA (grant No. 1/2467/05), and ESF (No. 54/04-I/32-DP, ITMS 131201 10048) for the financial support of this research.

References

1. Namiesnik J, Wardencki W (2000) J High Resol Chromatogr 23: 297
2. Fowler WK, Duffey CH, Miller HC (1979) Anal Chem 51: 2333
3. Jech L (1992), PhD Thesis, Charles University, Prague, Czech Republic.
4. Müller S, Efer J, Engewald W (1994) Chromatogr 38: 694
5. Qin T, Xu X, Polák T, Pacáková V, Štulík K, Jech L (1997) Talanta 44: 1683
6. McComb ME, Oleschuk RD, Giller E, Gesser HD (1997) Talanta 44: 2137
7. Shojanian S, Oleschuk RD, McComb ME, Gesser HD, Chow A (1999) Talanta 50: 193
8. Lipinski J (2001) Fresenius J Anal Chem 369: 57
9. Berezkin VG, Makarov ED, Stoljarov BV (2002) Neftekhim 42: 242
10. Berezkin VG, Makarov ED, Stoljarov BV (2003) J Chromatogr A 985: 63

3rd International Student Conference: “Modern Analytical Chemistry”

11. Wang A, Fang F, Pawliszyn J (2005) *J Chromatogr A* 1072: 127
12. Saito Y, Ueta I, Kotera K, Ogawa M, Wada H, Jinno K (2006) *J Chromatogr A* 1106: 190
13. Kubinec R, Berezkin VG, Górová R, Addová G, Mračnová H, Soják L (2004) *J Chromatogr B* 800: 295
14. Lord H, Pawliszyn J (2000) *J Chromatogr A* 885: 153
15. Water quality – Determination of benzene and some derivatives. ISO/DIS 11423 (1993)
16. Bianchi F, Careri M, Marengo E, Musci M (2002) *J Chromatogr A* 975: 113
17. EURACHEM Guide, 1st English ed (1998) *A Laboratory Guide to Method Validation and Related Topics*. In: *The Fitness for Purpose of Analytical Methods*, LGC, Teddington
18. Bruzzoniti MC, Cavalli S, Mangia A, Mucchino C, Sarzanini C, Tarasco E (2003) *J Chromatogr A* 997: 51
19. Kuráň P, Soják L (1996) *J Chromatogr A* 733: 119
20. Baltussen E, Cramers CA, Sandra PJF (2002) *Anal Bioanal Chem* 373: 3

GC STRUCTURE-RETENTION RELATION AND MASS SPECTROMETRY FOR IDENTIFICATION OF POLYALKENES DECOMPOSING PRODUCTS

Helena Jurdáková, Ladislav Soják, Róbert Kubinec, Žofia Krkošová, Jaroslav Blaško, Beáta Meľuchová, Eva Pavlíková

Faculty of Natural Sciences, Chemical Institute, Comenius University, Mlynská dolina CH-2, SK-842 15 Bratislava, Slovak Republic

Abstract

Low-density polyethylene and polypropylene were thermally decomposed individually in a batch reactor at temperatures up to 450 °C as a recycling route from the aspect of the production of petrochemical feedstock. More detailed separation of polyalkenes splitting compounds was achieved using high resolution GC (efficiencies up to 490 000 plates) than before. The GC-MS as well as the dependence of homomorphy factors and isopropyl group increments on the number of carbon atoms of alk-1-enes, alk-2-enes, alka- α,ω -dienes and alkanes were used for identification of separated analytes.

Thermal cracking of LDPE products in the range C₅-C₂₃ were characterized by quintets of peaks in the chromatogram which were assigned to *n*-alkanes, alk-1-enes, (*E*)-alk-2-enes, (*Z*)-alk-2-enes and alka- α,ω -dienes with average quantitative ratio 1 : 1.2 : 0.07 : 0.05 : 0.08. In fraction up to *n*-C₈ 140 GC peaks were separated and identified, including around 30 acyclic octenes.

In contrast to the polyethylene thermal cracking which yields products with straight-chain hydrocarbon structure, polypropylene cracking is characterized by the formation of compounds with branched and high prevalingly unsaturated hydrocarbon structure. The pretention of this analytical problem lies in stereoisomerism and corresponding multicomponentity of branched alkenes, alkadienes and alkanes in a broad range of carbon atoms number as characteristic decomposition products of polypropylene. Partial separation of all four diastereoisomers of

2,4,6,8-tetramethylundec-1-ene, which is the most abundant compound except for 2,4-dimethylhept-1-ene, was obtained. In the liquid fraction up to n -C₈ 84 peaks including around 40 acyclic octenes were identified. Other 149 GC peaks were analysed in the C₉-C₂₅ fraction with quantitative ratio of alkane : alkene : alkadiene equal to 1 : 17 : 4.

Keywords:

*High resolution gas chromatographic-mass spectrometric analysis.
Polyethylene and polypropylene thermal decomposition products.*

1. Introduction

Based on the analysis of oils and waxes from low-density polyethylene (LDPE) thermal decomposition at 500 °C to 700 °C, Williams and Williams [1] came to the conclusion that the wax was a very pure aliphatic material, with no aromatics and the oils produced up to 550 °C also contained no aromatic hydrocarbons or polycyclic aromatic hydrocarbons. Oil/wax products from polyethylene cracking are composed predominantly from straight-chain alkanes and alk-1-enes in the range of carbon atoms from C₈ to C₅₇. The products formed during PP cracking are mostly a complex mixture of branched alkenes and alkanes [2,3]. Such composition of oil/waxes from cracking of PE or PP at mild temperatures seems to be favourable, because these mixtures may be used as co-feed for many downstream processing units. They may be fed to a steam cracker, to produce reusable alkenes [4,5] or fed to a catalytic cracker to produce gasoline or upgraded in a hydrocracker [4]. The content of alkanes, alkenes, alkadienes, and aromatics determines the character of further chemical recycling of cracking products from waste polyalkenes.

The problems of identification of gas chromatographic separated analytes are related to the absence of reference materials, lack of published retention data as well as their insufficient reproducibility, insufficient precision of structure-retention relationships, and retention calculation methods, and with the limitation of hyphenated chromatographic-spectrometric techniques (GC-MSD-FTIRD) as well [6].

The product distribution of thermal decomposition of

polyalkenes has been studied by several authors. Gas chromatographic analysis with mass spectrometric detection showed that polyethylene (PE) degradation products display distinct gas chromatographic patterns of a series triplets composed of the aliphatic hydrocarbons having the same carbon atom number in a broad range of carbon atoms eluted on the apolar stationary phase in the order alka- α,ω -diene, alk-1-ene and n -alkane (Fig.1) [1]. Other authors stated that the thermal decomposition of high-density polyethylene (HDPE) yielded characteristic quartets of GC peaks in the chromatogram which were assigned to n -alkanes, alk-1-enes, alk- x -enes (alkenes with internal double bond), and alka- α,ω -dienes in the range C₄-C₂₂ [7,8]. Predel and Kaminsky [7] identified alk- x -enes in PE degradation product as alk-2-enes. The evolution of semivolatile compounds and toxic by-products in the pyrolysis of polyethylene has been studied from 600 to 900 °C and yields of around 150 semivolatile compounds were determined [9].

Thermal cracking of polypropylene (PP) in comparison with polyethylene gives different distribution components because of different splitting mechanisms of starting polyalkenes (Fig. 2.) [10,11]. In PP decomposition product the branched isomers are formed due to the branched structure. Marin et al. [11] determined about 50 compounds up to C₁₁, while 2,4-dimethylhept-1-ene was the most abundant compound. In higher boiling part of PP degradation product the presence of different stereoisomers in polypropylene degradation product was explained and analytically characterized by Jakab et al. [12]. Trimer 2,4-dimethylhept-1-ene was the main product of polypropylene splitting. Tetramer, pentamer, hexamer and heptamer, i.e. oligomeric alk-1-enes with carbon number $3n$ (C₁₂, C₁₅, C₁₈, C₂₁) where n is the number of monomeric units, were other significant splitting compounds. Also the presence of alk-1-enes with carbon number of $3n+1$ (C₁₀, C₁₃, C₁₆, C₁₉), alk-2-enes with carbon number $3n+2$ (C₁₁) and $3n$ (C₉, C₁₂), alkanes with carbon number $3n+2$ (C₈, C₁₁, C₁₄, C₁₇), and alka- α,ω -dienes $3n+1$ in a broad range of carbon atom numbers (C₁₀, C₁₃, C₁₆, C₁₉, C₂₂) was ascertained.

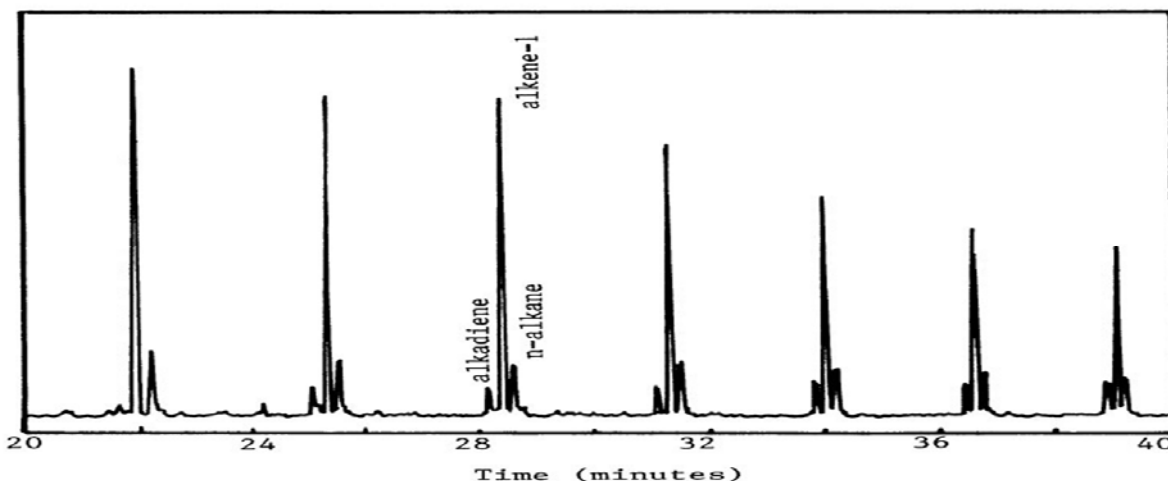


Fig.1. P.T. Williams, E.A. Williams, *J. Anal. Appl. Pyrolysis* 51 (1999) 107–126 [1].

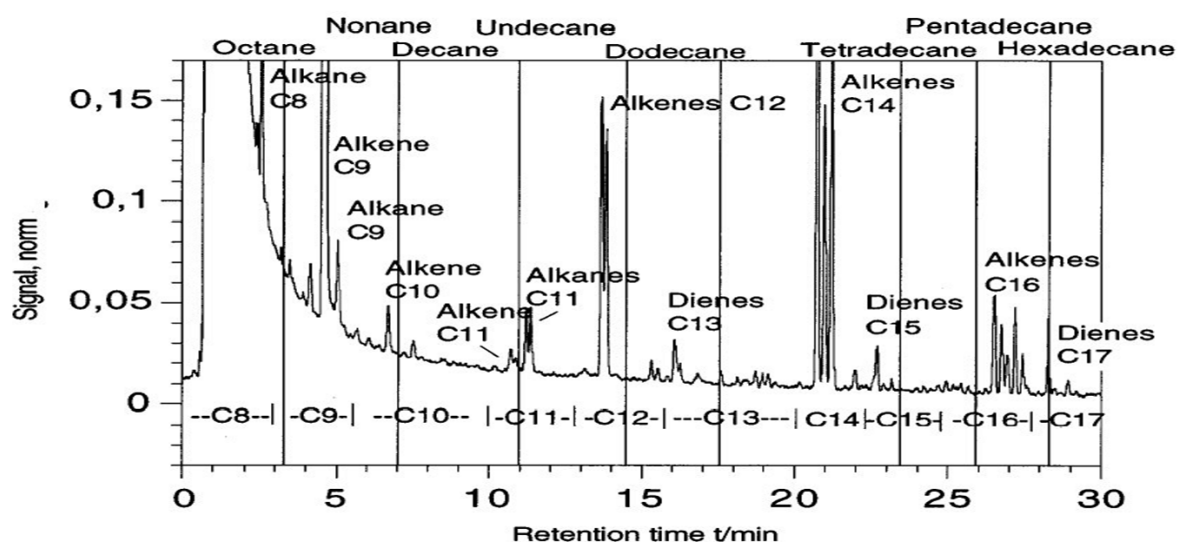


Fig.2. H. Bockhorn et al., *J. Anal. Appl. Pyrolysis* 48 (1999) 93–109 [10].

In previous works, the capillary gas chromatographic separation systems with moderate high separation efficiency were used for analytical separation of polyalkenes degradation products. The capillary columns (length 25 or 30 m and 250 μm I.D.) coated with a non-polar dimethylsilicone stationary phase were used regularly for separation, and maximum length was 60 m and 250 μm I.D. [13,14]. The aim of this work was to demonstrate the effect of using the more efficient gas chromatographic separation system for separation,

identification and quantification of LDPE and PP thermal cracking products for obtaining more detailed and reliable results on the liquid product composition.

2. Experimental

2.1. Material of LDPE and PP plastics

The polyalkenes: low-density polyethylene ($r = 919 \text{ kg.m}^{-3}$, $\overline{M}_n = 22.000$, $\overline{M}_w = 292.000$), and polypropylene (98% isotactic, $r = 903 \text{ kg.m}^{-3}$, $\overline{M}_n = 65.000$, $\overline{M}_w = 200.000$) were obtained from Slovnaft, Inc. (Bratislava, Slovak Republic) and are virgin plastics. The diameter of pellets ranged from 3.5 to 4.5 mm and 3.3 to 4.0 mm for LDPE and PP, respectively.

2.2. Preparation of liquid products from the thermal cracking of polyalkenes

The aim of the thermal cracking of the polyalkenes was to prepare high yields of oil/waxy products suitable for next recycling. LDPE and PP were thermally decomposed separately in a nitrogen atmosphere in a stainless-steel batch reactor. The substantial amount of the oil/wax product was formed in the narrow temperature range from 440 to 450°C. The low formation of gases and also of residue on the bottom of the reactor was observed. The final temperature of 450 °C in the reactor was reached after 45 minutes. This level of temperature in the reactor was maintained for another 35 minutes to allow the release of the maximum amount of decomposing products from the reactor.

Both LDPE and PP polyalkenes produced a hydrocarbon gas, a light yellow oil/wax fraction (80 mass % from LDPE and 85 mass % from PP) and little solid residue. The oil/wax products were subsequently separated into liquid and solid fractions by fractional distillations under atmospheric and reduced pressure (1.6 kPa) in nitrogen atmosphere. The distillation range of liquids from atmospheric distillation was from 40 to 180 °C (PE 1, PP 1) and the final boiling point of liquids from distillation under reduced pressure (PE 2, PP 2) was approximately 325 °C. In regard to the initial

polyalkene, the yield of liquid distillates from LDPE represented 51.9 mass % and that from PP represented 59.2 mass %. Thereafter, prepared liquid distillates were analysed by high resolution capillary gas chromatography with mass spectrometric detection.

2.3 GC-MS

The products of polyalkenes thermal cracking were separated by high resolution capillary gas chromatography with efficiency up to 490 000 effective plates (for (*Z*)-oct-2-ene with $k = 22.8$ at 30 °C) using Petrocol DH column 150 m x 250 mm i. d., 1.0 mm film (Supelco, Bellefonte, USA) under isothermal (up to C₈) [15] and temperature-programmed conditions in the range 40-300 °C with gradient 1 °C/min. (up to *n*-C₂₃). GC-MS measurements were performed on a gas chromatograph Agilent Technologies 6890N and 5973 Network mass selective detector. Degradation components were identified by comparing measured and published retention data and by structure-retention correlations of hydrocarbon homologues as well as oligomeric series, and mass spectra were interpreted by matching the results with library spectra.

3. Results and discussion

3.1 GC of polyethylene thermal cracking products

The chromatogram of PE 2 product is given in Fig. 3. and contains two dominant products which are alk-1-enes and *n*-alkanes in the range C₆-C₂₃. Beside these main PE decomposition products the chromatogram is fully occupied by several hundreds small peaks of other compounds. From comparison of published chromatograms (Fig. 1) and those measured in this work (Fig. 3) follows that the peak of alka- α,ω -dienes obtained in moderate efficient column by high resolution column shows the presence of at least two compounds. Follows that quantitative data of alka- α,ω -dienes measured in common efficient capillary columns are surplus value.

The presence of alk-*x*-enes, resp. alk-2-enes was documented in a polyethylene cracking product separated in common capillary column [7,8]. More efficient separation in high resolution column

(Fig. 3) showed that peaks which are eluted in this retention area are (*Z*)-alk-2-enes. In moderate efficient column with high probability these isomers interfered with other product compounds and quantitative data are also surplus value.

The determined presence of (*Z*)-alk-2-enes was ground to ascertain possible presence of (*E*)-alk-2-enes in the PE decomposition products. The chromatogram in Fig. 3 shows that these (*E*)-alk-2-enes are eluted immediately after *n*-alkanes. This finding suggests that the quantitation of *n*-alkanes is influenced by coelution of (*E*)-alk-2-enes in PE decomposition products analysed in capillary columns of moderate efficiency.

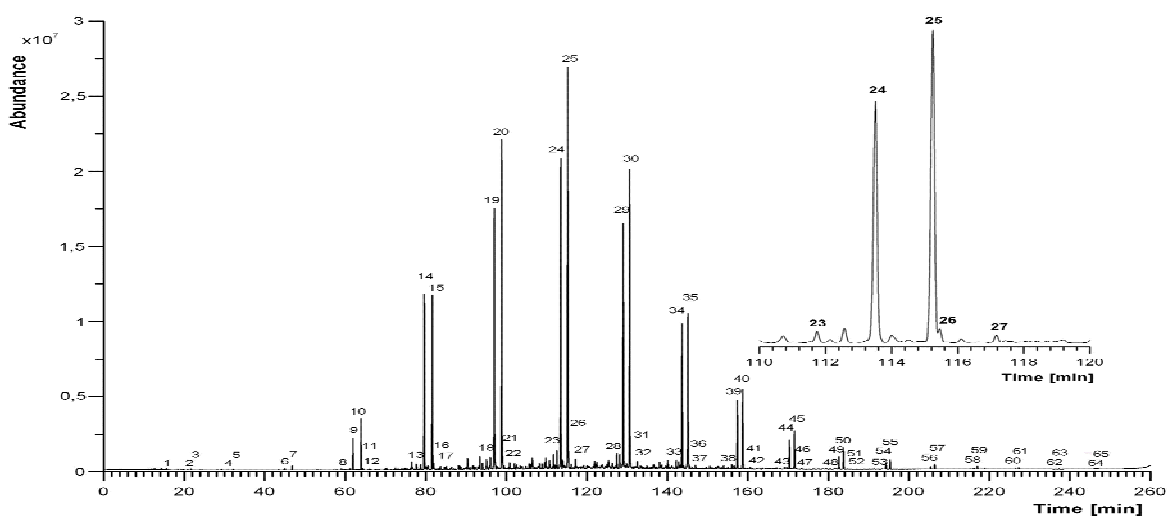


Fig. 3. GC-MS/TIC chromatogram of the separation of polyethylene thermal cracking products (PE 2 fraction).

Because of the lack of standard materials and retention data of alka- α,ω -dienes, (*E*)-alk-2-enes and (*Z*)-alk-2-enes with higher carbon atoms number and limitation of mass spectral data for resolution of (*E*)/(*Z*) isomers these analytes were preliminary identified on the basis of homomorphy factors H [6]. The H value is defined as the difference of retention index of the analyte and *n*-alkane with the same carbon atoms number. Under isothermic separation conditions the H values for hydrocarbon homologous series exhibit characteristic moderately non-linear asymptotical decreasing dependence on the number of carbon atoms of homologues. The decrease of H values is apparent up to about six carbon atoms from the beginning of the given homologous structural trait. Based on chromatogram obtained at linear

temperature programmed column in Fig. 3, the linear retention indices I_P and temperature programmed H_P values were calculated for alka- α,ω -dienes, alk-1-enes, n -alkanes, (E)-alk-2-enes and (Z)-alk-2-enes. The dependence $H_P = f(C_Z)$ at programmed column temperature is affected also by different retention temperature dependence of analytes. The H_P values increase with increasing number of carbon atoms for (Z)-alk-2-enes, alk-1-enes and alka- α,ω -dienes but decrease for (E)-alk-2-enes (Fig. 4). The regularities of these dependences allowed preliminary identification of these analytes. Negative temperature coefficients of Kováts retention indices (dI/dT values) of (E)-alk-2-enes [15] affected difficulties in their separation from corresponding n -alkanes with increasing carbon number of n -alkanes and increasing column temperature, respectively. This preliminary identification was confirmed by mass spectrometric detection of separated peaks. On the basis of these results the thermal decomposition of PE can be characterized by quintets of peaks in the chromatogram which were assigned to n -alkanes, alk-1-enes, (E)-alk-2-enes, (Z)-alk-2-enes and alka- α,ω -dienes. The average weight quantitative ratio for C_6 - C_{12} (area % of TIC) n -alkane: alk-1-ene : (E)-alk-2-ene : (Z)-alk-2-ene : alka- α,ω -dienes is 1 : 1.2 : 0.07 : 0.05 : 0.08. However, it must be noted that coelution of these with other compounds can not be excluded under high resolution separation system used.

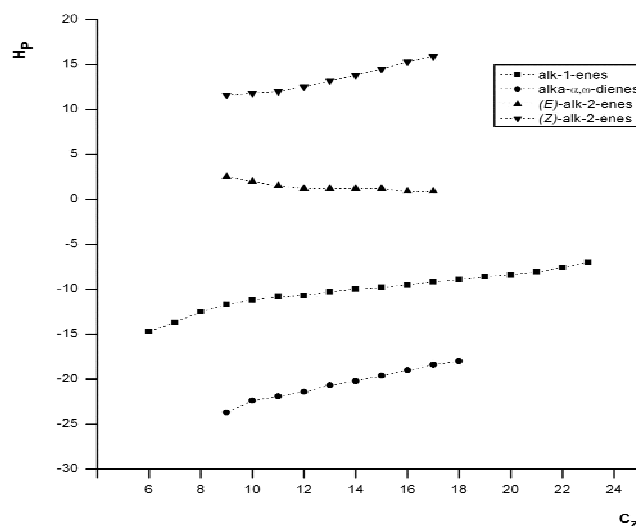


Fig. 4. Dependence of homomorphy factors $H_P = f(C_Z)$ at programmed column temperature for homologues series of alk-1-enes, alka- α,ω -dienes, (E)-alk-2-enes and (Z)-alk-2-enes from the PE 2 fraction on polydimethylsiloxane.

3.2 GC of polypropylene thermal cracking products

In contrast to the thermal polyethylene cracking products with straight-chain hydrocarbon structure, the formation of compounds with branched high prevailing unsaturated hydrocarbons structure is characteristic for polypropylene. It corresponds to the analogous free radical degradation mechanisms and different molecular structure of both polyalkenes [16]. Due to the polypropylene branched structure the variety of products is more complex than from PE degradation, and the stereoisomers are formed.

The chromatogram of PP 2 in Fig. 5 shows more than 400 partially separated GC peaks. For preliminary identification of PP 2 products the dependence of isopropyl group increments to the linear retention indices (I_{ip} values) on the number of carbon atoms of oligomeric $3n$ and $3n+1$ alk-1-enes, as well as $3n$ and $3n+2$ alk-2-enes, $3n+1$ alka- α,ω -dienes and $3n+2$ alkanes were used; first eluted diastereoisomers which are most abundant compounds were correlated. The regularities of these dependences are demonstrated in Fig. 6, and corresponding identification was confirmed by mass spectrometry.

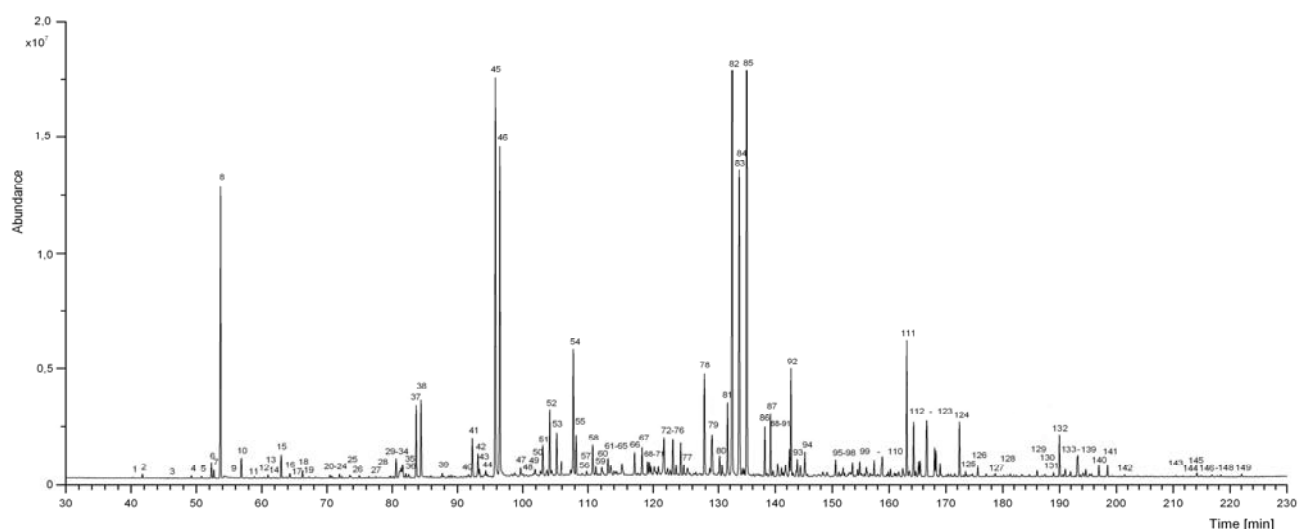


Fig. 5. GC-MS/TIC chromatogram of the separation of polypropylene thermal cracking products (PP 2 fraction).

Peak identification is in Table 2.

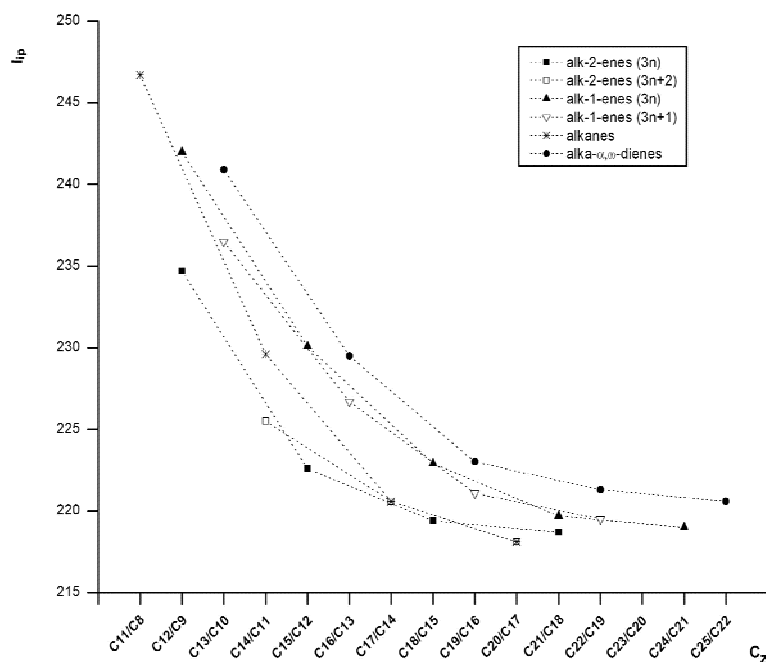


Fig. 6. Dependence of isopropyl group increments I_{ip} on the number of carbon atoms of alk-2-enes, alk-1-enes, alkanes and alka- α,ω -dienes from the PP 2 fraction on polydimethylsiloxane.

Under electron impact ($EI, 70\text{ eV}$) working conditions in the positive-ion mode, the molecular ions M^+ were observed for all identified compounds. As the specific MS ions were ascertained: for $3n$ alk-2-enes the abundances ratio of m/z 69 and 83 equal to 0.39, for $3n+2$ alk-2-enes m/z 69/83 = 10, for $3n+1$ alka- α,ω -dienes m/z 109/83 = 1.0, for $3n+2$ alkanes m/z 71/83 = 12, for $3n$ alk-1-enes and $3n+1$ alk-1-enes was the abundance ratio m/z 69/83 equal to 2.1 and 1.6 respectively and their resolution was completed on the basis of different molecular ions M^+ . The mass spectra of $3n$ alk-1-enes, $3n+1$ alk-1-enes, $3n$ alk-2-enes, $3n+2$ alk-2-enes, $3n+1$ alka- α,ω -dienes, and $3n+2$ alkanes with signed specific MS ions for most abundant diastereoisomers are given in Fig. 7.

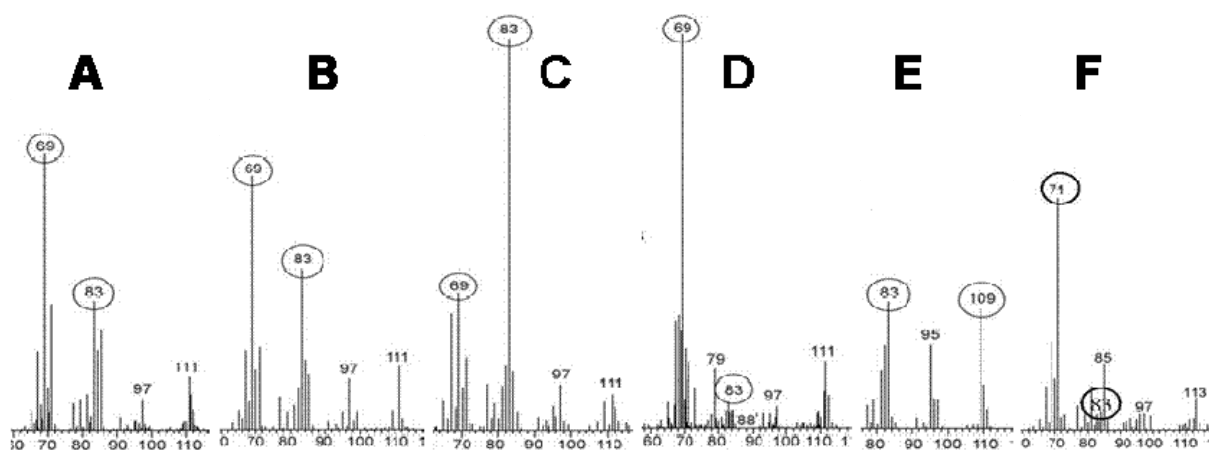


Fig. 7. Mass spectra of $3n$ alk-1-enes (A), $3n+1$ alk-1-enes (B), $3n$ alk-2-enes (C), $3n+2$ alk-2-enes (D), $3n+1$ alka- α,ω -dienes (E), and $3n+2$ alkanes (F) with signed specific MS ions.

Summary the following was found in the PP 2 product:

- C_9 , C_{12} , C_{15} , C_{18} , C_{21} and C_{24} $3n$ alk-1-enes, the most abundant were C_{15} diastereoisomers of 2,4,6,8-tetramethylundec-1-ene,
- C_{10} , C_{13} , C_{16} , C_{19} and C_{22} $3n+1$ alk-1-enes, the most abundant were C_{16} diastereoisomers of 2,4,6,8,10-pentamethylundec-1-ene,
- C_9 , C_{12} , C_{15} , C_{18} and C_{21} $3n$ alk-2-enes, the most abundant were C_{15} stereoisomers of 4,6,8,10-tetramethylundec-2-ene,
- C_{11} , C_{14} , C_{17} and C_{20} $3n+2$ alk-2-enes, the most abundant were C_{14} stereoisomers of 4,6,8-trimethylundec-2-ene,
- C_{10} , C_{13} , C_{16} , C_{19} , C_{22} and C_{25} $3n+1$ alka- α,ω -dienes, the most abundant were C_{16} diastereoisomers of 2,4,6,8,10-pentamethylundeca-1,10-diene,
- C_8 , C_{11} , C_{14} , C_{17} and C_{20} $3n+2$ alkanes, the most abundant were C_{14} diastereoisomers of 4,6,8-trimethylundecane.

The 149 GC peaks were analysed in the C_9 - C_{25} range. Overall quantified area of gas chromatographic peaks corresponds of 83.4 % to the identified compounds. On the basis of obtained chromatogram the calculated ratio of alkane : alkene : alkadiene in thermal cracking product of polypropylene is 1 : 17 : 4 (area % of TIC). Using an ASTM D 1319 method 5.5 % of alkanic, 93.3 % alkenic and 1.2 % vol. of aromatic hydrocarbons were determined. Obtained product distributions is valid for used non-isothermal cracking conditions, and for 98 % tacticity of the polypropylene. Polypropylene with other

tacticity afford different diastereomers because of the different stereochemistry along the backbone but the amounts of a given alkene or alkane product are the same [17].

The pretension of this analytical problem lies in stereoisomerism thus in the multicomponentity of branched alkenes, alkadienes and alkanes as main decomposition products of polypropylene. In the case of alk-1-enes which are the most abundant components, there are two possible diastereoisomers for 2,4,6-trimethylnon-1-ene, which are base-line separated also in column with moderate efficiency. For 2,4,6,8-tetramethylundec-1-ene, which is most abundant compound of PP 2, there are four possible diastereoisomers, and the moderate efficient capillary column these stereoisomers separated in three peaks [11]. Partial separation of all four diastereoisomers could have been obtained under extreme separation efficiencies only. The number of possible diastereoisomers increases with higher analysed alkene oligomers, e.g. there are eight possible diastereoisomers for analysed 2,4,6,8,10-pentamethyltridec-1-ene. For other hydrocarbon groups, e.g. for 4,6,8,10-tetramethyltridecane, there are six possible diastereoisomers, and for 2,4,6,8,10-pentamethylundeca-1,10-diene, there are three possible diastereoisomers. In the case of alk-2-enes the situation is more complex because of addition of asserting (*E*)/(*Z*) isomerism. Higher stereoisomers are eluted in a relative broad retention range, and the possibilities of separation interference of stereoisomeric alkenes, alkadienes and alkanes as well as other hydrocarbon types as PP cracking product components increases with an increasing number of carbon atoms.

Conclusions

The advantages of the use of high resolution GC in analysis of polyalkenes degradation products include better separation of multicomponent product mixtures and corresponding more characteristic measured mass spectra, that leads to the more reliable identification and to more precise quantitative results. Based on using high resolution GC, more compounds, mainly isomeric acyclic alkenes, were ascertained in polyethylene and polypropylene degradation products when compared with those described in earlier literature reports. More detailed and reliable qualitative and

quantitative results poses presumption for more detailed explanation of reaction mechanism and better optimization of reaction process for obtaining wishing products.

Acknowledgements

Support for this work was provided by VEGA-Slovakia (1/2467/05), and ESF (No. 54/04-I/32-DP, ITMS 131201 10048). The authors thank Dr. Andrej Boháč (Comenius University, Bratislava), for stereochemical analysis of diastereoisomeric hydrocarbon products.

References

- 1 P.T. Williams, E.A. Williams, *J. Anal. Appl. Pyrolysis*, 51 (1999) 107.
- 2 E. Kiran, J.K. Gillham, *J. Appl. Polym. Sci.*, 20 (1976) 2045.
- 3 T.M. Kruse, H.W. Wong, L.J. Broadbelt, *Macromolecules*, 36 (2003) 9594.
- 4 K.C. Kirkwood, S.A. Leng, W. David, *Polymer Cracking*, US Patent 5364995 (1992).
- 5 E. Hájeková, M. Bajus, *J. Anal. Appl. Pyrolysis*, 74 (2005) 270.
- 6 L. Soják, *Petroleum and Coal*, 46 (2004) 1.
- 7 Ch. Breen, Ph.M. Last, S. Taylor, P. Komadel, *Thermochim. Acta*, 363 (2000) 93.
- 8 M. Predel, W. Kaminsky, *Polym. Degrad. Stab.*, 70 (2000) 373.
- 9 R. Font, I. Aracil, A. Fullana, I. Martín-Gullón, J.A. Conesa, *J. Anal. Appl. Pyrolysis*, 69 (2003) 599.
- 10 H. Bockhorn, A. Hornung, V. Hornung, D. Schawaller, *J. Anal. Appl. Pyrolysis*, 48 (1999) 93.
- 11 N. Marin, S. Collura, V.I. Sharypov, N.G. Beregovtsova, S.V. Baryshnikov, B.N. Kuznetsov, V. Cebolla, J.V. Weber, *J. Anal. Appl. Pyrolysis*, 65 (2002) 41.
- 12 E. Jakab, G. Várhegyi, O. Faix, *J. Anal. Appl. Pyrolysis*, 56 (2000) 273.
- 13 L. Ballice, R. Reimert, *Chem. Eng. Process.*, 41 (2002) 289.
- 14 L. Ballice, *Fuel*, 81 (2002) 1233.
- 15 L. Soják, G. Addová, R. Kubinec, A. Kraus, A. Boháč, *J. Chromatogr. A*, 1025 (2004) 237.
- 16 R.P. Lattimer, *J. Anal. Appl. Pyrolysis*, 31 (1995) 203.
- 17 T.M. Kruse, H.W. Wong, L.J. Broadbelt, *Macromolecules*, 36 (2003) 9594.

ANALYSIS OF CONJUGATED LINOLEIC ACID ISOMERS IN EWE MILK PRODUCTS BY GC-MS

J. Blaško, L. Soják, R. Kubinec, Ž. Krkošová, H. Jurdáková, B. Meľuchová, E. Pavlíková,

Faculty of Natural Sciences, Chemical Institute, Comenius University, Mlynská dolina CH-2, SK-842 15 Bratislava, Slovak Republic

Abstract

High resolution GC-MS separation system with a polar stationary phase and efficiency of 450 000 plates was used for separation of fatty acid methylesters in ewe milk and cheese fats. The seasonal changes in *c*₉,*t*₁₁-18:2 isomer from two ewe milk processing plants were investigated. The content of CLA of dairy products decrease from 3.4.% in May to 1.5 % of FAME in October for first plant (Tisovec) (average content 2.5 %), and similarly from 3.2 to 1.5 % of FAME (average content 2.5 %) for second plant (Ružomberok). The determined contents of CLA in grazed ewe fats are higher than published contents. The seasonal variations of CLA in grazed ewe milk fat probably are connected mainly with seasonal changes in pasture composition.

1. Introduction

1.1 Isomeric conjugated linoleic acids

Conjugated linoleic acids (CLA) are octadecadienoic acids (18:2) that have a conjugated double-bond system. Interest in these compounds has expanded since CLA were found to be associated with a number of physiological and pathological responses such as cancer, metastases, atherosclerosis, diabetes, immunity, and body/fat protein composition [1-4].

CLA was originally intended to describe only those isomers in fats from ruminants showing anti-carcinogenic properties [5]. They were thought to be similar to the commercially available conjugated octadecadienoic acid isomers obtained by alkali isomerization of linoleic acid (*c*₉,*c*₁₂-18:2) [6]. Data from animal models reportedly

suggest that the *c9,t11*-isomer is responsible for CLA anti-carcinogenic properties [7].

The main sources of these conjugated fatty acids are dairy fats. Rumen bacteria convert polyunsaturated fatty acids, especially linoleic and linolenic acids, to CLA and numerous *trans*-containing mono- and diunsaturated fatty acids. An additional route of CLA synthesis in ruminants and monogastric animals, including humans, occurs via Δ^9 desaturation of the *trans*-18:1 isomers. The most abundant CLA and *trans*-18:1 isomers in normal dairy and beef fats are *c9, t11*-18:2 and vaccenic acid *t11*-18:1.

To date, a total of 6 positional CLA isomers have been found in dairy fats, each occurring in 4 geometric forms (*cis,trans*; *trans,cis*; *cis,cis* and *trans,trans*). Theoretical there are 14 possible positional isomers counting from carbons 2,4 to carbon 15,17 for a total of 56 possible isomers. The double bond positions of CLA isomers actually identified in rumen fat range from 6,8-18:2 to 12,14-18:2 in most of the possible geometric configuration for a total of about 20 isomers.

Dietary supplements enhanced in CLA are being developed and marketed in response to the reported physiological benefits found in animal models. Triacylglycerols containing CLA have recently been prepared by acidolysis of fish oils [8] and butterfat [9]. Other procedure includes of esterification of glycerol to triacylglycerols containing more than 95 % CLA [10]. The problem of determining the isomeric CLA composition of these products is a challenging analytical task.

It is essential that we know which isomers of CLA are contained in dietary supplements because our knowledge of the active isomers and models of action of CLA is incomplete. For example, the *c11,t13* isomer is reported to selectively concentrate in pig heart phospholipids [11] when pigs are fed CLA derived from extensive alkali isomerization of linoleic acid. As a result of this finding, most commercial CLA preparations now exclude the *c11,t13* isomer and consist primarily of the *c9,t11* and *t10,c12* isomers of CLA with lesser amounts of the *t8,c10* and *c11,t13* isomers [12] because the biological effects of *c11,t13* isomer remain to be explored.

The true impact of CLA in the diet must rely on availability of pure CLA isomers for the accurate identification and analysis of CLA isomers. No gas chromatographic columns or conditions have been

reported to date that will adequately resolve all the fatty acid methylesters of the isomers of CLA that have been identified in natural products and dietary supplements. The task requires high efficient separation systems and complementary techniques.

1.2 Dairy fats as source of CLA

The observation [1] that several CLA isomers are synthesized also in mammary and other tissues from 18:1 precursors in ruminants has forced researchers to consider the analyses of the 18:1 isomers as well as the CLA isomers. The most abundant CLA and *trans*-18:1 isomers in normal dairy and beef fats are *c9,t11*-18:2 and vaccenic acid *t11*-18:1.

Complex study about CLA composition in dairy fats of ruminants (cow, ewe, goat), mare milk, sow milk and human milk was realized by Jahreis et al. [4]. Its variation in milk fat of the bulk and individual samples was substantial (0.07 – 1.35 % of FAME). CLA in milk fat of all ruminants was season dependent. Ewe milk is rich in CLA (1.1 %). Among non-ruminants mare milk was nearly CLA-free (0.09 %). Human milk contained significantly more CLA (0.42 %) in comparison with the analyzed milk of the other monogastrides. There are differences between milk and non-milk drinkers. The order of the species according to the increasing CLA concentration in milk is: mare, sow, woman, goat, cow and ewe. The concentration of milk CLA in different ruminant species varied with the seasons. The greatest seasonal differences were measured in ewe milk which contains not only the highest content of CLA, but also the highest content of total *trans* fatty acids as well as *trans* vaccenic acid.

1.3 Analysis of isomeric CLA and other fatty acids in milk products

Our understanding of the biological role of CLA relies on the proper separation from biological and chemical matrices. Contemporary methods for CLA in biological samples consist of lipid extraction [13] and fractionation of lipid classes by thin layer chromatography (TLC) or high performance liquid chromatography (HPLC) as a prelude to further sample workup and analysis by silver

ion HPLC, gas chromatography (GC), mass spectrometry (MS), Fourier transform infrared (FTIR) spectroscopy [14], or nuclear magnetic resonance (NMR) [15].

Gas chromatography is often the only method used in the analysis of fatty acids for CLA, although the information on CLA isomeric composition is incomplete. Milk fats may contain up to 400 different fatty acids differing in chain length, branching, unsaturation, geometric and positional configuration, and functional groups [16]. A polar capillary GC column CP-Sil 88 or Supelcowax SP 2560 is absolutely mandatory for the analysis of isomeric CLA [17]. The CLA region of milk and tissue lipid extracts lies between the elution of 18:3 n -3/20:1 and 20:2 n -6. The region is essentially free of other fatty acids except for 21:0 FAME using a 100 m polar capillary column.

Capillary GC-MS combines an efficient separation and identification technique that can provide elemental composition, double bond equivalently and mass spectra indicating the location of double bonds for CLA and related compounds. However the electron impact (EI) mass spectra of individual CLA methyl esters are indistinguishable. The EI mass spectrum of the *c*9, *t*11-18:2 isomer

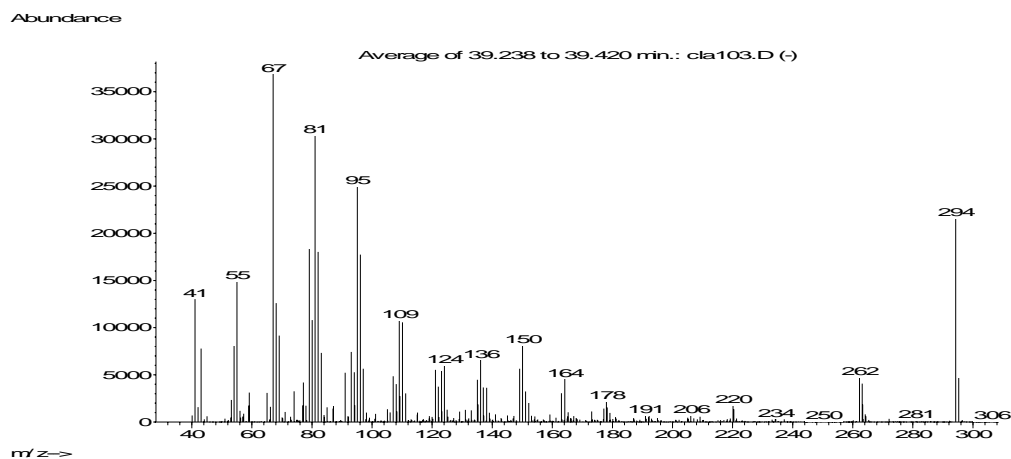


Fig.1: The EI mass spectrum of the of *c*9,*t*11-18:2

In the present study, under conditions of high resolution capillary gas chromatography hyphenated with mass spectrometric detection, the fatty acid compositions, mainly content of isomers of conjugated linoleic and oleic acid, of Slovak grazing ewe milks and milk products were investigated.

2. Experimental

2.1 Milk fat extraction

Lipids were extracted from the milk and milk products using chloroform and methanol as described by Bligh and Dyer [18] with some modifications regarding sample weight, solvent volume, and centrifugation speed and time. Approximately 200 mg of cheese or 2 mL of fluid milk products was homogenized with 2 mL of methanol and 2 mL of chloroform using a shaker (Heidolph, Rotamax 120, Germany) for 10 min at medium speed. Then, 2 mL of chloroform was added to the mixture, and homogenized for an additional 10 min on. The homogenate was centrifuged at 4000 rpm for 15 min using a Heraeus centrifuge (Heraeus Christ, Germany). The upper layer (methanol and water) was removed through aspiration. The middle and the lower layers (chloroform and precipitated protein, respectively) were filtered through filter paper to separate precipitate particles. The chloroform-lipid extracts were again filtered through anhydrous sodium sulfate (Na₂SO₄). The lipid extracts were dried under stream of nitrogen at 50 °C, and stored in 4-mL brown glass vials under nitrogen at -18 °C. The lipid samples were then used for the analysis of CLA and fatty acids *trans* isomers.

To prepare methylesters of fatty acids was used basic transesterifying agents, 0.5 M sodium methoxide in dry methanol. A sample of 10 to 50 mg of the extracted lipids was weighed and derivatized in screw-capped tubes with 2 mL of 0.5 M sodium methoxide in methanol for 30 min at 50 °C. At the end of the appropriate time, dilute acid is added to neutralize the sodium methoxide and so minimize the risk of hydrolysis occurring, and then was methyl esters extracted by 1 mL hexane for 10 min on shaker (Heidolph, Rotamax 120, Germany).

2.2 GC-MS analysis

An Agilent Technologies 6890N Network GC System Chromatograph (Waldbronn, Germany) equipped with an Agilent Technologies 7683 Series Splitless Injector and an Agilent Technologies 5973 Quadrupole Mass Selective Detector was used. A J

& W Scientific column DB-23 (60m×0.25mm I.D.), 0.25 µm film thickness column of polar stationary phase and coupled columns HP-88 (2 x 100m x 0.25 mm I.D.), 0.2 µm film thickness were employed with helium (99.999% purity) as carrier gas at a constant pressure of 1 mL/min. The oven temperature was programmed at 15 °C/min from 80 °C to 180 °C, and then held for 40 min. Injector temperature was set at 280 °C and the transfer line temperature at 260 °C. Split injection volume was 1 µL.

Identification of separated components was obtained on the basis of standard reference materials of FAs, published chromatograms and mass spectra data. Methyl esters of fatty acids were quantified by internal normalization.

3. Results and discussion

3.1 Analysis of Slovak ewe cheese "bryndza"

It was analyzed the sample of ewe's milk product - raw ewe milk, ewe's cheese, Slovak ewe cheese "bryndza", and "žinčica", from two regions of Slovakia around Ružomberok and around Tisovec. On the Figures 2 and 3 are GC-MS chromatograms of separation Slovak ewe cheese "bryndza" from Tisovec, during different seasons. From previous studies it is known that milk fat from ewes, cows and other ruminants grazing pasture had higher CLA content, than milk fat from ewes, cows and other ruminants feed a silage diet. Fig. 2 illustrates the chromatogram of "May bryndza" with the highest CLA content and Fig. 3 chromatogram "winter bryndza" of with the lowest CLA content. The CLA content depend on many factors, such as diet, animal's breed and age. We suppose that high content of CLA in Slovak ewe's milk products depends on the herbage effect upon the forage species.

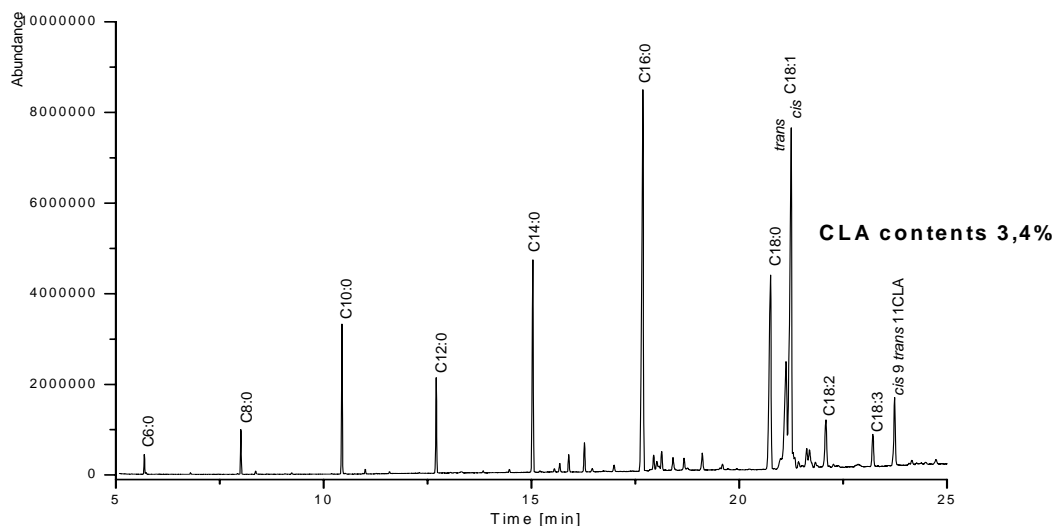


Fig. 2: GC-MS/TIC chromatogram of separation Slovak ewe cheese "bryndza" with the highest content of conjugated linoleic acid ("May bryndza").

Sample was separated in column DB-23.

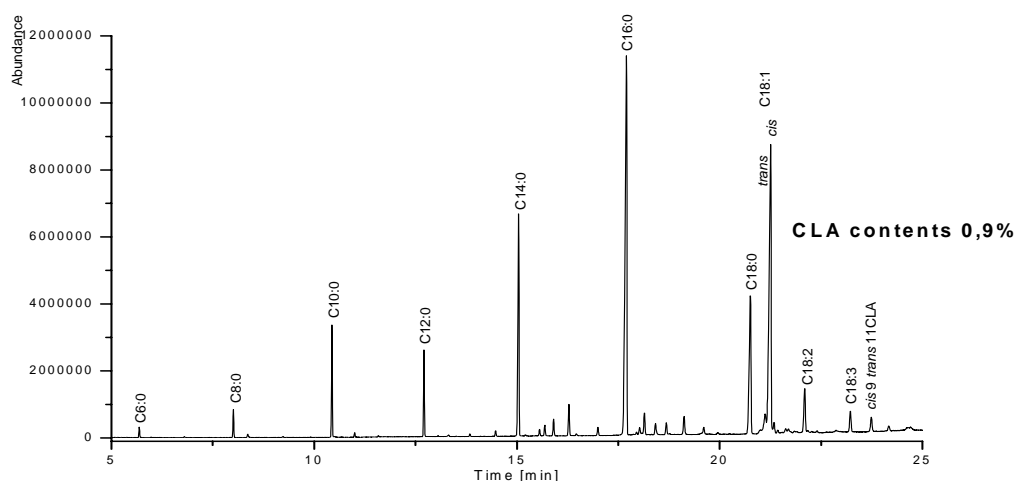


Fig. 3: GC-MS/TIC chromatogram of separation Slovak ewe cheese "bryndza" with lowest content of conjugated linoleic acid ("winter bryndza").

Sample was separated in column DB-23.

On Fig.4 is comparison of two chromatogram of separation of Slovak ewe cheeses - the "May bryndza" and "winter bryndza". Ewe's milk fat in spring season has the highest content of CLA, and also the highest content of *t11-18:1* (vaccenic acid). This isomer can act as a metabolic precursor of the bioactive conjugated linoleic acid isomer *c9,t11-18:2* [19]. Therefore CLA studies require also analyses of

C18:1 isomers. Most abundant CLA and *trans*-18:1 isomers in milk fat are *c9,t11*-18:2 and *t11*-18:1 isomeric acids.

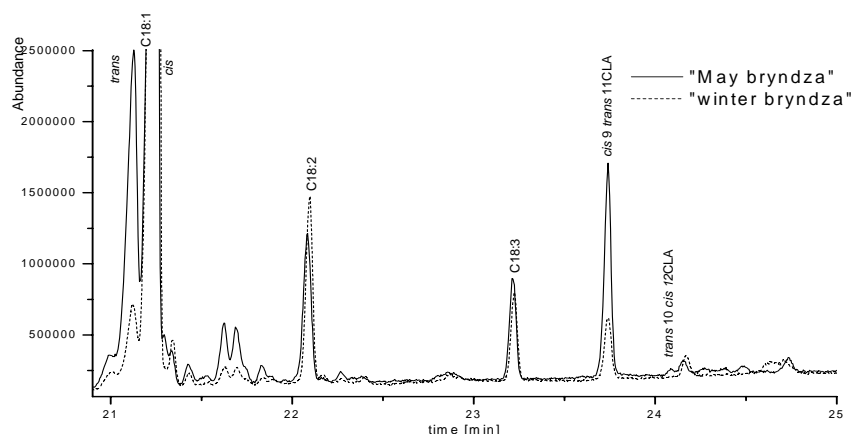


Fig. 4: Comparison of chromatograms of separation the "May bryndza" and "winter bryndza".

The concentration of CLA in ewe's milk fat varied with the season in similar way as in case of bryndza (Fig. 5 and 6). There was a distinct decrease at the end of the winter season (April). The greatest seasonal differences were measured in ewe milk: in spring (May) 3.4 % and at the end of the autumn period 1.5 %. However it must be noted, that with major CLA *c9,t11* isomer are coeluted minor CLA isomers *t7,c9* and *t8,c10*. Separation of these isomers needs substantially higher efficiencies than give a 60 m capillary column. Fig. 5 and 6 show on relatively regular decrease of CLA content of ewe's milk and bryndza in both regions. In Fig. 5 given value of 1.0 % CLA in "bryndza" is valid for "winter bryndza", which contents of 50 % of cow cheese. Ewe milk was collected up to end of October, because later most animals were not lactating.

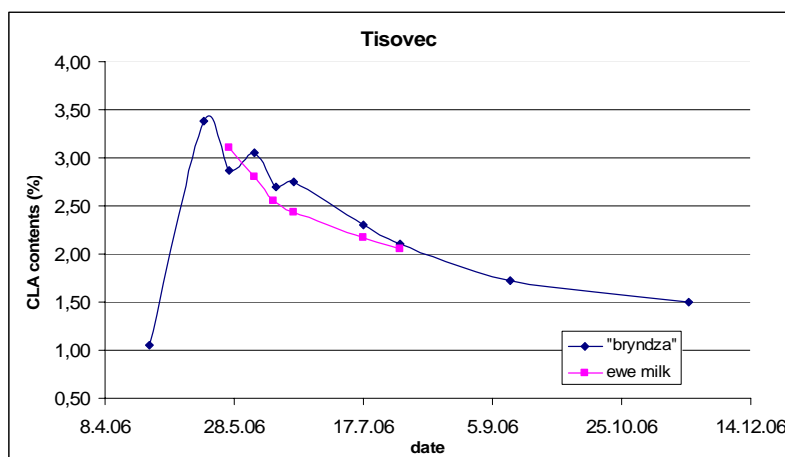


Fig. 5: CLA content of Slovak ewe milk and cheese "bryndza" in different seasons (% of total FAME) from Tisovec region.

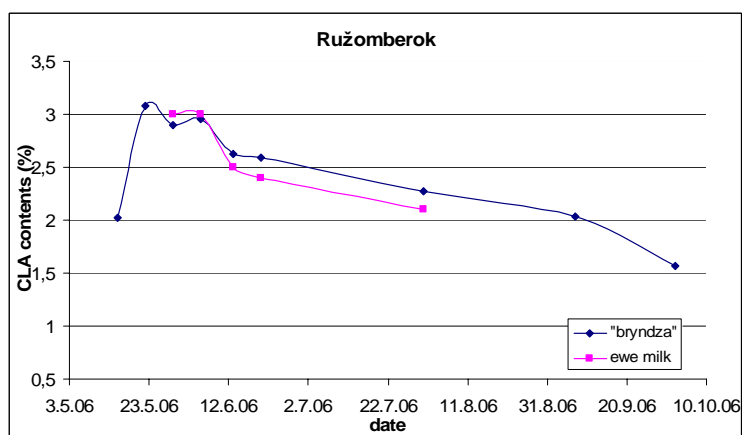


Fig. 6: CLA content of Slovak ewe milk and cheese "bryndza" in different seasons (% of total FAME) from Ružomberok region.

A possible explanation for fatty acids patterns can be found in the variation of animal diet during the survey period, particularly in the progressive variation of fatty acid profile as grass matures, with the quantitative and qualitative availability of pastures. The main fatty acid in grass lipids is α -linolenic acid (18:3n-3) that decreases, both in absolute and relative values, as grass matures. Such a decrease of 18:3n-3 could have resulted in a decrease of vaccenic acid produced in the rumen by biohydrogenation and, consequently, in a reduction of CLA that is mostly synthesized in mammary gland from vaccenic acid by Δ^9 -desaturase. It is also possible that something in green grass enhances the growth of particular bacteria in the rumen that are

responsible for producing CLA or blocks the final reduction of vaccenic acid to C18:0 [20].

3.2 High resolution separation and identification of FAME isomers oleic and conjugated linoleic acids in ewe's milk fat

No gas chromatographic separation columns or conditions have been reported to date that will adequately resolve all the fatty acid methyl esters of isomers of conjugated linoleic and oleic acids that have been identified in natural products. For separation used capillary columns 50-100 m long are not sufficient for resolution of these isomers. Most serious analytical problems consists that the second most abundant CLA isomer *t7,c9*, and *t8,c10* are not separated from the major CLA isomer *c9,t11*; other overlapping of CLA isomers are at *cis,trans*; *cis,cis*; *trans,trans* CLA isomers. Similar separation problems were found for isomers *trans*- and *cis*- 18:1, which eluate between C18:0 and C18:2 n-6. Nevertheless, after the class separation by Ag⁺ TLC, remain GC nonseparated 6- to 8-, 13- and *t14*- isomers 18:1, and 6- to 8-, 9- and *c10*- isomers 18:1. For solution of these separation problems we used the more efficient separation system with efficiency of 450 000 plates.

The high resolution separation of methyl esters of *t*-18:1 and conjugated linoleic acid isomers was performed on long capillary column HP-88 (2x 100 m x 0.25 mm x 0.2 μm) obtained by coupling of two columns in series in total length of 200 m. The chromatogram of separation of these isomers from Slovak ewe cheese "bryndza" is on Fig. 7. As a result of higher efficiency of this separation system, the isomers are substantially better separated as in Fig. 2 and 3.

Separated components were preliminary identified on the basis of retention and mass spectra data. This identification will be confirmed by GC-MS of DMOX derivates.

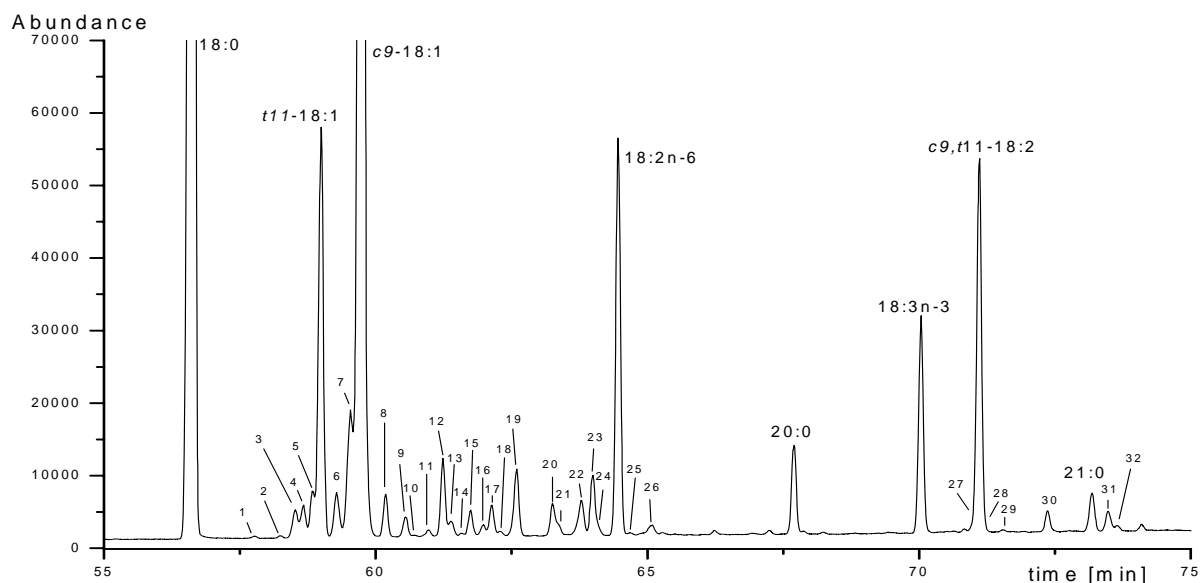


Fig. 7: The C18 region and the CLA region of a GLC of FAME from a Slovak ewe cheese "bryndza" sample

analysed using an HP-88 capillary column (200 m × 0.25 mm I.D., film thickness 0.2 μm), oven temperature was programmed at 15 °C/min from 80 °C to 180 °C and then programmed at 1 °C/min to 240 °C.

Peak identification:

1 = <i>t</i> 4-18:1	11 = <i>t</i> 16-18:1	24 = <i>c</i> 9, <i>c</i> 13-18:2
2 = <i>t</i> 5-18:1	12 = <i>c</i> 14-18:1	25 = <i>c</i> 9, <i>c</i> 14-18:2
3 = (<i>t</i> 6 + <i>t</i> 8)-18:1	13 = <i>c</i> 15-18:1	26 = <i>c</i> 9, <i>c</i> 15-18:2
4 = <i>t</i> 9-18:1	14–17 = <i>tt</i> -18:2	27 = <i>t</i> 7, <i>c</i> 9-18:2
5 = <i>t</i> 10-18:1	18 = <i>t</i> 9, <i>t</i> 12-18:2	28 = <i>t</i> 8, <i>c</i> 10-18:2
6 = <i>t</i> 12-18:1	19 = (<i>c</i> 9, <i>t</i> 13 + <i>t</i> 8, <i>c</i> 12)-18:2	29 = <i>t</i> 9, <i>c</i> 11-18:2
7 = (<i>t</i> 13+ <i>t</i> 14)-18:1+(<i>c</i> 6+ <i>c</i> 8)-18:1	20 = <i>c</i> 9, <i>t</i> 12-18:2	30 = <i>t</i> 11, <i>c</i> 13-18:2
8 = <i>c</i> 11-18:1	21 = <i>c</i> 8, <i>c</i> 13-18:2	31 = <i>t</i> 11, <i>t</i> 13-18:2
9 = <i>c</i> 12-18:1	22 = <i>t</i> 9, <i>c</i> 12-18:2	32 = <i>t</i> 8, <i>t</i> 10 - <i>t</i> 10, <i>t</i> 12-18:2
10 = (<i>c</i> 13+ <i>t</i> 15)-18:1	23 = (<i>t</i> 9, <i>c</i> 15+ <i>t</i> 10, <i>c</i> 15)-18:2	

4. Conclusions

High efficient separation system presenting of a column 200 m x 0.25 mm I.D. x 0.2 μm film thickness of polar stationary phase (efficiency of 450 000 plates) allows better separation of FAME in ewe milk as well as in cheese in comparison with separation in 60 m column. For samples obtained from two ewe milk processing plants in North and Middle Slovakia (Ružomberok and Tisovec) the estimated CLA concentration in unprocessed raw ewe milk and cheese shows the seasonal variation from 3.4 % of FAME in May to 1.5 % in

October. The results for two ewe milk processing plants (Tisovec and Ružomberok) are similar. Obtained CLA concentration of 3.4 % of FAME is highest in milk from animals fed pasture. The highest CLA ewe milk concentration and his seasonal variation are related to pasture quality.

5. Acknowledgements

Support for this work was provided by VEGA-Slovakia (1/2467/05), UK Grant (grant. No. UK/220/2006), ESF (No. 54/04-I/32-DP, ITMS 131201 10048) and LPP-0089-06 and 0198-06.

6. References

- 1.C. Cruz-Hernandez, Z. Deng, J. Zhou, A.R. Hill, M.P. Yurawecz, P. Delmonte, M.M. Mossoba, M.E.R. Dugan, J.K.G. Kramer, *J. AOAC Int.*, 87, 545-562 (2004).
- 2.J.A.G. Roach, M.M. Mossoba, M.P. Yurawecz, J.K.G. Kramer, *Anal. Chim. Acta*, 465, 207-226 (2002).
- 3.R.G. Ackman, *Anal. Chim. Acta*, 465, 175-192 (2002).
- 4.G. Jahreis, J. Fritsche, P. Möckel, F. Schöne, V. Möller, H. Steinhart, *Nutrition Research*, 19, 1541-1549 (1999).
- 5.Y.L. Ha, N.K. Grimm, M.W. Pariza, *J. Agric. Food Chem.*, 37, 75 (1989).
- 6.N. Sehat, J.K.G. Kramer, M.M. Mossoba, M.P. Yurawecz, J.A.G. Roach, K. Eulitz, K.M. Morehouse, Y. Ku, *Lipids*, 33, 963 (1998).
- 7.Y. Park, J.M. Storkson, K.J. Albright, W. Liu, M.W. Pariza, *Lipids*, 34, 235 (1999).
- 8.H.S. Garcin, J.A. Arcos, D.J. Ward, C.G. Hill Jr., *Biotechnol. Bioeng.*, 70, 587 (2000).
- 9.H.S. Garcia, K.J. Keough, J.A. Arcos, C.G. Hill Jr., *J. Dairy Sci.*, 83, 371 (2000).
10. F. Trimmerman, R. Gaupp, J. Gierke, R. von Kries, W. Adams, A. Sander, *German DE* 19, 718, 245 (1997).
11. J.K.G. Kramer, N. Jehat, M.E.R. Dugan, M.M. Mossoba, M.P. Yurawecz, J.A.G. Roach, K. Eulitz, J.A. Aalhus, A.L. Schaefer, Y. Ku, *Lipids*, 33, 549 (1998).
12. J.K.G. Kramer et al., in *Advances in Conjugated Linoleic Acid Research*, Vol. 1, Eds. M.P. Yurawecz et al., AOCS Press, Champaign, IL, 83 (1999).
13. M.P. Yurawecz, in *Advances in Conjugated Linoleic Acid Research*, Vol. 1, Eds. S. Banni et al., AOCS Press, Champaign, IL, 307 (1999).
14. J. Fritsche et al., *Fett/Lipid*, 101, 272 (1999).
15. A.L. Davis, G.P. McNeil, D.C. Caswell, *Chem. Phys. Lipid*, 97, 155 (1999).
16. R.G. Jensen, A.M. Ferris, C.J. Lammi-Keffe, *J. Dairy Sci.*, 74, 3228 (1991).
17. J.K.G. Kramer, J. Zhou, *Eur. J. Lipid Sci. Technol.* 103, 594 (2001).
18. E.G. Bligh, and W.J. Dyer, *Can. J. Physiol.*, 37, 911-917 (1959).
19. J. Molquentin, D. Precht, *Kiel. Milchwirtsch. Forschungsber.*, 56, 53-63 (2004).
20. A. Nudda, M. A. McGuire, G. Battacone, G. Pulina, *J. Dairy Sci.*, 88, 1311-1319 (2005).

DEVELOPMENT OF L-SHAPED HYDRIDE MULTIATOMIZER FOR ATOMIC ABSORPTION SPECTROMETRY

Olga Grossová^{a,b} and Jiří Dědina^a

^a *Academy of Sciences of the Czech Republic, Institute of Analytical Chemistry, Vídeňská 1083, 142 20 Prague 4, Czech Republic, e-mail: grossova@biomed.cas.cz*

^b *Charles University, Faculty of Science, Albertov 8, 128 40 Prague 2, Czech Republic*

Abstract

The aim of this work is to develop an advanced type of multiple microflame hydride atomizer (multiatomizer) for atomic absorption spectrometry. In an ideal case, usage of multiatomizer would eliminate inherent disadvantages of a conventional externally heated quartz tube atomizer (QTA) by keeping the analyte in the state of free atoms. This can be achieved by filling the multiatomizer optical tube with hydrogen radicals (H-radicals).

The H-radicals are produced in the multiatomizer optical tube by reactions between hydrogen and oxygen. As the oxygen supply to the optical tube plays a crucial role in atomizer performance, it has to be introduced as uniformly as possible over the whole length of the optical tube.

To reach this aim, we have tested various approaches to the optical tube design, including different types of quartz tubes with perforated wall, with various size and number of holes, and some porous materials such as ceramics and porous quartz tube.

Any of these tubes could not be attached to the previously introduced T shaped multiatomizer since they cannot be joined to the central inlet arm of atomizer. Therefore, a new, L shaped multiatomizer arrangement was designed. The substantial advantage of the multiatomizer L design is that the optical tubes can be simply replaced.

Employing selenium hydride as an analyte and arsine as an interferent, an evaluation of the L shaped multiatomizer

performance, in terms of sensitivity, calibration graph linearity and resistance to atomization interferences, is discussed.

Keywords

quartz tube atomizer, multiatomizer, porous quartz, hydride generation atomic absorption spectrometry

Introduction

At first an analyte is converted to the form of volatile compound in hydride generation atomic absorption spectrometry. Then the volatile form of the analyte is converted into the state of free atoms in an atomizer.

Popular atomizers for hydride generation atomic absorption spectrometry are QTA that are T shaped tubes with an externally heated optical tube aligned in an optical axis of the spectrometer. The inlet arm of the T tube serves to introduce the analyte hydride, supported by the flow of carrier gas, to the horizontal optical tube.

The hydride is atomized by H-radicals, which are formed by reactions between hydrogen and oxygen in the heated part of the atomizer. As the hydride is transported to the atomizer directly from the reaction cell, there is enough hydrogen present since it is formed by decomposition of tetrahydroborate during hydride generation. Oxygen traces present in the system are usually sufficient to produce enough H-radicals. The H-radicals, produced in QTA, form a spatially limited cloud situated in the T-junction of the atomizer. Free analyte atoms created in the H-radical cloud are transported farther to the atomizer.

Nevertheless the free analyte atoms react immediately after leaving the H-radical rich atmosphere, since they are thermodynamically forbidden outside the H-radical atmosphere. This is the only reason for all the troubles inherent to the conventional QTA, namely the poor resistance to the atomization interferences and insufficient linearity of calibration.

T multiatomizer

To sum up, the drawbacks of QTA can be substantially suppressed by reatomization approach, because once decayed analyte

forms can be reverted to the free atoms by another contact with H-radicals.

Consequently the analyte is maintained in the state of free atoms by recurrent atomization in multiatomizer. The horizontal arm of the multiatomizer consists of two concentric tubes. The inner tube (optical tube) of the previously introduced T shaped multiatomizer has over its length 14 holes about 0.5 mm in diameter (Fig. 1)^{1,2}. Air is introduced to the cavity between the outer and the inner tube, from where it enters the optical tube through the holes. In any of the holes, oxygen reacts with hydrogen presented inside the tube. The H-radical cloud is thus formed in each hole.

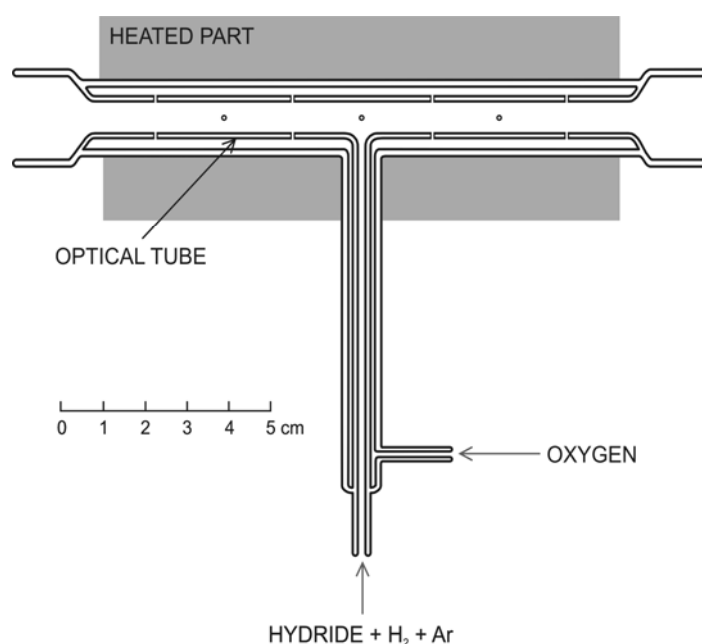


Fig.1 T multiatomizer

The T multiatomizer provides better linearity and one to two orders of magnitude better resistance to interferences than the QTA. However, the resistance to the interferences is still substantially worse than observed if a diffusion flame atomizer is used. This indicates that the performance of the T multiatomizer is still far from ideal.

L multiatomizer

The aim of this work is to develop an improved type of multiatomizer enabling uniform distribution of H-radicals inside the optical tube. To reach this aim a porous optical tube or tube with multiple perforated walls has to be used.

In the T multiatomizer these kinds of tubes could not be sealed to the form of T shape. Therefore, a new modular L shaped multiatomizer was devised (Fig. 2). The main feature of the L multiatomizer is that the hydride enters the optical tube edgewise. The horizontal arm of L multiatomizer consists of two concentric tubes. The cavity between the tubes is sealed tightly with two removable teflon o-rings with teflon coated silicon padding. A teflon cap closes the horizontal arm with a quartz window and hydride inlet on one side. To prevent gas leakage the L multiatomizer is fixed firmly to a metal frame (is not shown). Another benefit of the L multiatomizer is its modular arrangement as optical tube is conveniently exchangeable.

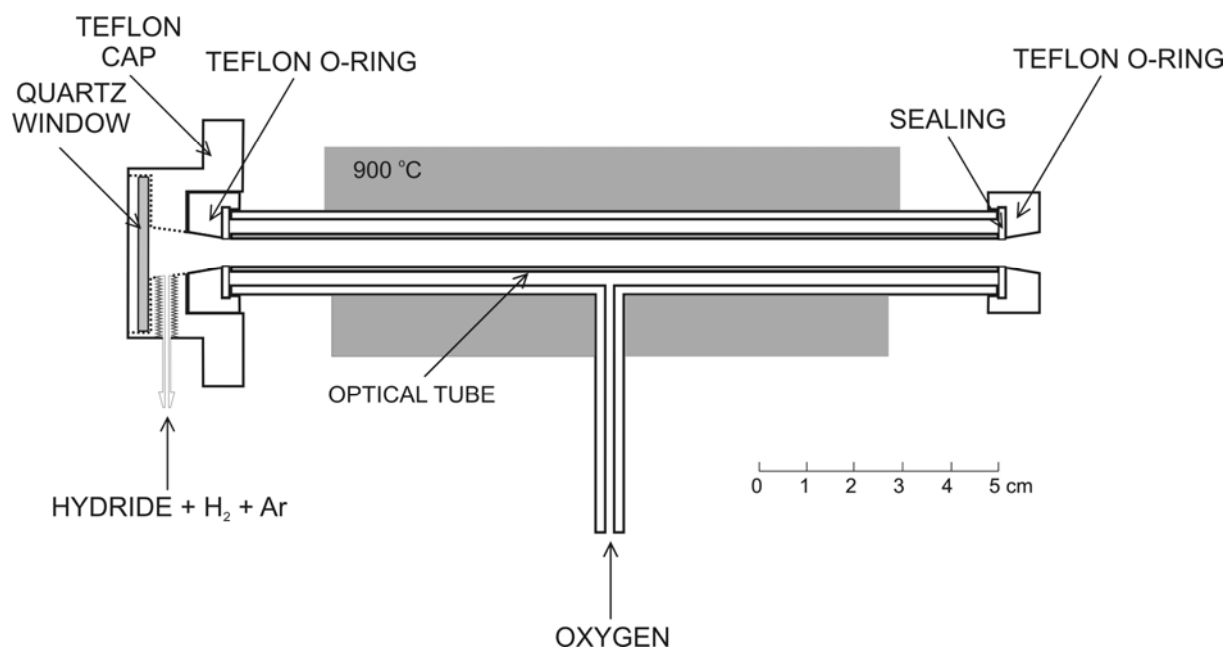


Fig.2 L multiatomizer

It has been found that the L multiatomizer with the same optical tube (with 14 holes) as has the T multiatomizer provides the same performance (in terms of calibration graph linearity and resistance to interferences) compared to the T multiatomizer. This is a proof that the convenient modular L multiatomizer could be employed for the subsequent optimization studies.

Several types of porous or perforated optical tubes were tested in L multiatomizer.

There were quartz tubes with multiple perforated walls, with 50 and 170 holes. The holes were made by optical beam drilling (Institute

of Scientific Instruments of the ASCR). These tubes were evaluated in terms of the holes volume and its spatial distribution. The holes size was found to be about 5 μm in diameter.

The other tested material was porous quartz (Vycor 7930, Corning) with very narrow pore size distribution, with the average pore radius about 4 to 6 nm^(3,4). As it rapidly absorbs water and organic contaminants, it had to be heated extremely slowly to prevent its breakage from steam expansion. Another problem was shrinkage due to a meltdown of the internal porous structure when the glass was subjected to the high temperature. The porous membrane shrank even at temperature as low as 200 °C. The shrinkage gradually increases and when the temperature is above 900 °C a dramatic changes occurred. For that reason the atomization temperature was set to 800 °C.

Firstly an oxygen flow rate optimization for all the optical tube was done. For all the measurements selenium was chosen as the model analyte and arsenic as the interferent. Fig. 3 shows the calibration graph for L multiatomizers with the perforated optical tubes.

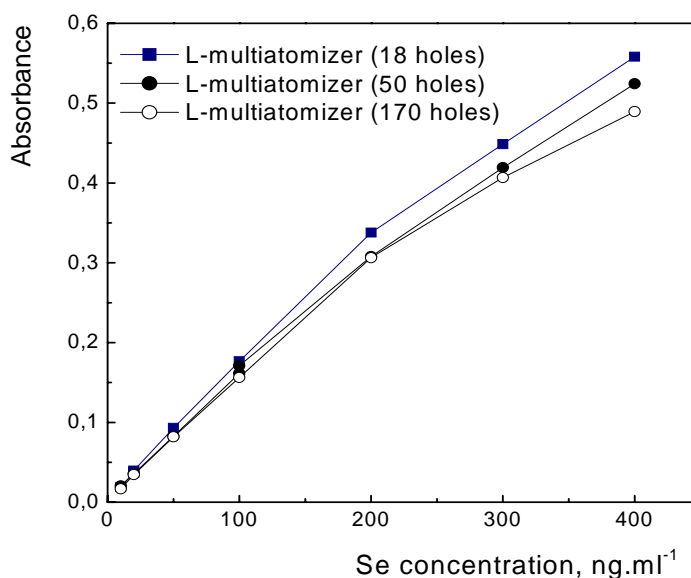


Fig. 3 Calibration graph for Se, 204 nm

The sensitivity and linear portion of the calibration graph for both atomizers with the multiple perforated optical tubes did not differ from the performance of the original T multiatomizer. The resistance

to interferences was not improved as well. Such a results cannot be properly explained until another experiments will be done.

On the other hand the sensitivity of the L multiatomizer with porous quartz optical tube reaches only up to 50% compared to the multiatomizer with perforated optical tubes This is probably due to the much bigger surface area of the porous quartz compared to the plain quartz. Nevertheless the porous glass seems to be a promising material for optical tube, since the signal depression with increasing amount of interferent is less significant than if perforated glass optical tube is used (Fig. 4). The testing of porous quartz is still in progress.

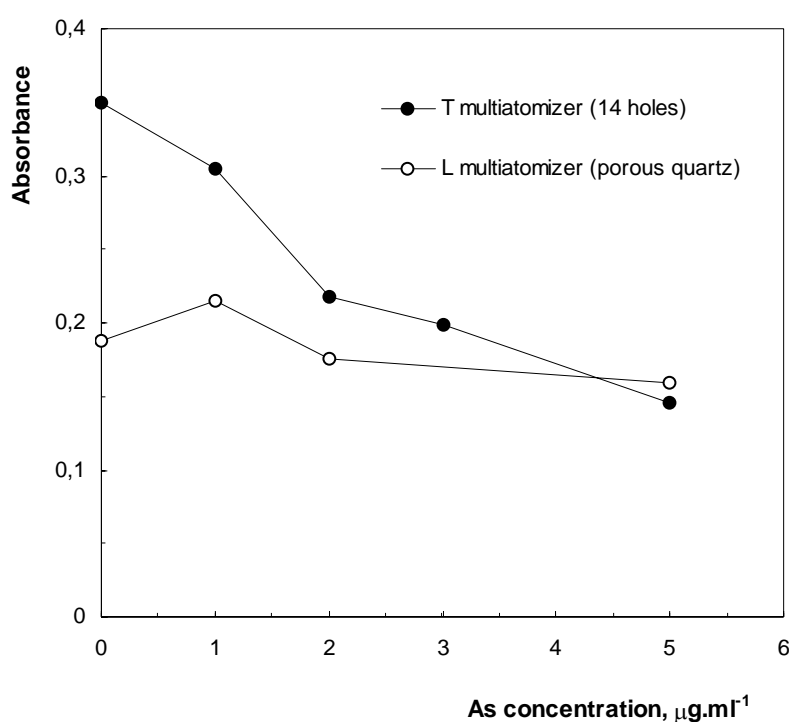


Fig. 4 Effect of As concentration in the sample on the observed absorbance

Acknowledgment

Financial support from the Grant Agency of the ASCR (Project No. A400310507), the Grant Agency of Charles University (Project No. GAUK 306/2006/B-CH/PrF) is gratefully acknowledged. We are also indebted to Dr. Jan Dupák and Dr. Libor Dupák, Team of New Technologies, Institute of Scientific Instruments, Academy of Sciences of the Czech Republic for making holes to quartz tube by using the electron beam technology.

References

- [1] Dědina, J.; Matoušek, T.: *J. Anal. At. Spectrom.* **15** (2000) 301–304
- [2] Matoušek, T.; Dědina, J.; Selecká, A.: *Spectrochim. Acta Part B* **57**(2002) 451–462
- [3] Elmer, T. H.: *Porous and Reconstructed Glasses*. Accessible from URL:
<http://www.corning.com/lightingmaterials/products/index_vycor.html> [cit. 12.4.2005]
- [4] Shelekhin, A. B.; Pien, S.; Ma, Y. H.: *Journal of Membrane Science* **103**(1995) 39–43

USE OF BORON-DOPED DIAMOND ELECTRODE IN VOLTAMMETRY OF BIOLOGICALLY ACTIVE ORGANIC COMPOUNDS

Jana Musilová^a, Jiří Barek^a and Karolina Pecková^a

^a Charles University in Prague, Faculty of Science, Department of Analytical Chemistry, UNESCO Laboratory of Environmental Electrochemistry, Hlavova 2030, 12843 Prague 2, Czech Republic

Abstract

Boron-doped diamond (BDD) films have been studied intensively just over the past ten years as electrode materials for electrochemistry. The diamond thin-films are prepared in many cases by the technique of chemical vapor deposition (CVD). Because of excellent electrochemical properties and high sensitivity for many species, BDD thin film electrodes can be used to determine a great variety of organic and inorganic compounds.

Keywords:

Boron-doped diamond electrode, voltammetry

1. Introduction

Boron-doped diamond (BDD) films have been studied intensively just over the past ten years as electrode materials for electrochemistry. During this time, it has become apparent that BDD films are in many ways ideal for high-sensitivity analytical measurements of a wide variety of inorganic and organic species.

2. Preparation and Characterization

Diamond thin films can be grown from dilute mixtures of a hydrocarbon gas (methane) in hydrogen using CVD (chemical vapor deposition) methods, the most popular being hot-filament and microwave discharge. A carbon-containing gas is energetically activated to decompose the molecules into methyl radicals and atomic-hydrogen source gas mixture is used.¹

Typical growth conditions are C/H volume ratios of 2.5-2%, pressures of 10-100 Torr, substrate temperatures of 800-1000°C, and microwave powers of 1000-1300 W, or filament temperatures of ~ 2100°C. The films grow by nucleation at rates in the 0.1-1 µm/h range. For the substrates to be continuously coated with diamond, the nominal film thickness must be ~ 1 µm. Microwave CVD growth of nanocrystalline diamond using a unique fullerene-argon gas mixture produces continuous films at thicknesses as low as 30 nm. Boron doping is accomplished from the gas phase by diborane. Typical boron doping level is 10²⁰ cm⁻³ (Ref.²).

The substrate is pretreated by cleaning with a series of solvents and seeding it with small diamond particles by polishing the substrate with diamond powder. The embedded particles serve as nucleation centers for film growth.

Atomic hydrogen prevents surface reconstruction from a saturated sp³-hybridized diamond microstructure to an unsaturated sp²-hybridized graphite microstructure, suppresses the formation of nondiamond impurity, and abstracts hydrogen from hydrocarbon surface sites and gas-phase hydrocarbon species to form reactive radicals.

The film is composed of sharp, well-faceted microcrystallites ranging in size from 0.5 to 3 µm, with many twinned and misoriented crystallites with no obvious preferential orientation.

Films can be prepared in one of several possible particle sizes, depending upon the growth conditions, ranging from microcrystalline, with crystallites typically in the 1 – 10 µm range to nanocrystalline, with particles in the range below 1 µm, down to ultrananocrystalline, with particles in the range down to 1 nm.

The quality of microcrystalline CVD films is conveniently assessed with scanning electron microscopy (SEM) to ensure that the crystallinity is good.

Raman spectroscopy is an essential characterization technique, one of the routine ways Raman is used is to gauge the presence of sp² carbon, which shows up typically as a very broad peak centered at 1600 cm⁻¹, while diamond itself has a highly characteristic peak, due to the principal phonon mode, at very close to 1332 cm⁻¹. This peak is extremely intense for highly crystalline diamond. The presence of a high concentration of boron as a dopant leads to an increase in a broad

peak at 1200 cm^{-1} . Weak scattering intensity in the region around 1520 cm^{-1} can be caused by nondiamond carbon impurity incorporated into the film.

The surface termination of the diamond film, whether hydrogen or oxygen, can affect the electrochemical properties greatly. This can be established through the use of x-ray photoelectron spectroscopy.^{1,3}

3. Electrochemical Properties

Boron-doped diamond thin-film electrodes possess excellent electrochemical properties, such as extreme hardness, corrosion resistance, high thermal conductivity, a low and stable background current over a wide potential range, microstructural stability at extreme cathodic and anodic potentials, high current densities, good responsiveness for many redox analytes without pretreatment, and resistance to electrode fouling. Diamond thin-film surfaces are relatively inert to impurity adsorption.^{1,4,5}

4. Chemically Modified Diamond Electrodes

The chemical modification of the BDD surface can provide enhanced sensitivity and selectivity for the detection of various species. Several approaches for modification have been developed thus far; these include surface oxidation, attachment of organic functional groups, attachments of biomolecules and the deposition of metal or metal oxide particles. These modified surfaces have been used more extensively for the analysis of organic and biochemical compounds, but some have also been used for inorganic species.³

5. Microelectrodes

Sharpened platinum wires (76, 25, and 10- μm diameter) are suitable substrate for the deposition of boron-doped polycrystalline diamond films to form microelectrodes useful for electroanalytical measurements. Microelectrodes with a combined conical and cylindrical shape that exhibit reproducible voltammetric responses, at least in terms of the peak and half-wave potentials, for a variety of aqueous redox analytes. The voltammetric response is affected by boron-doping level and the shape of the electrode. Several methods were evaluated for their ability to insulate the cylindrical portion of

the microelectrode, reproducibly exposing a disk geometry at the end, including polyimide, nail polish, epoxy, and polypropylene coatings. Although all of the coatings appear to adhere strongly to the diamond surface, the limited chemical or electrochemical stability of some restrict their use to certain environments and potential ranges.⁴

6. Effect of Nondiamond Carbon Impurity

Polycrystalline diamond films commonly contain varying amounts of nondiamond carbon impurity, depending on the growth conditions. The nondiamond carbon likely consists of a mixture of sp^3 and sp^2 -hybridized bonding, similar to diamond like or amorphous carbon. This impurity was introduced through adjustment of the C/H source gas ratio used during the deposition. Proportional increases in the fraction of grain boundary, the extent of secondary nucleation, and the sp^2 -bonded carbon impurity content occurred with increasing C/H ratio. The electrode response was assessed⁶ using $Fe(CN)_6^{3-/4-}$, $Ru(NH_3)_6^{3+/2+}$, $Fe^{3+/2+}$, and 4-tert-butylcatechol as model reversible redox systems. While the increasing sp^2 -bonded carbon content had little effect on the cyclic voltammetric peak separation (ΔE_p) or peak current for the first two redox systems, the impurity had a significant impact on the latter two, as ΔE_p decreased proportionally with the increased sp^2 -bonded carbon content. The effect of the impurity on the reduction of oxygen in 0.1 M $HClO_4$ and 0.1 M $NaOH$ was also investigated. A direct correlation was found between the relative amount of the impurity, and the overpotential for the reaction. The greater the nondiamond content, the lower the kinetic overpotential for the reduction and the higher the exchange current density. The results demonstrate that the grain boundaries, and the sp^2 carbon impurity presumably residing there, can have a significant impact on the electrode reaction kinetics for certain redox systems and little influence for others.

7. Applications

BDD electrodes can be used to determine a great variety of organic compounds. These can undergo either reversible or irreversible (due to the complexity of the processes) electrochemical

reactions. Recent developments in specific organic determination are reviewed in ³.

Methods using diamond film electrodes as electrochemical sensors for organic species involve:

- Cyclic voltammetry
- Differential pulse voltammetry
- Square wave voltammetry
- Hydrodynamic voltammetry
- Laser ablation voltammetry
- FIA with diamond thin-film amperometric detectors
- Chronoamperometry
- Chronocoulometry
- HPLC with BDD electrode as amperometric detector
- Ultrasonically facilitated BDD electrochemical technique

8. Construction of Boron-Doped Diamond Electrode

The scheme of a BDD electrode constructed in our laboratory is depicted in Fig. 1. The use of this electrode for voltammetric determination of trace amounts of biologically active nitro compounds in various environmental matrices is under investigation.

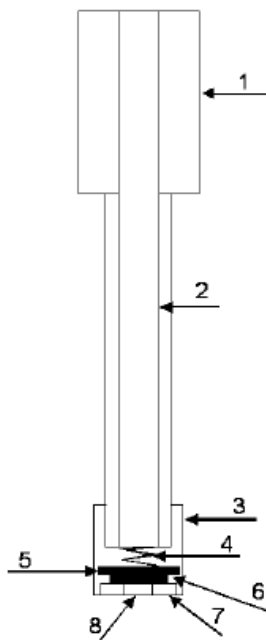


Fig.1: Scheme of BDD electrode: *electrode body (1), stainless steel (2), screw attachment (3), small metal spring (4), brassy sheet (5), boron doped diamond thin-film electrode (6), Viton® gasket (7), access for solution (8)*

Acknowledgement

This work was financially supported by the Czech Ministry of Education, Youth and Sports (project LC06035 and project MSM 0021620857).

Reference list

- [1] Xu J.; Granger M.C.; Chen Q.; Strojek J.W.; Lister T.E.; Swain G.M.: *Anal. Chem.* **69** (1997), 591A-597A
- [2] Cvačka J.; Swain G.M.; Barek J.; Zima J.: *Chem. Listy* **96** (2002), 33-38
- [3] Chailapakul O.; Siangproh W.; Tryk D.A.: *Sensor Lett.* **4** (2006), 99-119
- [4] Cvačka J.; Quaiserova V.; Park J.; Show Y.; Muck A.; Swain G.M.: *Anal. Chem.* **75** (2003), 2678-2687
- [5] Xu J.; Qingyun C.; Swain G.M.: *Anal. Chem.* **70** (1998), 3146-3154
- [6] Bennet J.A.; Wang J.; Show Y.; Swain G.M.: *J. Electrochem. Soc.* **151** (2004), E306-E313

STUDY OF ELECTROCHEMICAL BEHAVIOR OF 2,7-DINITRO-9-FLUORENONE

Vlastimil Vyskočil^a, Jiří Barek^a, Karel Čížek^a, Zbigniew Zawada^b

^a Charles University in Prague, Faculty of Science, Department of Analytical Chemistry, UNESCO Laboratory of Environmental Electrochemistry, Hlavova 2030, 128 43, Prague 2, Czech Republic; e-mail: barek@natur.cuni.cz

^b Charles University in Prague, Faculty of Pharmacy in Hradec Králové, Department of Inorganic and Organic Chemistry, Heyrovského 1203, 500 05, Hradec Králové, Czech Republic; e-mail: zavadaz@faf.cuni.cz

Abstract

The electrochemical reduction of the nitro and carbonyl groups in 2,7-dinitro-9-fluorenone at mercury electrodes has been studied in buffered water-methanolic solutions over a pH range of about 2 – 12. The number of electrons involved in the reduction steps was measured using potentiostatic coulometry at large surface mercury pool electrode in acid, neutral and alkaline medium. Acquired results have been compared with results obtained by using direct current polarography and cyclic voltammetry. On the basis of these methods, a possible mechanism of the electrochemical reduction of 2,7-dinitro-9-fluorenone has been discussed and proposed.

Keywords

2,7-dinitro-9-fluorenone; Mechanism of reduction; Number of exchanged electrons; DC polarography; DC TAST polarography; Cyclic voltammetry; Potentiostatic coulometry; Dropping mercury electrode; Hanging mercury drop electrode; Mercury pool electrode

1. Introduction

The approximately 20% cancer mortality together with the fact that environmental causes contribute to the significant number of cancers, emphasize the potential benefits of environmental detection of chemical carcinogens and raises carcinogenic substances monitoring in general and working environment to the highest priority¹. Nitrated polycyclic aromatic hydrocarbons (NPAHs) belong among the substances whose occurrence in the environment can be

causally connected with an increased cancer rate². NPAHs have been found e.g. in incinerators emissions, exhaust gases, fossil fuel combustion products, cigarette smoke or in natural waters, river sediments in river water and food, too³.

Main problem in NPAHs effect on organisms is the fact that the pernicious tumor grow can be provoked by small amount of carcinogen. Whereas the disease can manifest itself after many years since the initiatory exposition. That is why the need for extremely sensitive and selective methods of NPAHs determination is still growing.

Nitro compounds belong between relatively easy reducible compounds, chemically as well as electrochemically. Study of NPAHs electrochemical reduction can contribute to elucidation of mechanism of their genotoxic effect and can lead to better understanding of processes that occur during the degradations of these compounds in organism.

Studied compound 2,7-dinitro-9-fluorenone (2,7-DNFN) (structural formula see Fig. 1) belongs to the group of NPAHs. 2,7-DNFN is suspected of carcinogenicity⁴, even though direct acting carcinogenicity was not proved up to now. However, possible products of 2,7-DNFN chemical reduction – polycyclic amino derivatives – are known as carcinogenic agents⁵.

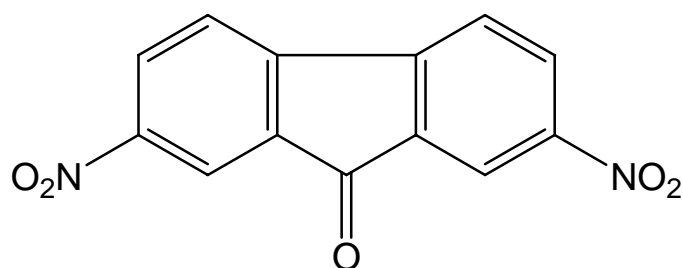


Fig. 1 – Structural formula of 2,7-dinitro-9-fluorenone

2. Experimental Part

2.1 Reagents

The stock solution of 2,7-dinitro-9-fluorenone (97%, Sigma-Aldrich, Prague, Czech Republic) in methanol ($c = 2 \cdot 10^{-4} \text{ mol} \cdot \text{L}^{-1}$) was prepared by dissolving 0.0270 g of the substance in 500 ml of

methanol (Lachema, Brno, Czech Republic). The lower concentration of 2,7-DNFN was used due to its limited solubility in methanol. More diluted solutions were prepared by exact dilution of the stock solution with methanol. All solutions were kept in dark. Other chemicals (boric acid, glacial acetic acid, phosphoric acid, sodium hydroxide, potassium chloride, all p.a. purity) were supplied by Lachema, Brno, Czech Republic. Deionized water from Millipore, USA, was used. All solutions were kept in glass vessels in dark.

2.2 Apparatus

Direct current fast polarographic (DCTP), cyclic voltammetric (CV) and potentiostatic coulometric (PC) measurements were carried out using Eco-Tribo electrochemical analyzer driven by PolarPro 5.1 software (all Polaro-Sensors, Prague, Czech Republic). The software worked under the operational system Microsoft Windows XP Professional (Microsoft Corporation). Direct current polarographic (DCP) measurements were carried out using PO4 Polariter polarograph (Radiometer, Copenhagen, Denmark).

DCTP measurements were carried out in a three-electrode system – platinum electrode PPE (Monokrystaly, Turnov, Czech Republic) as auxiliary electrode, silver/silver chloride reference electrode RAE 113 ($1 \text{ mol}\cdot\text{L}^{-1}$ KCl) (Monokrystaly, Turnov, Czech Republic) and dropping mercury electrode (DME) as working electrode. The mercury drop lifetime was 1 s, the height of the mercury reservoir was 36 cm (mass flow rate of mercury through the capillary was $6.96 \text{ mg}\cdot\text{s}^{-1}$). Unless stated otherwise, the scan rate $4 \text{ mV}\cdot\text{s}^{-1}$ was used.

CV measurements were carried out in a three-electrode system – platinum electrode PPE (Monokrystaly, Turnov, Czech Republic) as auxiliary electrode, silver/silver chloride reference electrode RAE 113 ($1 \text{ mol}\cdot\text{L}^{-1}$ KCl) (Monokrystaly, Turnov, Czech Republic) and miniaturized hanging mercury drop electrode (HMDE), type UM μ E (Polaro-Sensors, Prague, Czech Republic) as working electrode. The valve opening time was 300 ms, the mercury drop surface was 0.0196 cm^2 . The pulse amplitude -50 mV, pulse width 80 ms and scan rate $50 \text{ mV}\cdot\text{s}^{-1}$ was used.

PC measurements were carried out in a three-electrode system – platinum electrode PPE (Monokrystaly, Turnov, Czech Republic) as auxiliary electrode, silver/silver chloride reference electrode RAE 113 ($3 \text{ mol}\cdot\text{L}^{-1} \text{ KCl}$) (Monokrystaly, Turnov, Czech Republic) and mercury pool (MPE) as working electrode. The MPE surface was 2.41 cm^2 . The sampling rate 1 s was used.

DCP measurements were carried out in a two-electrode system (Kalousek cell) – mercury/mercury(I) chloride reference electrode (saturated KCl solution) and classical DME as working electrode. The mercury drop lifetime was 2 s, the height of the mercury reservoir was 81 cm (mass flow rate of mercury through the capillary was $4.09 \text{ mg}\cdot\text{s}^{-1}$). The scan rate $200 \text{ mV}\cdot\text{min}^{-1}$ were used.

2.3 Procedures

Unless stated otherwise, appropriate amount of 2,7-DNFN stock solution was measured into a polarographic vessel (or Kalousek cell), methanol was added to total volume of 5.0 ml and the solution was filled up to 10.0 ml with Britton-Robinson (BR) buffer of appropriate pH. All curves were measured 3 times.

While using potentiostatic coulometry, modified polarographic vessel with large surface mercury pool electrode was used and the measured solution was mechanically stirred during the analysis (time of analysis was 20 minutes). A concentration decrease of 2,7-DNFN during electrolysis was monitored using DPV at HMDE.

Oxygen was removed from the measured solutions by bubbling with nitrogen for five minutes.

3. Results and Discussion

3.1 Investigation of Electrochemical Reduction of

2,7-Dinitro-9-fluorenone

The influence of pH on polarographic behavior of 2,7-DNFN was investigated using DCTP in a mixture of methanol – BR buffer (1:1). It can be seen from Fig. 2 that 2,7-DNFN gives 2 – 3 well-developed irreversible waves. At pH 2 and 3 it is possible to differentiate 3 waves, in pH range 4 – 7 2 waves (at pH 4 the first wave is not splitted and the second wave is partially splitted, at pH 5 –

7 the first wave is partially splitted and the second wave is not splitted) and in pH range 8 – 12 to differentiate 3 waves.

We can suppose that the reduction of 2,7-DNFN proceeds in two or three consecutive reduction steps. On the basis of Ilkovic equation we can estimate number of exchanged electrons from the diffusion currents⁶.

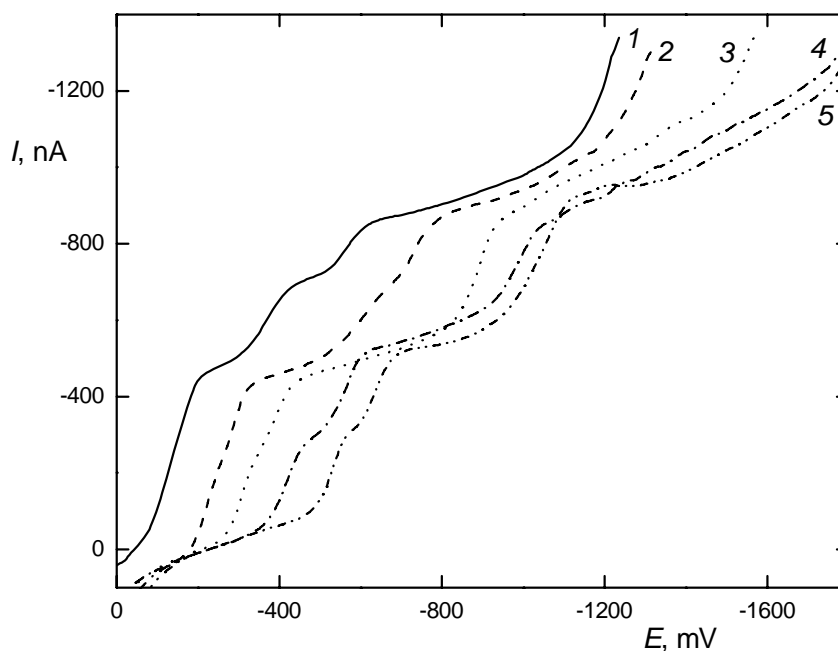


Fig. 2 – Selected DCT polarograms of 2,7-DNFN ($c = 1 \cdot 10^{-5} \text{ mol} \cdot \text{L}^{-1}$) at DME in methanol – BR buffer (1:1); resulting pH 2.7 (1), 4.9 (2), 7.0 (3), 9.3 (4), 12.4 (5).

On the basis of analogy with polarographic reduction of various dinitrofluorenes⁶, we can assume that in acid medium 2,7-DNFN exchanges consecutively 8 electrons in the first wave, 4 electrons in the second wave and 2 electrons in the third wave. In neutral medium, we can assume that 2,7-DNFN exchanges consecutively 4 electrons in the first wave, 4 electrons in the second wave and 4 electrons in the third wave. In alkaline medium 2,7-DNFN exchanges consecutively 4 electrons in the first wave, 4 electrons in the second wave and 6 electrons in the third wave. We compared this behavior with results obtained using DCP and the results have confirmed our presumptions. The ratio of limiting currents of individual waves corresponds to presumed numbers of exchanged electrons in corresponding steps.

The number of exchanged electrons was determined by potentiostatic coulometry. Constant potential electrolysis of 2,7-DNFN was carried out in a coulometric cell. Hydrodynamic

voltammetric curves at a mercury pool electrode were measured at resulting pH 2.7, 7.0 and 11.2. The values of exchanged electrons were rounded off to the nearest whole number. In acid media 2,7-DNFN exchanges overall 14 electrons, in neutral media overall 12 electrons and in alkaline medium overall 14 electrons.

Cyclic voltammetric measurements of 2,7-DNFN were used to obtain an overall view of electrochemical behavior. It can be seen that at low pH (see Fig. 3) neither of the peaks corresponds to a reversible process while at high pH (see Fig. 4 and 5) there are signs of quasi-reversible character of some processes. The observed linear dependence of peak currents on the square root of the scan rate confirms the diffusion control of the observed processes.

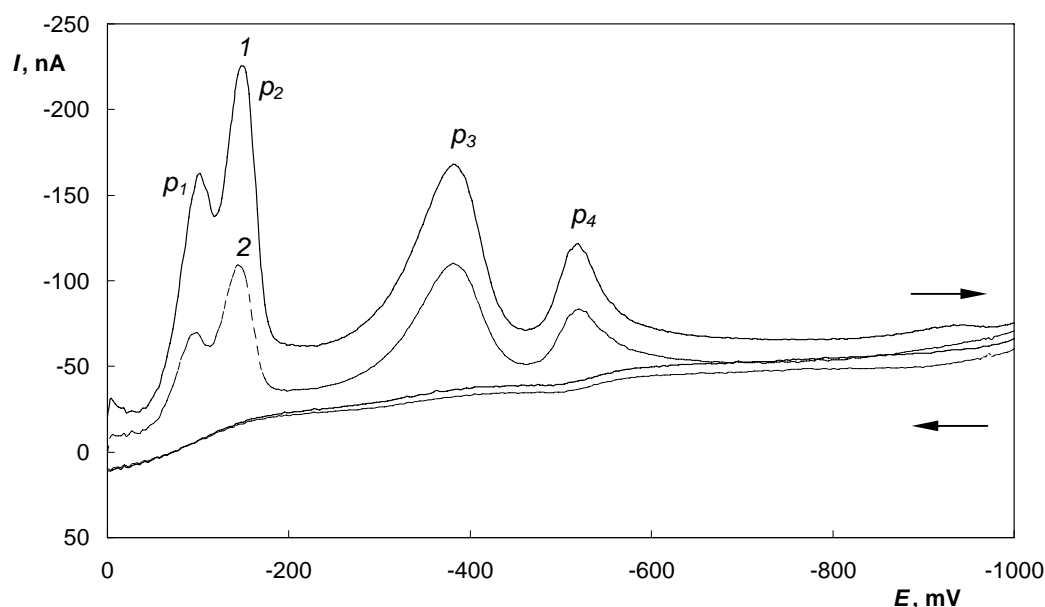


Fig. 3 – Cyclic voltammograms of 2,7-DNFN ($c = 1 \cdot 10^{-5} \text{ mol} \cdot \text{L}^{-1}$) at HMDE in methanol – BR buffer (1:1); resulting pH 2.6; first (1) and second(2) scan in the potential window from 0 to -1000 mV, scan rate $50 \text{ mV} \cdot \text{s}^{-1}$.

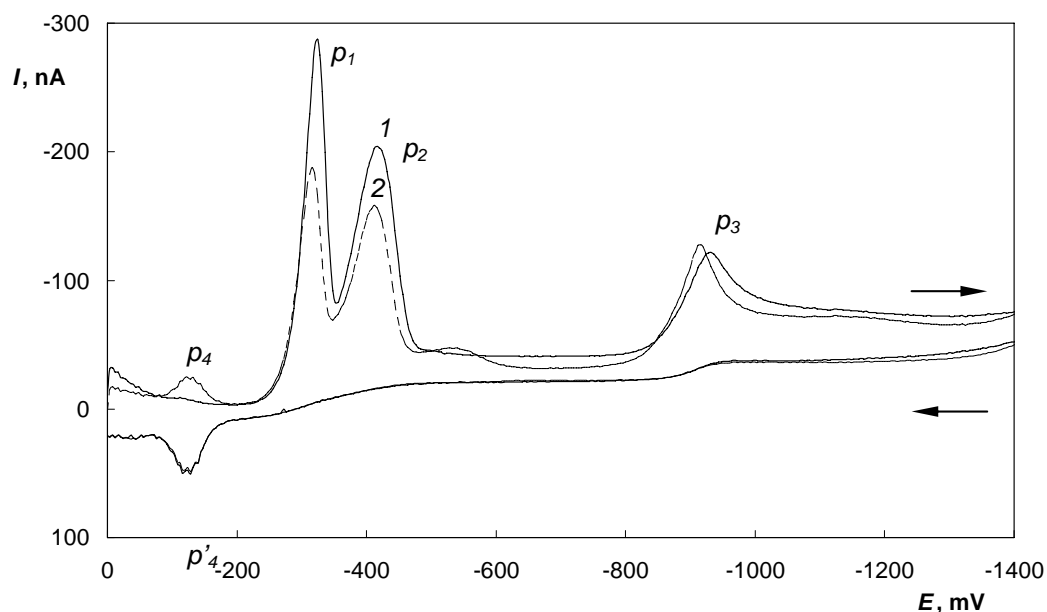


Fig. 4 – Cyclic voltammograms of 2,7-DNFN ($c = 1 \cdot 10^{-5} \text{ mol} \cdot \text{L}^{-1}$) at HMDE in methanol – BR buffer (1:1); resulting pH 7.2; first (1) and second(2) scan in the potential window from 0 to -1400 mV, scan rate $50 \text{ mV} \cdot \text{s}^{-1}$.

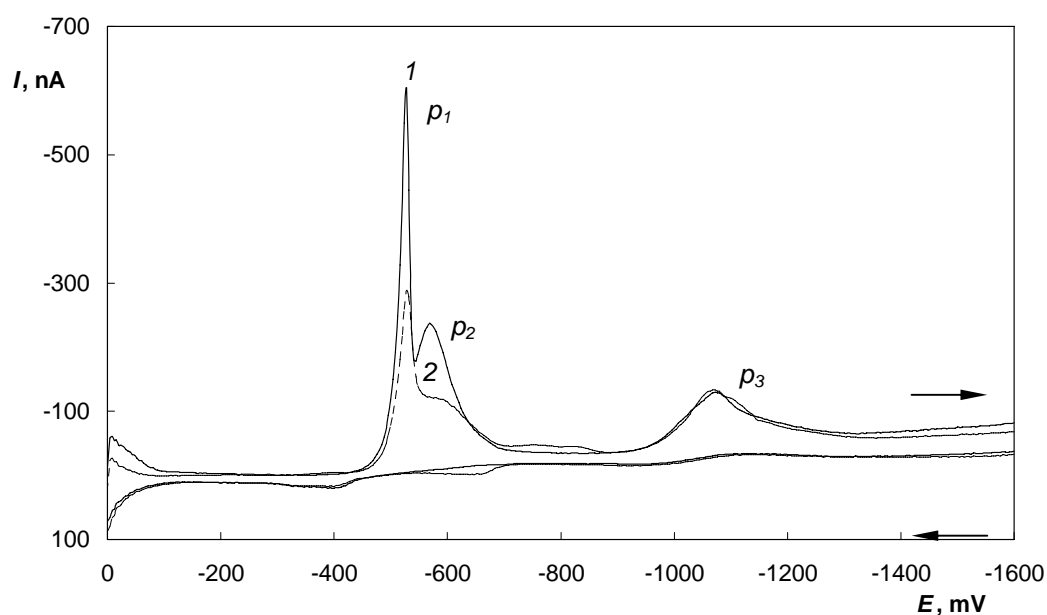


Fig. 5 – Cyclic voltammograms of 2,7-DNFN ($c = 1 \cdot 10^{-5} \text{ mol} \cdot \text{L}^{-1}$) at HMDE in methanol – BR buffer (1:1); resulting pH 11.1; first (1) and second(2) scan in the potential window from 0 to -1600 mV, scan rate $50 \text{ mV} \cdot \text{s}^{-1}$.

3.2 Proposed Mechanism of Electrochemical Reduction of 2,7-Dinitro-9-fluorenone

Gary and Day⁶, who studied the polarographic reduction of 2,7-DNFN in a buffered mixture of water and acetone at pH 1.4, 4.3, 6.6, 7.7, 10.4 and 11.3, found at pH 1.4 one eight-electron wave followed by a four-electron wave and a two-electron wave; at pH 4.3 they found one eight-electron wave followed by a four-electron wave; and at pH 6.6 they found they found two consecutive four-electron waves followed by a two-electron wave. They did not determined the number of exchanged electrons in the alkaline medium.

Our findings in the mixture of water and methanol (1:1) are different. On the basis of our results we have proposed a scheme of electrochemical reduction of 2,7-DNFN different in the acid medium (see Fig. 6), in neutral medium (see Fig. 7) and in alkaline medium (see Fig. 8).

In the acid medium (see Fig. 3 and 6), first cathodic peak p_1 corresponds to 4-electron reduction of one nitro group to hydroxylamino group and second peak p_2 corresponds to 4-electron reduction of the second nitro group to hydroxylamino group in the presence of the previously formed hydroxylamino group (this reduction step is corresponding to the polarographic first 8-electron wave, which splits above pH 5 into two 4-electron waves). The separation of the first polarographic wave can be explained by the fact that first nitro group is reduced in the presence of second nitro group with the pronounced negative mesomeric ($-M$) effect which decreases the electron density in the region of the first nitro group thus making its reduction easier. The second nitro group is reduced in the presence of $-\text{HN}_2^+\text{OH}$ group (in acid media) or $-\text{NHOH}$ group (in neutral and alkaline media). The NHOH group with the positive mesomeric ($+M$) effect increases the electron density in the region of the second nitro group thus making its polarographic reduction more difficult. This assumption is in agreement with the observed fact that the separation of the first 8-electron wave is higher in alkaline than in acid region. Protonated $-\text{NH}_2^+\text{OH}$ group withdraws electrons from the second group thus making its reduction easier, i.e. shifts its half-wave potential closer to the first wave.

Third cathodic peak p_3 in acid media corresponds to 4-electron simultaneous reduction of one hydroxylamino group to amino group and carbonyl group to secondary alcohol group⁶. And fourth peak p_4 in acid media corresponds to 2-electron reduction of the second hydroxylamino group to amino group.

In neutral region (see Fig. 4 and 7), cathodic peaks p_1 and p_2 represents the same 8-electron and peak p_3 the same 4-electron reduction process as in acid media. Peak p_4 is not observed and the reduction process is stopped in the state, where one hydroxylamino group stays unreduced and the second hydroxylamino group is reduced to amino group. The presence of unreduced hydroxylamino group is indicated by the reversible anodic peak p_4' , which can be assigned to a 2-electron oxidation of hydroxylamino group to nitroso group (-NO). The cathodic peak p_4 was observed in second cathodic scan around -150 mV, which is in agreement with the well-known reversibility of NO/NHOH system.

In alkaline region (see Fig. 5 and 8), the reduction is similar to the reduction in acid medium (peaks p_1 and p_2 represents two 4-electron reductions of nitro groups). Whereas the reduction from 2,7-di(hydroxylamino)-9-fluorenone to 2,7-diamino-9-fluorenol goes in two consecutive steps in acid medium, simultaneous 6-electron reduction is observed in alkaline medium. Peak p_3 corresponds to this reduction step. The presumption that neither hydroxylamino group is present after last reduction step is supported by absence of peak of reversible NO/NHOH system.

Acknowledgement

This work was financially supported by the Czech Ministry of Education, Youth and Sports (project LC06035 and project MSM 0021620857).

References

- [1] Moreira J. C., Barek J.: *Quimica Nova*. **18** (2005), 362-367.
- [2] Jacob J., Karcher W., Belliaro J. J., Dumler R., Boeneke A.: *Fresenius J. Anal. Chem.* **340** (1991) 755-767.
- [3] Barek J., Cvačka J., Moreira J. C., Zima J.: *Chem Listy*. **90** (1996), 805-817.
- [4] Rafii F., Selby A. L., Newton R. K., Cerniglia C. E.: *Appl. Environ. Microbiol.* **60** (1994), 4263-4267.
- [5] Pumera M., Muzikář J., Barek J., Jelínek I.: *Anal. Lett.* **34** (2001), 1369-1375.
- [6] Gary J. T., Day R. A.: *J. Electrochem. Soc.* **107** (1960), 616-618.

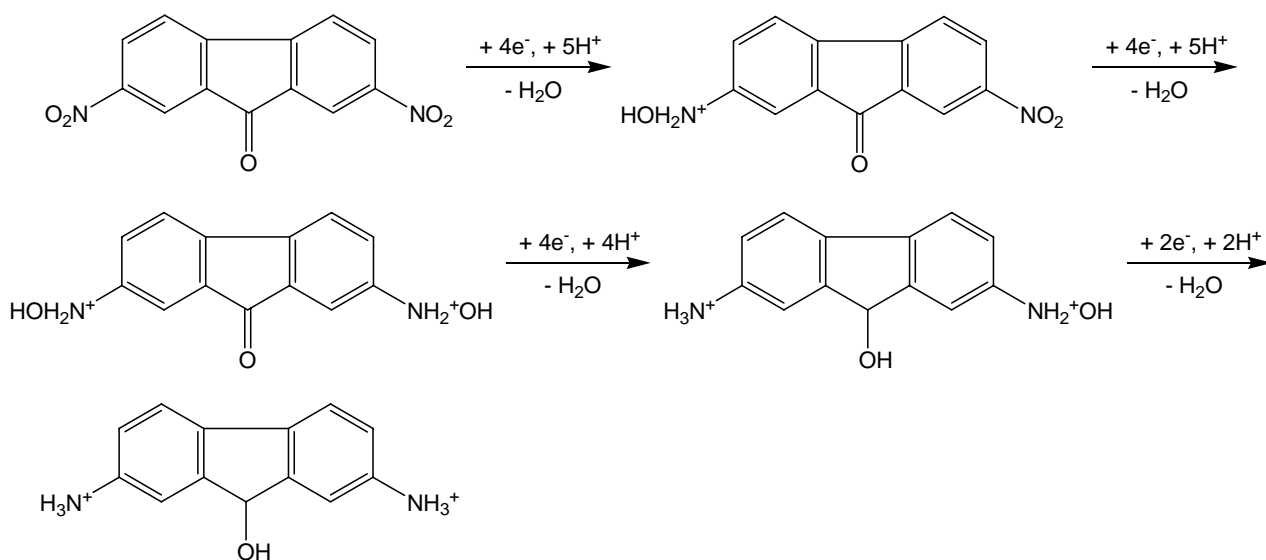


Fig. 6 – Proposed electrochemical reduction of 2,7-DNFN in acid medium.

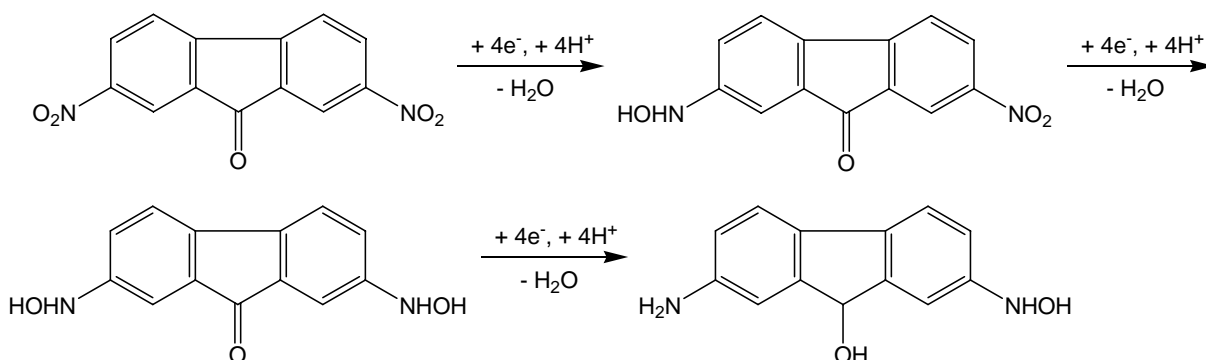


Fig. 7 – Proposed electrochemical reduction of 2,7-DNFN in neutral medium.

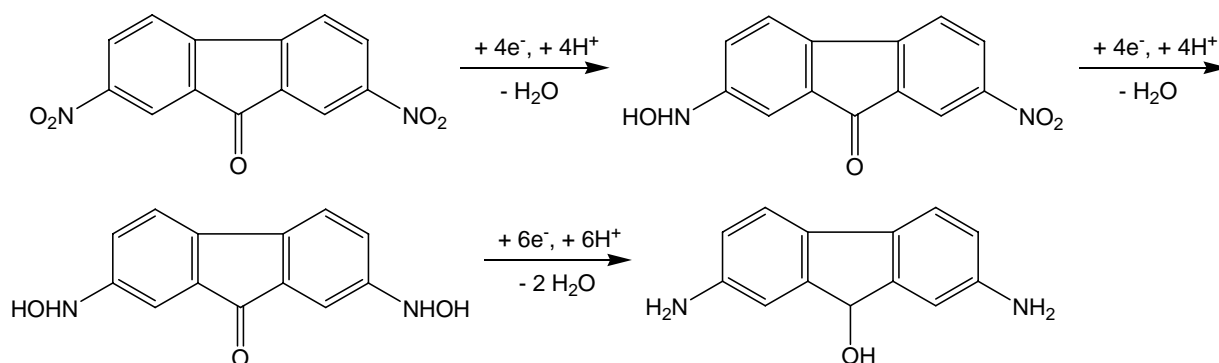


Fig. 8 – Proposed electrochemical reduction of 2,7-DNFN in alkaline medium.

VOLTAMMETRIC DETERMINATION OF GENOTOXIC NITROCOMPOUNDS USING SILVER AMALGAM ELECTRODES

Aleš Daňhel^a, Jiří Barek^a, Bogdan Yosypchuk^b and Karolina Pecková^a

^a Charles University in Prague, Faculty of Science, Department of Analytical Chemistry, UNESCO Laboratory of Environmental Electrochemistry, Albertov 8, 128 40 Prague 2, Czech Republic; e-mail: ales.danhel@seznam.cz

^b Academy of Sciences of the Czech Republic, Jaroslav Heyrovsky Institute of Physical Chemistry, Dolejškova 3, 182 23 Praha, Czech Republic

Abstract

Silver amalgam is an electrode material suitable for construction of new types of electrodes. It is a non-toxic electrode material that can substitute "toxic" mercury in modern voltammetric methods. In this work, a new type of electrode was prepared. It is a silver paste amalgam electrode where the pastes were mixed from a silver amalgam powder and a mineral oil, silicone oil, paraffin oil and tricresylphosphate (TCP), stuffed into a Teflon body of electrode. Potential windows of those electrodes were studied in aqueous solutions of 0,1 mol.L⁻¹ HClO₄; 0,1 mol.L⁻¹ HCl; 0,2 mol.L⁻¹ acetate buffer pH 4,8; 0,5 mol.L⁻¹ EDTA and 0,2 mol.L⁻¹ acetate buffer pH 4,8; 0,1 mol.L⁻¹ NaClO₄; 0,05 mol.L⁻¹ Na₂B₄O₇ pH 9,2; 0,1 mol.L⁻¹ NaOH and compared with polished silver solid amalgam electrode (p-AgSAE). The concentration dependences and reproducibility were measured by DPV for 4-nitrophenol (4-NP) on the paraffin oil paste (Ag-amalgam: paraffin oil = 20:1) in 0,2 mol.L⁻¹ acetate buffer pH 4,8. Relative standard deviation of these measurements was lower than ±5% and the limit of quantification was found to be 1 μmol.L⁻¹ for 4-NP. The silver paste amalgam electrodes are expected to provide new possibilities for determinations of electrochemically reducible compounds by modern voltammetric methods. The main expected advantage is the possibility of easily renewable surface as in the case of carbon paste electrodes.

Keywords

Voltammetry; DC voltammetry (DCV); differential pulse voltammetry (DPV); silver amalgam electrode; silver paste amalgam electrode (AgPAE); 4-nitrophenol (4-NP)

Introduction

Voltammetric methods are used very often to determine electrochemically reducible compounds, such as some agrochemicals, medicaments, industry dyes and many environmental pollutants¹. Mercury electrodes have been used for these determinations most frequently. But since European Union bans the usage of "toxic" mercury on the workplace, new non-toxic electrode materials are looked for^{2,3}. Metal amalgams are the most commonly used types of non-toxic electrode materials for electrochemical reduction in modern electroanalytical chemistry. Solid amalgam electrodes have a good mechanical stability, simple handling and regeneration and a potential window comparable with hanging mercury drop electrode (HMDE)^{4,5}.

Testing the silver paste amalgam electrode as a possible substitution of mercury electrodes is the aim of this work.

Experimental

Voltammetric measurements were done on Eco-Tribo Polarograph with software PolarPro version 5.1 (Polaro-Sensors, Praha, ČR) in a three electrodes system, where the AgPAE (diameter 2,99 mm) was used as the working electrode, the Ag/AgCl electrode (3 M KCl) of type 10-20+ (Electrochemical Detectors, Turnov, ČR) was the referent electrode and the platinum wire electrode (Monocrystals, Turnov) was the auxiliary electrode.

The polarization rate $20 \text{ mV}\cdot\text{s}^{-1}$, the pulse width -50 mV and the modulation amplitude 80 ms were used in differential pulse voltammetry (DPV) and the same polarization rate $20 \text{ mV}\cdot\text{s}^{-1}$ in DC voltammetry.

The solutions were prepared from the deionized water (Milli-Q plus system, Millipore, USA) and analytical reagents of p.a. purity (Lachema Brno, ČR). The solutions were bubbled by nitrogen of 4.0 purity (Linde, Praha, ČR). Mineral oil – ultra purity (69794, Fluka),

silicone oil (MV 15500, Lukoil, Kolín), paraffin oil (Paraffinum liquidum, Phar B, p. 2459. Grada Publishing, Prague 1997) and tricresylphosphate (92100, Fluka) were used to make the paste with silver amalgam powder. The silver amalgam was prepared by mixing mercury and silver powder (3:2, w/w) by 5 min shaking in dental amalgamator (Dentomat compact, Degussa, Brazil). After that the amalgam was comminuted to fine powder in agate dish. The pastes were prepared by mixing suitable weight ratio of the amalgam and the pasting liquid. This ratio must be chosen to prepare paste of optimal consistency. The pastes were stuffed into the Teflon body of the electrode and after that, this electrode was activated by imposing a constant potential -2200 mV for 5 min in 0,2M KCl solution. This electrochemical activation was repeated every day before measurement. Regeneration was done before every measurement by switching between two potentials E_{in} and E_{fin} in 150 cycles for a period 0,1 s. If the electrode did not work, a disk surface had to be wiped off, new paste was forced out from the electrode and electrochemically activated in KCl.

Result and Discussion

The pastes were made by appropriate weight ratio of amalgam and the pasting liquid. The optimum ratio of components was found experimentally. The paste must not be washy, because it would flow out, and it must not be too compact (dry), because it would fall apart. Therefore, small variation of the amalgam pasting liquids can be done to obtain the optimum consistency in dependence on the consistency of silver amalgam powder. Behavior of those electrodes in dependence of pH was investigated by DCV in aqueous solutions of 0,1 mol.L⁻¹ HClO₄; 0,1 mol.L⁻¹ HCl; 0,2 mol.L⁻¹ acetate buffer pH 4,8; 0,5 mol.L⁻¹ EDTA and 0,2 mol.L⁻¹ acetate buffer pH 4,8; 0,1 mol.L⁻¹ NaClO₄; 0,05 mol.L⁻¹ Na₂B₄O₇ pH 9,2 and 0,1 mol.L⁻¹ NaOH. The measured potential windows of amalgam paste electrodes looked very similar to each other, but in comparison with p-AgSAE and HMDE they are narrower (Table I).

For testing of electrochemical activity of amalgam pastes, an aqueous solution of 4-nitrophenol (10, 20 and 100 μmol.L⁻¹) in 0,1

mol.L⁻¹ HCl, 0,2 mol.L⁻¹ acetate buffer and 0,1 mol.L⁻¹ NaOH was chosen. (See Fig. 1 for the sake of illustration).

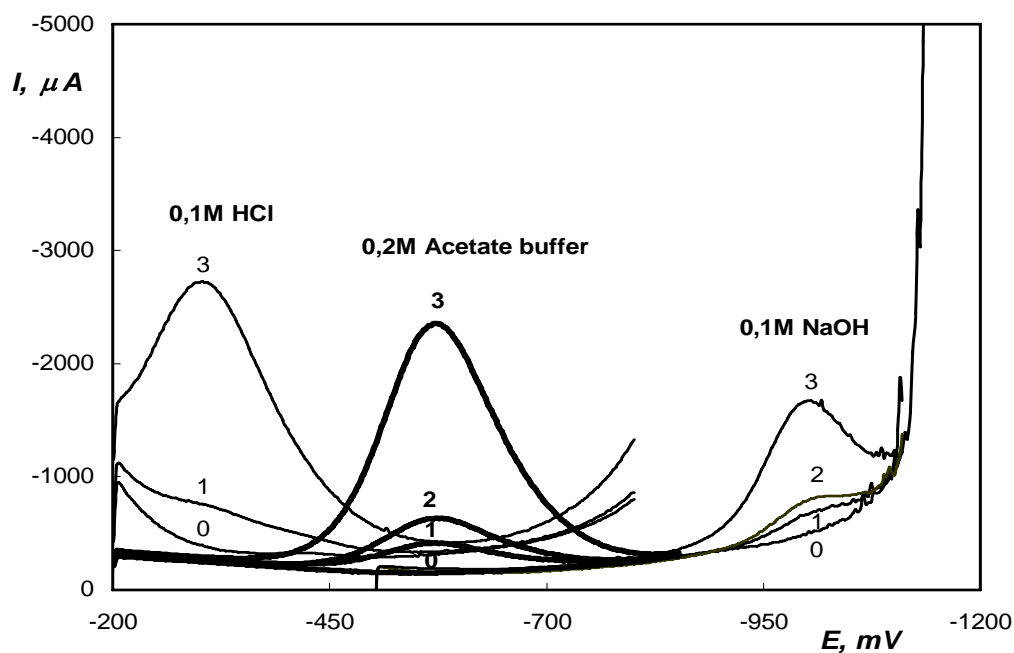


Fig. 1 - DP voltammograms of 4-nitrophenol on the AgPAE

(*amalgam : paraffin oil* = 20:1); *c* (4-NP): 0-base electrolyte (0); 10 (1); 20 (2); 100 (3) $\mu mol.L^{-1}$.

From all tested pastes, paraffin oil paste was chosen, because it gave the best DPV signal of all base electrolytes tested (the lowest background signal of base electrolyte), a good signal for 4-nitrophenol and good repeatability.

Table I – Experimental range of working potentials measured by DCV at AgPAE in different aqueous base electrolytes

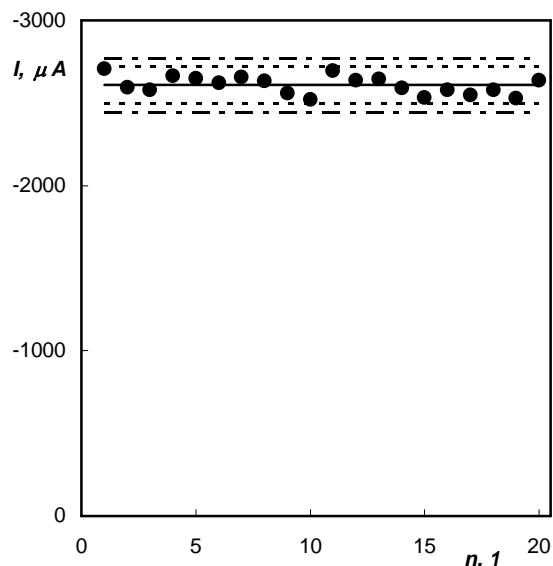
Electrode + paste liquid (current, μA)	Constitution	Range of AgPAE working potentials, V						
	amalgam: paste liquid (w/w)	0.1M HClO ₄	0.1M HCl	0.2M acetate buffer, pH 4.8	0.05M Na ₂ EDTA, 0.2M acetate buffer, pH 4.8	0.1M NaClO ₄	0.05M Na ₂ B ₄ O ₇ pH 9.2	0.1M NaOH
HMDE (1 μA)^a	-	-1,19 ... +0,44	-1,27 ... +0,11	-1,70 ... +0,31	-1,55 ... +0,31	-	-1,98 ... +0,15	-1,97 ... -0,07
p-AgSAE (1 μA, 0,70 mm)^a	-	-1,12 ... +0,45	-1,12 ... +0,11	-1,51 ... +0,31	-1,45 ... +0,11	-	-1,88 ... +0,16	-1,96 ... -0,06
AgPAE+mineral oil (1 μA)	44:1	-0,82 ... 0,13	-0,67 ... -0,50	-0,89... 0,11	-0,83 ... -0,20	-0,71 ... 0,60	-1,02 ... 0,50	-0,76 ... -0,14
AgPAE+mineral oil (5 μA)		-0,94 ... 0,31	-0,79 ... 0,16	-1,03 ... 0,30	-0,96 ... 0,24	-1,24 ... 0,33	-1,24 ... 0,16	-1,25 ... -0,40
AgPAE+mineral oil (20 μA)		-1,04 ... 0,36	-0,90 ... 0,21	-1,15 ... 0,38	-1,09 ... 0,360	-1,36 ... 0,51	-1,50 ... 0,24	-1,45 ... 0,30
AgPAE+silicone oil (1 μA)	15:1	-0,16 ... -0,04	-0,23 ... -0,10	-0,22 ... -0,04	-0,19 ... -0,08	-0,20 ... -0,13	-0,18 ... -0,10	-0,20 ... -0,17
AgPAE+silicone oil (5 μA)		-0,79 ... -0,07	-0,70 ... -0,01	-0,84 ... 0,13	-0,91 ... 0,00	-0,77 ... -0,05	-0,93 ... 0,00	-0,73 ... -0,11
AgPAE+silicone oil (20 μA)		-0,93 ... 0,28	-0,84 ... 0,18	-1,14 ... 0,36	-1,13 ... 0,33	-1,17 ... 0,44	-1,20 ... 0,18	-1,15 ... -0,03
AgPAE+parafine oil (1 μA)	20:1	-0,34 ... 0,06	-0,23 ... -0,03	-0,26 ... 0,09	-0,16 ... -0,03	-0,20 ... 0,00	-0,24 ... -0,06	-0,28 ... -0,16
AgPAE+parafine oil (5 μA)		-0,85 ... 0,24	-0,70 ... 0,15	-0,96 ... 0,29	-0,85 ... 0,12	-0,70 ... 0,35	-0,85 ... 0,12	-0,71 ... -0,07
AgPAE+parafine oil (20 μA)		-0,97 ... 0,26	-0,83 ... 0,18	-1,15 ... 0,35	-1,08 ... 0,34	-1,19 ... 0,45	-1,21 ... 0,17	-1,20 ... -0,03
AgPAE+TCP (1 μA)	13:1	-0,79 ... 0,13	-0,67 ... -0,03	-0,86 ... 0,17	-0,83 ... -0,03	-1,03 ... 0,17	-1,10 ... 0,09	-1,20 ... -0,11
AgPAE+TCP (5 μA)		-0,92 ... 0,31	-0,79 ... 0,14	-0,98 ... 0,30	-0,96 ... 0,28	-1,28 ... 0,35	-1,25 ... 0,15	-1,30 ... -0,06
AgPAE+TCP (20 μA)		-1,03 ... 0,46	-0,87 ... 0,18	-1,07 ... 0,37	-1,07 ... 0,36	-1,35 ... 0,45	-1,35 ... 0,32	-1,33 ... -0,03
AgPAE+TCP (1 μA)	11:1	-0,83 ... 0,14	-0,82 ... -0,07	-1,06 ... 0,07	-1,03 ... -0,02	-1,03 ... 0,05	-1,14 ... 0,03	-1,12 ... -0,10
AgPAE+TCP (5 μA)		-1,01 ... 0,42	-0,98 ... 0,16	-1,27 ... 0,31	-1,27 ... 0,20	-1,37 ... 0,32	-1,36 ... 0,15	-1,32 ... -0,05
AgPAE+TCP (20 μA)		-1,15 ... 0,52	-1,11 ... 0,22	-1,44 ... 0,44	-1,44 ... 0,44	-1,47 ... 0,58	-1,42 ... 0,26	-1,37 ... 0,02

diameter of AgPAE (2,99 mm); TCP – tricresylphosphate; ^a taken from reference ⁶

After that, the repeatability of DPV signals for 4-NP ($1 \mu\text{mol.L}^{-1}$) was tested by 20 consecutive measurements using AgPAE (amalgam : paraffin oil = 20:1) in $0,2 \text{ mol.L}^{-1}$ acetate buffer with regeneration potentials $E_{\text{in}} -200 \text{ mV}$ and $E_{\text{fin}} -800 \text{ mV}$ (Fig. 2).

Fig. 2 - 20 consecutive DPV measurements of $1 \mu\text{mol.L}^{-1}$ 4-NP at AgPAE in $0,2 \text{ mol.L}^{-1}$ acetate buffer

$\text{pH } 4,8$: (—) average peak current; (- -) twice RSD; (-.-.-) three times RSD;
 $E_{\text{in}} -200 \text{ mV}$ and $E_{\text{fin}} -800 \text{ mV}$.



The calibrations curves of 4-NP were measured by DPV using AgPAE in $0,2 \text{ mol.L}^{-1}$ acetate buffer $\text{pH } 4,8$ in two concentration ranges from 10 to $100 \mu\text{mol.L}^{-1}$ (Fig. 3) and from 1 to $10 \mu\text{mol.L}^{-1}$ (Fig. 4). Potentials of regenerations AgPAE were $E_{\text{in}} -200 \text{ mV}$ and $E_{\text{fin}} -800 \text{ mV}$ and from the linear concentration range (Fig, 3 and Fig. 4) was constructed the logarithmic diagram of concentration dependences (Fig. 5).

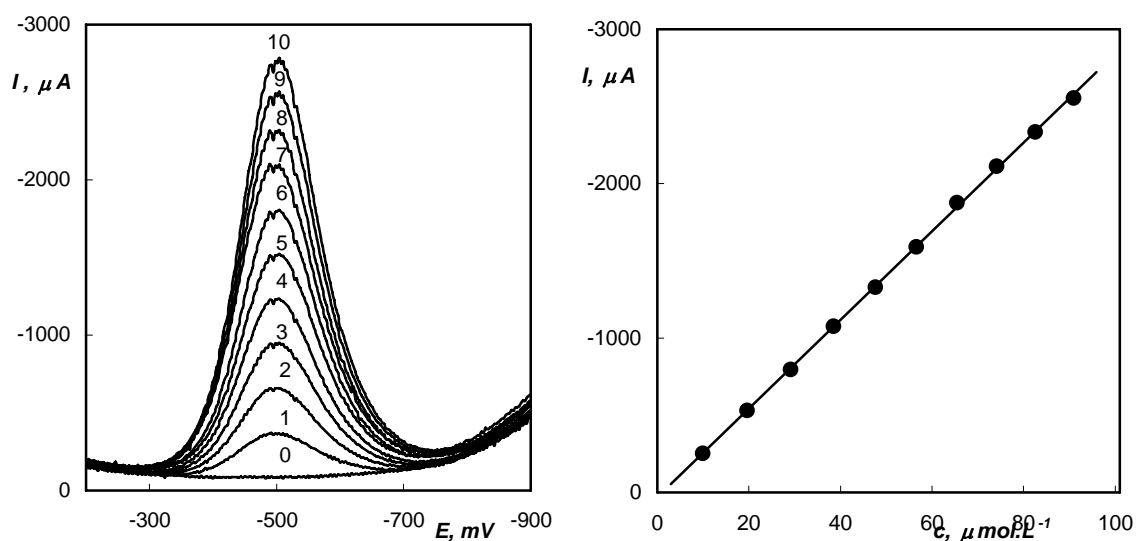


Fig. 3 - DP voltammograms and calibration dependence for 4-NP in 0,2 mol.L⁻¹ acetate buffer

pH 4,8 measured at AgPAE; E_{in} -200 mV and E_{fin} -800 mV; c (4-NP): 0 (0); 9,9 (1); 19,6 (2); 29,1 (3); 38,5 (4); 47,6 (5); 56,6 (6); 65,4 (7); 74,1 (8); 82,6 (9); 90,9 (10) $\mu\text{mol.L}^{-1}$.

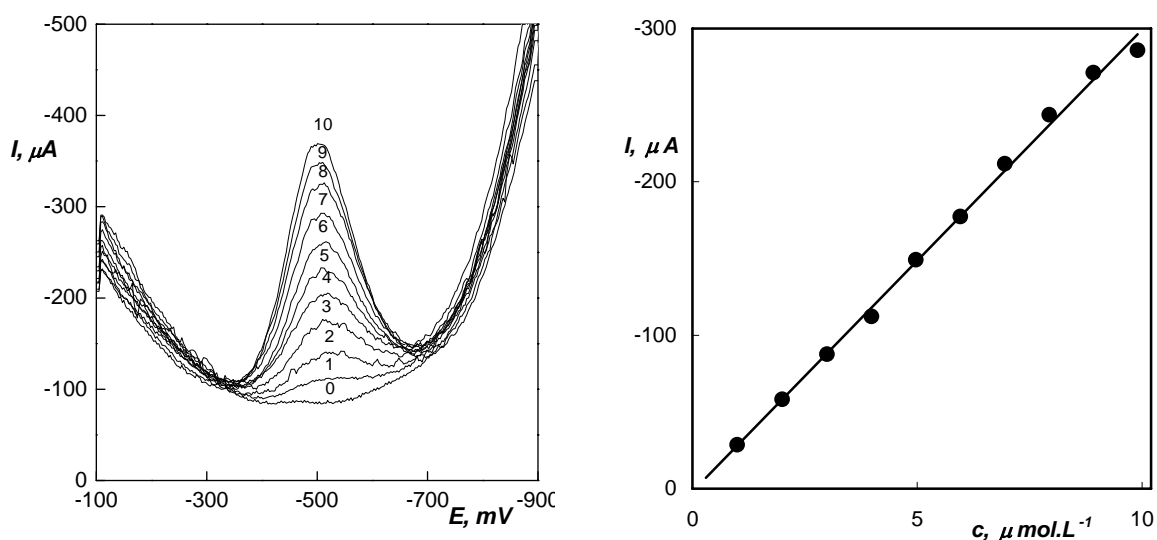
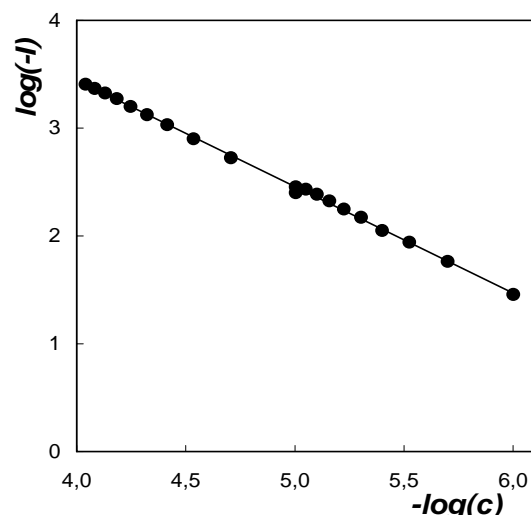


Fig. 4 - DP voltammograms and calibration dependence for 4-NP in 0,2 mol.L⁻¹ acetate buffer

pH 4,8 measured at AgPAE; E_{in} -200 mV and E_{fin} -800 mV; c (4-NP): 0 (0); 1,0 (1); 2,0 (2); 3,0 (3); 4,0 (4); 5,0 (5); 6,0 (6); 7,0 (7); 7,9 (8); 8,9 (9); 9,9 (10) $\mu\text{mol.L}^{-1}$.

Fig. 5 - Logarithmic dependence of DPV peak high and c (4-NP) measured at AgPAE in 0,2 mol.L⁻¹ acetate buffer pH 4,8



The parameters of calibrations curves and parameter of logarithmic dependence are summarized in Table II.

Table II Parameters of the calibration curves and of the logarithmic dependence

Dependence	Concentration range, $\mu\text{mol.L}^{-1}$	Slope, $\mu\text{A.L.}\mu\text{mol}^{-1}$	Intercept, μA	R ²	LOQ, $\mu\text{mol.L}^{-1}$
calibration 4-NP	10-100	-28,7	30,1	0,9997	-
calibration 4-NP	1-10	-30,1	1,93	0,9969	1
logarithmic	1-100	-0,989	7,4	0,9990	-

Conclusion

The silver paste amalgam electrode can be used to determine electrochemically reducible compounds. The limit of quantification was found to be 1 $\mu\text{mol.L}^{-1}$ for 4-nitrophenol by differential pulse voltammetry at silver paste amalgam electrode in aqueous solution of 0,2 mol.L⁻¹ acetate buffer of pH 4,8.

Acknowledgements

Authors thank the Ministry of Education, Youth and Sports of the Czech Republic (projects LC 06035 and MSM 0021620857) for the financial support.

References

1. Yosypchuk B., Novotny L.: *CRC Crit. Rev. Anal. Chem.* **32**, 141 (2002).
2. http://www.europarl.eu.int/meetdocs/2004_2009/documents/pr/585/585664/585664cs.pdf, obtained 3.12.2005.
3. Eley B.M.: *British Dental J.* **182**, 373 (1997).
4. Yosypchuk B., Novotny L.: *Electroanalysis* **15**, 121 (2003).
5. Yosypchuk B., Heyrovsky M., Palecek E., Novotny L.: *Electroanalysis* **14**, 1488 (2002).
6. Bogdan Yosypchuk: PhD Thesis. Faculty of Chemical Technology, University of Pardubice, Pardubice 2003.
7. Aleš Daňhel: Thesis. Faculty of Science, Charles University, Prague 2006.

CAPILLARY ELECTROPHORESIS OF ANTHRAQUINONE DYES EMPLOYED IN WORKS OF ART

Eva Svobodová, Marie Vadinská, Zuzana Bosáková

Charles University in Prague, Faculty of Science, Department of Analytical Chemistry, Hlavova 2030, 128 43 Prague 2, Czech Republic; e-mail: eduscho@seznam.cz

Abstract

Two CZE and MEKC methods have been developed for identification and quantitation of seven natural hydroxyderivatives of anthraquinone dyes. A fused-silica capillary was used, with a $0.01 \text{ mol}\cdot\text{dm}^{-3}$ borate buffer, $\text{pH} = 10.1$, as the running electrolyte for CZE, permitting separation of all the analytes (except for 1,5-dihydroxyanthraquinone) within 17 minutes, with a satisfactory resolution, at a voltage of 20 kV. The effects of the electrolyte concentration, the pH value, the presence of organic modifiers and the separation voltage on the analyte migration have been studied. The MEKC separation used a $0.01 \text{ mol}\cdot\text{dm}^{-3}$ borate buffer of $\text{pH} = 9.7$, with an addition of $0.02 \text{ mol}\cdot\text{dm}^{-3}$ sodium dodecylsulfate (SDS), which even permits the detection of 1,5-dihydroxyanthraquinone. Analytes with analogous structures exhibit similar migration times and thus cannot be mutually separated. The MEKC method has been used to quantify 2-hydroxyanthraquinone.

Keywords:

CZE, MEKC, Anthraquinone

1 Introduction

Anthraquinone derivatives belong among the main components of natural dyes which are produced by various plants and animals, especially insects. The composition of natural dye mixtures used in historical objects of art is important for the dating of these objects, locating the place of their origin and their restoration. Hydroxyderiva-

tives of anthraquinone, studied in this work, are at present of special interest because of their wide applicability. They have been used not only in works of art, but also in foodstuff industry, medicine, agriculture, in studies of hydrogen bonding, complexation reactions, etc.

To identify mono-, di- and trihydroxyderivatives of anthraquinone, colorimetric tests^{1,2} and spectrometric methods³⁻⁵ have been employed, mostly molecular UV/VIS absorption spectrometry and infrared microscopy, followed by Raman, X-ray fluorescence and electron microscopy. The electrochemical method of voltammetry⁶ has been used to identify impurities in the anthraquinone derivatives. Separations have mostly been carried out chromatographically, using paper chromatography (PC) and thin-layer chromatography (TLC)^{6,7} because of their simplicity and low cost. But especially reversed-phase high-performance liquid chromatography (HPLC)⁷⁻¹⁰ has been used. To identify anthraquinone dyes (alizarin and purpurin) in historical objects, capillary zone electrophoresis (CZE)^{10,11,14} has been employed with UV/VIS and mass spectrometric (MS) detection. Glucosides of hydroxyderivatives of anthraquinone have been determined by CZE employing cyclodextrins¹². Micellar electrokinetic chromatography (MEKC)¹²⁻¹⁴ with MS detection has been used to quantify natural anthraquinones and natural pigments as foodstuff colorants.

This work deals with separations of 1- and 2-hydroxy-, 1,2-, 1,4-, 1,5- and 1,8-dihydroxy- and 1,2,4-trihydroxyanthraquinone, using capillary zone electrophoresis (CZE) and micellar electrokinetic chromatography (MEKC).

2 Experimental

2.1 Chemicals

The analytes, namely 1- and 2-hydroxy-, 1,2-dihydroxyanthraquinone (alizarin), were isolated at the Institute of Microbiology of the Academy of Sciences of the Czech Republic with a purity better than 98 % and the other ones, 1,4- (quinizarin), 1,5- (anthrarufin), 1,8-dihydroxy- (danthron) and 1,2,4-trihydroxyanthraquinone (purpurin), were obtained from Fluka with a purity better than 95 %. All the analytes were dissolved in 1.5 cm³ CH₃CN (Sigma-Aldrich) and then diluted at a ratio of 33/67 (v/v) with the CH₃CN/electrolyte (danthrone solution was diluted in the 0.01 mol·dm⁻³ borate buffer, pH 11.0, for

its identification using CZE). The analyte solutions were stored in a fridge and remained stable within a year. The running CZE electrolytes were prepared by mixing the 0.01 mol·dm⁻³ borate buffer, pH 10.1 (Lachema), with CH₃CN. The MEKC running electrolytes were prepared by mixing the 0.01 mol·dm⁻³ borate buffer, pH 9.7, with SDS (Sigma-Aldrich). The other chemicals were purchased from Lachema and Lach-Ner. Distilled water was used throughout.

2.2 Instruments

The CZE measurements were carried out using a PrinCE 250 (PrinCE Technologies B.V., NL) with an autosampler and an on-column UV/VIS absorbance detector Spectra 100 (Therma Separation Products, USA) operated at 250 nm for mixtures. To detect single analytes, their local absorption maxima wavelengths were used. UV spectra of individual anthraquinones were measured using Pye Unicam PU 8800 UV/VIS spectrophotometer (Philips, GB) in a wavelength range from 190 to 500 nm. Fused-silica capillaries (CACO s.r.o., SK and Composite Metal Services Ltd., GB) of $L_D = 55.8$ cm, $L_C = 69.8$ cm, i.d. = 75 μm and o.d. = 380 μm were used, with hydrodynamic sample injection at 2 kPa for 10 s. The separation voltage was 20 – 30 kV.

3 Results and Discussion

3.1 Separation

The wavelengths of the local absorption maxima of the individual analytes have been found to attain high analyte responses. All the analytes absorb within a narrow range around 250 nm, except for anthrarufin. Thus CZE method sensitivity of anthrarufin was lower and anthrarufin wasn't detected using this method.

The CZE separation is based upon charged analytes and thus requires pH values close to dissociation constant of analytes, in alkaline area. Hence a 0.02 mol·dm⁻³ borate buffer has been selected as the CZE running electrolyte. The effect of organic modifiers in the electrolyte on the higher analyte solubility and baseline stabilization has been studied. With increasing concentration of CH₃CN (to 40 vol. %), the electroosmotic flow slowed down, the peak profile

deteriorated and the analyte solubility didn't increased (Fig. 5). Therefore, the borate buffer was used as the running electrolyte without an addition of the organic modifier.

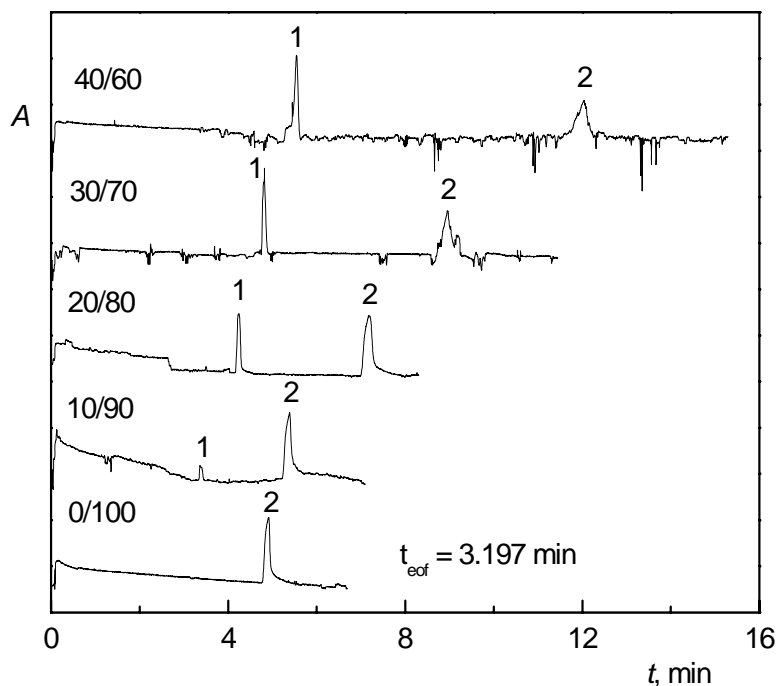


Fig. 5 Dependence of the electroosmotic flow (peak 1 corresponding to thiourea) and electrophoretic mobility of 1,2-dihydroxyanthraquinone (peak 2) on the composition of the running electrolyte consisting of CH₃CN and 0.02 mol·dm⁻³ borate buffer (pH 9.5) at various ratios (v/v);

$V = 30 \text{ kV}$, $\lambda = 250 \text{ nm}$.

The effect of electrolyte's pH value (9.5 – 11.0) on the analyte migration has been studied. The pH exceeding 10.0, needed for the analyte ionization, caused too high electric currents in the capillary. Hence the concentration of the borate buffer had to be reduced from value 0.02 mol·dm⁻³ to 0.01 mol·dm⁻³ and also the value of the separation voltage from 30 kV to 20 kV.

The optimum running electrolyte is the 0.01 mol·dm⁻³ borate buffer, pH = 10.1, which permits separation of all the above analytes (except for 1,5-dihydroxyanthraquinone) with a satisfactory resolution, at a voltage of 20 kV, within 17 min. (Fig. 6) The analyte effective mobilities under these conditions are listed in

Table 1.

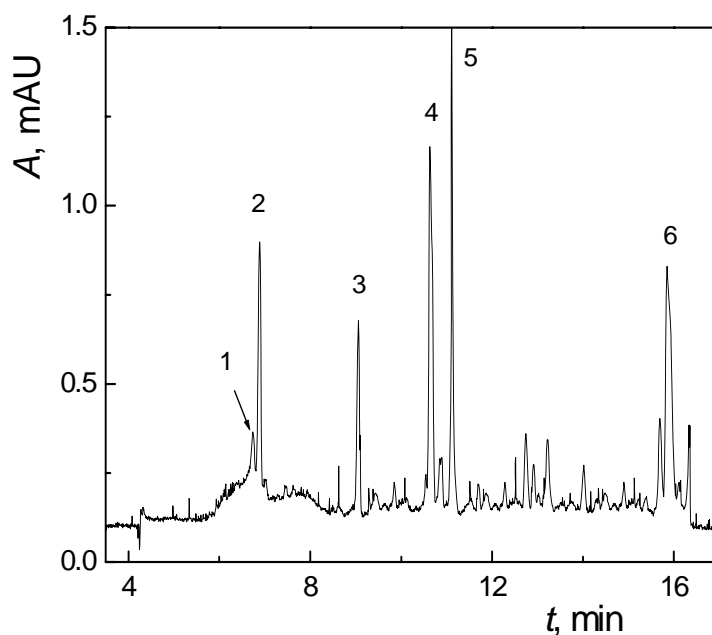


Fig. 6 Separation of six analytes: (1) 1,2-dihydroxyanthraquinone, (2) 2-hydroxy-anthraquinone, (3) 1,4-dihydroxyanthraquinone, (4) 1-hydroxyanthraquinone, (5) 1,2,4-trihydroxyanthraquinone and (6) 1,8-dihydroxyanthraquinone;

the 0.01 mol·dm⁻³ borate buffer (pH 10.1), $V = 20$ kV, detection at $\lambda = 250$ nm.

Table 1 Effective mobilities of the analytes in a 0.01 mol·dm⁻³ borate buffer (pH 10.1);

detection at the wavelengths of the local absorption maxims, $V = 20$ kV, fused--silica capillary CACO ($L_D = 55.8$ cm, $L_C = 69.8$ cm, $d_i = 75$ μ m, $d_o = 380$ μ m).

Substance	μ_{eff} 10^{-4} cm ² ·V ⁻¹ ·s ⁻¹
1-HA	-2.76
2-HA	-1.76
1,2-DHA (alizarin)	-1.72
1,4-DHA (quinizarin)	-2.55
1,2,4-THA (purpurin)	-3.03
1,5-DHA (anthrarufin)	-
1,8-DHA * (danthron)	-3.42

* 1,8-dihydroxyanthraquinone was diluted in pH 11.0

The solution of 1,8-dihydroxyanthraquinone was diluted in the $0.01 \text{ mol}\cdot\text{dm}^{-3}$ borate buffer, pH 11.0, and injected into the electrolyt ($0.01 \text{ mol}\cdot\text{dm}^{-3}$ borate buffer, pH 10.1), because it wasn't ionized at a lower pH value.

The MEKC separation is based upon not only charged analytes but also uncharged analytes and thus requires lower pH values. The running electrolyte contained a $0.01 \text{ mol}\cdot\text{dm}^{-3}$ borate buffer of pH 9.7, with an addition of the SDS anionogenic tenside. The effect of the SDS concentration ($0.01 - 0.02 \text{ mol}\cdot\text{dm}^{-3}$) on the analyte response can be seen in Fig. 7. The highest response is obtained at the highest SDS concentration ($0.02 \text{ mol}\cdot\text{dm}^{-3}$) due to the greatest solubility of the analytes. The greater solubility even permits the detection of 1,5-dihydroxyanthraquinone (Fig. 8).

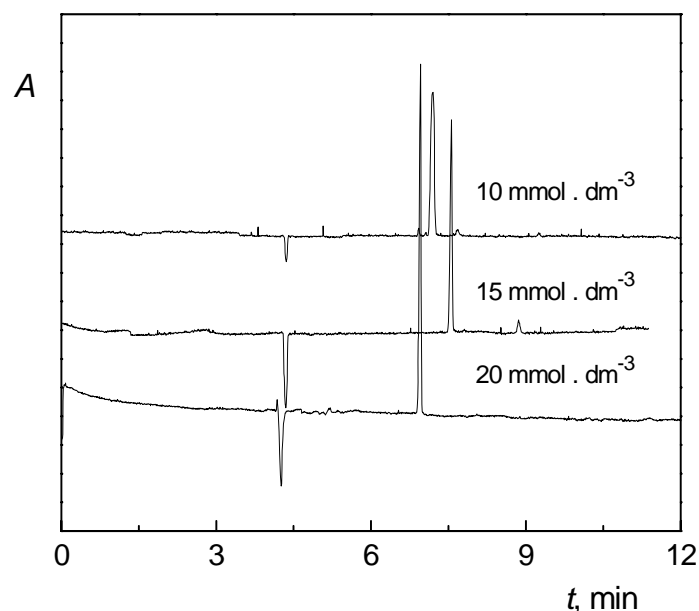


Fig. 7 The effect of the SDS concentration on the $1.5 \cdot 10^{-4} \text{ mol}\cdot\text{dm}^{-3}$ 2-hydroxyanthraquinone response;

the $0.01 \text{ mol}\cdot\text{dm}^{-3}$ borate buffer (pH 9.7) with $(1.0; 1.5; 2.0) \cdot 10^{-2} \text{ mol}\cdot\text{dm}^{-3}$ SDS, $V = 20 \text{ kV}$, $\lambda = 250 \text{ nm}$.

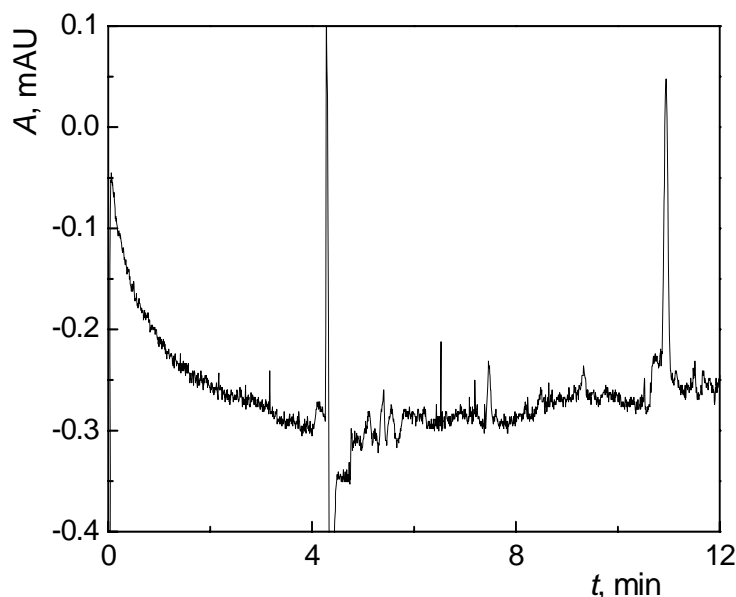


Fig. 8 Electropherogram of 1,5-dihydroxyanthraquinone;

the $0.01 \text{ mol}\cdot\text{dm}^{-3}$ borate buffer (pH 9.7) with $0.02 \text{ mol}\cdot\text{dm}^{-3}$ SDS, $V = 20 \text{ kV}$, $\lambda = 250 \text{ nm}$.

The analyte pseudoeffective mobilities under these conditions (the $0.01 \text{ mol}\cdot\text{dm}^{-3}$ borate buffer of pH = 9.7 with the $0.02 \text{ mol}\cdot\text{dm}^{-3}$ SDS at a voltage of 20 kV) are given in Table 2.

Table 2 Pseudoeffective mobilities of the analytes in a $0.01 \text{ mol}\cdot\text{dm}^{-3}$ borate buffer (pH 9.7) with various concentrations of SDS;

$\lambda = 250 \text{ nm}$, $V = 20 \text{ kV}$, fused-silica capillary by CACO ($L_D = 55.8 \text{ cm}$, $L_C = 69.8 \text{ cm}$, $d_i = 75 \mu\text{m}$, $d_o = 380 \mu\text{m}$).

Substance	$\mu_{\text{eff}}^{\text{ps}}$ ($10^{-4} \text{ cm}^2\cdot\text{V}^{-1}\cdot\text{s}^{-1}$)		
	Concentrations of SDS ($\text{mol}\cdot\text{dm}^{-3}$)		
	$1.0\cdot 10^{-2}$	$1.5\cdot 10^{-2}$	$2.0\cdot 10^{-2}$
1-HA	-2.80	-2.52	-2.93
2-HA	-1.96	-1.90	-1.97
1,2-DHA	-1.68	-1.80	-1.88
1,4-DHA	-2.53	-2.58	-2.91
1,2,4-THA	-3.14	-3.06	-3.12
1,5-DHA	-	-	-2.99
1,8-DHA	-	-	-2.97

Analytes with analogous structures exhibit similar migration and from this point of view, they can be classified into two groups. The one contains 2-hydroxyanthraquinone and 1,2-dihydroxyanthraquinone; the second contains 1-hydroxyanthraquinone, 1,4-dihydroxyanthraquinone, 1,5-dihydroxyanthraquinone, 1,8-dihydroxyanthra-

quinone and 1,2,4-trihydroxyanthraquinone. Mixture prepared by mixing the analytes from the same group cannot be mutually separated.

3.2 Calibration

The MEKC method, permitting greater analyte solubility, was used to quantify 2-hydroxyanthraquinone within a range from $1.0 \cdot 10^{-6}$ to $8.0 \cdot 10^{-5}$ mol·dm⁻³. The peak height (area) vs. the analyte concentration dependence is linear over the whole studied range (Fig. 9). The limits of detection ($1.0 \cdot 10^{-6}$ mol·dm⁻³) and determination ($2.6 \cdot 10^{-6}$ mol·dm⁻³) were obtained from the regression analysis as the background noise multiplied by three and ten, respectively.

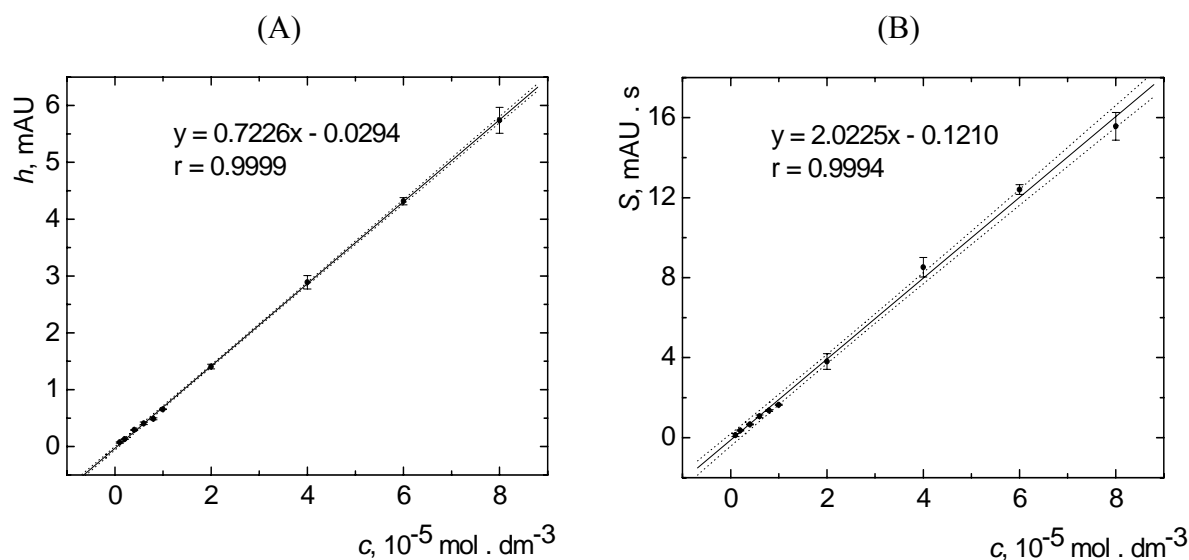


Fig. 9 Calibration curves for peak height (A) and peak area (B) of 2-hydroxyanthraquinone;

the 0.01 mol·dm⁻³ borate buffer, pH 9.7, with 0.02 mol·dm⁻³ SDS, $V = 20$ kV, $\lambda = 250$ nm.

4 Conclusions

The CZE method is preferable for separations of the analyte mixtures for pH > 10, whereas MEKC is advantageous for quantitation because of a greater solubility of the analytes in the micellar system. The MEKC method is suitable for detection of 1,5-dihydroxyanthraquinone.

Acknowledgements

The authors are grateful to the Ministry of Education, Youth and Sports of the Czech Republic for financial support, grant No. 41-202181.

References

- [1] Karsbeek, N.: *Stud. Conserv.* **50** (3) (2005), 205-229.
- [2] Schweppe, H.: *Handbuch der Naturfarbstoffe: Vorkommen, Verwendung, Nachweis. Landsberg/Lech, Ecomed* (1992), ISBN 3-609-65130-X.
- [3] Jacquemin, D.; Preat, J.; Charlot, M.; Wathélet, V.; André, J.M.; Perpète, E.A.: *J. Chem. Phys.* **121** (4) (2004), 1736-1743.
- [4] Čechák, T.; Gerndt, J.; Kopecká, I.; Musílek, L.: *Nucl. Instrum. Methods Phys. Res. Sect. B* **213** (2004), 735-740.
- [5] Čechák, T.; Gerndt, J.; Musílek, L.; Kopecká, I.: *Radiat. Phys. Chem.* **61** (2001), 717-719.
- [6] Grygar, T.; Kučková, Š.; Hradil, D.; Hradilová, J.: *J. Solid State Electrochem.* **7** (2003), 706-713.
- [7] Hofenk de Graaff, J.H.; Roelofs, W.G.Th.; van Bommel, M.R.: *The Colourful Past: Origins, Chemistry and Identification of Natural Dyestuffs. Abegg-Stiftung* (ISBN 3-905014-25-4) and *Archetype Publications* (ISBN 1-873132-13-1) (2004).
- [8] Novotná, P.; Pacáková, V.; Bosáková, Z.; Štulík, K.: *J. Chromatogr. A* **863** (1999), 235-241.
- [9] Bosáková, Z.; Peršl, J.; Jegorov, A.: *J. High Resol. Chromatogr.* **23** (10) (2000), 600-602.
- [10] Weng, W.C.; Sheu, S.J.: *J. High Resol. Chromatogr.* **23** (2) (2000), 143-148.
- [11] Puchalska, M.; Orlińska, M.; Ackacha, M.A.; Połec-Pawlak, K.; Jarosz, M.: *J. Mass Spectrom.* **38** (2003), 1252-1258.
- [12] Koyama, J.; Morita, I.; Fujiyoshi, H.; Kobayashi, N.: *Chem. Pharm. Bull.* **53** (5) (2005), 573-575.
- [13] Shang, X.; Yuan, Z.: *Bioorg. Med. Chem. Lett.* **13** (2003), 617-622.
- [14] Atanabe, T.; Terabe, S.: *J. Chromatogr. A* **880** (2000), 311-322.

HPLC - ED DETERMINATION OF EPINEPHRINE AT CARBON PASTE ELECTRODE

Zuzana Jemelková, Jiří Zima, Jiří Barek

Charles University in Prague, Faculty of Science, Department of Analytical Chemistry, Albertov 6, 128 43 Prague 2, Czech Republic; e-mail: Zuzana.Jemelkova@seznam.cz

Abstract

Catecholamines are widely distributed and they are important neurotransmitters and hormones in mammalian species. They are highly reactive and are readily oxidized to aminochromes. That enables the use of electrochemical method for the determination of epinephrine. In this paper, HPLC-ED is described because of its high sensitivity and selectivity. The carbon paste electrode (CPE) prepared of glassy carbon spherical microparticles was applied in amperometric detection. The measurement was carried out in media of pH 6, in phosphate buffer:methanol mobile phase. The lowest determined concentration was $4 \cdot 10^{-6} \text{ mol} \cdot \text{dm}^{-3}$.

Keywords

Epinephrine, high-performance liquid chromatography, carbon paste electrode, amperometric detection

1 Introduction

Catecholamines (e.g. epinephrine, norepinephrine and dopamine) include compounds with a dihydroxyphenyl group and an amino group. Historically, epinephrine was first extracted in 1901 from the adrenal glands of animals by Jokichi Takamine and it was synthesized in 1904 by Friedrich Stolz¹. Epinephrine is an adrenal medulla hormone. It occurs also in sympathetic postganglionic terminal and in some parts of central nervous system. It is sympathicus activator and humoral transmitter of sympathetic excitement to target tissue. Epinephrine affects both, α and β receptors and it is the most powerful α receptors stimulator.

High-performance liquid chromatography (HPLC) with electrochemical detection (ED) is most often used technique for analysis of catecholamines and their metabolites because of its high sensitivity and selectivity²⁻⁶. By electrochemical oxidation, catecholamines are easily converted into quinone species. Catecholamines oxidation is electrochemically reversible and this fact eliminates or limits the interference from compounds whose oxidation is not chemically reversible, e.g. from oxygen. ED also enables to obtain high sensitivity without derivatization. Other methods for epinephrine assay and study are capillary electrophoresis^{7,8} and flow injection analysis⁹⁻¹¹. Very often used detection methods are fluorescence, chemiluminescence and mass spectrometry.

2 Experimental

2.1 Reagents

All reagents were of analytical-reagent grade and all solutions were prepared with water obtained from a Millipore Q-plus System (Millipore, Bedford, MA, USA). Epinephrine was purchased from Zentiva (Prague, Czech Republic) as a solution containing epinephrini hydrochloridum 1.2 mg (epinephrinum 1 mg) in 1 cm³ of injection solution. Mobile phase contained methanol for HPLC (Chromservis, Czech Republic) and phosphate buffer solution. Phosphate buffer solution (pH 5) consisted of 0.01 mol·dm⁻³ sodium dihydrogenphosphate (Lachema Brno, Czech Republic). Carbon paste was prepared by mixing 250 mg of glassy carbon spherical powder 0.4-12 micron, type 2 (Alfa Aesar, Karlsruhe, Germany) and 0.09 cm³ of mineral oil Nujol (Fluka, Buchs).

2.2 Apparatus

A 4330 Conductivity & pH Meter (Jenway Ltd., Essex, UK) fitted with the combined glass electrode was employed to measure the pH of the solutions. An HPLC system consisted of a high-pressure pump HPP 5001 (Laboratorní přístroje, Prague, Czech Republic), injector valve CI-30 (Laboratorní přístroje, Prague, Czech Republic) with 10 µl loop, column Kromasil 100-7 µm, 250 × 4.6 mm I.D., C18 (Prochrome, India), UV/VIS detector LCD 2040 (Laboratorní

přístroje, Prague, Czech Republic), amperometric detector ADLC 1 (Laboratorní přístroje, Prague, Czech Republic) and software CSW 32 (DataApex Ltd.) working under Win98 (Microsoft Corp.). Amperometric detection was carried out in the three-electrode system consisting of working glassy carbon paste electrode (Vývojové dílny, Univerzita Pardubice, Czech Republic), silver/silver chloride, 3 mol·dm⁻³ KCl reference electrode RE-5B (BASi, USA) and a platinum wire as the auxiliary electrode (Monokrystaly, Turnov, Czech Republic).

2.3 Procedures

The mobile phase for HPLC of epinephrine consisted of methanol and phosphate buffer of appropriate pH. The mobile phase pH was chosen on the basis of previous measurements when studying the voltammetric determination of epinephrine¹². 1·10⁻⁴ mol·dm⁻³ stock solution was prepared diluting 0.183 cm³ of epinephrini hydrochloridum in methanol. 0.01 cm³ of 1·10⁻⁴ mol·dm⁻³ epinephrine were injected to the HPLC system. All measurements were performed under the laboratory temperature. The column dead time was determined injecting 1·10⁻³ mol·dm⁻³ NaNO₃.

3 Results and Discussion

The phosphate buffer of appropriate pH was mixed with methanol (10:90, 20:80, 30:70 and 60:40, 70:30, 80:20, v/v) to study the conditions for optimal HPLC separation of epinephrine. The dependencies of the peak height and the retention time of epinephrine on methanol content are shown in Fig. 1 and 2. The peak height increased with increasing volume of methanol, but the retention time was almost the same as the column dead time with amount of methanol higher than 60 %. Therefore the mobile phase containing phosphate buffer (pH 5):methanol (70:30, v/v) was chosen for following measurement. The final pH value of the mobile phase was 5.7.

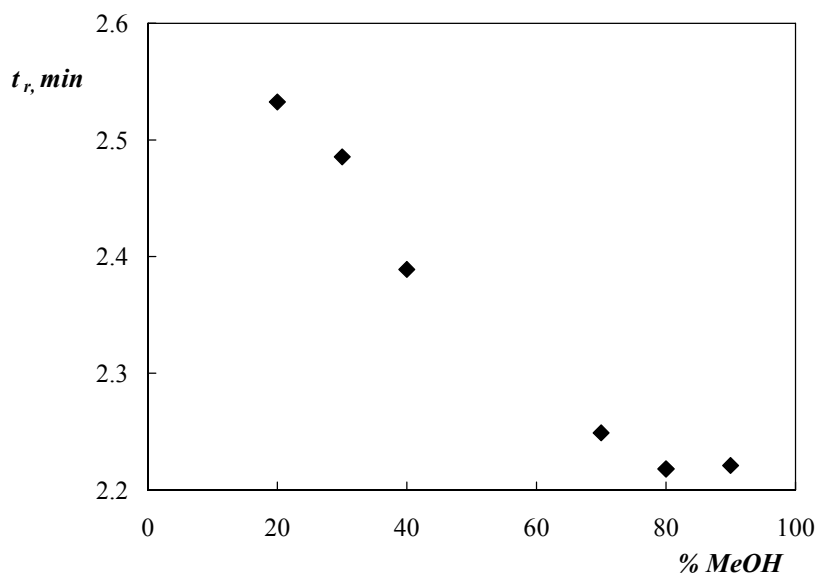


Fig. 1 The dependency of epinephrine retention time t_r (min) on the methanol content;

$0.01 \text{ mol}\cdot\text{dm}^{-3}$ phosphate buffer (pH 5), column Kromasil 100-7 μm , $250 \times 4.6 \text{ mm I.D.}$, C18, $F_m = 1 \text{ cm}^3\cdot\text{min}^{-1}$, $0.01 \text{ cm}^3 1\cdot 10^{-4} \text{ mol}\cdot\text{dm}^{-3}$ injected.

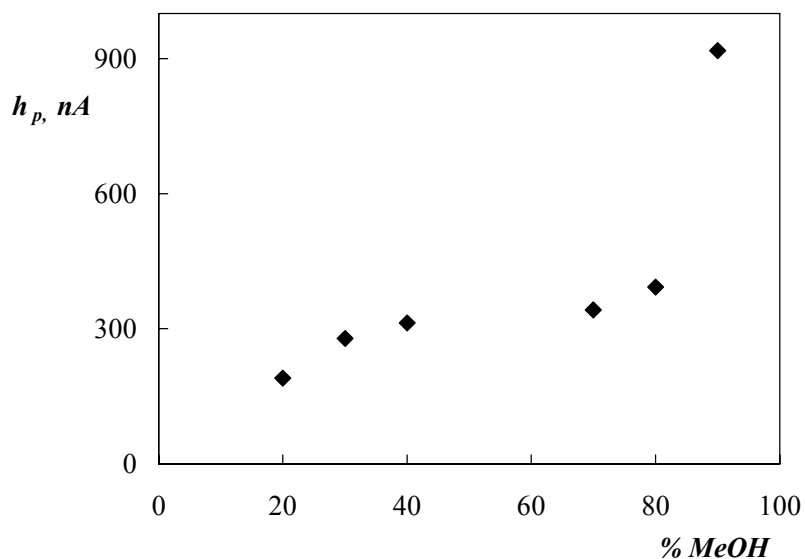


Fig. 2 The dependency of epinephrine peak height h_p (nA) on the methanol content;

$0.01 \text{ mol}\cdot\text{dm}^{-3}$ phosphate buffer (pH 5), column Kromasil 100-7 μm , $250 \times 4.6 \text{ mm I.D.}$, C18, $F_m = 1 \text{ cm}^3\cdot\text{min}^{-1}$, $0.01 \text{ cm}^3 1\cdot 10^{-4} \text{ mol}\cdot\text{dm}^{-3}$ injected.

The optimal potential of working electrode was found out by measuring the hydrodynamic voltammograms, which is the dependence of peak height on the polarization potential of the working

electrode. The voltammograms were measured in the potential range from +0.3 to +1.4 V and Fig. 3 shows the dependence of the peak height on the polarization potential. The polarization potential +1.2 V was considered as the optimal potential for the detection of epinephrine.

Under optimized instrument conditions, the calibration curve was measured in the concentration range from $1 \cdot 10^{-4} \text{ mol} \cdot \text{dm}^{-3}$ to $4 \cdot 10^{-6} \text{ mol} \cdot \text{dm}^{-3}$. HPLC-ED chromatograms and the dependence of the peak height on epinephrine concentration are shown in Fig. 4.

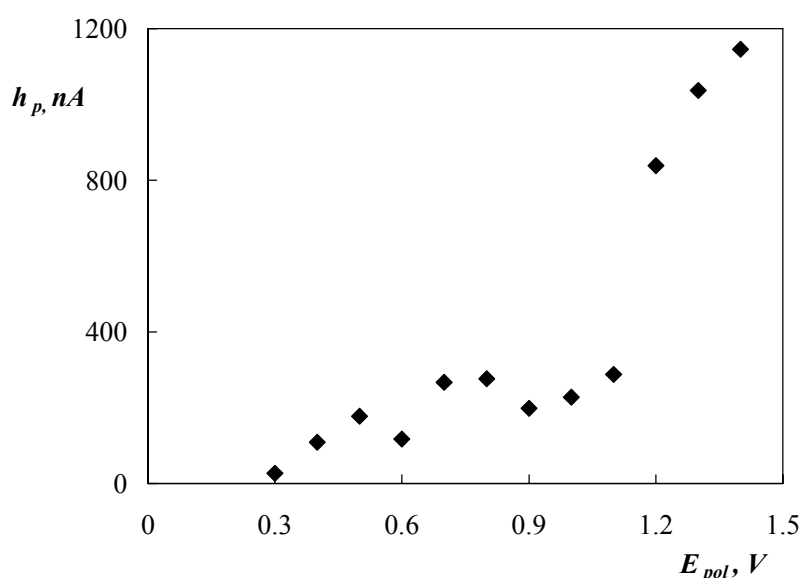


Fig. 3 The dependency of peak height h_p (nA) on the polarization potential of the working electrode E_{pol} (V);

phosphate buffer (pH 5): methanol (70:30, v/v) mobile phase, column Kromasil 100-7 μm , $250 \times 4.6 \text{ mm I.D.}$, C18, $F_m = 1 \text{ cm}^3 \cdot \text{min}^{-1}$, $0.01 \text{ cm}^3 1 \cdot 10^{-4} \text{ mol} \cdot \text{dm}^{-3}$ injected.

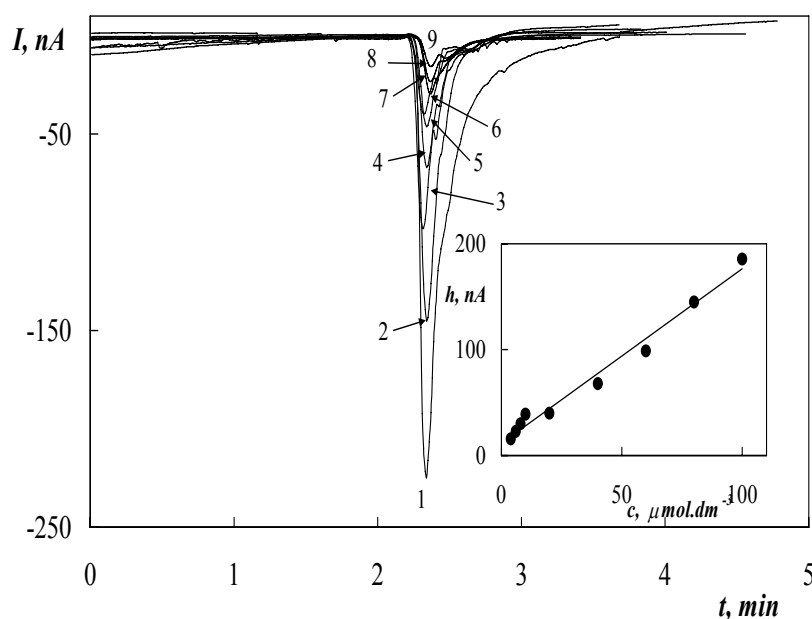


Fig. 4 HPLC chromatograms of epinephrine and the dependence of the peak height h_p (nA) on epinephrine concentration;

ED at CPE, $E_{pol} = +1.2$ V, phosphate buffer (pH 5):methanol (70:30, v/v) mobile phase, column Kromasil 100-7 μm , 250×4.6 mm I.D., C18, $F_m = 1 \text{ cm}^3\cdot\text{min}^{-1}$, 0.01 cm^3 $1\cdot 10^{-4} \text{ mol}\cdot\text{dm}^{-3}$ injected, $c(\text{epi}) = 1\cdot 10^{-4}$ (1); $8\cdot 10^{-5}$ (2); $6\cdot 10^{-5}$ (3); $4\cdot 10^{-5}$ (4); $2\cdot 10^{-5}$ (5); $1\cdot 10^{-5}$ (6) $\text{mol}\cdot\text{dm}^{-3}$.

Conclusion

In this work, the use of CPE as the working electrode in electrochemical detection in RP HPLC was studied. It is shown that it is possible to use CPE prepared of glassy carbon spherical microparticles for electrochemical detection in flow methods e.g. HPLC. The lowest determined concentration was $4\cdot 10^{-6} \text{ mol}\cdot\text{dm}^{-3}$ and the limit of detection for this method was $2\cdot 10^{-6} \text{ mol}\cdot\text{dm}^{-3}$.

Acknowledgment

This work was financially supported by the Grant Agency of the Czech Republic (project No. 203/04/0136) and the Czech Ministry of Education, Youth and Sports (projects No. LC 06035 and No. MSM 0021620857).

References

- [1] *The Columbia Encyclopedia*. Accessible on:
<<http://www.bartleby.com/65/ep/epinephr.html>> [cit. 9.1.2007].
- [2] Ochs, S.C.; Westfall, T.C.; Macarthur, H.: *J. Neurosci. Methods* **142** (2005), 201-208.
- [3] Sastre, E.; Nicolay, A.; Bruguerolle, B.; Portugal, H.: *J. Chromatogr. B* **801** (2004), 205--211.
- [4] Ueyama, J.; Kitaichi, K.; Iwase, M.; Takagi, K.; Takagi, K.; Hasegawa, T.: *J. Chromatogr. B* **798** (2003), 35-41.
- [5] Sabbioni, C.; Saracino, M.A.; Mandrioli, R.; Pinzauti, S.; Furlanetto, S.; Gerra, G.; Raggi, M.A.: *J. Chromatogr. A* **1032** (2004), 65-71.
- [6] Kumarathasan, P.; Vincent, R.: *J. Chromatogr. A* **987** (2003), 349-358.
- [7] Sanger-van de Griend, C.E.; Ek, A.G.; Widahl-Nasman, M.E.: *J. Pharm. Biomed. Anal.* **41** (2006), 77-83.
- [8] Wei, S.L.; Song, G.Q.; Lin, J.M.: *J. Chromatogr. A* **1098** (2005), 166-171.
- [9] Kojlo, A.; Nalewajko, E.: *Chem. Anal.* **49** (2004), 653-663.
- [10] Du, J.X.; Shen, L.H.; Lu, J.R.: *Anal. Chim. Acta* **489** (2003), 183-189.
- [11] Michalowski, J.; Halaburda, P.: *Talanta* **55** (2001), 1165-1171.
- [12] Jemelková, Z.; Zima, J.; Barek, J.; Kucukkolbasi, S.: *Proceedings of international seminar Analytical Chemistry and Toxicology* (2006), 71-76.

FIA DETERMINATION OF CHONDROITIN SULFATE BY AZURE B WITH SPECTROPHOTOMETRIC DETECTION

R. Pospíchal*, K. Nesměrák, P. Rychlovský

Department of Analytical Chemistry, Faculty of Science, Charles University, Department of Albertov 6, CZ-128 43 Prague 2, Czech Republic

** Corresponding author. E-mail address: pospichalr@seznam.cz.*

Abstract

A new method for the flow-trough spectrophotometric determination of chondroitin sulfate in presence of Azure B was developed. A study was done under both static and flow-trough conditions. Statistic factorial design was used to find the significant experimental parameters for the flow-trough configuration and their optimal values were found: pH = 5.5, $c_{\text{Azure B}} = 4 \times 10^{-5} \text{ mol L}^{-1}$, the flow rate 5.8 mL min^{-1} , sample volume injected of $100 \text{ }\mu\text{L}$, reaction coil length of 20 cm . The calibration curves are linear in the concentration range of $0\text{--}5 \text{ }\mu\text{g mL}^{-1}$ of chondroitin sulfate, the limit of detection of about $0.29 \text{ }\mu\text{g mL}^{-1}$, the limit of determination of about $1.22 \text{ }\mu\text{g mL}^{-1}$. The stoichiometry of an ion aggregate chondroitin sulfate:Azure B was determined in ratio of 1:3 per one disaccharide unit under the optimal conditions.

Keywords:

Chondroitin sulfate; Thiazine dyes; Flow injection analysis; Factorial design

1. Introduction

Chondroitin sulfates (CS) are important members of glycosaminoglycans family, containing repeating structures of N-acetylgalactosamine and glucuronic acid. According to position of sulphonate group on structure of N-acetylgalactosamine the CS can be divided into chondroitin 4-sulfate (referred to as chondroitin sulfate *a*;

CSA) and chondroitin 6-sulfate (referred to as chondroitin sulfate *c*, CSC); see Fig. 1. The linear chain of CS is composed of repeating disaccharide units of β -glucuronic acid-[1 \rightarrow 3]-N-acetyl- β -D-galactosamine-6-sulfate-[1 \rightarrow 4], which has two negative charges. CS are a major constituent of cartilage and are also present in the lining of blood vessels. They belong to the pharmacological agents used as a prevention of osteoarthritis and atherosclerosis.

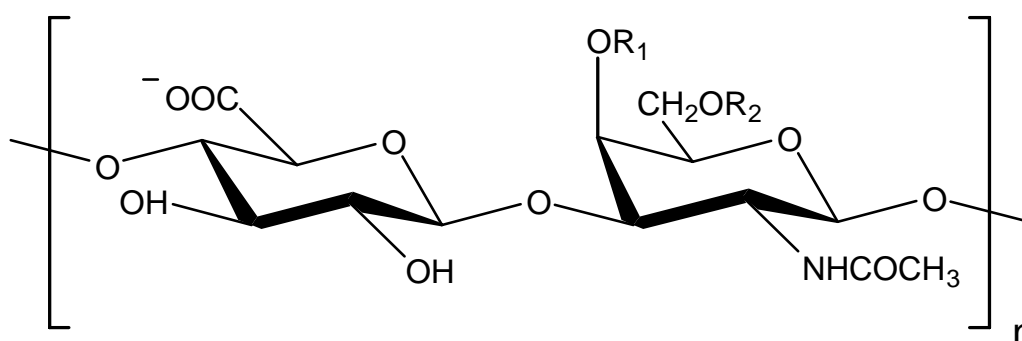


Fig. 1 Basic unit of chondroitin 4-sulfate ($R_1 = \text{SO}_3^-$, $R_2 = \text{H}$) and chondroitin 6-sulfate ($R_1 = \text{H}$, $R_2 = \text{SO}_3^-$)

The determination of CS is carried out by chromatographic [1–4], electrophoretic [5–8] and spectrophotometric methods [9, 10]. The spectrophotometric determination of CS is based on its interaction with the thiazine cationic dye Azure B (AB), see Fig. 2, which is often used as a biological staining reagent. Compared to the other methods, the spectrophotometric determination of CS is easier, cheaper and very sensitive.

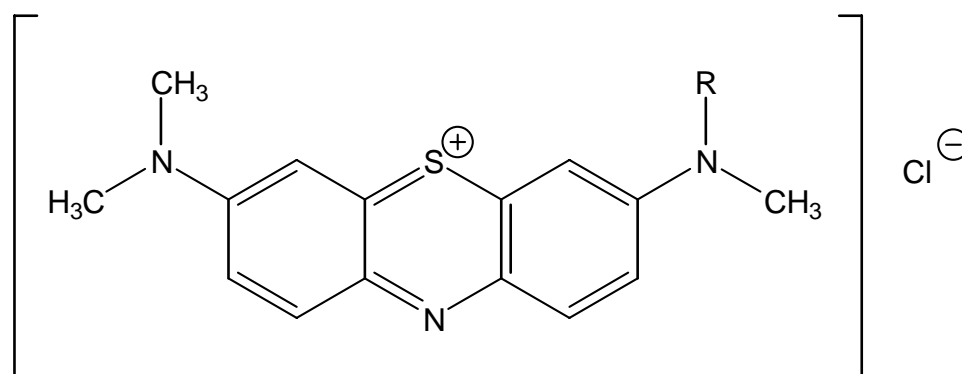


Fig. 2 The structure formula of Azure B, $R = \text{H}$.

The aim of this work was the development of new method for the flow-through spectrophotometric determination of CSC in presence of Azure B. As CSC does not absorb in visible region of electromagnetic spectra, the decrease of absorption of the thiazine dye in consequence of forming an ion aggregate was observed as an analytical signal.

2. Experimental

2.1. Chemicals

Chondroitin 6-sulfate, CAS 12678-07-8, was used as a sodium salt (Sigma-Aldrich, Germany). A 10 $\mu\text{g mL}^{-1}$ stock solution was prepared in distilled water; the pH of the solution was adjusted by hydrochloric acid. Stock solution was stored in the refrigerator at 4°C.

Azure B, 3-methylamino-7-dimethylaminofenothiazinium chloride, CAS 531-55-5, $M_r = 305.8$ (Loba-Chemie, Austria) was used. A 5.0×10^{-5} mol L⁻¹ stock solution was prepared in distilled water; the pH was adjusted by hydrochloric acid.

The tested mass-produced medicinal form was Condrosulf® 400 (400 mg of chondroitin sulfate per capsule; IBSA, Switzerland). Determination in medicinal form was carried out by dissolving of the content of the capsule in 250 mL of distilled water (pH = 5.5 adjusted by hydrochloric acid). The 0.5 mL of this solution was transferred into volumetric flask of 250 mL and diluted by distilled water.

All other chemicals used were of analytical grade.

2.2. Apparatus

The static spectrophotometric measurements were carried out using a spectrophotometer Agilent 8453 (Hewlett Packard) with quartz cuvettes with an optical path of 10 mm.

The flow-through measurements were carried out by Skalar 2000/195 (Holand), with a built-in peristaltic pump. The sample was injected using a PTFE six-way injection port. A dye solution was pumped through Tygon tubes 0.5 and 0.75 mm i.d. A reaction coils were made by PTFE tubes 0.5 mm i.d. in required length. A PYE UNICAM PU 8800 spectrophotometer (England) with 80 μL flow-

through quartz cell with an optical path of 10 mm was used for spectrophotometric detection.

2.3. Procedure

Scheme of the apparatus used for the flow injection analysis is depicted in Fig. 3. The solution of the dye is propelled by peristaltic pump and sample of CSC is injected into the dye stream through the sampling valve. The reaction of CSC with the thiazine dye takes place in the reaction coil. The absorbance of the reaction product is measured by the connected spectrophotometer with recording of the signal by computer. The absorbance of the dye was set as the zero value.

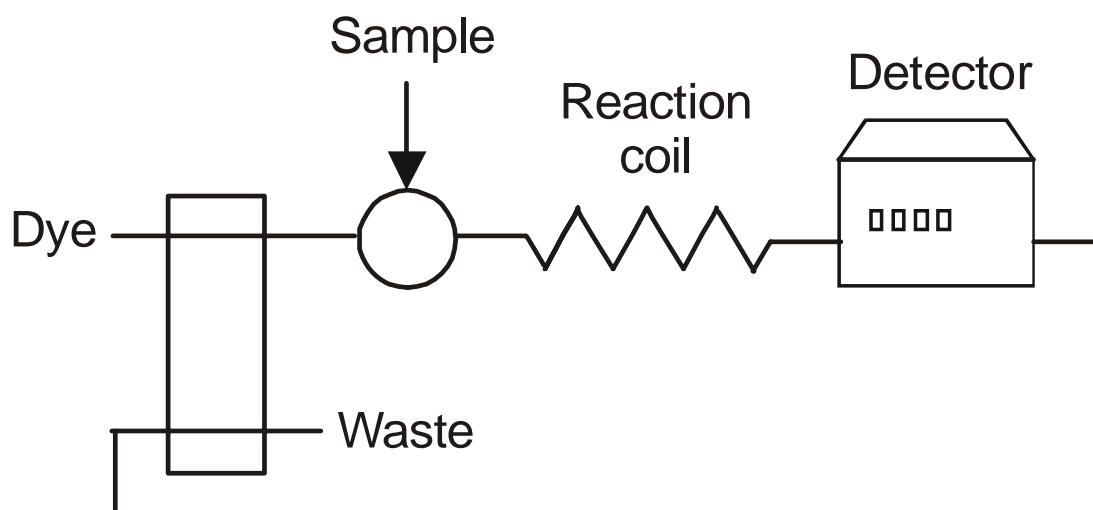


Fig. 3. Scheme of the apparatus for the flow injection analysis.

3. Results and discussion

3.1. Optimization of the reaction conditions

The essential conditions for the optimal flow measurement were obtained by measuring the spectral changes of AB under the different conditions.

The absorption spectra of AB in solutions were measured. Up to $1.0 \times 10^{-5} \text{ mol L}^{-1}$ of AB only the absorption band at 647 nm was observed. At concentration of AB higher than $1.0 \times 10^{-5} \text{ mol L}^{-1}$ a new peak appeared at 601 nm, which referred to aggregation of thiazine dye [10]. The absorption changes at 647 nm were linear over the concentration range $0.5 - 5.0 \times 10^{-5} \text{ mol L}^{-1}$ AB.

The presence of CSC in solution appears in absorption spectrum of AB as a decrease in the absorbance at 647 nm and the formation of maxima at 554 nm (Fig. 4), which can be explained by the formation of ion associate of AB-CSC. The decrease of the absorption at 647 nm is linear over the range of 0–8 $\mu\text{g mL}^{-1}$ CSC.

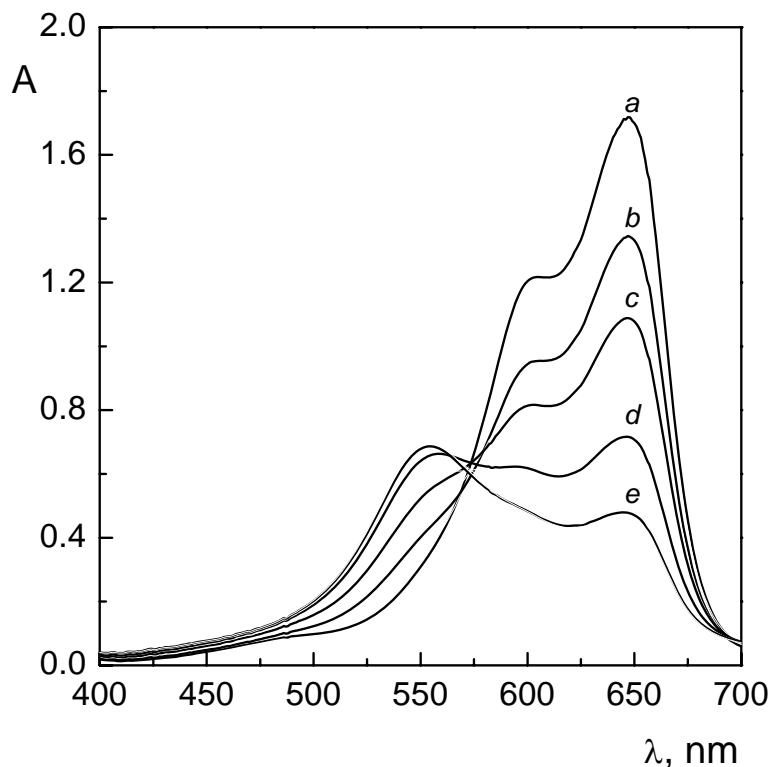


Fig. 4 Absorption spectra of Azure B with increasing concentration of CSC:

$a - 0$; $b - 2$; $c - 4$; $d - 6$; $e - 8 \mu\text{g mL}^{-1}$
($c_{AB} = 4.0 \times 10^{-5} \text{ mol L}^{-1}$, $\lambda_{max} = 647 \text{ nm}$, $\text{pH} = 5.5$).

The concentration of dye was set at $4 \times 10^{-5} \text{ mol dm}^{-3}$ as it guarantees the $A_{\text{dye}} \approx 1.5$. The maximum value of ΔA ($\Delta A = A_{\text{dye}} - A_{\text{dye+CSC}}$) was registered at $\text{pH} = 5.5$ in studied range of $\text{pH} 4-8$. The buffer selection was evaluated by measuring of ΔA between $4 \times 10^{-5} \text{ mol dm}^{-3}$ of dye and the same solution containing $3 \mu\text{g mL}^{-1}$ CSC (Fig. 5). The maximum value of ΔA was observed in the solution treated by hydrochloric acid, in comparison with citrate, acetate, phosphate and ammoniac buffer. This phenomenon can be explained by interaction of the buffering components with an ion associate AB:CSC.

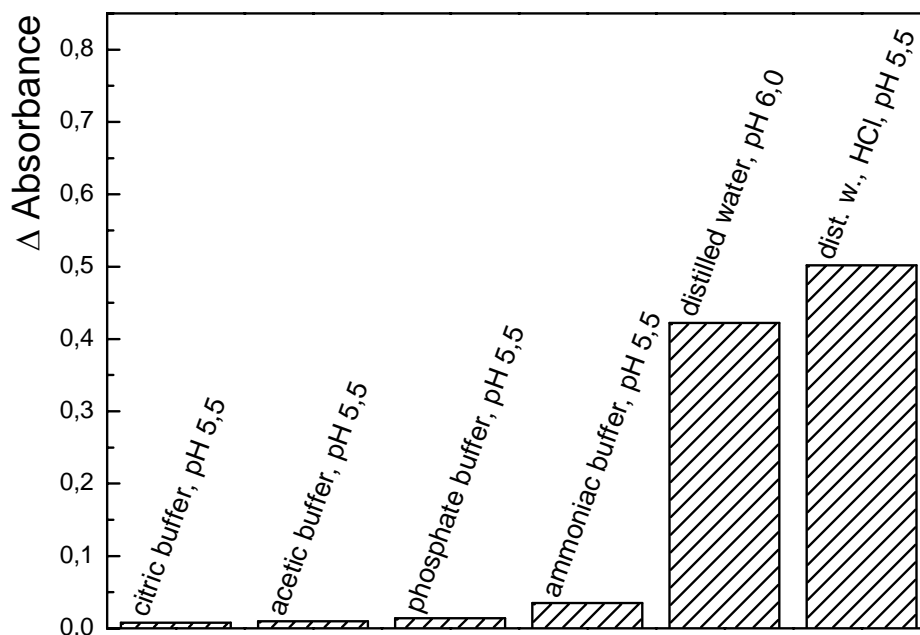


Fig. 5 The influence of buffer on the absorption changes of AB ($4 \times 10^{-5} \text{ mol L}^{-1}$) in presence of CSC ($3 \mu\text{g mL}^{-1}$).

The stoichiometry of an ion associate was determined under listed conditions by Job's method of continual variation [11] as AB:CSC = 3:1 per one disaccharide unit of CSC (Fig. 6).

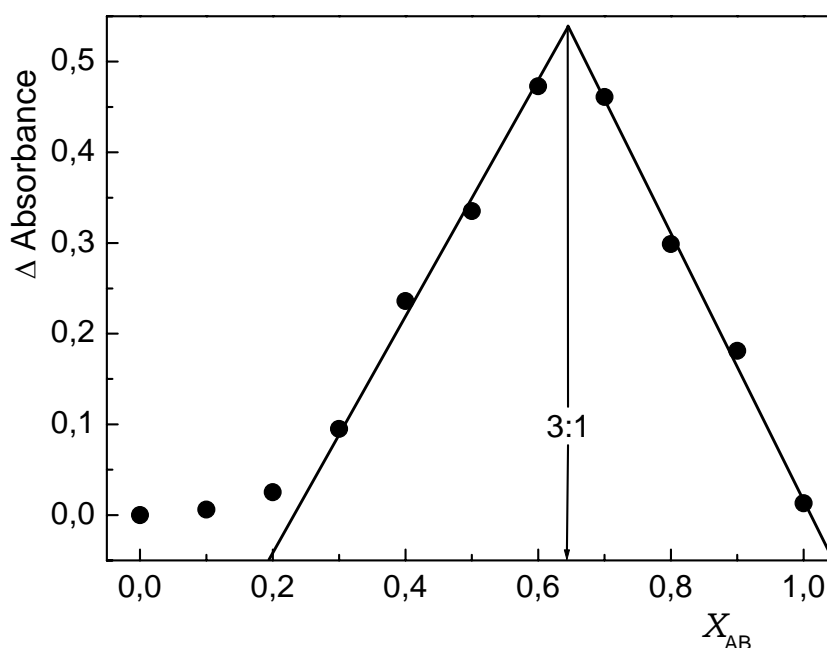


Fig. 6 The curve of continual variation of an aggregate AB:CSC,

$$c_{AB} + c_{CSC} = 10 \mu\text{g mL}^{-1}, \text{pH} = 5.5.$$

3.2. Optimization of the flow-trough determination

A stock solution $4 \times 10^{-5} \text{ mol L}^{-1}$ AB, pH = 5.5, was used as the absorption background in the flow-trough configuration where the influence of the sampled volume of CSC and the dye flow rate on the absorption changes were studied. The high of the FIA peak served as an analytical signal. The high of the FIA peak increases with increasing of sample injected volume over the studied range of 30–1000 μL . The high of the FIA peak decreases with increasing flow rate over the studied range of 5.1–6.7 mL min^{-1} .

The significance of the individual parameters was determined by the factorial design [12]. If k factors (parameters) is checked and each factor has I levels than I^k experiments must be carried out. The effect of the individual factors w_i follows from the relationship

$$w_i = 2^{1-k} (\sum y^+ - \sum y^-) \quad (1)$$

where y^+ is result of the experiment in which the factor is on level (+) and y^- is result of the experiment in which the factor is on level (–).

Factorial design was used to determine the significance of the length of the reaction coil (Factor A), the flow rate (Factor B) and the sample injected volume (Factor C). For each factor two levels were selected (Table 1). Optimization was carried out at a wavelength of 647 nm. The i.d. of the tubes and the detection cell and the shape of the reaction coil were unvarying during the experiment. The effect of the individual factors is shown in Table 2.

Table 1 Studied parameters and their levels.

Parameter	Factor	Level of the factor
Length of the reaction coil	A	– 20 cm
		+ 100 cm
Flow rate of AB	B	– 3.1 mL min ⁻¹
		+ 5.8 mL min ⁻¹
Sample volume injected	C	– 30 µL
		+ 100 µL

Table 2 Effect of the individual parameters and their combinations.

Factor	A	B	C	AB	AC	BC	ABC
Effect w_i	-0.143	0.005	0.464	0.003	-0.052	-0.019	-0.034

The sample volume injected has the greatest impact on the high of the FIA peak. The length of the reaction coil and the flow rate has the effect smaller and negative. The influence of the flow rate and the sample volume injected on the absorption was observed (Fig. 7). As the sample volume increases, the high of the FIA peak also increases over the range of used flow rates. With increasing sample volume the FIA peak becomes broader and the time to achieve the maximum signal also increases. Thus, 100 µL was chosen since it provides symmetrical and pointed peaks. The length of the reaction coil has a negative impact. The longer reaction coil leads to larger dispersion, thus the length of 20 cm was used. The effect of the flow rate is small. Since the high flow rate causes smaller dispersion of the injected zone, the 5.8 mL min⁻¹ was chosen.

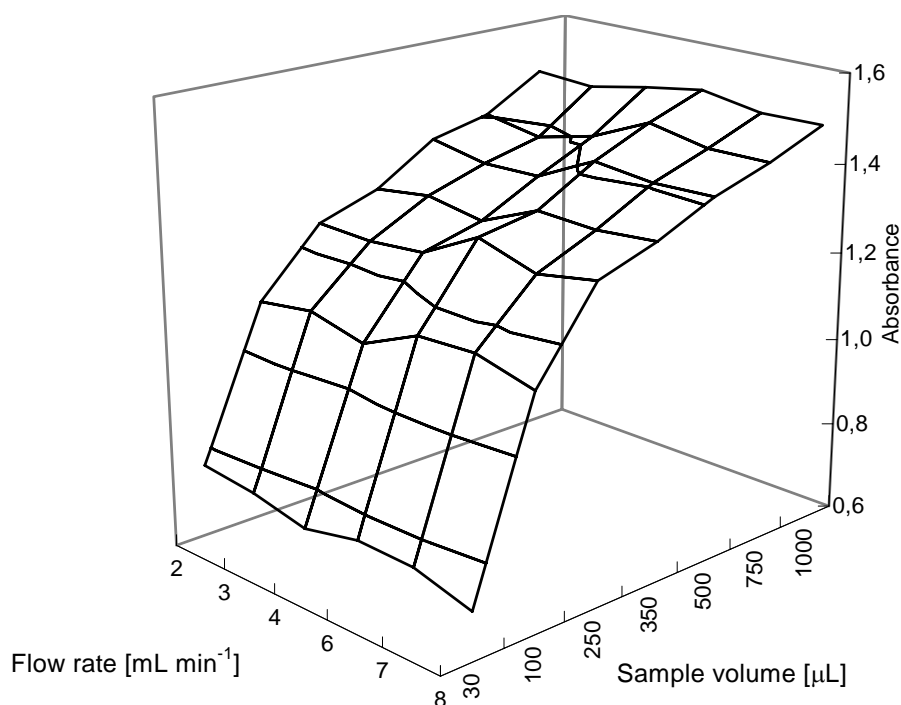


Fig. 7 Dependence of the high of the FIA peak on the sample volume injected and the flow rate of AB

($c_{AB} = 4 \times 10^{-5} \text{ mol L}^{-1}$, $\text{pH} = 5.5$, $c_{\text{CSC}} = 10 \text{ } \mu\text{g mL}^{-1}$, length of the reaction coil 20 cm).

Under the optimal conditions of the flow-trough measurement ($c_{AB} = 4 \times 10^{-5} \text{ mol L}^{-1}$, $\text{pH} = 5.5$, $\lambda = 647 \text{ nm}$, the flow rate 5.8 mL min^{-1} , the sample volume injected $100 \text{ } \mu\text{L}$, length of the reaction coil 20 cm) the calibration curve

$$A = 0.0647 (\pm 0.0026) c_{\text{CSC}} + 0.7375 (\pm 0.0078) \quad (2)$$

$$n = 6, r = 0.9969, \text{SD} = 0.0110$$

was measured. The calibration curve is linear over the range of $0\text{--}5 \text{ } \mu\text{g mL}^{-1}$ CSC. The limit of detection (LOD) and the limit of determination (LOQ) were determined in values $\text{LOD} = 0.29 \text{ } \mu\text{g mL}^{-1}$, $\text{LOQ} = 1,22 \text{ } \mu\text{g mL}^{-1}$.

3.3. Application of developed method on medical form

The developed method of flow-trough determination of CSC was employed for analysis of mass-produced medicinal preparation (Condrosulf[®], 400 mg of chondroitin sulfate per capsule). The total concentration of CS was determined in value $382.5 \pm 7.5 \text{ mg}$ per one capsule with sampling frequency 1.6 min^{-1} .

Acknowledgements

This work was financially supported by the Czech Ministry of Education, Youth and Sports (project LC06035 and project MSM 0021620857).

References

1. H. Toyoda, K. Motoki, M. Tanikawa, K. Shinomiya, H. Akiyama, T. Imanari, J. Chromatogr. Biomed. Appl. 565 (1991) 141.
2. H. Akiyama, S. Shidawara, A. Mada, H. Toyoda, T. Toida, T. Imanari, J. Chromatogr. Biomed. Appl. 579 (1992) 203.
3. J. Du, N. Eddington, Anal. Biochem. 306 (2002) 252.
4. D. W. Choi, M. J. Kim, H. S. Kim, S. H. Chang, G. S. Jung, K. Y. Shin, S. Y. Chang, J. Pharm. Biomed. Anal. 31 (2003) 1229.
5. S. Michaelsen, M. B. Schröder, H. Sörensen, J. Chromatogr. 652 (1993) 503.
6. D. H. Vynios, A. Faraos, G. Spyropoulou, A. J. Aletras, C. P. Tsiganos, J. Pharm. Biomed. Anal. 21 (1999) 859.
7. N. K. Karamanos, S. Axelsson, P. Vanky, G. N. Tzanakakis, A. Hjerpe, J. Chromatogr. 696 (1995) 295.
8. N. Volpi, Carbohydrate Research 247 (1993) 263.
9. S. Zhang, N. Li, F. Zhao, K. Li, S. Tong, Spectrochim. Acta 58 (2002) 273.
10. L. Zhang, N. Li, F. Zhao, K. Li, Anal. Sci. 20 (2004) 445.
11. K. A. Connors, Binding Constants, J. Wiley and Sons, 1987, 24.
12. J. N. Miller, J. C. Miller, Statistics and Chemometrics for Analytical Chemistry, 5th edn., Pearson Education Limited, 2005, 181.

VOLTAMMETRIC DETERMINATION OF TRACE AMOUNTS OF NITRO AND AMINO DERIVATIVES OF QUINOLINE

Ivan Jiránek^a, Jiří Barek^a, Bogdan Yosypchuk^b, Karolina Pecková^a, Karel Čížek^a

^a Charles University in Prague, Faculty of Science, Department of Analytical Chemistry, UNESCO Laboratory of Environmental Electrochemistry, Hlavova 2030, 128 43 Prague 2, Czech Republic; e-mail: ijirane@gmail.com

^b J. Heyrovský Institute of Physical Chemistry, Academy of Science of the Czech Republic, Dolejškova 3, 182 23 Prague 8, Czech Republic

Abstract

Determination of 5-nitroquinoline (5-NQ) and 5-aminoquinoline (5-AQ) by differential pulse voltammetry (DPV) at Hanging Mercury Drop Electrode (HMDE) and at carbon paste electrode (CPE) was developed and applied for the determination of test substance in model samples of 5-NQ prepared from drinking and river water. At first, the possibility of direct determination of 5-NQ in model samples was verified. Afterwards, the voltammetric determination of 5-NQ after preliminary separation and preconcentration using solid phase extraction (SPE) was performed. The attempt to increase the sensitivity of the determination by means of adsorptive stripping voltammetry (AdSV) was not successful.

Keywords:

Differential Pulse Voltammetry, Adsorptive Stripping Voltammetry, Hanging Mercury Drop Electrode, Carbon Film Electrode, Solid Phase Extraction, 5-Nitroquinoline, 5-Aminoquinoline

Introduction

Nitro and amino derivatives of quinoline are suspicious of carcinogenic and mutagenic effects¹⁻³. Thanks to the presence of nitro or amino groups these substances are easily electrochemically

reducible or oxidizable. The ever increasing demand for analytical methods suitable for the determination of trace amounts of these substances prompted us to investigate the possibility of voltammetric determination of these substances. The aim of this study was to find out optimal conditions for the determination of trace amounts of nitro and amino derivatives of quinoline using modern voltammetric methods, namely differential pulse voltammetry (DPV) at a hanging mercury drop electrode (HMDE) and at a carbon film electrode (CFE). Other aim was to reach the lowest concentration limits of determination of these substances using some preconcentration techniques like adsorptive stripping voltammetry (AdSV) and solid phase extraction (SPE). Finally, we tried to verify practical applicability of new methods on model environmental samples. Among the advantages of HMDE are mainly the broad cathodic potential window, easy renewable and atomically smooth surface. The disadvantages consist in narrow anodic potential window, so limiting the use of mercury electrodes for anodic oxidations. Furthermore, the concern of mercury toxicity is in question. On the other hand, carbonaceous materials have much broader anodic potential window. There is a possibility to cover surface of conventional solid electrode by a film made of polymer containing conductive particles⁴. Conductive microparticles provide the contact between analyzed solution and conductive part of electrode. Such film electrode behaves like material that conductive microparticles are made of so there is possibility to broaden potential window of original solid electrode by covering it with the film. The biggest problem of all solid electrodes lies in the reproducibility of their surface and their passivation strongly influencing their analytical performance. In the case of film electrode this problem is solved very elegantly. When the old film is not useful anymore it can be easily and quickly renewed by wiping the film electrode with a filter paper, and immerse the electrode's surface to an ink solution to form a new film. However, when a suitable electrochemical pretreatment of the film electrode is applied, the same film can be used for reproducible measurement for several days. In our case we chose for measuring combination of Silver Amalgam Solid Electrode (AgSAE) and carbon film. The AgSAE electrode was chosen because its electrochemical behavior is very similar to any mercury electrode and if there is no need to measure oxidations in

anodic area, the film can be removed and cathodic measurement can be realized with AgSAE as a working electrode. We assume that a film electrode will be used only for anodic oxidations whereas AgSAE would rather be used for cathodic reductions.

Differential pulse voltammetry is well known electroanalytical method. Great sensitivity and relatively low price of instrumentation belong among advantages of this method which is well described for example in monographs^{5,6}.

Experimental Part

Reagents

The stock solution of 5-nitroquinoline (99%, Aldrich Chem. Co.) in deionized water ($c = 1 \cdot 10^{-3} \text{ mol.l}^{-1}$) was prepared by dissolving 0,01742 g of the substance in 100 ml of deionized water and sonication for 30 minutes. The stock solution of 5-aminoquinoline (97%, Aldrich Chem. Co.) in deionized water ($c = 1 \cdot 10^{-3} \text{ mol.l}^{-1}$) was prepared by dissolving 0,01442 g of the substance in 100 ml of deionized water. More diluted solutions were prepared by exact dilution of the stock solution with deionized water. All solutions were kept in the dark, at laboratory temperature and in glass vessels. Other chemicals (boric acid, glacial acetic acid, phosphoric acid, sodium hydroxide, potassium chloride, all p.a. purity) were supplied by Lachema Brno, Czech republic. Deionized water from Millipore, USA, was used. The conductive carbon ink solution was prepared by mixing 0,01 g of polystyrene, 0,09 g of carbon powder (crystalline graphite 2 μm , CR 2 Maziva Týn, Czech Republic). The mixture was thoroughly homogenized by sonication or by intensive agitation.

Apparatus

Voltammetric measurements were carried out using Eco-Tribo Polarograph driven by software PolarPro version 5.1 (Polaro-Sensors, Prague). The software worked under the operational system Microsoft Windows XP (Microsoft Corp.).

All measurements were carried out in a three-electrode system. Platinum wire as an auxiliary electrode, silver/silver chloride

reference electrode RAE 113 (1 mol.l⁻¹ KCl, Monokrystaly Turnov, Czech republic) and HMDE (calculated value of surface of drop was 7,66.10⁻³ cm²) or CFE (AgSAE, disk diameter 0.55 mm, covered by carbon ink film) as a working electrode.

Unless started otherwise, the scan rate 20 mV.s⁻¹ was used in the case of both electrodes. The pulse amplitude -50 mV (HMDE) or 50 mV (CFE) and pulse width 80 ms were used.

Good reproducibility of determinations at CFE was assured by a suitable electrochemical regeneration of CFE. Optimal results were obtained by the application of 50 potential jumps between -200 mV and +600 mV for 0.3 s.

For SPE techniques columns LiChrolut RP – 18e (1000 mg; CAT.NO.: 1.02124.0001, Merck, Darmstadt, Germany) were used.

Procedures

Appropriate amount of 5-NQ or 5-AQ stock or more diluted solution (0.02 – 1 ml) was measured out into a voltammetric vessel and it was filled up to 10 ml with Britton-Robinson (BR) buffer of appropriate pH. All curves were measured 3 times. The parameters of calibration curves (e.g., slope, intercept, limit of determination) were calculated using statistic software Adstat. This software uses confidence bands ($\alpha = 0.05$) for calculation of the limit of determination (L_Q). It corresponds to the lowest signal for which relative standard deviation is equal 0.1⁷.

Model samples

Drinking water from public water line in the building of Faculty of Science of Charles University or river water from the river “Vltava” near the location “Výtoň” in Prague spiked with appropriate amount of 5-NQ stock solution was used as a model sample.

Results and Discussion

Differential Pulse Voltammetry at a Hanging Mercury Drop

Electrode

It follows from DP voltammograms that 5-NQ gives one well developed cathodic peak in the whole investigated pH region (Fig.1). Other strongly irreversible and badly developed peaks were observed at more negative potentials and are not analytically useful. The best developed peak was obtained in BR buffer pH 13 medium, which was further used for measuring calibration curves. Parameters of calibration curves are summarized in Table I. DP voltammograms and calibration plot corresponding to the lowest attained concentration range are for the sake of illustration depicted in Fig. 2.

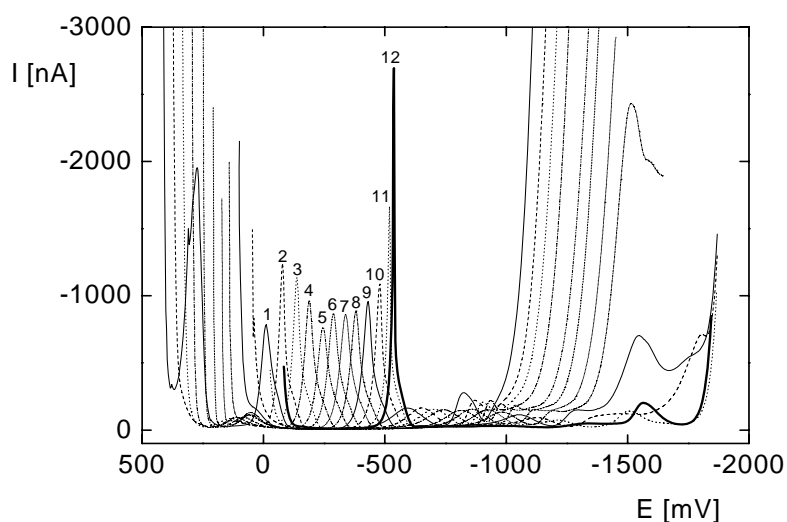


Fig. 1 Differential pulse voltammograms of 5-NQ ($c = 1.10^{-4} \text{ mol.l}^{-1}$) at HMDE in BR buffer, pH 2,0 (1); 3,0 (2); 4,0 (3); 5,0 (4); 6,0 (5); 7,0 (6); 8,0 (7); 9,0 (8); 10,0 (9); 11,0 (10); 12,0 (11), and 13,0 (12).

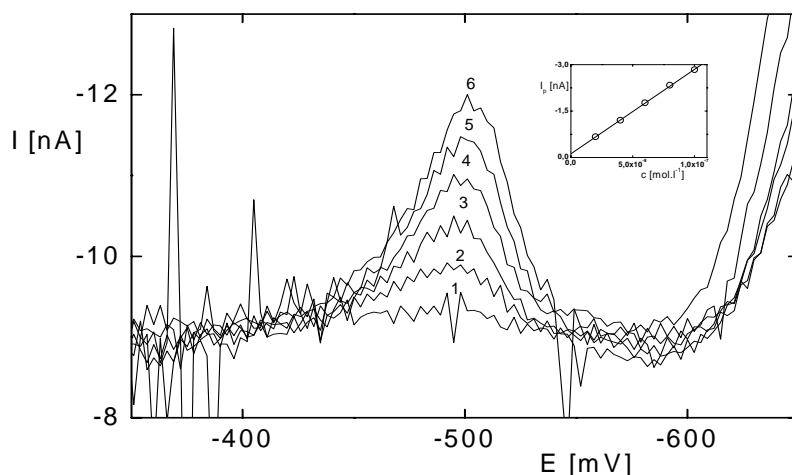


Fig. 2 DP voltammograms and calibration plot of 5-NQ at HMDE in BR buffer pH 3 medium at the lowest attained concentrations

$c(5\text{-NQ}) = 0$ (1), 2.10^{-8} (2), 4.10^{-8} (3), 6.10^{-8} (4), 8.10^{-8} (5), and 1.10^{-7} (6) mol.l^{-1} .

Table I

Parameters of calibration straight lines for DPV determination of 5-NQ at HMDE in 0.2 M NaOH medium.

Concentration [mol.l^{-1}]	Slope [$\mu\text{A.mol}^{-1}.\text{l}$]	Intercept [μA]	Correlation coefficient	L_Q [mol.l^{-1}]
$(2 - 10) \cdot 10^{-5}$	$-2.71 \cdot 10^7$	-78.3	0.9998	-
$(2 - 10) \cdot 10^{-6}$	$-3.15 \cdot 10^7$	2.10	0.9997	-
$(2 - 10) \cdot 10^{-7}$	$-2.76 \cdot 10^7$	0.23	0.9999	-
$(2 - 10) \cdot 10^{-8}$	$-2.73 \cdot 10^7$	-0.12	0.9999	$2.0 \cdot 10^{-8}$

Determination of 5-NQ in drinking and river water

The optimum conditions found for DPV determination of 5-NQ above were used for direct determination of 5-NQ in model samples of drinking and river water. It was found that calibration curves are linear and their parameters are presented in Table II. Voltammograms and calibration plot corresponding to the lowest attained concentration range are shown in Fig. 3 and 4.

Furthermore, we tried to preconcentrate the 5-NQ by solid phase extraction (SPE). The procedure for DP voltammetric determination of 5-NQ in model samples of drinking or river water after SPE was as follows: An SPE column was connected to a vacuum manifold and activated by washing with 5 ml of methanol and 5 ml of deionized

water. Afterwards, the model water sample spiked with different amounts of 5-NQ was sucked through the column using volumetric flasks as sample reservoirs and PTFE tubing as connector of the reservoirs and SPE columns. Adsorbed analyte was then eluted with 1 ml of methanol, the solution was made up to 10.0 ml with 0.2 mol.l⁻¹ NaOH and after deaeration DP voltammogram was recorded. The recoveries were calculated from the ratio I_p/I_p^o , where I_p is the height of the peak of the analyte of interest after solid phase extraction and I_p^o is the height of peak in a reference solution prepared by the addition of the standard solution of studied analyte to the blank solution. DP voltammograms of the lowest attained concentration range with appropriate calibration plot after solid phase extraction from drinking and river water are shown in figures 5 and 6 for illustration and parameters of extraction and parameters of obtained regression dependences are presented in Tables III and IV.

Table II

Parameters of calibration straight lines for direct DPV determination of 5-NQ at HMDE in 0.2 M NaOH medium.

Matrice	Concentration [mol.l ⁻¹]	Slope [$\mu\text{A}\cdot\text{mol}^{-1}\cdot\text{l}$]	Intercept [μA]	Correlation coefficient	L_Q [mol.l ⁻¹]
Drinking water	$(2 - 10)\cdot 10^{-7}$	$-2.80\cdot 10^7$	1.08	0.9999	-
Drinking water	$(2 - 10)\cdot 10^{-8}$	$-2.72\cdot 10^7$	0.11	0.9996	$1.5\cdot 10^{-8}$
River water	$(2 - 10)\cdot 10^{-7}$	$-2.48\cdot 10^7$	0.34	0.9999	-
River water	$(2 - 10)\cdot 10^{-8}$	$-2.38\cdot 10^7$	-0.01	0.9998	$6.5\cdot 10^{-9}$

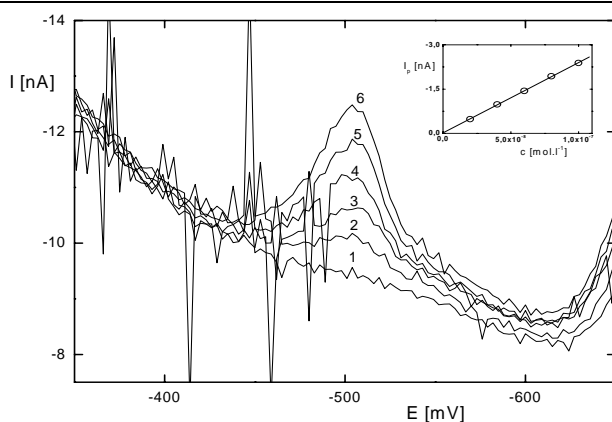


Fig. 3 DP voltammograms and calibration plot of 5-NQ in drinking water, containing 0 (1), 2 (2), 4 (3), 6 (4), 8 (5) and 10 (6) $\cdot 10^{-8}$ mol.l⁻¹ of this substance. Measured by DPV at HMDE in 0.2 M NaOH medium.

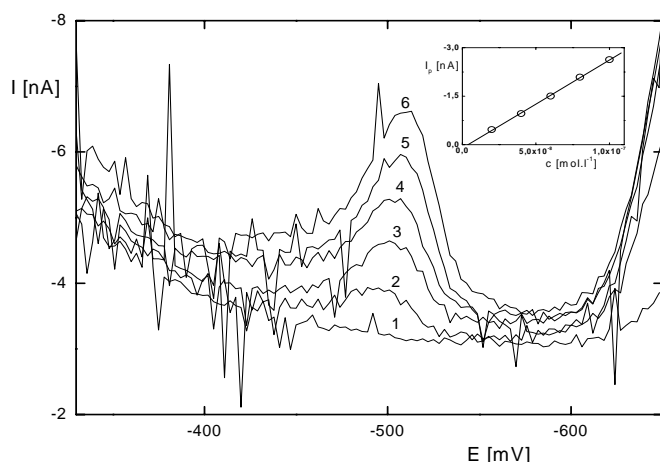


Fig. 4 DP voltammograms and calibration plot of 5-NQ in river water, containing 0 (1), 2 (2), 4 (3), 6 (4), 8 (5) and 10 (6) · 10⁻⁸ mol.l⁻¹ of this substance. Measured by DPV at HMDE in 0.2 M NaOH medium.

Tab. III Recovery of extraction of 5-NQ from drinking and river water.

Measured by DPV at HMDE in 0.2 M NaOH – methanol (9:1) medium.

Matrice	Extracted volume [ml]	c (5-NQ) in water [mol.l ⁻¹]	$-I_p^0$ [μA]	$-I_p$ [nA]	Yield [%]
Drinking water	100	1 · 10 ⁻⁸	1.65	1.31	79.5
Drinking water	1000	1 · 10 ⁻⁹	0.95	0.22	22.7
River water	100	1 · 10 ⁻⁸	1.20	1.16	96.6

Tab. IV Parameters of calibration dependences of 5-NQ after extraction from drinking and river water.

Measured by DPV at HMDE in 0.2 M NaOH – methanol (9:1) medium.

Matrice	Extracted volume [ml]	Concentration [mol.l ⁻¹]	Slope [μA · mol ⁻¹ · l]	Intercept [μA]	Correlation coefficient	L_Q [mol.l ⁻¹]
Drinking water	100	(2 – 10) · 10 ⁻⁹	-1.31 · 10 ⁸	0.02	0.9983	2.5 · 10 ⁻⁹
River water	100	(2 – 10) · 10 ⁻⁹	-1.12 · 10 ⁸	-0.04	0.9994	1 · 10 ⁻⁹

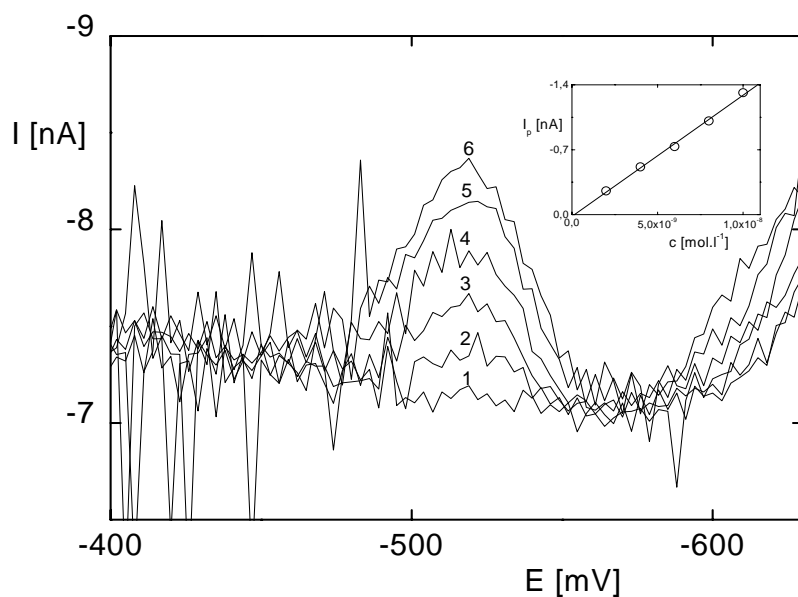


Fig. 5 Voltammograms and calibration plot of 5-NQ after extraction from 100 ml of drinking water,

containing 0 (1), 2 (2), 4 (3), 6 (4), 8 (5) and 10 (6) $\cdot 10^{-9}$ mol.l⁻¹ of this substance. Measured by DPV method at HMDE in 0.2 M NaOH – methanol (9:1) medium.

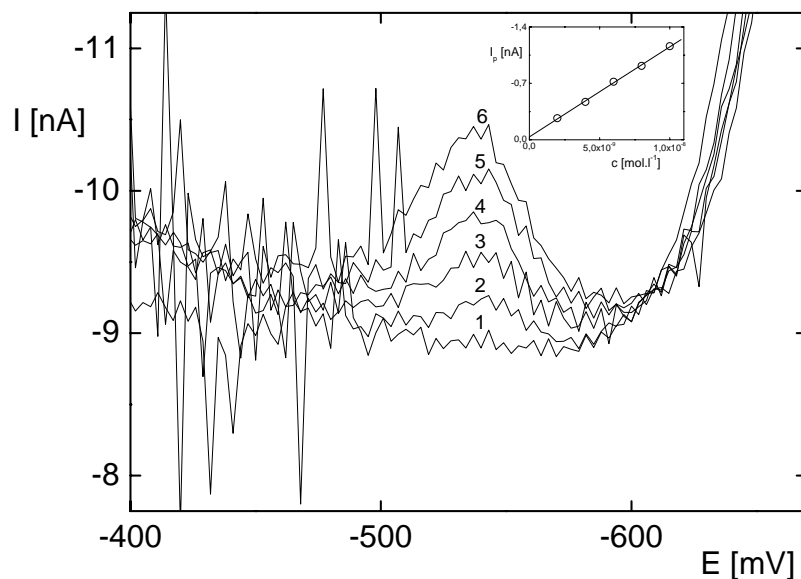


Fig. 6 Voltammograms and calibration plot of 5-NQ after extraction from 100 ml of river water,

containing 0 (1), 2 (2), 4 (3), 6 (4), 8 (5) and 10 (6) $\cdot 10^{-9}$ mol.l⁻¹ of this substance. Measured by DPV method at HMDE in 0.2 M NaOH – methanol (9:1) medium.

Differential Pulse Voltammetry at a Carbon Film Electrode

5-AQ gives one anodic peak in the whole investigated pH region (see Fig.7). The best developed peak was obtained in BR buffer pH 6 medium. This medium was further used for measuring of calibration curves. Parameters of calibration dependences are summarized in Table V and voltammograms connected with the lowest attained concentration range are shown in Figure 8 for illustration.

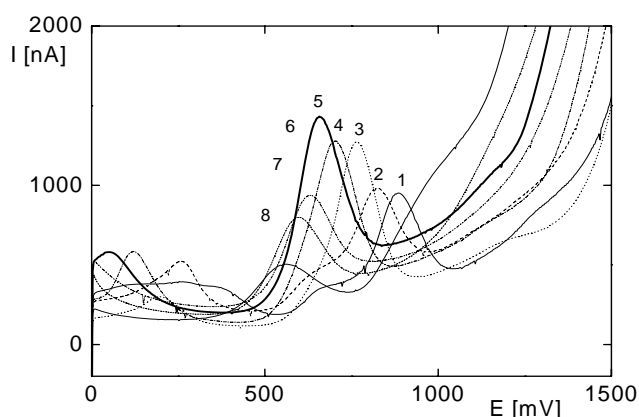


Fig. 7 Differential pulse voltammograms of 5-AQ ($c = 1.10^{-4} \text{ mol.l}^{-1}$) at CFE in BR buffer,

pH 2,0 (1); 3,0 (2); 4,0 (3); 5,0 (4); 6,0 (5); 7,0 (6); 9,0 (7); 12,0 (8).

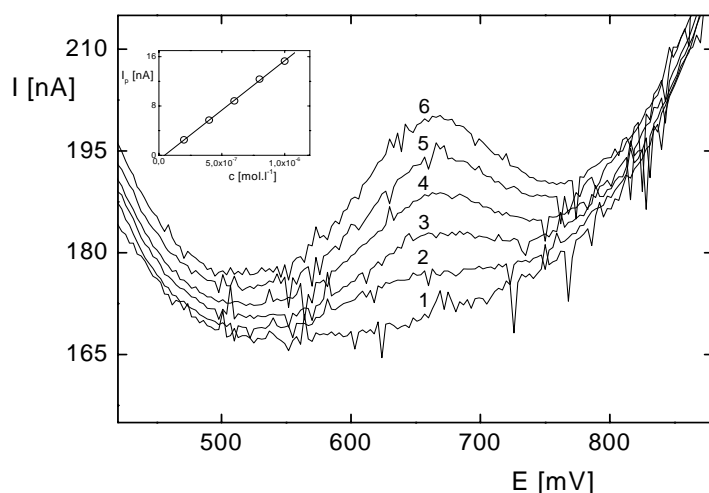


Fig. 8 DP voltammograms and calibration plot of 5-AQ at CFE in BR buffer pH 6 medium at the lowest attained concentrations.

$c(5\text{-AQ}) = 0$ (1), 2.10^{-7} (2), 4.10^{-7} (3), 6.10^{-7} (4), 8.10^{-7} (5) and 1.10^{-6} (6) mol.l^{-1} .

Table V Parameters of calibration straight lines for DPV determination of 5-AQ at CFE in BR buffer pH 6 medium.

Concentration [mol.l ⁻¹]	Slope [μA.mol ⁻¹ .l]	Intercept [μA]	Correlation coefficient	L _Q [mol.l ⁻¹]
(2 – 10)·10 ⁻⁵	5.99·10 ⁶	31.25	0.9962	-
(2 – 10)·10 ⁻⁶	8,67·10 ⁶	4,18	0.9994	-
(2 – 10)·10 ⁻⁷	1,61·10 ⁷	-0,74	0.9997	1.5·10 ⁻⁷

Summary

By DP Voltammetry at HMDE, the limit of quantification of 5-NQ equal to 2·10⁻⁸ mol.l⁻¹ was reached.

In the case of direct determination of 5-NQ in model samples the limit of quantification equal to 1.5·10⁻⁸ mol.l⁻¹ in drinking water and 6.5·10⁻⁹ mol.l⁻¹ in river water was reached.

After soild phase extraction 5-NQ from drinking resp. river water the limit of quantification of 5-NQ equal to 2.5·10⁻⁹ mol.l⁻¹ resp. 1·10⁻⁹ mol.l⁻¹ was reached.

By DP Voltammetry at CPE, the limit of quantification of 5-AQ equal to 1.5·10⁻⁷ mol.l⁻¹ was reached.

Acknowledgements

This work was financially supported by the Czech Ministry of Education, Youth and Sports (project LC06035 and project MSM 0021620857).

References

- [1] Marhold J.: *Přehled průmyslové toxikologie 2. Avicenum, Praha 1986.*
- [2] Tachibana M.; Shoei S.; Kawazoe Y.: *Chem. Pharm. Bull.* **15** (1967), 1112-1119.
- [3] Kawazoe Y.; Araki M.; Nakahara W.: *Chem. Pharm. Bull.* **17** (1969), 544-549.
- [4] Yosypchuk B.; Berek J.; Fojta M.: *Electroanalysis* **18** (2006), 1126-1130.
- [5] Wang J.: *Analytical Electrochemistry, 2nd edition. VCH, Weinheim 2000.*
- [6] Bard A. J.; Faulkner L. R.: *Electrochemical Methods: Fundamentals and Applications, 2nd edition. John Wiley, New York 2001.*
- [7] Meloun M.; Militký J.: *Statistické zpracování experimentálních dat na osobním počítači. Finish, Pardubice 1992.*

POSTCOLUMN ELECTROCHEMICAL HYDRIDE GENERATION USED FOR SPECIATION ANALYSIS OF ARSENIC COMPOUNDS

V. Červený, J. Hraníček and P. Rychlovský

Charles University, Faculty of Science, Department of Analytical Chemistry, Hlavova 2030, 128 43 Prague 2, Czech Republic; e-mail: cerven2@natur.cuni.cz

Abstract

The evaluation of an alternative and universal usable method of speciation analysis of Arsenic is presented in this work. The system employs electrochemical and (for comparison) chemical hydride generation for its easy on-line connection of the AAS detector with HPLC device. Externally heated quartz tube atomizer was chosen as the best atomization device for analysis of substituted arsenic hydrides. The electrochemical hydride generation is characterized by more than 95% efficiency of arsenic volatile compound generation for all oxidation states of arsenic at the same conditions except arsenobetaine (only 4% efficiency). Various types of generation cell were tested and optimum separation conditions were found.

Keywords

Arsenic, speciation analysis, electrochemical hydride generation, atomic absorption spectroscopy

1. Introduction

Speciation analysis is defined as “the determination of the exact chemical form or compound in which an element occurs in a sample and the quantitative distribution of the different chemical forms that may coexist”. [1]

The knowledge of various species toxicity resulted in the need of the speciation analysis of samples from the environment. Speciation

analysis of pollutants like arsenic is used for drinking and waste water samples, health service samples, soil or metal industry samples.

The main meaning about speciation today is that it can be provided using the efficient separation methods and the high sensitive detection technique. Choice of the methods depends on the number of samples, analyte concentration, time consuming and other parameters which can influence the usability of the method for the proposed purpose.

There are many ways which can be used for separation of various species. Firstly, the extraction serves for distribution of an analyte in the organic and inorganic phases [2, 3]. Secondly, gas chromatography (GC) serves for separation of gas or volatile analytes and their derivatives [4]. Third, another possibility for a separation of species is liquid chromatography, especially High Performance Liquid Chromatography (HPLC) [5]. Capillary electrophoresis (CE) is other separation techniques which can be used for the separation included in speciation analysis [6]. The easier speciation way is a choice of the reaction conditions that provides the only one product and on the base of the change of these conditions can be generated other derivatives of species. This way can be called “selective generation” and is commonly used for hydrides [7].

UV/VIS spectroscopy, atomic absorption (AAS) [8] or more sensitive atomic fluorescence spectroscopy (AFS) [9] can be chosen as the detection method for the speciation analysis for example. Furthermore, more expensive methods using Inductively Coupled Plasma (ICP) can be used for Mass Spectroscopy (ICP-MS) [5] or Atomic Emission Spectroscopy (ICP-AES) [10] as the excitation or ionization source. Electrochemical detectors are not as universal because some species may not be electrochemically active. The only one useful electrochemical system for automation is contactless conductivity detector but it is characterized by none selectivity.

For this study, the HPLC separation of arsenic species was chosen. The atomic absorption spectrometer was employed as the detector. Hydride generation (HG) is the best way to avoid of interferences in this detection method. Produced volatile compounds are separated from liquid matrix in gas – liquid separator; this resulted in employing of convenient atomization in quartz furnace and interferenceless detection. Common way of hydride generation is

using the chemical reduction. NaBH_4 is usually employed as the reducing agent. Sodiumborohydride solutions are unstable, thus there is necessary to prepare daily fresh solutions of this agent which can influence the limits of detection and determination in negatively way because of adulterants content.

The aim of this work was to find other possibilities in speciation analysis of arsenic. Postcolumn electrochemical hydride generation is an alternative method to the traditionally used chemical HG. Instead of reducing agent solution a cathode and electric current were used. Thus the acidified analyzed solution can not be contaminated from other added solutions. Other advantage of electrochemical HG is that hydrides can be obtained from organic arsenic compounds with efficiency higher than 95 % (except Arsenobetaine; only 4 % efficiency) at the same experimental conditions for all oxidation states of arsenic. This fact enables possible universal application and automation of method proposed.

2. Experimental

2.1. Reagents

A standard solution of As^{III} , As^{V} (Merck, BRD), monomethyl arsonic acid (MMAs^{V}) and dimethylarsinic acid (DMAs^{V}) (Prof. Miroslav Stýblo; Center for Environmental Medicine, Asthma and Lung Biology, University of North Carolina, Chapel Hill, NC 27599, USA) were used throughout and were diluted with $0.5 - 2.0 \text{ mol}\cdot\text{l}^{-1}$ hydrochloric acid. A suprapure grade hydrochloric acid (Merck, Germany) served as the catholyte. The anolyte solution was prepared from analytical grade sulfuric acid (Merck, Germany). Deionized water was obtained from the Milli Qplus system (Millipore, USA). Argon of the 99.999% purity was used as the carrier gas. A solution of 0.5 % (w/w) NaBH_4 (Merck, Germany) in 0.4 % (w/w) NaOH was used for the chemical hydride generation.

2.2. Instrumentation

An AA300 atomic absorption spectrometer (Varian, Australia) with externally heated quartz tube atomizer (RMI, Czech Republic) were used for selective and high sensitive detection of generated arsenic hydrides and substituted hydrides. The advantages of this

setup are in low atomization temperature and easy on-line connection with HPLC column. Arsenic Superlamp (Photron, Australia) was used as the radiation source for atomic absorption measurements. A LPS 303 laboratory power supply (American Reliance, Taiwan) was used as the electric current source for laboratory made hydride generation cells. All solutions were pumped through Tygon and PTFE tubing (0.5 mm ID, minimum length) by peristaltic pump (Cole-Parmer, USA). An anion exchange column Hamilton PRP – X 100 (250 x 2.1 mm; 10 μ m), sample injection valve 7125 (Rheodyne, USA) and HPLC pump Bromma 2150 (Sveden) were used as the separation unit. The whole instrumental setup is shown in the Figure 1. The optimum detection conditions are summarized in Table 1.

Table 1: Atomic absorption spectrometer condition:

Atomic absorption spectrometer	SpectrAA 300A (Varian, Australia)
Super lamp (Photron, Australia)	As ($\lambda = 193.7$ nm); $\Delta\lambda = 0.5$ nm; I = 15 mA
Externally heated quartz tube atomizer	QF (RMI, Czech Republic); 950°C
Deuterium background correction	

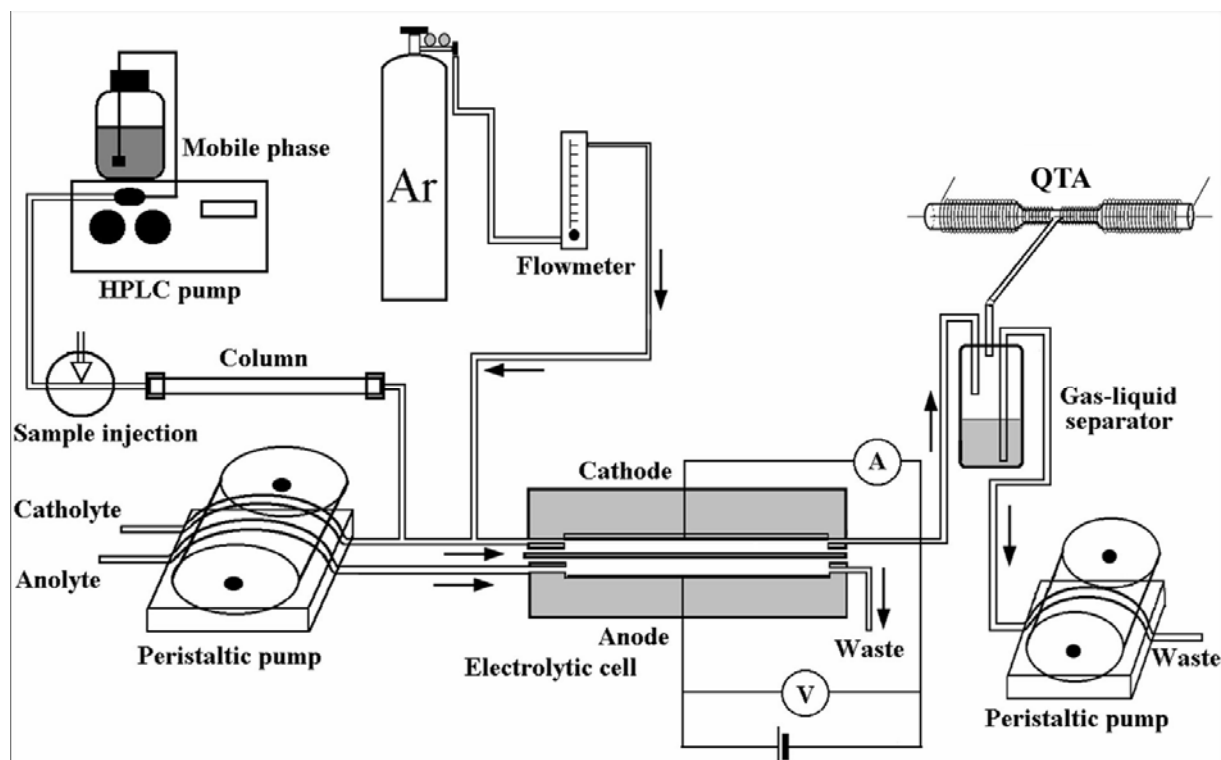


Figure 1: Scheme of used electrochemical hydride generation system

2.3. Laboratory made flow through cells

Perspex was chosen for electrochemical hydride generation cells because of easy working (drilling) with this transparent material. Platinum was selected as anode material because of its inert properties. On the base of the preliminary results lead wire was used as the best cathode material because of its high hydrogen overvoltage. The scheme of the most studied type thin layer electrolytic hydride generation cell (Cell I) is presented in Figure 2; other studied types schemes are given in Figures 3 and 4. Inner volumes, electrode surface areas and electric current densities are listed in Table 2.

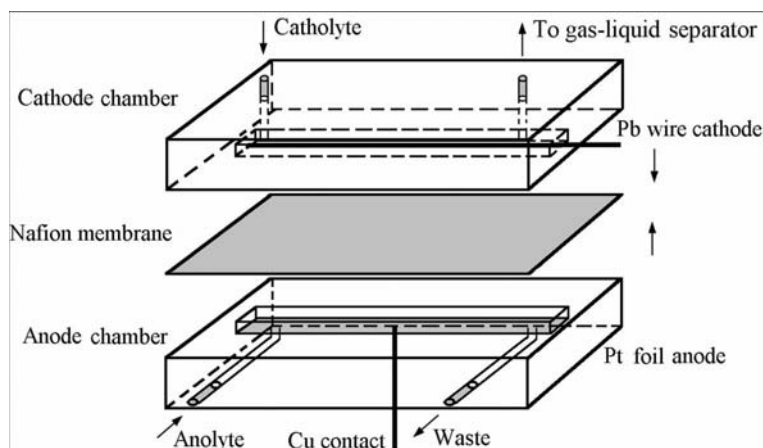


Figure 2: Scheme of thin layer electrolytic hydride generation cell (Cell I)

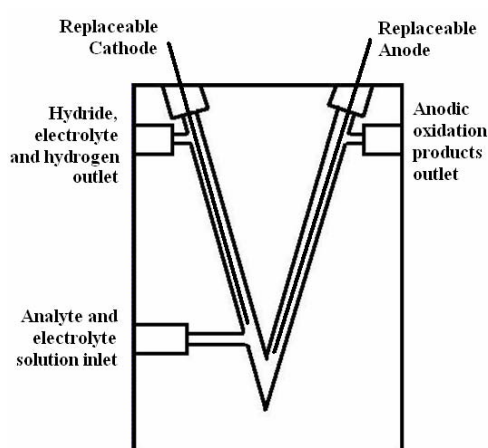


Figure 3: Scheme of V-type of electrolytic hydride generation cell (Cell II)

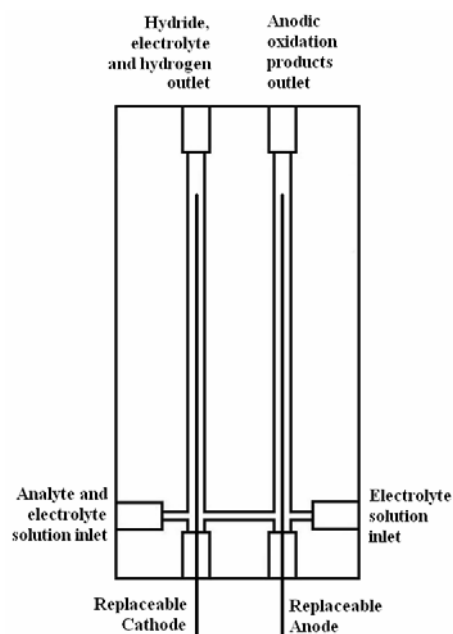


Figure 4: Scheme of H-type of electrolytic hydride generation cell (Cell III)

3. Results and discussion

3.1. HG cells testing

Three electrolytic HG cell were tested till today. Relative HG efficiencies attained were compared to the traditional chemical HG. The speed of signal response with a change of analyte concentration was another criterion. It means the time following sampling in which the signal can be observed. Reached values of these two parameters are listed in Table 1 as well. This resulted in that Cell III (the H-type) was chosen as the actual best. The advantage of Cell III is in the separated electrolyte inlet for the anode department which enables to introduce analyte to the cathode department direct through the chromatographic capillary (from the column outlet).

So far, the connection to the chromatographic system was realized only with Cell I (thin layer electrolytic hydride generation cell). The cathode and anode departments in this HG cell are isolated with ion exchange membrane Nafion 117. The best of Cell II, Cell III and Cell IV is going to undertake this connection too to obtain a comparison with the old one.

3.2. Chromatography

With Cell I the optimum separation conditions for the mixture solution of inorganic (As^{III} and As^{V}) and organic (MMA^{V} and DMA^{V}) arsenic were investigated. The optimized parameters and values are listed in Table 3. The example of attained chromatogram at these conditions with Cell I is shown in Figure 5.

Table 2: Electrolytic hydride generation cell type's properties

	Cell I	Cell II	Cell III	Cell IV
Cathode chamber volume (mm^3)	890	880	450	200
Anode chamber volume (mm^3)	1100	290	450	200
Lead wire cathode diameter (mm)	2	1	1	1
Cathode length (mm)	100	40	40	40
Cathode surface area (mm^2)	630	125	125	125
Anode surface area	300	125	125	125
Optimum cathode electric current density ($\text{mA}\cdot\text{mm}^{-2}$)	1.9	3.2	4.0	*
Relative HG efficiency (%)	100	80	98	*
Time of reaching the signal (s)	90	94	72	*

* till not measured

Table 3 Optimized separation parameters:

Parameter	Value
Column	PRP-X100; 10 μm (250 mm x 2.1 mm) (Hamilton, USA)
Sample volume	50 μl
Mobile phase	2 $\text{mmol}\cdot\text{l}^{-1}$ $\text{NaH}_2\text{PO}_4/\text{Na}_2\text{HPO}_4$ buffer; pH 5.0
Mobile phase flow rate	1.0 $\text{ml}\cdot\text{min}^{-1}$

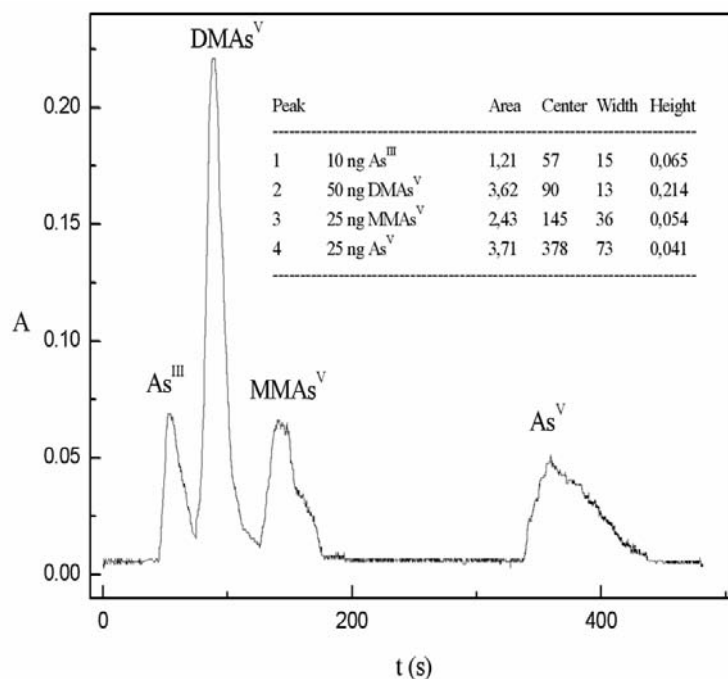


Figure 5: Chromatogram example

attained at optimum conditions listed in Table 2 with Cell I

4. Conclusions

On the base of these experiments it was found that postcolumn electrochemical hydride generation can fully substitute the traditional chemical generation with NaBH_4 . Its biggest advantage is that hydrides and substituted hydrides are generated with the efficiency more than 95 % (except of Arsenobetaine – 4 %) independent of the oxidation state of the analyte. One more advantage is that there is no contamination of analyzed solution with adulterants from added reducing agent solution in contrary to using electrochemical HG. Moreover difficulties of working with unstable NaBH_4 are avoided too. In this state of measurement, LOD and LOQ values are not comparable with that listed for more sensitive detection methods like atomic fluorescence.

4.1. Future plans

This project still continues. Possible evolution of instrumentation is in miniaturization of generation cells and reducing of dead volumes. One type else (triangle-type Cell IV, see in Figure 6) is to be made and investigated. Plans for future include finishing of testing of proposed miniaturized cells and experiments with

radioisotopes. Furthermore, there will be repeating of chromatographic optimization with temperature dependences. There will be tested the influence of preliminary UV photooxidation on the generating efficiency of hydrides from Arsenobetaine. The final step of the theme is going to be connection with atomic fluorescence detector and comparing of attained LOD values with published data.

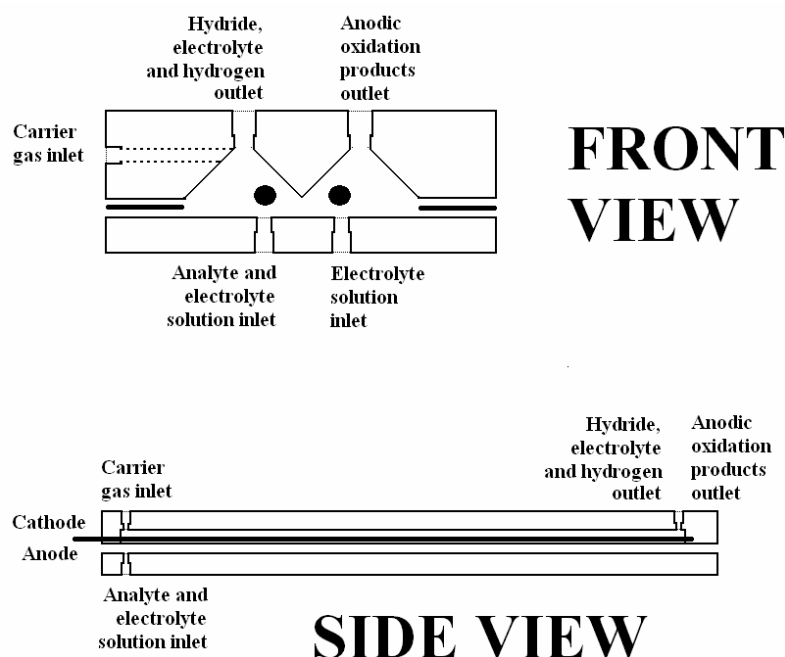


Figure 6: Scheme of triangle-type electrolytic hydride generation cell (Cell IV)

Acknowledgment:

The authors thank The Grant Agency of the ASCR (project: A400310507/2005) and MSMT CR (project MSM0021620857) for the financial support.

References:

- [1] Compendium of Chemical Terminology, IUPAC, 2nd Edition (1997), 1993, **65**, 2099
- [2] Daus B. et al., *Microchim Acta* **151**, 175-180, 2005
- [3] Raab A., Feldmann J., *Anal Bioanal Chem* **381**, 332-338, 2005
- [4] Killelea D.R., Aldstadt J.H., *J. Chromatogr. A* **918**, 169-175, 2001
- [5] Coelho N.M.M. et al., *Talanta* **66**, 818-822, 2005
- [6] Yeh Ch.-F., Jiang S.-J., *Electrophoresis* **26**, 1615-1621, 2005
- [7] Dědina J., Tsalev D.: Hydride Generation Atomic Absorption Spectrometry, *Wiley and Sons, Chichester*, 1995
- [8] Tseng W.-C. et al., *Analytica Chim Acta* **543**, 38-45, 2005
- [9] Schaeffer R., Soeroes C., Ipolyi I, Fodor P., Thomaidis N.S., *Analytica Chim Acta* **547**, 109-118, 2005
- [10] Narváez J., Richter P., Toral M.I., *Anal Bioanal Chem* **381**, 1483-1487, 2005

PRODUCTION OF GAS WITH LOW CONTENT OF TAR IN PLASMA GASIFICATION REACTOR

M. Hlina^a, M. Hrabovsky^a, V. Kopecky^a, M. Konrad^a, T. Kavka^a,
S. Skoblja^b

^a Institute of Plasma Physics, ASCR, Za Slovankou 3, 182 00 Prague 8, Czech Republic; e-mail: hlina@ipp.cas.cz

^b Department of Gas, Coke and Air Protection, Institute of Chemical Technology, Technická 5 166 28 Prague 6, Czech Republic

Tar content in gas produced by the gasification of biomass always plays an important role because high tar content disables some potentialities of the further treatment of the produced gas. There is a strong effort to produce gas with low tar content from this point of view. High concentrations of hydrogen and carbon monoxide also advance possibilities of the usage of the produced gas. Experiments were carried out in a reactor for plasma gasification equipped with hybrid gas-water stabilized DC torch. They confirmed that the reactor is absolutely suitable for this purpose mainly due to extremely low flow of plasma composed of argon, hydrogen and oxygen and its high inner temperature. The measurements of the tar content, using wood as a treated material, were based on SPE method and the determination of benzene and toluene in a gas phase revealed really low concentrations of tar, mostly below 10 mg/Nm³.

Key words:

tar, plasma, biomass gasification

1 Introduction

The new ways, how to satisfy increasing world population and its energy consumption are needed. Fossil fuels run low and it is obvious they cannot fulfil world demands. Nuclear energy represents an alternative, but there still remain problems with nuclear refuse. So renewable energy sources play more and more important role today. One method how to renewably obtain energy is to gasify biomass.

The plasma gasification of biomass is a smart way how to produce the mixture of hydrogen and carbon monoxide, which can be easily used for energy production. Hydrogen can be isolated and used separately if its concentration is high enough. The mixture of hydrogen and carbon monoxide produced by the gasification of biomass is called synthetic gas, or syngas. The quality of syngas depends on many factors, very important is the content of tar. Tar is a complex mixture of many organic compounds. There are several definitions of tar and it is impracticable to find one definition that satisfies all meanings. Tar is commonly mentioned as all organic contaminants with a higher molecular weight than benzene or the mixture of organic compounds which condensate at room temperature [1]. The classification of tar is presented in Table 1.

The presence of tar is a serious problem, which limits utilization of syngas for power generation or in chemical industry, so tar removal or conversion is required. Typical gas quality and tar content required for specific application can be found in [2]. There are two general groups of methods how to do it [3]:

- Primary methods - in-situ removal of tar. These methods try to adjust and control the conditions of gasification to achieve the desired composition of the produced gas. The geometrical design of a gasifier and various catalysts enhancing a chemical reactivity inside the gasifier are considered as the primary methods of reducing the tar content.

- Secondary methods - ex-situ removal of tar or gas cleanup. The gas cleaning is done by tar condensing (scrubbers) or chemical conversion (partial oxidation, catalytic cracking) in this approach.

The task of tar removal is technically complicated and expensive problem and its solution determines the capacity of industrial utilization of syngas.

This paper describes experiments with plasma-assisted gasification of biomass. The goal of the experiments was testing the possibility of production of syngas with reduced content of tar in the reactor with high temperature and high enthalpy thermal plasma flow. High temperatures in plasma reactor and absence of combustion ensure conditions for suppression of tar production. The content of oxygen in biomass is in such a degree that only small amount of oxygen is needed to be added to provide appropriate composition of

the produced gas and suppression of production of solid carbon. Almost all energy for biomass decomposition is delivered by plasma flow, the partial oxidation is needed only for the tuning of composition of the produced gas, so the process of the plasma gasification has characteristics of pyrolysis. This results in high content of hydrogen and carbon monoxide and low content of other species.

Table 1. Tar classification [4]

Tar class	Class name	Property	Representative compounds
1	GC-undetectable	Very heavy tars	
2	Heterocyclic	Containing hetero atoms, highly water soluble	Pyridine, Phenols, Cresols etc.
3	Light aromatic	One ring compounds	Toluene, Xylenes etc.
4	Light polyaromatic	Two and three ring compounds	Indene, Naphtalene etc.
5	Heavy polyaromatic	More than three rings	Fluoranthene, Pyrene etc.

3 Experimental setup

The experimental plasma-chemical reactor with water-cooling system was operated at a wall temperature 1100 – 1400 °C. Crushed wood (humidity 10.1, 20.2 % w/w) was supplied to the reactor at the rate of 10-50 kg/hour and encountered a plasma jet in the position about 30 cm downstream of the input plasma entrance nozzle at the reactor top. It was partially gasified during its flight within the jet, the non-gasified part of the wood falls onto the bottom of the reactor where it was gasified in the hot gas flow. The exit tube for exhaust gas was in the upper part of the reactor, so as the produced gases passed through the zone of high temperature within plasma jet or close to it. Inputs for additional gases for control of reactor atmosphere are at three positions in the upper part of the reactor. Produced gas leaves the gasification chamber and is cooled down approximately to 250 °C by water spray. More detailed description of the reactor is presented in [6].

Plasma was produced in the torch with DC arc stabilized by combination of gas flow and water vortex. The torch generates an oxygen-hydrogen-argon plasma jet with extremely high plasma enthalpy and temperature. Mean plasma temperature in the plasma torch is more than 15 000 K [5]. The torch is attached to the reactor at

the reactor top. Plasma enters the reactor volume through the nozzle with diameter of 40 mm in the top of the reactor. High velocity of plasma and high level of turbulence ensure good mixing inside the reactor and homogeneous heating of its volume.

Plasma torch power varied from 95 to 138 kW. The power available for gasification depends on the plasma torch power and was roughly one half of the plasma torch power. There was also added small amount of carbon dioxide into the gasification chamber to set up right conditions for stoichiometric gasification, it means to increase an oxygen content and reduce the production of solid carbon deposits. The molecular formula of dry wood was assumed as $C_{1,61}H_{2,24}O$ for the calculation of the amount of added carbon dioxide.

The measuring system included monitoring of plasma torch operation parameters, temperatures in several positions inside the reactor and calorimetric measurements on cooling water loops. The composition of produced gas was measured at the output of the reactor. The results of these measurements are given in [6]. The samples for tar analysis are withdrawn from the duct between the gasification chamber and the quenching chamber (Fig.1). The tube for collection of samples was cooled by the water spray in the quenching chamber. Tar was captured onto DSC-NH₂ adsorbent or silica gel positioned at the tube and the samples were analysed by means of gas chromatography. Other analyses of the composition of the produced syngas and the content of tar were measured by the means of mass spectroscopy and gas and liquid chromatography.

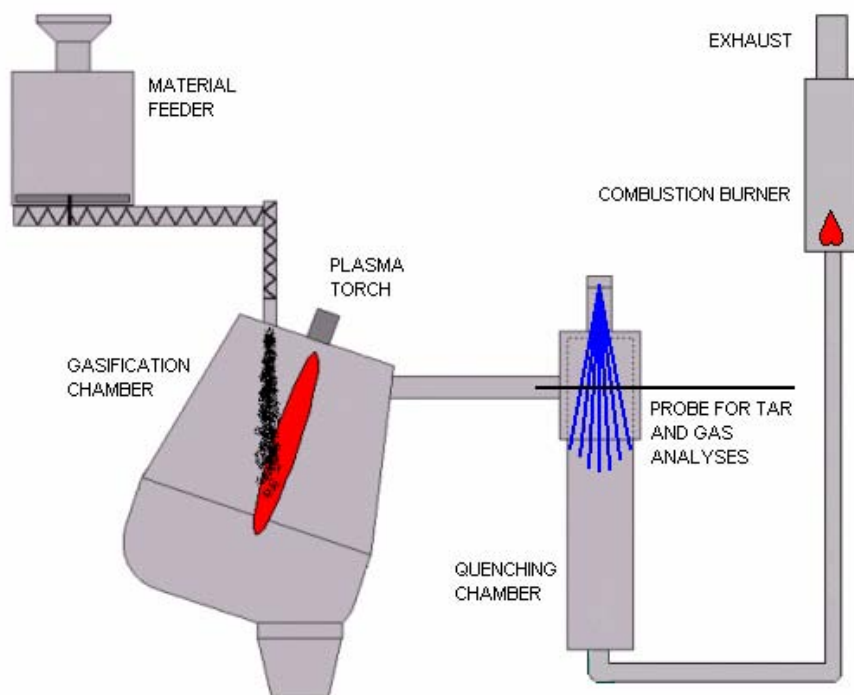


Fig. 1. Schematics of the plasma gasification reactor

4 Results and Conclusions

The measurements of the content of tar were based on solid phase extraction (SPE) method and the determination of benzene and toluene in a gas phase also directly on gas chromatography with thermo conductive detector (TCD). This paper includes the results from two series of experiments (A and B). These series differed in conditions. The results are summarized in Tables 2 and 3. Samples for SPE analyses were withdrawn also during B experiments, but overall content of tar was lower than 10 mg/Nm^3 , which was under the detection limit of used TCD. This occurred even with toluene, but it is obvious that concentration of tar in produced gas is really low in comparison with other gasification plants [4]. Especially in the case of lower flows of treated material the tar content is minimal. Low tar content is caused mainly by the high temperatures in the reactor and the fast quenching. However, it is necessary to point out that many improvements are taking place in this field [7], but the plasma gasification by gas-water stabilised torch has one very important advantage and it is the fact that the mass flow rate of plasma is almost inconsiderable compared to the flow rate of added material. It results

in high concentrations of hydrogen and carbon monoxide, which range between 40-50 % (vol.) [6].

The gasifier equipped with the gas-water stabilised plasma torch represents a unique system with superior features, which cannot be obtained by any other system built for the gasification of biomass. Further experiments will focus on the adjusting of experimental conditions, the gasification of other materials and energy and mass balances.

Table 2. Content of polyaromatic hydrocarbons in produced gas (A experiments)

Plasma torch power [kW]	95	138
CO ₂ flow rate [slm]	23	13
Humidity of treated wood [w/w]	10.1	10.1
Wood flow rate [kg/hour]	20	20
Fluorene [$\mu\text{g}/\text{m}^3$]	45.5	6.0
Phenanthrene [$\mu\text{g}/\text{m}^3$]	223.5	56.0
Anthracene [$\mu\text{g}/\text{m}^3$]	1.0	0.5
Fluoranthene [$\mu\text{g}/\text{m}^3$]	199.0	535.5
Pyrene [$\mu\text{g}/\text{m}^3$]	814.0	2 331.0
Benz[a]anthracene [$\mu\text{g}/\text{m}^3$]	<1	<1
Chrysene [$\mu\text{g}/\text{m}^3$]	7.0	4.0
Benzo[ghi]fluoranthene [$\mu\text{g}/\text{m}^3$]	0.8	<1
Benzo[a]pyrene [$\mu\text{g}/\text{m}^3$]	11.5	11.0
Benzo[ghi]perylene [$\mu\text{g}/\text{m}^3$]	250.5	282.0

Table 3. Content of benzene in produced gas (B experiments)

Plasma torch power [kW]	107	107	107
CO ₂ flow rate [slm]	5	10	60
Humidity of treated wood [w/w]	20.2	20.2	20.2
Wood flow rate [kg/hour]	10	20	50
Benzene [mg/Nm^3]	1,5	2,7	116,2
Toluene	< 1 mg/Nm^3		
Tar - SPE	< 10 mg/Nm^3		

Acknowledgement

The authors gratefully acknowledge the support of this work by the Grant Agency of the Czech Republic under the project No. 202/05/0669.

References

- [1] <http://www.tarweb.net/> (2006)
- [2] Hasler P., Nussbaumer T., Gas cleaning requirements for IC engine applications fixed bed biomass gasification, *Biomass and Bioenergy*, 16(1999) 385-395
- [3] Nair S.A., Corona Plasma for Tar Removal, PhD thesis, Eindhoven University of Technology, 2004
- [4] Devi L., Ptasinski K.J., Janssen F.J.J.G., van Paasen S.V.B., Bergman P.C.A., Kiel J.H.A., Catalytic decomposition of biomass tars: use of dolomite and untreated olivine, *Renewable Energy*, 30 (2005) 565-587
- [5] Brezina V., Hrabovsky M., Konrad M., Kopecky V., Sember V., New plasma spraying torch with combined gas-liquid stabilization of arc, *Proceedings of the 15th international symposium on plasma chemistry*, vol. III, Orleans. 2001, 1021-6
- [6] Hrabovsky M., Konrad M., Kopecky V., Hlina M, Kavka T., Oost G., Beeckman E., Gasification of Biomass in Water/Gas-Stabilized Plasma for Syngas Production, *Czechoslovak Journal of Physics* 56, Part 6 suppl. B (2006) B1199-B1206
- [7] Bhattacharya S.C., Siddique A.H.M.M.R., Pham H.L., A study on wood gasification for low-tar gas production, *Energy*, 24 (4) (1999) 285-286

3rd International Student Conference: “Modern Analytical Chemistry”

Vydala Česká společnost chemická. Za obsah veškerých textů nesou plnou zodpovědnost autoři. Publikace neprošla odbornou ani jazykovou úpravou a je určena pro účastníky semináře a členy pořádajících organizací. Není určena k volnému prodeji. Zveřejněné informace mohou být dále použity za předpokladu úplného citování původního zdroje. Přetiskování, kopírování či převádění této publikace do jakékoliv tištěné či elektronické formy a její prodej je možný pouze na základě písemného souhlasu vydavatele. (Bona fide vědečtí pracovníci si mohou pořídit jednotlivé xerox kopie).

Published by the Czech Chemical Society in collaboration with organizers of the conference. This publication is made available for the conference participants, members of the organizing institutions and for documentary purposes.

Some products named or cited in this publication and other materials of the congress are registered as trademarks or proprietary names even in the case this fact is being explicitly shown or acknowledged. It is not to be considered as fail to notice the ownership or authorship by the publisher. All the texts are published with the full responsibility of authors for their content. The publication was not content or language-polished. Its content could be used on the condition of full acknowledgement and citation of the source. Direct reprinting, transformation to any means of electronic form is restricted (bona fide scientist may xerox single copies in accordance of their local copyright laws and regulations) and is possible upon written agreement with the publisher only.

Vydala / Published by



**Česká společnost chemická
Czech Chemical Society**

Novotného lávka 5, CZ 116 68, Praha 1

v roce 2007

1. vydání, brož., náklad 50 výtisků

Editor: Mgr. Václav Červený

© Charles University in Prague

ISBN 80 - 86238 - 96 – 2